POSTTRANSCRIPTIONAL AND POSTTRANSLATIONAL REGULATION OF VIRULENCE IN ERWINIA AMYLOVORA

BY

JAE HOON LEE

DISSERTATION

Submitted in partial fulfillment of the requirements
for the degree of Doctor of Philosophy in Crop Sciences
in the Graduate College of the
University of Illinois at Urbana-Champaign, 2018

Urbana, Illinois

Doctoral Committee:

Associate Professor Youfu Zhao, Chair
Professor Steven C. Huber
Assistant Professor Nathan E. Schroeder
Assistant Professor Li-Qing Chen

ABSTRACT

Erwinia amylovora is the causal agent of fire blight, the most destructive bacterial disease of the *Rosaceae* family plants. Two virulence factors, the type III secretion system (T3SS) and the exopolysaccharide (EPS) amylovoran, are strictly required for its pathogenicity. Our previous studies have determined the role of several transcription factors in the regulation of *E. amylovora* virulence; however, molecular mechanisms of virulence regulation at the posttranscriptional and posttranslational levels have still remained elusive. In this dissertation, our goal was to understand new regulatory mechanisms in *E. amylovora* virulence.

First, we characterized the molecular mechanism of Lon protease-mediated virulence regulation. Mutation of the *lon* gene caused the amylovoran overproduction, the increased T3SS expression and the non-motile phenotype. In the absence of Lon, abundance and stability of the HrpS/HrpA and RcsA proteins were significantly increased, and the resulting accumulation of the RcsA/RcsB proteins influenced the expression of *flhD*, *hrpS* and *csrB*. In addition, *lon* expression is under the control of the RNA-binding protein CsrA, possibly at both the transcriptional and post-transcriptional levels, suggesting a possible interplay between Lon and the Csr system.

Second, we examined the role of ClpXP protease in virulence regulation and its potential interaction with Lon. Mutation in *clpXP* diminished the T3SS expression, amylovoran production and motility, resulting in delayed disease progress. Highly accumulated RpoS proteins were detected in the *clpXP* mutant, and mutation of *rpoS* in the *clpXP* mutant background restored virulence to the wild-type level. These suggest that ClpXP-dependent RpoS degradation positively affects virulence traits. In addition, lack of both ClpXP and Lon resulted in significantly reduced virulence independently of RpoS level, suggesting that ClpXP and Lon are indispensable for full virulence.

Third, transcriptional regulation mechanism of the *hrpS* gene, encoding the essential T3SS activator, was examined. We found that the *hrpS* gene contains two promoters driven by HrpX/HrpY and the Rcs system, respectively. IHF also positively regulates *hrpS* expression

through directly binding to the *hrpX* promoter and positively regulating *hrpX/hrpY* expression. Moreover, *hrpX* expression was down-regulated in the ppGpp-deficient mutant and the *dksA* mutant, but up-regulated when the wild-type strain was treated with serine hydroxamate, suggesting that ppGpp might induce *hrpX/hrpY* and *hrpS* expression. Furthermore, CsrA positively regulates *hrpS* expression mainly through the Rcs system. These results suggest that *E. amylovora* recruits multiple stimuli-sensing systems to regulate *hrpS* and T3SS gene expression.

Fourth, we examined the global effect of CsrA and determined potential molecular mechanisms of CsrA-dependent virulence regulation in *E. amylovora*. Using REMSA, direct interaction between CsrA protein and *csrB* sRNA was confirmed, while CsrA did not bind to the transcripts of T3SS activators, *hrpL* and *hrpS*. Transcriptomic analyses under the T3SS-inducing condition revealed that mutation in *csrA* led to differential expression in more than 20% genes in the genome. Of these, T3SS genes and those required for cell growth and viability were significantly down-regulated, explaining the pleiotropic defects in the *csrA* mutant. On the other hand, the *csrB* mutant exhibited significant up-regulation of the major virulence genes, further suggesting antagonistic effects of *csrB* on CsrA. Through REMSA combined with site-directed mutagenesis and LacZ reporter gene assay, three CsrA targets (*flhD*, *rcsB* and *relA*) were identified that positively regulate *E. amylovora* virulence. Overall, this dissertation demonstrates that *E. amylovora* employs multiple layers of gene regulatory networks to effectively control the expression of virulence factors.

ACKNOWLEDGEMENTS

My dissertation research would not have been possible without the support of many people. First, I would like to thank my advisor Prof. Youfu 'Frank' Zhao for giving me this invaluable opportunity to learn and grow in his lab. I am truly grateful for the productive and educational atmosphere of the Zhao laboratory. His guidance and support throughout my Ph.D. training led me to become a better scientist.

I would like to extend my thanks to all my committee members Prof. Steven Huber, Prof. Nathan Schroeder and Prof. Li-Qing Chen for their feedback on my projects throughout the years. My special thanks also go to Dow AgroSciences Fellowship, USDA-SCRI and USDA-NIFA-AFRI, for financial assistance of my degree and the research projects. I am also grateful to Prof. James Slauch and his student Kyungsub Kim for letting me use his lab equipment and all kinds of discussion and help on my experiments.

I would also like to thank current and former members of the Zhao laboratory for providing me with cheerful support and friendship. It has been a great pleasure to have everyone as my colleague. My special thanks to Dr. Veronica Ancona and Dr. Tiyakhon Chatnaparat for their encouragements and advices on my research and career.

Last, but not the least, I would like to thank my parents for their endless love and support. I feel truly blessed to be their son, and I could not have completed this long journey without their encouragements.

TABLE OF CONTENTS

LIST OF FIGURES

LIST OF TABLES

CHAPTER 1

Literature review

1.1 Fire blight pathogen, *Erwinia amylovora*

Fire blight is the most destructive bacterial disease of the *Rosaceae* family plants, including apple and pear trees. Since the first observation in the Hudson Valley of New York over 200 years ago, the occurrence of fire blight has been reported worldwide (Denning, 1794; Bonn and Zwet, 2000). The rosaceous plants are one of the most economically important fruit crops in many countries. However, losses and costs associated with fire blight are serious. The estimated annual damages to fire blight are over $100 million in the United States alone, and a single fire blight epidemic can cause a loss of more than $68 million as reported in northwest USA in 1998 (Bonn, 1999; Norelli et al., 2003). The causal agent of fire blight is *Erwinia amylovora*. It was first isolated by Thomas Burrill in Illinois, 1980 and is now described as the first bacterium proven to be a plant pathogen. As the control of fire blight has become serious concern in pome fruit industry, a better understanding of the disease and its pathogen is necessary.

1.1.1 Fire blight: disease cycle, symptoms and signs

Fire blight, as the name implies, is characterized by scorched appearance of affected trees and rapid development of epidemics. Fire blight has a complex disease cycle that can develop several distinct phases throughout the season. The causal agent, *E. amylovora*, overwinters mainly in the cankers on the branches and trunks of previously infected trees. Dormant buds, fruit mummies and other alternate hosts are also sites for survival during the winter (Anderson 1952; Goodman 1954; Baldwin and Goodman, 1963; Keil and van der Zwet, 1972). In the spring, bacteria are released as ooze from the primary source of inoculum and

disseminated to blossoms by wind, rain and insects. The stigma exduates from flowers, especially within 2 days after opening, provide a favorable condition for bacterial growth (Thomson, 1986; Gouk et al., 1996). Pathogen colonization and multiplication on flower lead to blossom blight and also become the secondary source of inoculum for subsequent infections (Malnoy et al., 2012). In the summer, other phases of blight symptoms become distinct, especially in young shoot, immature fruit, and rootstock. Since invasion of *E. amylovora* occurs through natural openings and wounds, all the above-ground parts of tree can be a site for secondary infection. The diseased tissues generally exhibit wilting and blackened necrotic lesions and produce droplets of bacterial ooze under humid conditions. The characteristic shepherd's crook-like bending of the shoot tip and canker formation are also often observed. Rootstock infection causes the most devastating phase that girdles susceptible rootstock and occasionally kills trees (Momol et al., 1998). Therefore, conditions favorable for severe epidemics of fire blight are warm and humid weather in the spring for the establishment of blossom blight, followed by frequent heavy rain and wind during the active growth period of *E. amylovora* (Biggs et al., 2008). Since young succulent tissues are more susceptible to *E. amylovora* infection, cultural practices that stimulate rapid growth of trees, such as excess fertilizer and heavy pruning, also increase the severity of fire blight (Schroth et al., 1974).

1.1.2 General characteristics of *Erwinia amylovora*

E. amylovora is a Gram-negative, plant-pathogenic bacterium of the *Enterobacteriaceae* family. Several clinically important pathogens, such as *Escherichia coli*, *Salmonella* and *Shigella*, and plant-associated bacteria, such as *Pantoea* and *Pectobacterium* are closely related to *E. amylovora* as the same family member. Like other enteric bacteria, *E. amylovora* is short rod-

shaped, motile by peritrichous flagella, non-sporulated, and weakly fermentative (Brenner, 1984; Holt et al., 1994). Two pathogenicity factors, the exopolysaccharide (EPS) amylovoran and a hypersensitive response (HR) and pathogenicity (*hrp*)-type III secretion system (T3SS), are essential for *E. amylovora* to cause disease (Khan et al., 2012). *E. amylovora* is capable of growing between 4℃ and 37℃, but the optimal growth temperature is between 21℃ and 30℃ (Billing, 1974). Bacterial growth rate is significantly increased as the temperature exceeds 18℃, indicating the minimum temperature required for establishment of the fire blight (Billing, 1974). Among several *Erwinia* spp., *E. amylovora* is distinguishable by its cultural, physiological and biochemical characteristics, including motility, facultative anaerobe, mucoid growth, reducing substances from sucrose, acetoin production, and gelatin liquefaction (Holt et al., 1994). Motility of *E. amylovora* is pH- and temperature-dependent and stimulated by chelating metal ions (Raymundo and Ries, 1981). Motility plays a significant role in apple blossom infection, although it is not indispensable for infection of other tissues, such as shoot seedlings (Bayot and Ries, 1986). Consistently, *E. amylovora* is attracted to asparatate and several dicarboxylic acids that are present in the nectar of apple flowers (Raymundo and Ries, 1980; Vanneste, 2000).

In addition to apple and pear trees, *E. amylovora* can affect more than 180 species from 39 genera of the *Rosaceae* family (Zwet and Keil, 1979; Bradbury, 1986). This wide range of host plants might result in two different host specificities within *E. amylovora* species: strains infecting the Spiraeoideae subfamily, such as apple and pear, and strains infecting the *Rubus* genus, such as raspberry and blackberry. Although both host-specific groups utilize the same two major pathogenicity factors, amylovoran and T3SS, *Rubus*-infecting strains exhibit less or no virulence on apple and pear (Heimann and Worf, 1985; Braun and Hildebrand, 2005). This

indicates that there are intraspecies genetic diversities between different *E. amylovora* strains. Since the complete genome sequence of *E. amylovora* was first revealed in 2010, about 140 strains have been sequenced (Sebaihia et al., 2010; Smits et al., 2010a). Comparative genomic analysis revealed that average amino acid identities of all *E. amylovora* strains are 99.72%, those of only Spiraeoideae-infecting strains are 99.98%, but those of two individual genomes in different host-specific group decreases to 99.19% (Mann et al., 2013). *Rubus*-infecting strains and Spiraeoideae-infecting strains exhibit variations in the lipopolysaccharide biosynthesis pathway, effector proteins and avirulence proteins. In addition, *Rubus*-infecting strains uniquely contain genes responsible for a putative secondary metabolite pathway, suggesting the putative host-specific determinants (Mann et al., 2013). However, despite high genetic homogeneity, four wild-type strains of Spiraeodieae-infecting strains (Ea1189, Ea273, Ea110, and CFBP1430) cause different levels of disease severity on apple plants (Wang et al., 2010). Understanding how different *E. amylovora* strains have evolved to display different virulence patterns with such low levels of genetic diversity remains elusive.

E. amylovora contains a circular chromosome of 3.8 Mb containing about 3500 coding sequences (Sebaihia et al., 2010; Smits et al., 2010a). This is relatively small compared to 4.5 to 5.5 Mb of other sequenced enterobacterial genomes. Components for amylovoran biosynthesis and T3SS are encoded in a cluster of 12 *ams* genes and the Hrp pathogenicity island (PAI), respectively, in the chromosome (Oh and Beer, 2005). All *E. amylovora* strains, except UPN527, also contain plasmid pEa29 which encodes thirteen genes including histone-like nucleoid structuring protein (*hns*) and thiamine biosynthesis componenets (*thiF*, *thiG*, and *thiO*) (McGhee and Jones, 2000; Mann et al., 2013). The pEa29-cured strain exhibits a less virulent phenotype,

suggesting that pEa29 contributes to bacterial virulence and survival in plants (McGhee and Jones, 2000). Other plasmids have been also observed in different strains of *E. amylovora*, but there is no clear evidence for their role in virulence regulation (Llop et al., 2012).

1.2 Type III secretion system of plant-pathogenic bacteria

T3SS is a major virulence factor widely found in Gram-negative bacteria. Type III effectors (T3Es), which allow suppression of basal host defense, bacterial growth, and subsequent disease development, are directly injected into the host cells through T3SS. Although the impact of T3SS on bacterial virulence can vary between species, studies of T3SS in many important pathogens have enhanced our understanding of bacterium-host interactions. It is generally believed that T3SS contributes to early stages of infection in plant pathogenic bacteria that establish a population in the apoplast, including *Pseudomonas*, *Erwinia*, *Ralstonia*, and *Xanthomonas* spp. (Alfano and Collmer, 2004). Their T3Es play a central role in suppressing plant innate immunity, determining host range at the race-cultivar level (Lindeberg, 2012). In *E. amylovora*, mutant deficient in T3SS is unable to cause necrosis in apple leaf mesophyll and a hypersensitive response (HR) in tobacco, while mutant deficient in amylovoran production is still able to cause both reactions (Metzger et al., 1994). T3SS of *E. amylovora* also elicits oxidative burst and related reactions, such as lipid peroxidation and electrolyte leakage, which are always accompanied before successful pathogensis (Venisse et al., 2001; Venisse et al., 2003). Due to its critical role in pathogenesis, T3SS has been extensively characterized, and this review will focus on architecture and regulation mechanisms of T3SS in plant-pathogenic bacteria.

1.2.1 Architecture of type III secretion system

T3SS is one of the most complex bacterial nanomachines generated by over 20 different proteins. T3SS can refer to two different systems in bacteria: the flagellar T3SS that secretes extracellular components of flagellum, such as hook and filament subunits, and the non-flagellar T3SS that translocates T3Es into eukaryotic cells. Despite different overall organization and function, they share a highly conserved core structure. Phylogenomic and comparative analyses revealed that the non-flagellar T3SS arose from the flagellar T3SS by a series of genetic alteration, in other words, by evolutionary exaptations (Abby and Rocha, 2012). The assembled non-flagellar T3SS is composed of four main parts: a cytoplasmic ATPase; a basal body that spans bacterial inner and outer membranes; extracellular needle (animal pathogens) or pilus (plant pathogens) that serves as a secretion conduit; and a translocon that forms a pore in the host plasma membrane and allows the delivery of effectors into the host cytosol (Fig. 1.1). At least 9 intracellular components in the non-flagellar T3SS are conserved among plant- and animal-pathogens, and most of them are also homologous to flagellar components (Abby and Rocha, 2012; Büttner, 2012; Portaliou et al., 2015).

T3SS of plant-pathogenic bacteria have been grouped into two different families, Hrp (HR and pathogenicity) 1 for *Pseudomonas* and *Erwinia* spp., and Hrp2 for *Xanthomonas* and *Ralstonia* spp., and the conserved structural components in both families are encoded by *hrc* (HR and conserved) genes. Two highly conserved components of the non-flagellar T3SS in the cytoplasm are ATPase and putative C-ring, which are part of secretion apparatus and implicated in rotor/switch complex in the flagellar T3SS (Erhardt et al., 2010). The structure of T3SS ATPase is related to F_1 domain of F_oF_1-ATPase. The F_1 domain generally consists of a

heterohexamer ($\alpha_3\beta_3$), while T3SS ATPase consists of a homohexameric $FliI_6$ and $HrcN_6$ in flagellum and plant-pathogens, respectively (Pozidis et al., 2003; Imada et al., 2007; Zarivach et al., 2007). ATPase is mainly involved in recognition and unfolding of type III secretion substrates by dissociating the substrate-chaperon complexes (Akeda and Galan, 2005). ATPase was thought to drive protein translocation across the bacterial membranes. However, it has been reported that ATP hydrolysis is not essential for protein translocation, and the energy source for T3SS is the electrical potential difference ($\Delta\psi$) and the proton concentration difference (ΔpH), together called the proton motive force (Wilharm et al., 2004; Paul et al., 2008; Minamino et al., 2011). The role of putative C-ring (HrcQ in plant pathogens) in the non-flagellar T3SS is not clear yet, but suggested to provide docking sites for the T3Es due to its interaction with T3Es and T3E-chaperon complexes (Morita-Ishihara, 2006; Spaeth et al., 2009).

Cytoplasmic components of T3SS are associated with the export apparatus in the inner membrane. The export apparatus is composed of five highly conserved proteins (HrcR, HrcS, HrcT, HrcU, and HrcV in plant pathogens), which are essential for the formation of functional T3SS machinery (Allaoui et al., 1994). HrcR, HrcS, and HrcT homologues contain several transmembrane helices, possibly forming a ring-shaped protein channel in the inner membrane. In contrast, HrcU and HrcV homologues contain C-terminal cytosolic domains, whose auto-cleavage events promote a secretion-competent state and contribute to regulation of the ordered export of T3SS substrates (Ferris et al., 2005; Zarivach et al., 2008). In this process, type III secretion substrate specificity switch (T3S4) proteins interact with HrcU homologues, induce conformational changes in the cytoplasmic domain, and mediate the recognition of appropriate substrates sequentially from structural components to T3Es (Büttner, 2012). T3S4 proteins in

different species exhibit limited homology, and their actions during secretion switches also appear to vary. For example, T3S4 proteins suppress the secretion of pilus subunits in *X. campestrics* pv. *vesicatoria*, but is required for full secretion of pilus subunits in *P. syringae* pv. *tomato* (Lorenz et al., 2008; Morello and Collmer, 2009).

T3SS chaperone proteins in the cytoplasm are also often required to promote substrate targeting. They specifically bind their cognate substrates and enhance interactions between substrates and T3SS machinery (Büttner, 2012). In some cases, the chaperone proteins also contribute to the substrate stability. For example, one of *E. amylovora* T3SS chaperones, DspB/F, is required for DspA/E effector secretion by preventing its intracellular degradation during secretion process (Gaudriault et al., 2002). In addition to the substrate recognition with the aid of accessory proteins, there are several evidences that the N-terminal region of T3SS substrates also important for the T3SS machinery recognition (Michiels and Cornelis, 1991; Sory et al., 1995; Schesser et al., 1996). In plant-pathogenic bacteria, analysis of 28 candidates of T3S substrates in *P. syringae* revealed that T3SS substrates contain solvent-exposed amino acids in the first five amino acids, lack aspartate or glutamate resides in the first 12 amino acids, and exhibit amphipathicity in the first 50 amino acids (Petnicki-Ocwieja et al., 2002).

T3SS machinery consists of ring structures in the inner and outer membranes that enclose the channel for the protein secretion (Kubori et al., 1998; Marlovits et al., 2004). The membrane-spanning components are localized by sec-dependent translocation, followed by several maturation steps, including signal peptide cleavage and oligomerization (Kubori et al., 1998; Yip et al., 2005). In the inner membrane, the membrane and supramembranous ring (MS)

is formed by surrounding the export apparatus and provides a scaffold for the overall assembly processes. The conserved component of the MS ring is HrcJ homologues that are located at the periplasm and interact with the needle or pilus subunits (Ogino et al., 2006). The outer membrane ring of the non-flagellar T3SS is structurally distinct from the flagellar T3SS by forming homomultimeric rings of the secretin-family proteins (HrcC in plant pathogens) (Abby and Rocha, 2012). They are also found in the other secretion systems, including type II secretion systems, type IV pili, and extrusion machinery of filamentous phages, and crucial for providing pores in the outer membrane (Korotkov et al., 2011). Small lipoprotein, called pilotins, is associated with seretins in animal pathogens to facilitate the formation and localization of the outer membrane ring, while no such protein was observed in plant pathogens (Daefler and Russel, 1998; Burghout et al., 2004; Büttner, 2012).

The extracellular components of non-flagellar T3SS are highly variable in their structure between species. The pilus of plant pathogens can be extended up to several micrometers long to penetrate the plant cell wall, while the needle of animal pathogens is only about 40 to 80 nm long (Tamano et al., 2000; Hu et al., 2001; Jin and He, 2001). Electron microscopy analysis showed that the pilus components of *E. amylovora* (HrpA) form a helical structure with a diameter of about 8 nm, which is thinner than flagellar filaments with a diameter of about 15 nm (Jin et al., 2001). Despite high sequence variability, the pilus components in different species exhibit similar physiocochemical properties, structural flexibilities, and polymerization modes (Tampakaki et al., 2010).

1.2.2 Regulation of Hrp1 type III secretion system

Phylogenetic analysis based on amino acid sequences of HrcV homologues showed that T3SS of *Erwinia* spp. belongs to the Hrp1 group with *P. syringae* (He et al., 2004). Despite different host specificities, bacteria carrying the Hrp1-T3SS have been reported to share similar regulatory mechanisms for T3SS activation, and their structural and functional components tend to be encoded in gene clusters or pathogenicity islands (PAI). All the *hrp* and *hrc* genes of *E. amylovora* are clustered in *hrp*-PAI (Fig, 1.2), which is composed of four distinct regions: the *hrp*/*hrc* region, the Hrp effectors and elicitors (HEE) region, the Hrp-associated enzymes (HAE) region and the island transfer (IT) region ((Oh and Beer, 2005). The *hrp*/*hrc* region contains 25 genes, including four genes (*hrpL*, *hrpS*, and *hrpXY*) encoding regulators of T3SS gene expression and nine *hrc* genes encoding the T3SS machinery (Bogdanove et al., 1996; Oh et al., 2005). The HEE region contains seven genes, including two harpin genes (*hrpN* and *hrpW*) and two *dsp* genes (*dspA*/*E* and *dspB*/*F*) (Oh et al., 2005). Since the *hrp*/*hrc* region and the HEE region include most *hrp* and *dsp* genes, these two regions are called the *hrp*/*dsp* gene cluster.

The *hrp* and *hrc* genes of Hrp1 T3SS carry a consensus sequence (GGAACC-N_{16}-CCACNNA), called *hrp* box or *hrp* promoter, at the -35 and -10 upstream regions, which is transcriptionally activated by the exocytoplasmic function (ECF) sigma factor, HrpL (Wei and Beer, 1995; Xiao and Hutcheson, 1994). To date, 30 putative *hrp* promoters including all T3SS genes have been identified in *E. amylovora* (McNally et al., 2012). In general, the activity of ECF sigma factors is restricted by tightly bound anti-sigma factors and released through either conformational change or proteolysis in response to a specific stimulus (Mascher, 2013). However, no apparent anti-sigma factors for HrpL have been identified. Instead, HrpL activity is

transcriptionally regulated by RpoN (σ^{54}) and its three associated transcription regulators, including HrpS/HrpR, IHF, and YhbH (Wei et al., 2000; Hendrickson et al., 2000; Hutcheson et al., 2001; Jovanovic et al., 2011; Ancona et al., 2014; Lee and Zhao, 2015). An alternative sigma factor, RpoN, directs RNA polymerase (RNAP) to consensus -24 (GG) and -12 (TGC) regions of the promoter. Unlike other σ^{70} family members, the RpoN-RNAP holoenzymes form an energetically stable closed complex that rarely isomerizes into the open complex. For the transcription initiation, the closed complex must be remodeled by interacting with bacterial enhancer binding proteins (bEBPs) that couple chemical energy derived from ATP hydrolysis to a mechanical action using the AAA^+ (ATPase associated with various cellular activities) (Bush and Dixon, 2012). Homohexameric HrpS and heterohexameric HrpS/HrpR acts as a bEBP of the RpoN-dependent *hrpL* transcription in *Erwinia* spp. and *P. syringae*, respectively (Wei et al., 2000; Hutcheson et al., 2001). Since the binding site of oligomeric HrpS and HrpR proteins is located at about 150 bp upstream of the transcription start site, IHF, a nucleoid associated protein (NAP), is required to ensure interaction between RpoN and bEBPs through DNA bending (Jovanovic et al., 2011; Lee and Zhao, 2015). Additionally, YhbH is annotated as a σ^{54} modulation protein, but its exact role in *hrpL* transcription is still unclear (Smits et al., 2010a; Ancona et al., 2014).

In *E. amylovora*, the HrpS binding site (TGCAA-N_4-TTGCA) is observed only in the upstream region of *hrpL* gene among 38 genes containing a potential RpoN binding site, suggesting that HrpS might only serves as an activator of T3SS, and the activation of HrpS might be a critical step for T3SS activation (Lee et al., 2016). The activity of bEBPs is generally modulated by signal transduction intermediates, including the phosphoryl group, ligands, and

anti-activator proteins, that target the N-terminal regulatory domain of bEBPs (Bush and Dixon, 2012). However, HrpS and HrpR lack the N-terminal domain and have unique regulatory mechanisms. In *Erwinia* spp., the HrpX/HrpY two-component system regulates the HrpS activity at the transcription level (Wei et al., 2000; Merighi et al., 2003). The response regulator HrpY is activated by the sensor kinase HrpX and binds to direct repeats (AAATCCTTAC-N_{11}-AATTCCTTAC) on the *hrpS* upstream sequence to activate the transcription (Merighi et al., 2006). Genetic analyses of *E. stewartii* (*Pantoea stewartii* subsp. *stewartii*), *Dickeya dadantii* (*E. chrysanthemi*) and *E. herbicola* pv. *gypsophilae* (Pantoea agglomerans) showed that HrpY is essential for virulence and can retain some activity without HrpX, presumably due to cross talk from other sensor kinases or acetyl phosphates (Nizan-Koren et al., 2002; Yap et al., 2005; Merighi et al., 2006). However, mutations in *hrpX* and *hrpY* genes in *E. amylovora* failed to abolish the ability of causing HR on tobacco leaves and pathogenicity on immature pear fruits, suggesting the presence of an alternative pathway of *hrpS* gene expression in HrpY-independent manner (Zhao et al., 2009b). The HrpS/HrpR activity in *P. syringae* has evolved to be mainly regulated through protein-protein interactions. In non-inducing conditions, formation of HrpS/HrpR oligomers is inhibited by Lon-dependent HrpR degradation and interaction of HrpS with HrpV (Preston et al., 1998; Bretz et al., 2002; Wei et al., 2005). In inducing conditions, up-regulated gene expression of *hrpRS* allows HrpR accumulation, and a chaperone-like protein HrpG disrupts the negative regulation of HrpV on HrpS by binding to HrpV (Wei et al., 2005; Ortiz-Martín et al., 2010b; Jovanovic et al., 2011). In *P. syringae* pv. *averrhoi*, HrpF binds to either HrpG or HrpA, and these direct interactions are proposed to contribute to the regulation of free HrpS level from HrpV (Huang et al., 2015). *E. amylovora* also contains HrpV and HrpG that

interact with each other, but their roles in the regulation of HrpS activity and T3SS gene expression remain unknown (Gazi et al., 2015).

The optimal conditions that induce the expression of Hrp1-T3SS genes have been reported to mimic the environment in the apoplast, including low temperature, low pH, low salt concentration and the presence of certain carbon sources (Huynh et al., 1989; Wei et al., 1992b). Direct contact with the plant cells and the water-soluble plant compounds also maximizes the induction of T3SS (Haapalainen et al., 2009). However, how pathogens sense and respond to these environmental stimuli is not fully understood. In addition to HrpX/HrpY, one of the widely studied two-component system involved in T3SS regulation is GacS/GacA system. Its homologue BarA/UvrY in *E. coli* responds to carboxylate compounds, including acetate and formate (Chavez et al., 2010). Many γ-proteobacteria, including *Erwinia* spp. and *P. syringae*, carry GacS/GacA, which is predominantly associated with the regulation of RsmA/CsrA RNA binding protein activity (Lapouge et al., 2008). The response regulator GacA indirectly up-regulates the expression of *hrpRS* genes, and thus is required for full T3SS expression and virulence in various *P. syringae* pathovars (Chatterjee et al., 2003; Ortiz-Martín et al., 2010a). GacA of *E. carotovora* subsp. *carotovora* and *D. dadantii* also acts as a positive regulator of T3SS (Cui et al., 2001; Yang et al., 2007). On the other hand, GacS/GacA negatively regulates T3SS expression in *E. amylovora* (Li et al., 2013). In both cases, direct GacA or RsmA/CsrA targets responsible for the altered phenotypes have not been identified yet. The response regulator OmpR in EnvZ/OmpR two-component system functions as a negative regulator of T3SS in *E. amylovora* and *P. syringae*, but its exact targets also remain unknown (Xiao et al., 2007; Li et al. 2013).

Bacteria utilize nucleotide-based secondary messengers to regulate T3SS expression upon sensing environmental signals. The linear nucleotide guanosine tetraphosphate (ppGpp) and guanosine pentaphosphate (pppGpp), collectively known as ppGpp, act as the bacterial alarmone and are synthesized from ATP and either GTP or GDP by RelA-SpoT homologues. Under nutrient starvation, the intracellular concentration of ppGpp is increased, leading to the stringent response (Hauryliuk et al., 2015). Diverse physiological changes associated with the increased ppGpp concentration are partially achieved by promoting an alternative sigma factor-mediated transcription in synergy with the transcription factor DskA (Dalebroux and Swanson, 2012). Given that T3SS is highly induced in the limited nutrient conditions, ppGpp and DksA are identified as key factors for T3SS expression and pathogenesis in *E. amylovora* and *P. syringae*, possibly through activating an alternative sigma factor cascade from RpoN to HrpL (Ancona et al., 2014; Chatnaparat et al., 2015a; Chatnaparat et al., 2015b). The cyclic diguanylate (c-di-GMP) is also a second messenger involved in T3SS expression. Biosynthesis and degradation of c-di-GMP is regulated by diguanylate cyclase containing GGDEF domains and phosphodiesterase containing EAL or HD-GYP domains, respectively. c-di-GMP binds to a wide range of RNA or protein effector components and modulates their activities (Hengge, 2009). In *E. amylovora* and *D. dadantii*, c-di-GMP negatively regulates T3SS expression and may play an important role in the transition between different infection stages (Yi et al., 2010; Edmunds et al., 2013). Our current model of T3SS activation mechanism in *E. amylovora* is shown in figure 1.3.

1.3 Alternative sigma factor transcription

Control of transcription initiation is a primary regulatory step of gene expression in all domains of life. It determines which and how much mRNA will be produced under given

conditions, allowing substantial changes in cell physiology. Transcription starts with binding of RNAP and its associated transcription factors on the promoter and upstream regulatory elements of the gene. Core RNAP in bacteria is composed of five subunits (α2ββ'ω) whose sequence, structure, and functions are evolutionarily well conserved (Murakami and Darst, 2003). Unlike other organisms, bacterial RNAP requires a sixth dissociable subunit, called sigma factor, for promoter recognition and transcription initiation. Therefore, two forms of RNAP exist in bacteria, holoenzyme (α2ββ'ωσ) for initiation, and core RNAP (α2ββ'ω) for elongation (Feklístov et al., 2014).

Bacteria genomes encode multiple sigma factors. The number of sigma factors in the genome range from 1 in *Mycoplasma genitalium* to 63 in *Streptomyces coelicolor* (Fraser et al., 1995; Bentley et al., 2002). Comparison of the sigma factors in different species suggested that bacteria having complex life cycles tend to contain more sigma factors (Mittenhuber, 2002). Since each sigma factor directs the holoenzyme to specific promoters with conserved sequences, transcription regulation of individual genes and operons can be effectively achieved by different holoenzyme species (Haugen et al., 2008). The most abundant and primary sigma factor in many bacterial species, including *E. coli* and *E. amylovora*, is σ^{70} (σ^{D} and RpoD). The σ^{70}-RNAP holoenzyme is responsible for transcription of housekeeping genes and other majority of genes during exponential growth (Paget and Helmann, 2003). However, if bacteria need to express genes involved in the stringent response and survival, the σ^{70} should be replaced by other alternative sigma factors, such as σ^{S} (σ^{38} and RpoS) and σ^{54} (σ^{N} and RpoN). In this process, the intracellular signaling nucleotides, ppGpp, modulates the availability of RNAP to alternative

sigma factors (Dalebroux and Swanson, 2012). By altering the level of ppGpp, bacteria can switch the global gene expression pattern in response to external stimuli.

Sigma factors are grouped into two families: the σ^{70} family and the σ^{54} family. The majority of sigma factors, including σ^{70}, σ^{S} and ECF sigma factors, belong to the σ^{70} family, while only a single member, σ^{54}, comprises the σ^{54} family. Due to their differences in domain structure, two families exhibit different transcription initiation mechanism. The σ^{70} family-RNAP holoenzyme binds to the consensus -35 and -10 sequences and simultaneously promotes the formation of an open complex for transcription initiation (Guo et al., 2000). On the other hand, the σ^{54}-RNAP holoenzyme binds to the consensus -24 and -12 sequences and forms an energetically stable closed complex that is incompetent for transcription initiation (Guo et al., 2000). To mediate transition into an open complex, the σ^{54}-dependent transcription requires bEBPs that couples ATP hydrolysis to remodeling of the closed complex (Bush and Dixon, 2012). Since the binding site of bEBPs is generally located 80 to 150 bp upstream of the transcription start site, IHF-dependent DNA bending is often required to allow interaction between bEBP and the σ^{54}-RNAP holoenzyme.

1.3.1 RpoS

RpoS is an alternative sigma factor induced during stationary phase and various stress conditions. The RpoS-mediated stress response is found in the β- and γ-proteobacteria that have a broad host range, including animal, insect and plants (Dong et al., 2008). The contribution of RpoS to cell survival is variable in different species. RpoS in *Yersinia enterocolitica* is important for survival against oxidative, osmotic, acid and heat stress, while RpoS in *Ralstonia*

solanacearum, a soil-borne plant pathogen, is not required for survival against oxidative, heat and osmotic stress (Badger et al., 1995; Flavler et al., 1998). In *E. amylovora*, *rpoS* mutant exhibited viable but non-culturable (VBNC) response after starvation in natural water and became more sensitive to oxidative, osmotic, acid and heat stresses (Santander et al., 2014). Nevertheless, RpoS is still believed to serve as a central response regulator for adaptation to hostile environments. The transcriptome analysis of *E. coli* revealed that expression of about 10% of the genome, including genes for not only starvation/stress response but also metabolism, transport and membrane proteins, is directly or indirectly dependent on RpoS under unfavorable conditions for growth (Pattern et al., 2004; Lacour and Landini, 2004; Weber et al., 2005).

The RpoS activity is tightly restricted during exponential growth by low transcription level and rapid degradation by ClpXP immediately after its production (Schweder et al., 1996). Although most genes containing RpoS-dependent promoter can be co-transcribed by RpoD, the nucleoid-associated protein, H-NS, selectively blocks the transcription initiation by RpoD and represses the basal expression of these genes (Shin et al., 2005; Grainger et al., 2008). As ppGpp levels increase in response to stress, a combined effect of small molecules, small RNAs, and various global regulators up-regulates RpoS levels (Battesti et al., 2011). Among multiple layers of RpoS regulatory mechanism, reduced degradation rate largely accounts for accumulation of RpoS. The rate-limiting factor for RpoS degradation is an adaptor protein RssB (Becker et al., 1999; Pruteanu and Hengge-Aronis, 2002). RssB mediates RpoS recognition of ClpXP and facilitates its degradation (Muffler et al., 1996; Zhou et al., 2001). Three inhibitors of RssB, including IraP, IraM, and IraD, have been identified under phosphate starvation, magnesium starvation and DNA damage, respectively (Bougdour et al., 2006; Bougdour et al., 2008;

Merrikh et al., 2009). They are induced in response to specific stress stimuli, bind directly to RssB and block RpoS degradation. In carbon starvation condition, instead of the Ira proteins, low ATP levels in cells increase RpoS stability by slowing ClpXP proteolysis (Peterson et al., 2012).

RpoS is also involved in virulence regulation of many bacterial species. In *Salmonella*, RpoS is critical for virulence by positive regulation of SpvR and SpvABCD, required for intracellular growth and systemic infection, and YedI, required for persistence (Fang et al., 1992; Kowarz et al., 1994; Erickson and Detweiler, 2006). RpoS of *Legionella pneumophila*, the pneumonia pathogen, positively regulates Mip isomerase and hydrolytic enzymes, required for invasion and multiplication (Bachman and Swanson, 2004; Broich et al., 2006). The role of RpoS in virulence regulation has been also reported in plant pathogens. Mutation in *rpoS* in the rice seedling blight pathogen, *Burkholderia plantarii*, delayed disease development, indicating that RpoS is required for full virulence (Solis et al., 2006). RpoS of the soft rot pathogen *D. dadantii* is involved in negative regulation of T3SS and virulence (Li et al., 2010). On the other hand, RpoS in *E. amylovora* is likely to have a minor effect on virulence regulation. Although mutation in *rpoS* affected the regulation of EPS production and motility, disease severity and progress of the mutant was not significantly different from WT in pear plantlets (Santander et al., 2014). Whether *E. amylovora* RpoS participates in the regulation of other virulence factors, such as T3SS, still needs to be determined.

1.4 Rsm/Csr system

Small RNAs (sRNAs) are functional non-coding RNA transcripts with a major role in transcriptional or post-transcriptional regulation of gene expression in both prokaryotes and

eukaryotes. Divergent regulatory outcomes from sRNAs have been observed in a wide range of biological processes. Despite bacterial sRNA and eukaryotic sRNA share certain similarities in the regulation of target gene expression, their structural and functional details are fundamentally different. In general, bacterial sRNAs are about 50 to 300 nucleotides in length and are synthesized with relatively short processing steps (Storz et al., 2011). Long bacterial sRNAs are often folded into secondary structures, such as stem-loop, to stabilize the molecule and also to be recognized by regulatory proteins (Gottesman, 2005). Depending on the mode of action, bacterial sRNAs work in conjugation with different regulatory proteins, most of which lead to regulation of target gene expression at post-transcriptional level. Unlike eukaryotic sRNAs, bacterial sRNAs can be involved in not only translation repression but also mRNA stabilization and translation activation (Gottesman, 2005).

One of the unique features of bacterial sRNAs is its capacity to modulate protein function. The most well characterized protein-binding sRNAs in bacteria is RsmB (or its homolog CsrB/CsrC and RsmX/RsmY/RsmZ) that antagonize the activity of RsmA (or its homolog CsrA and RsmE). RsmA/CsrA, an RNA binding protein, acts as a homodimer and binds to target transcripts for the post-transcriptional regulation. Structural analyses of RsmA/CsrA proteins revealed that each monomer is composed of five tandem β-sheets and a short α-helix, and a homodimer is formed by interwoven anti-parallel β-sheets (Gutierrez et al., 2005; Heeb et al., 2006). Alanine-scanning mutagenesis of *E. coli* CsrA revealed that two distinct subdomains, β_1 residue 2-7 and β_5 residue 40-47, are critical for RNA binding and regulatory effect (Mercante et al., 2006). CsrA binds preferentially to RNA that contains GGA motif within the loop of hairpin structure (Dubey et al., 2005). Approaches combining *in vivo* UV crosslinking with RNA

deep sequencing (CLIP-seq) of CsrA protein in *Salmonella* found that 467 transcripts are potential targets of direct CsrA binding (Holmqvist et al., 2016). Numerous global regulators were listed, indicating that CsrA/RsmA is directly or indirectly associated with diverse cellular processes as a major post-transcriptional regulator. The expression of *csrA* gene in *E. coli* is subject to complex regulatory networks, including transcription by five different promoters and a negative feedback loop regulation (Yakhnin et al., 2011). However, the CsrA/RsmA activity is rapidly adjusted by Csr/Rsm sRNAs in response to environmental stimuli (Vakulskas et al., 2015). Since the Rsm/Csr sRNAs contain many GGA motifs in their multiple stem-loops, they can effectively compete with mRNAs for RsmA/CsrA binding and determine the concentration of free RsmA/CsrA (Romeo et al., 2013).

In γ-proteobacteria, GacS/GacA system (or its homolog BarA/UvrY, VarS/VarA, ExpS/ExpA and LetS/LetA) is a key activator for the expression of Rsm/Csr sRNAs (Brencic et al., 2009; Waters and Storz, 2009; Ancona and Zhao, 2013; Martinez et al., 2014). Transcriptome analysis in *P. aeruginosa* showed that the sets of genes differentially expressed in *rsmY*/*rsmZ* mutant and *gacA* mutant compared to WT were nearly identical (Brencic et al., 2009). A comprehensive genomic DNA-protein interaction assay of *E. coli* and *Salmonella* using ChIP-exo also showed that *csrB/csrC* genes were the strongest targets of crosslinking in both species (Zere et al., 2015). These results suggest that the GacS/GacA system responds to external stimuli mostly through the regulation of RsmA/CsrA-inhibitory sRNAs expression. Several other global regulators that sense growth and external stimuli also control the level of RsmA/CsrA-inhibitory sRNAs. The consensus IHF-binding site is identified in the promoter region of *csrB* in several species, including *E. coli*, *Salmonella* and *E. amylovora*, and IHF-binding is critical for its

transcription (Martinez et al., 2014; Lee and Zhao, 2015; Zere et al., 2015). The consensus RcsAB-binding site (reviewed in 1.5.3) is also identified in the promoter region of *rsmB* in *Pectobacterium* spp., but its effect on the transcription is unknown (Andresen et al., 2010). In *E. coli*, DeaD, the DEAD-box RNA helicase that alters RNA structure and stability, facilitates *uvrY* translation by remodeling the leader sequence, leading to the activation of *csrB*/*csrC* transcription (Vakulskas et al., 2014). Other DEAD-box RNA helicase SrmB also activates *csrB*/*csrC* transcription by an unknown mechanism (Vakulskas et al., 2014). The bacterial alarmone ppGpp and its partner transcription factor DksA are required for full activation of *csrB*/*csrC* transcription (Edwards et al., 2011). CsrA also indirectly activates *csrB*/*csrC* transcription through up-regulating transcription and translation of *uvrY* and promoting BarA kinase activity (Camacho et al., 2015).

E. coli and some other bacteria, including *E. amylovora*, also contain CsrD that controls the stability of the Rsm/Csr sRNAs by mediating RNase E or PNPase-dependent degradation (Suzuki et al., 2006). CsrD is a membrane protein, and its cytoplasmic region contains putative GGDEF and EAL domains originally involved in biosynthesis and degradation of the second messenger c-di-GMP. However, the CsrB/CsrC degradation activity of CsrD is not dependent on c-di-GMP, and the two domains also exhibit no ci-di-GMP synthetic/hydrolytic activity (Suzuki et al., 2006). There are several evidences that the putative GGDEF and EAL domains of CsrD have evolved to respond to the availability of a preferred carbon source. In *E. coli* and *Vibrio cholerae*, $EIIA^{Glc}$, a glucose-specific enzyme II A, is found to interact with the cytoplasmic region of CsrD and its homologue MshH, respectively (Pickering et al., 2012). As a part of phosphoenolpyruvate carbohydrate phosphotrasnferase system (PTS) that regulates glucose

uptake, $EIIA^{Glc}$ plays a central role in carbon metabolism. The unphosphorylated form of $EIIA^{Glc}$ in glucose-rich conditions binds to and regulates several transporters or catabolic enzymes, while the phosphorylated form of $EIIA^{Glc}$ in glucose-limited conditions is incapable of interacting with the majority of its interaction partners (Deutscher et al., 2014). In *E. coli*, only the unphosphorylated $EIIA^{Glc}$ interacts with the EAL domain of CsrD and activates the CsrB/CsrC degradation activity (Leng et al., 2016). Although it is recently reported that CsrD-mediated RNase E cleavage targets unstructured segment of CsrB at 3' end, the exact molecular mechanism of CsrD-dependent sRNA decay is still unclear (Christopher et al., 2016). However, no CsrD homologues have been identified in *Pseudomonas* spp. (Vakulskas et al., 2015). In *P. fluorescens*, RsmE binding protects RsmZ from RNase E cleavage, suggesting that a sequential process of RsmE dissociation and RsmZ degradation may lead to a unidirectional release of RsmE (Duss et al., 2014).

Multiple mechanisms of gene regulation via RsmA/CsrA have been reported. RsmA/CsrA generally binds to the 5' UTR of target mRNA, and the conserved binding sequence (GGA motif) is similar to Shine-Dalgarno (SD) sequence. Therefore, its predominant effect is to regulate translation rate by modulating ribosome accessibility (Vakulskas et al., 2015). In *E. coli*, CsrA binds to the SD sequence of *glgCAP* transcripts and blocks ribosome binding (Backer et al., 2002). Since these genes are involved in glycogen biosynthesis, mutation in *csrA* results in glycogen accumulation due to up-regulated translation of *glgCAP* (Romeo et al., 1993). *P. aeuruginosa* RsmA also inhibits translation of *psl* operon, required for biofilm formation, by stabilizing a stem-loop structure that blocks ribosome binding (Irie et al., 2010). RsmA/CsrA also can activate translation. *P. aeruginosa* RsmA binding on the 5' UTR of phenazine biosynthesis

transcript *phz2* destabilizes the stem-loop structure in the SD sequence and enhances ribosome access (Ren et al., 2013). RsmA/CsrA binding sometimes increases translation rate by stabilizing the target mRNAs. In *E. coli*, CsrA activates the expression of *flhDC*, encoding the master regulator of flagellum biosynthesis, by protecting the transcripts from RNase E-mediated cleavage (Yakhnin et al., 2013). In addition to post-transcriptional regulation, RsmA/CsrA also mediates transcription termination by altering the transcript structure for Rho-dependent transcription. *E. coli* CsrA binding to the leader sequence of *pgaABCD*, involved in the biofilm formation, causes premature termination of transcription (Figueroa-Bossi et al., 2014).

.

The role of Rsm/Csr system in virulence regulation has been extensively studied in plant pathogens. The majority of research revealed that RsmA plays a central role in regulation of diverse virulence factors. In *Pectobacterium carotovorum* and *Pectobacterium wasabiae*, mutation in *rsmA* resulted in increased virulence on potato tuber by up-regulation of plant cell wall degrading enzymes (PCWDEs), type VI secretion systems, flagellar components, and butanediol fermentation components (Chatterjee et al., 1995; Koiv et al., 2013). Negative regulation of virulence and host colonization via RsmA is also observed in *P. syringae* pv. tabaci BR2R, *P. syringae* pv. *syringae* B728a, and *P. syringae* pv. *phaseolicola* NPS3121 (Kong et al., 2012). RsmA also acts as a positive regulator of virulence. RsmA is essential for virulence of *Xanthomonas. campestris* pv. *campestris* and *X. oryzae* pv. *oryzae* by activating PCWDEs, EPS production, and T3SS (Chao et al., 2008; Zhu et al., 2011). *X. citri* subsp. citri (XCC) utilizes RsmA to activate T3SS gene expression by protecting *hrpG* mRNA (encoding the master regulator of T3SS in XCC) from RNase E cleavage (Andrade et al., 2014). In this case, RsmA binding on the 5’ UTR stabilizes the *hrpG* mRNA, thereby enhancing the HrpG translation and

its downstream T3SS gene expression. RsmA is also critical for virulence of *E. amylovora*. Mutation in *rsmA* caused significantly reduced T3SS, motility, and amylovoran production (Ancona and Zhao, 2014). However, the direct RsmA targets responsible for these phenotypes have not been identified yet.

1.5 Bacterial proteases

The abundance and quality of more than 4000 proteins in bacteria are constantly controlled to adjust their fitness in a wide variety of environments. The physiological needs of the cell are efficiently met by degradation and modification of functional proteins. Damaged or misfolded proteins are also removed to prevent a formation of toxic aggregates and to recycle amino acids (Sauer and Baker, 2011). In the cell, most of these post-translational regulation processes are mediated by proteases. Bacteria utilize two major intracellular proteases, ClpXP and Lon, which are members of the AAA^+ (ATPases associated with diverse cellular activities) family protein. In *E. coli*, more than 50 proteins, including metabolic enzymes and transcription factors, are targeted by ClpXP, and about half of the misfolded protein degradation is carried out by Lon (Chung and Goldberg, 1981; Flynn et al., 2003). Since protein degradation is irreversible process, proteolytic activity is required to be highly specific, especially for the regulatory function. The AAA^+ proteases consist of several structurally and functionally distinct components that enable the regulation of dynamic proteome changes.

1.5.1 AAA^+ protease

Proteins carrying AAA^+ domain, which can convert chemical energy derived from ATP to mechanical energy, are present in all kingdoms of life and found in various processes in

bacteria, including protein degradation, the σ^{54}-dependent transcriptional activation, DNA repair and recombination (Tucker and Sallai, 2007). In general, AAA^+ family proteins exist as a ring-shaped hexamer (Sauer and Baker, 2011; Bush and Dixon, 2012; Costa et al., 2013). Each AAA^+ domain consists of two subdomains, an N-terminal α/β subdomain ($\alpha_5\beta_5$) and a C-terminal α subdomain (α_4), and contains several conserved motifs implicated in ATP hydrolysis and oligomerization (Neuwald et al., 1999). The Walker A and Walker B motifs are responsible for nucleotide binding and hydrolysis, respectively, and the sensor 1 and 2 regions also further contribute to these processes (Hanson and Whiteheart, 2005). Arginine residues, called R fingers, on the interface of subunits are also required for nucleotide sensing and interaction between subunits (Ogura et al., 2004). The resulting energy release from ATP hydrolysis induces an allosteric conformational change that generates mechanical motion within the hexamer (Tucker and Sallai, 2007)

Functional diversity of AAA^+ protease is conferred by additional domains necessary for three major steps of proteolytic activity, recognition, unfolding and degradation. Hexameric AAA^+ ring is involved in ATPase and unfoldase, while compartmental protease acts as a degradation chamber (Erzberger and Berger, 2006). Coordination of each step has evolved to ensure the substrate specificity of AAA^+ protease. Upon ATP binding, AAA^+ proteases recognize substrate by targeting specific degradation recognition motifs called degrons. They can be directly recognized by AAA^+ protease at the place where unfolding occurs, such as the pore of hexameric ring, or associated with the adaptors that mediate binding to AAA^+ protease (Gur et al., 2013). In the later case, competition between adaptors and anti-adaptors can control the rate of substrate delivery to AAA^+ protease (Turgay et al., 1998; Neher et al., 2003). If the

recognition motifs are not exposed to the exterior, post-translational modifications or specific cellular conditions that alter the tertiary structure of substrate could also be a determinant for substrate recognition (Sauer and Baker, 2011).

Following recognition, substrates are unfolded to be translocated into the degradation chamber. Several motifs and loops lining the axial pore of AAA^+ ring generates pulling force from ATP hydrolysis and induces unfolding of substrates through the narrow channel (Hinnerwisch et al., 2005). Coupling of ATP hydrolysis to unfolding/translocation is rate-limiting for the proteolytic activity, and thus degradation efficiency of the proteases is determined by AAA^+ ATPase domain (Martin et al., 2008). Since substrates are sequentially unfolded from the attachment point, the structure and stability adjacent to the recognition motifs also can control their susceptibility to AAA^+ protease (Lee et al., 2001). However, the specific motifs gripped by the pore loops during translocation have not yet been clarified. It has been proposed that the pore loop may use non-covalent, long-ranged interactions, such as van der Waals force, to contact unfolded polypeptides of variable composition (Barkow et al., 2009).

The protease domain forms a barrel-shaped chamber, composed of six or seven subunits, and sequesters their active site away from the cytosol. To avoid aberrant degradation and permit only unfolded proteins that are specifically recognized, entry portal of the degradation chamber is narrow (~10 Å) and gated by the AAA^+ domain (Gur et al., 2013). Degradation of small peptides or unfolded proteins in the absence of the AAA^+ ATPase domain has been observed, but at greatly reduced rate (Jennings et al., 2008). Once the substrates reach the chamber, they are completely degraded into small peptides, ranging in size from 3 to 30 residues, without the

release of large intermediates (Nishii and Takahashi, 2003; Choi and Licht, 2005; Nishii et al., 2005).

1.5.2 ClpXP protease

Clp protease is an ATP-dependent cytosolic protease composed of AAA^+ ATPase and protease that are present on separate subunits. Five different ATPase components (ClpA, ClpC, ClpE, ClpX and ClpY) and two different protease components (ClpP and ClpQ) can form several possible Clp protease complexes, and five active Clp protease complexes (ClpAP, ClpCP, ClpEP, ClpXP and ClpYQ) have been observed in bacteria. Although each Clp protease has a distinct role in selective degradation of cellular proteins, Proteobacteria, including *E. coli* and *E. amylovora*, contain three active Clp proteases, ClpAP, ClpXP and ClpYQ (Kress et al., 2009). ClpXP is the most widely distributed and highly conserved in various bacteria species, and its functional roles are also relatively well characterized. Protease subunits of ClpXP form a barrel-like structure stacked by two ring-shaped ClpP heptamers carrying 14 proteolytic active sites (His-Asp-Ser catalytic triad) inside the chamber (Wang et al., 1997). Since the pore entrance of ClpP is too narrow, both sides of the subunit associates with a hexameric ring of ClpX to mediate substrate recognition, unfolding and translocation (Grimaud et al., 1998). Although ClpP alone still can degrade damaged or misfolded peptides, its proteolytic activity becomes selective and tightly controlled only after binding to ClpX (Frees et al., 2013).

Like other AAA+ proteases, substrate recognition by ClpXP largely depends on either the N- or C-terminal ends of target proteins. Approximately 50 putative substrates for ClpXP degradation have been identified in *E. coli* using inactive variant of ClpXP ($ClpXP^{trap}$) that can

capture substrates without degradation. Analysis of the amino acid sequences from these proteins revealed three N-terminal and two C-terminal ClpX-recognition motifs (Flynn et al., 2003). In addition to intrinsic recognition motifs, ClpXP also can recognize proteins tagged with SsrA, which consists of 11 amino acids (AANDENYALAA) (Gottesman et al., 1998). The SsrA-tagging occurs co-translationally on C-terminal end of incomplete proteins stalled on ribosome to prevent their subsequent misfolding and aggregation (Moore and Sauer, 2007). In this process, SspB adaptor protein binds to SsrA tag and increase substrate affinity for ClpX, leading to rapid substrate delivery for degradation (Bolon et al., 2004). Similarly, two more adaptor protein-assisted substrate recognition in ClpXP have been identified: RssB for RpoS (σ^S) and UmuD for UmuD' (component of DNA polymerase V) (Zhou et al., 2001; Neher et al., 2003).

The functional significance of ClpXP in stress responses has been apparent from altered stress sensitivity of *clpXP* mutant in a number of bacterial species (Damerau et al., 1993; Thomsen et al., 2002; Frees et al., 2007). The ClpXP-mediated proteome changes against environmental stimuli are largely achieved by regulating sigma factor activity. The stationary phase sigma factor, RpoS, is one of the major substrates for ClpXP, and mutations in *clpXP* caused RpoS accumulation in early growth phase (Schweder et al., 1996). Although RpoS has an N-terminal ClpX-recognition motif, the rate of degradation is enhanced with the aid of RssB adaptor protein (Muffler et al., 1996; Zhou et al., 2001). RssB acts as a limiting factor for degradation of RpoS, and its activity is modulated via phosphorylation and antiadaptors (Becker et al., 2000; Bougdour et al., 2006). Indeed, many $ClpXP^{trap}$-associated proteins and RpoS were coordinately regulated during stationary phase and stress conditions (Flynn et al., 2003). For example, Rsd, anti-RNA polymerase sigma 70, is transcriptionally activated by RpoS, and DksA

(RNA polymerase-binding transcription factor) is critical for inducing optimal concentration of RpoS under appropriate conditions (Jishage and Ishihama, 1998; Webb et al., 1999; Brown et al., 2002). ClpXP also regulates the activity of the heat shock sigma factor, RpoE, by degrading its anti-sigma factor, RseA (Ades et al., 1999; Flynn et al., 2004). RpoE plays a key role in maintaining cell envelope integrity by expressing genes associated with extracytoplasmic stress response (De Las Penas et al., 1997). RpoE activity is normally inhibited via its direct interaction with RseA. However, under stress conditions, SspB adaptor protein binds to RseA and facilitates delivery to ClpXP, leading to release of free RpoE (Flynn et al., 2004).

ClpXP is also important for the virulence regulation in many Gram-negative bacteria. In Enterohemorrhagic *E. coli* (EHEC), *clpXP* mutant showed significantly reduced expression of the locus of enterocyte effacement (LEE)-encoded T3SS largely due to accumulation of two ClpXP substrates, RpoS and GrlR (Iyoda and Watanabe, 2005). Mutations in *clpXP* of the soft rot plant pathogen, *D. dadantii*, caused RpoS accumulation, resulting in down-regulation of T3SS and virulence (Li et al., 2010). However, the downstream regulators of RpoS during T3SS activation are still unclear. Molecular mechanisms underlying ClpXP-mediated virulence regulation are better understood in *S. typhimurium*. *Salmonella* utilizes *Salmonella* pathogenicity island 1 (SPI-1)-encoded T3SS to manipulate host immunity and metabolism, including macrophage apoptosis (Brennan and Cookson, 2000). Since its survival and replication within the macrophage is critical for systemic infection, macrophage apoptosis by effectors of SPI-1 T3SS must be strictly regulated. The current model of the regulation of SPI-1 gene expression suggests that ClpXP negatively regulates SPI-1 T3SS by degrading $FlhD_4C_2$ that activates transcription of FliZ, the positive regulator of SPI-1 transcription factor (Kage et al., 2008).

Therefore, mutations in *clpXP* of *S. typhimurium* significantly increased the cellular levels of SPI-1 products, thereby precluding its ability to cause systemic disease in mice (Yamamoto et al., 2001; Kage et al., 2008).

1.5.3 Lon protease

Lon is a cytosolic protease belonging to the AAA^+ superfamily of ATPase and highly conserved in all kingdoms of life. Unlike ClpXP, Lon is a homohexamer containing AAA^+ ATPase and protease on the same subunit and utilizes Ser-Lys catalytic dyad in the active site instead of classical Ser-His-Asp triad (Amerik et al., 1990; Amerik et al., 1991). Two hexamers of Lon also can stack together to form dodecamers. This assembly, however, creates narrow entry sites only in ~45 Å, resulting in lower activity against large protein substrates (Vieux et al., 2013). Lon is divided into two subfamilies, LonA and LonB, based on the differences in sequence and domain organization. Over 80% of all known Lon proteases, including that of *E. coli* and *E. amylovora*, are a member of LonA subfamily and contain a family-specific N-terminal domain in addition to AAA^+ and proteolytic domains (Rotanova et al., 2004). The N-terminal domain is involved in hexamerization and substrate recognition (Ebel et al., 1999; Melnikov et al., 2008). Interaction between the N-terminal domain and substrates also can induce allosteric conformational changes that enhance proteolytic activity (Wohlever et al., 2013). On the other hand, LonB subfamily, found only in Archaea, lacks the N-terminal domain and contains transmembrane segment within the AAA^+ domain (Rotanova et al., 2004).

Lon, as a major player in protein quality control, prevents cytotoxicity induced by damaged or misfolded proteins using its proteolytic activity. Indeed, inhibition of AAA^+

proteases caused a 70% reduction in degradation of abnormal proteins, while *lon* mutation solely resulted in a 50% reduction (Chung and Goldberg, 1981). To recognize potentially deleterious proteins, Lon binds to a cluster of aromatic and non-polar residues, which is not exposed in most native proteins (Gur and Sauer, 2008). This Lon activity is associated with heat shock responses. Expression of *lon* is up-regulated under heat stress, and the *lon* mutant contained a larger amount of protein aggregates after heat stress compared to mutants lacking other AAA^+ proteases (Phillips et al., 1984; Rosen et al., 2002) Lon post-translationally regulates the level of IbpA and IbpB small heat-shock proteins that facilitate chaperone-mediated disaggregation and refolding (Ratajczak et al., 2008; Bissonnette et al., 2010). In some cases, Lon itself exhibits a chaperone activity in a proteolysis-independent manner and contributes to protection against proteotoxic stress by remodeling misfolded proteins (Lee et al., 2004; Coleman et al., 2009; Wohlever et al., 2014).

Lon also participates in various cellular processes by targeting other regulatory proteins. One of the well known Lon substrates is RcsA. Under normal conditions, RcsA is highly unstable, and the amount of RcsA is also found at very low levels in the cells mainly due to Lon (Torres-Cabassa and Gottesman, 1987). RcsA is an auxiliary protein of the RcsBCD two-component system that regulates a wide range of virulence-associated phenotypes, including EPS production, motility and biofilm formation (Ebel and Trempy, 1999; Ferrieres and Clarke, 2003; Francez-Charlot et al., 2003; Huang et al., 2006; Wang et al., 2009). It is uniquely composed of three core proteins, RcsB, RcsC and RcsD. Multiple steps of phosphorelay between histidine and aspartate residues occur in the core proteins to activate this system (Majdalani and Gottesman, 2006). Upon sensing environmental signals, RcsC is autophosphorylated at the conserved

histidine residue, and the phosphate is transferred to RcsB through the phosphotransfer protein RcsD (Takeda et al., 2001). The response regulator RcsB is a cytoplasmic protein that contains a DNA binding domain and binds to the promoter region of target gene in homodimeric form (Stout and Gottesman, 1990). RcsB also can form a heterodimer with RcsA and binds to a specific site termed the RcsAB box (Wehland et al., 1999). Therefore, mutation in *lon* causes RcsA accumulation, stimulating the high activity of RcsAB. Its binding at the RcsAB box can result in either positive or negative regulation of target gene expression. For example, in *E. coli*, RcsAB activates capsule biosynthesis gene (*cps*) expression but negatively regulates *flhD* expression (Torres-Cabassa and Gottesman, 1987; Francez-Charlot et al., 2003). In *E. amylovora*, the RcsAB box has been also identified in the promoter region of the *ams* operon and *flhD* (Wehland et al., 1999; Ancona et al., 2015a). However, there is no report yet on the characterization of Lon-RcsA regulatory pathway in *E. amylovora*.

The flagellar biosynthesis is further subject to Lon-dependent proteolysis following transcriptional regulation of *flhD* via RcsA. Two major transcription activators of flagellar gene expression, $FlhD_4C_2$ and FliA, are rapidly degraded by Lon (Claret and Hughes, 2000; Barembruch and Hengge, 2007). This indicates that complex transcriptional control of flagellar biosynthesis is partially accomplished by the proteolytic action of Lon at different levels. Lon has been also studied in T3SS regulation of several important Gram-negative bacteria (Bretz et al., 2002; Jackson et al., 2004; Takaya et al., 2005). In *P. syringae*, which shares similar pathways of T3SS regulation with *E. amylovora*, Lon appears to be involved as a negative regulator at two different stages of regulation. Under non-inductive condition for T3SS, the level of HrpR is maintained low by Lon degradation (Bretz et al., 2002). Once T3SS gene expression

is activated, Lon affects the stability of effector proteins, thereby modulating secretion (Losada and Hutcheson, 2005). Interestingly, Lon also participates in the Gac/Rsm signal transduction pathway by regulating GacA stability. In *P. protegens*, GacA is accumulated in *lon* mutant, resulting in up-regulation of *rsmY* and *rsmZ* sRNAs (Takeuchi et al., 2014). *E. amylovora* Lon is reported to be involved in UV tolerance and EPS regulation, but its contribution to virulence regulation has not been fully characterized (Eastgate et al., 1995).

1.6 Research objectives

Since T3SS plays a critical role in disease development and/or bacterium-host interaction in many pathogenic bacteria, diverse aspects of T3SS, including structure, gene regulation and effector function, have been extensively studied. One of the major projects that have been focused in Zhao lab over the last few years is to characterize the regulatory networks that activate T3SS in *E. amylovora*. We have determined the role of several transcription factors, including sigma factor, bacterial enhancer binding protein, nucleoid-associated protein and two-component systesm, in T3SS regulation. Based on this, we have also proposed the model of T3SS activation mechanism in *E. amylovora* (Fig. 1.3). Given that the ECF alternative sigma factor HrpL acts as the master regulator of T3SS, we have shown that RpoN, YhbH, HrpS and IHF are critical for the *hrpL* transcription in a ppGpp-dependent manner (Ancona et al., 2014; Ancona et al., 2015b; Lee and Zhao, 2015). We have also shown that GacS/GacA and EnvZ/OmpR two-component systems are indirectly involved in the negative regulation of *hrpL* transcription (Li et al., 2013). My dissertation research will focus on another layer of regulatory control over transcription. Molecular mechanisms underlying the regulation of T3SS through two major cytosolic proteases, Lon and ClpXP, and an RNA-binding protein, CsrA, will be examined.

Therefore, the objectives of this study are:

1) To examine the role of Lon protease in *E. amylovora* virulence (Chapter II);

2) To examine how ClpXP protease-dependent degradation of RpoS affects the regulation of T3SS (Chapter III);

3) To characterize the regulatory mechanism of *hrpS* expression through integration of multiple stimuli-sensing systems (Chapter IV);

4) To identify targets of CsrA and to examine CsrA-mediated post-transcriptional regulation during T3SS induction (Chapter V).

1.7 Figures

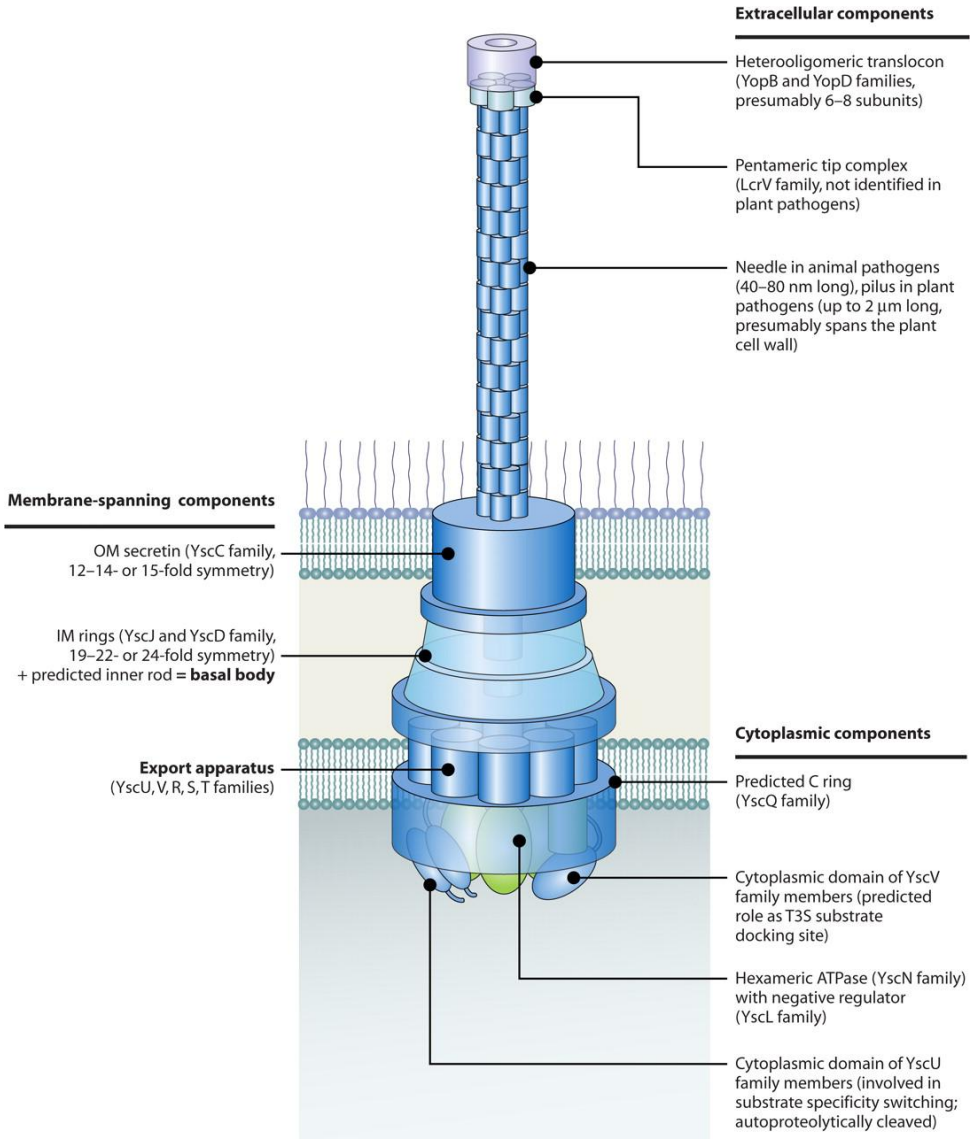

Figure 1.1 Schematic diagram of the non-flagellar type III secretion system from animal- and plant-pathogenic bacteria (from Büttner, 2012)

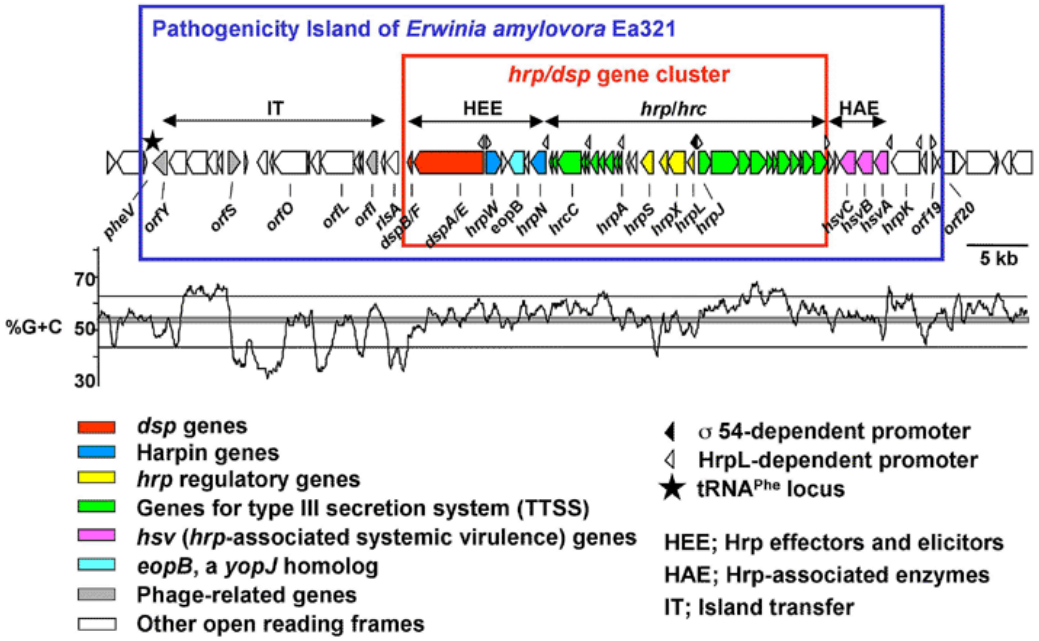

Figure 1.2 Schematic diagram of the *hrp*-pathogenicity island of *Erwinia amylovora* (from Oh and Beer, 2005)

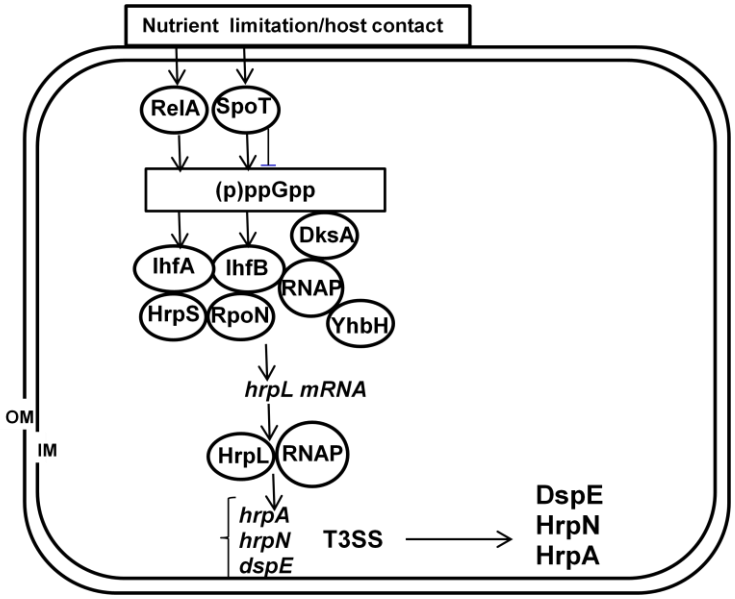

Figure 1.3 Current model of T3SS activation mechanism in *Erwinia amylovora* (From Ancona et al., 2015b)

CHAPTER 2

Lon protease modulates virulence traits in *Erwinia amylovora* by direct monitoring of major regulators and indirectly through the Rcs and Gac-Csr regulatory systems

2.1 Abstract

Lon, an ATP-dependent protease in bacteria, influences diverse cellular processes by degrading damaged, misfolded and short-lived regulatory proteins. In this study, we characterized the effects of *lon* mutation and determined the molecular mechanisms underlying Lon-mediated virulence regulation in *Erwinia amylovora*, an enterobacterial pathogen of apple. *E. amylovora* depends on the type III secretion system (T3SS) and the exopolysaccharide (EPS) amylovoran to cause disease. Our results showed that mutation of the *lon* gene led to overproduction of amylovoran, increased T3SS gene expression and non-motile phenotype. Western blot analyses showed that mutation in *lon* directly affected the accumulation and stability of HrpS/HrpA and RcsA. Mutation in *lon* also indirectly influenced the expression of *flhD*, *hrpS*, and *csrB* through accumulation of the RcsA/RcsB proteins, which bind to the promoter of these genes. In addition, *lon* expression is under the control of CsrA, possibly at both transcriptional and posttranscriptional levels. Although mutation in *csrA* abolished both T3SS and amylovoran production, deletion of the *lon* gene in the *csrA* mutant only rescued amylovoran production, but not T3SS. These results suggested that CsrA might positively control both T3SS and amylovoran production partially by suppressing Lon, whereas CsrA may also play a critical role in T3SS by affecting unknown targets.

2.2 Introduction

Erwinia amylovora, an enterobacterial plant pathogen, causes fire blight disease of apples and pears in more than 50 countries around the world. The type III secretion system (T3SS) and the exopolysaccharide (EPS) amylovoran are two major pathogenicity factors of the pathogen (Khan et al., 2012; Zhao, 2014). The T3SS in *E. amylovora* is encoded by the hypersensitive response and pathogenicity (*hrp*) island. It has been demonstrated that expression of the *hrp*-T3SS genes is activated by the master regulator HrpL, a member of the exocytoplasmic functions (ECF) subfamily of sigma factors (Wei and Beer, 1995, McNally et al., 2012). In turn, *hrpL* transcription is positively regulated by alternative sigma factor 54 (RpoN), its modulation protein YhbH, bacterial enhancer binding protein (bEBP) HrpS and integration host factor IHF (Ancona et al., 2014; Lee and Zhao, 2016). HrpS, a member of the NtrC family, activates RpoN-dependent transcription by mediating the isomerization of RpoN-RNA polymerase (RNAP) complex, whereas the nucleoid-associated protein IHF enables the interaction between HrpS and RpoN (Bush and Dixon, 2012; Lee and Zhao, 2016; Lee et al., 2016). Moreover, the RpoN-HrpL alternative sigma factor cascade is further activated by linear nucleotide second messengers (p)ppGpp, which are also essential for T3SS gene expression and virulence under nutrient stress conditions (Ancona et al., 2015b).

In addition, amylovoran plays an important role in virulence, biofilm formation, and survival of the bacterium (Sjulin and Beer, 1978; Koczan et al., 2009). Genome-wide screening of two-component systems (TCS) identified major regulators of amylovoran production in *E. amylovora* (Zhao et al., 2009b). Among them, the enterobacterial-specific Rcs phosphorelay system is essential for pathogenicity and amylovoran production (Ancona et al., 2015a; Bernhard

et al., 1990; Bereswill and Geider, 1997; Wang et al., 2009; Wang et al., 2012). The Rcs system is an unusual complex TCS, comprised of three core proteins RcsBCD and one auxiliary protein RcsA without the phosphorylation site (Bernhard et al., 1990; Gottesman et al., 1985; Majdalani and Gottesman, 2005; Wehland et al., 1999). RcsB homodimer or RcsA/RcsB heterodimer binds to conserved RcsAB box to regulate gene expression, including *amsG*, the first gene of amylovoran biosynthetic operon, and *flhD* in *E. amylovora* (Ancona et al., 2015a; Bernhard et al., 1993; Wehland et al., 1999). Furthermore, the GacS/GacA (GrrS/GrrA and BarA/UvrY) system, widely distributed TCS in gamma-Proteobacteria, negatively regulates amylovoran biosynthesis and T3SS in *E. amylovora* (Li et al., 2014). It was recently shown that negative regulation of virulence by GacS/GacA in *E. amylovora* acts through the non-coding small regulatory RNA (sRNA) *csrB*, which binds to and neutralizes the positive effect of the RNA-binding protein CsrA on T3SS gene expression and amylovoran production, indicating critical role of CsrA in *E. amylovora* virulence (Ancona et al., 2016). However, the targets of CsrA remain unknown in *E. amylovora*.

Lon is a highly conserved cytosolic protease belonging to the AAA^+ superfamily of ATPase, and acts as a major player in general protein quality control by degrading damaged or misfolded proteins (Chung and Goldberg, 1981). The proteolytic activity of Lon also contributes to the post-translational regulation of functional proteins. To recognize potentially deleterious proteins, Lon tends to bind a cluster of aromatic and non-polar residues, which are embedded in most native proteins (Gur and Sauer, 2008). As one well-characterized Lon substrate, RcsA protein level is generally maintained low by HN-S-mediated transcriptional repression and Lon-dependent degradation (Torres-Cabassa and Gottesman, 1987; Sledjeski and Gottesman, 1995).

Increased stability of RcsA and its associated overproduction of EPS in the *lon* mutant of some enterobacterial species lead to mucoid colonies (Gottesman et al., 1985; Lai et al., 2003). Lon also controls SulA protein level, which inhibits cell division as part of the SOS response under DNA damage-inducing conditions (Huisman and D'Ari, 1981). Failure to remove accumulated SulA in the *lon* mutant strain blocks cell division, leading to the irradiation sensitivity phenotype (Gottesman et al., 1981; Mizusawa and Gottesman, 1983).

Furthermore, Lon has been implicated in regulation of the T3SS in several important gram-negative bacteria (Bretz et al., 2002; Jackson et al., 2004; Takaya et al., 2005). In *Yersinia pestis*, Lon positively regulates the T3SS by degrading YmoA, a small histone-like protein that suppresses T3SS gene expression (Jackson et al., 2004). In *Pseudomonas syringae*, Lon acts as a negative regulator of the T3SS by degrading HrpR and effector proteins. HrpR, a homologue of HrpS, forms heterohexamer with HrpS and is maintained low by Lon under non-inductive conditions (Bretz et al., 2002). Once HrpL-dependent T3SS gene expression is activated, Lon affects the stability of effector proteins, thereby modulating secretion rate (Losada and Hutcheson, 2005). In *E. amylovora*, Lon is involved in EPS regulation and UV tolerance, but is not required for infection of apple seedlings (Eastgate et al., 1995). However, the effect of *lon* mutation on *E. amylovora* virulence and its underlying molecular mechanisms have not been fully characterized.

The purpose of this study is to characterize the effect of *lon* mutation in *E. amylovora*, to identify potential targets of Lon, and to determine the molecular mechanisms underlying Lon-mediated virulence regulation. Our results showed that mutation of the *lon* gene led to

amylovoran overproduction, increased T3SS gene expression and non-motile phenotype by directly targeting RcsA and HrpS/HrpA, and indirectly affecting the expression of the *flhD*, *hrpS,* and *csrB* sRNA genes through accumulation of the RcsA/RcsB proteins. Moreover, mutation of the *csrA* gene led to up-regulation of *lon* expression, suggesting that positive regulation of T3SS and amylovoran production by CsrA could be partially through suppression of *lon* expression.

2.3 Materials and methods

2.3.1 Bacterial strains and growth conditions

Bacterial strains and plasmids used in this study are listed in Table 2.1. *E. amylovora* and *E. coli* strains were routinely grown in LB broth. For T3SS gene expression, a *hrp*-inducing medium (HMM) (1g $(NH_4)_2SO_4$, 0.246 g $MgCl_2 \bullet 6H_2O$, 0.1 g NaCl, 8.708 g K_2HPO_4, 6.804 g KH_2PO_4) supplemented with 10 mM galactose as carbon source was used (Ancona et al., 2014). For amylovoran production, MBMA minimal medium (3 g KH_2PO_4, 7 g K_2HPO_4, 1g $(NH_4)_2SO_4$, 2 ml glycerol, 0.5 g citric acid, 0.03 g $MgSO_4$) supplemented with 1% sorbitol was used (Wang et al., 2009). Antibiotics were used at the following concentrations when appropriate: 100 μg ml^{-1} ampicillin (Ap), 50 μg ml^{-1} kanamaycin (Km), and 10 μg ml^{-1} chloramphenicol (Cm). Primer sequences used for mutant construction, mutant confirmation, qRT-PCR, inverse PCR, cloning and electrophoretic mobility shift assay (EMSA) in this study are listed in Table 2.2.

2.3.2 Mutant generation by λ-Red recombinase cloning

As described previously, *E. amylovora* Ea1189 mutant strains were generated using λ phage recombinase method (Zhao et al., 2009a). Briefly, competent cells were prepared from overnight cultures of *E. amylovora* strains carrying pKD46 which were subcultured to

exponential phase (OD_{600} = 0.8) in LB containing 0.1% arabinose. Recombination DNA fragments, which contain a Cm^R or Km^R gene with their own promoter flanked with a 50-nucleotide homology from the target genes, were generated by PCR using plasmids pDK32 or pKD13 as a template and transformed into competent cells by electroporation. The resulting mutants were selected on LB plates with appropriate antibiotics, and confirmed by PCR. In the corresponding mutant strains, the coding regions of the target genes were deleted, except for the first and last 50 nucleotides. Double mutant strains were generated using single mutants as a background strain as indicated.

2.3.3 Virulence, amylovoran production, and motility assays

Virulence assay on immature Bartlett pear fruits (*Pyrus communis* L. cv. Bartlett) was performed as described previously (Ancona et al., 2014, 2016; Wang et al., 2009). Briefly, bacterial inoculum was prepared from overnight cultures and was resuspended in PBS to OD_{600} = 0.1 and then diluted 100-times (approximately 10^6 CFU/ml). Surface-sterilized immature pears were air dried, pricked with a sterile needle, inoculated with 2 μl of cell suspensions, and incubated in a humidified chamber at 28 ℃. Symptoms were recorded at 4 and 8 days post-inoculation. Pears were assayed in triplicate for each strain, and the experiments were repeated three times.

Amylovoran production was determined using the cetylpyrimidinium chloride (CPC) method as described previously (Bellemann et al., 1994, Zhao et al. 2009b). Briefly, overnight-grown cultures were re-inoculated into 5 ml MBMA medium to OD_{600} = 0.2. After 24 h incubation at 28 ℃ with shaking, 1 ml of each culture was centrifuged at 4,500 g for 10 min, and

50 µl of 50 mg/ml CPC was added to the supernatant. After 10 min incubation at room temperature, amylovoran concentration was quantified by measuring OD_{600} turbidity and normalized for a cell density of 1.0. Each experiment was performed in triplicate and repeated three times.

Motility was performed on the motility agar plates (10 g tryptone, 5 g NaCl and 2.5 g agar per liter) as described previously (Zhao et al., 2009b). Diameters were measured at 24 and 48 h post-inoculation, and each experiment was performed in triplicate and repeated three times.

2.3.4 Quantitative real-time PCR (qRT-PCR)

For *in vitro* gene expression of T3SS and amylovoran production, RNA was isolated from cultures in HMM for 6 h at 18 ℃, and in MBMA medium for 18 h at 28 ℃, respectively (Wang et al., 2012, Ancona et al., 2016). To avoid RNA degradation, 4 ml of RNA protect reagent (Qiagen, Hilden, Germany) was added to 2 ml of bacterial cell cultures and then cells were harvested by centrifugation. RNA was extracted using RNeasy® mini kit (Qiagen) following the manufacturer's instructions and DNase I treatment was performed with TURBO DNA-free kit (Ambion, TX, USA). RNA was quantified using Nano-Drop ND100 spectrophotometer (Nano-Drop Technologies; Wilmington, DE, USA).

Reverse transcription was performed using Superscript III reverse transcriptase (Invitrogen, Carlsbad, CA) following the manufacturer's instructions. Power SYBR® Green PCR master mix (Applied Biosystems, CA, USA) with appropriate primers (Table 2.2) was mixed with cDNAs of selected genes, and qRT-PCR was performed using the StepOnePlus Real-Time

PCR system (Applied Biosystems) under the following conditions: 95 ℃ for 10 min, followed by 40 cycles of 95 ℃ for 15 s and 60 ℃ for 1 min. Dissociation curve was measured after the program was completed and relative gene expression was calculated with the relative quantification (ΔΔCt) method using the *rpoD* gene as an endogenous control. The experiment was repeated at least twice.

2.3.5 Western blot

Western blot was performed as described previously (Ancona *et. al.*, 2015, 2016). The genomic DNA regions containing the promoter and coding sequence of the *hrpS*, *hrpA*, *rcsA*, *rcsB*, and *lon* genes with six-His tag at the C-terminus were cloned into pWSK29. Genes were oriented opposite to vector promoters, and expression of genes was driven only by their native promoters. The resulting plasmids were sequenced at the University of Illinois at Urbana-Champaign core sequencing facility and transformed by electroporation into the WT and the mutants. For western blot, equal amount of *E. amylovora* cells grown in HMM at 18 ℃ for 6 h or MBMA at 28 ℃ for 24 h were collected. To test protein stability, tetracycline was added to cell cultures with the final concentration of 50μg/ml, and equal amount of cells were collected at different time points. Cell lysates were resolved by sodium dodecyl sulfate polyacrylamide gels and transferred to polyvinylidene fluoride membrane (Millipore, MA, USA). After blocking with 5% milk in PBS, membranes were probed with 1.0 μg/ml rabbit anti-His antibodies (GeneScript, NJ, USA) or rabbit anti-RNA polymerase beta (*E. coli* RpoB) antibodies (Abcam, MA, USA) diluted 1:2,000 and then horseradish peroxidase-linked anti-rabbit IgG antibodies (Amersham Bioscience, Uppsala, Sweden) diluted 1:10,000. Immunoblots were developed using enhanced

chemiluminescence reagents (Pierce, IL, USA) and visualized using ImageQuant LAS 4010 CCD camera (GE Healthcare, NJ, USA). The experiment was performed at least three times.

2.3.6 Transposon mutagenesis and screening for the motile mutants

The EZ::T5^{TM} <KAN-2> Tnp Transposome^{TM} kit (Epicentre, WI, USA) was used for the random mutagenesis following the manufacturer's instructions. Briefly, to prepare the competent cells, overnight culture of the *lon* mutant was subcultured to exponential phase (OD_{600} = 0.8) in LB. Cells were then harvested, washed with cold sterile water and transformed with 1 μl of the EZ-Tn5 <Kan> Tnp transposome by electroporation. After 3 h incubation at 28 ℃, transformants were plated on LB with Km. A total of 1045 colonies were picked and stored at -20 ℃. For screening, the wild-type (WT), *lon* mutant and Tn5 mutant strains were grown overnight in LB in 96-well microwell plates, and 2 μl of each culture were directly inoculated on the motility agar plate. After 24 and 48 h incubation at 28 ℃, the mutants with restored motility were then selected and the motility of the mutants were re-examined as described above.

Inverse PCR was performed to determine the transposon insertion site as described previously with a few modifications (Martin and Mohn, 1999). Genomic DNA of overnight cell cultures was isolated using MasterPure^{TM} complete DNA & RNA purification kit (Epicenter), digested with the restriction enzyme (PstI or PvuI) and re-ligated using T4 DNA ligase. For PCR reactions, DNA samples treated with PstI were amplified with a primer pair of KAN-2 FP-1/KAN-2 RP-1, while DNA samples treated with PvuI were amplified with a primer pairs of either KAN-2 FP1/PvuI-right or KAN-2 RP1/PvuI-left (Table 2.2). The PCR products were gel-purified and then sequenced at the UIUC core sequencing facility. The flanking sequences of

transposon insertion site were analyzed using BLAST search on the National Center for Biotechnology Information (NCBI).

2.3.7 Electrophoresis mobility shift assay (EMSA)

EMSA assays for RcsA/RcsB bindings to the upstream regions of the *rsmB* sRNA and the *hrpS* gene were performed as described previously (Ancona et al., 2015b, 2016; Lee and Zhao, 2016). Briefly, complementary oligonucleotides (Table 2.2) were 3' biotinylated using the biotin 3' end DNA labeling kit (Pierce) and annealed before use. Reaction volumes of 10 µl with 20 fmol of labeled oligonucleotides were incubated with 5 pmol either or both of RcsA/RcsB proteins in 1X binding buffer, 50 ng/µl Poly(dI·dC), 0.5 mM $MgCl_2$, 0.1% Nonidet P-40, 0.05 mg/ml bovine serum albumin, and 5% glycerol. Reactions were incubated for 20 min at room temperature, mixed with 2.5 µl of 5X loading buffer, and resolved into a 6% native polyacrylamide gel in 0.5X TBE buffer. The resolved reactions were transferred to a positively charged nylon membrane and UV cross-linked. The chemiluminescent signals were developed using the lightshift chemiluminescent EMSA kit (Pierce) and visualized using ImageQuant LAS 4010 CCD camera (GE Healthcare). The experiment was repeated at least twice.

2.4 Results

2.4.1 Characterization of the Ea1189 *lon* mutant in *Erwinia amylovora*

It was reported earlier that *E. amylovora* Lon is involved in EPS production, but is not required for infection of apple seedlings (Eastgate et al., 1995). In this study, we generated an insertional mutant strain defected in lon gene in the background of the wild-type strain Ea1189 (Table 2.1). Consistent with previous reports, the Ea1189 *lon* mutant exhibited mucoid colony on

growth media (Fig. 2.1A) and produced about 10 times more amylovoran than that of the wild type (WT) strain, which could be partially complemented (Fig. 2.2A). Transcript levels of *rcsA* (a rate-limiting regulatory gene) and *amsG* (the first gene in the *ams* operon for amylovoran biosynthesis) were about 5- and 40-fold higher in the *lon* mutant, respectively (Fig. 2.2B). The Ea1189 *lon* mutant induced typical HR lesion on tobacco (data not shown) and was as pathogenic as the WT on immature pears, though the disease progress was similarly or slightly faster in the mutant at 4 days post inoculation (Fig. 2.2C). We also found that expression of the T3SS regulatory (*hrpL*) and effector (*hrpA*) genes was about 6-fold higher in the *lon* mutant as compared to the WT (Fig. 2.2D). These results indicate that Lon suppresses expression of genes required for T3SS and amylovoran in *E. amylovora*, but is not indispensable for its virulence.

2.4.2 Lon negatively regulates the T3SS by targeting HrpS and HrpA

Previous studies in *P. syringae* showed that Lon negatively regulates the T3SS by targeting HrpR and effector proteins, but not HrpS (Bretz et al., 2002; Losada and Hutcheson, 2005). *E. amylovora* only contains HrpS, which shares about 40 to 44% amino acid identities with HrpR and HrpS of *P. syringae*, respectively. We examined the abundance and stability of HrpS and HrpA proteins in the WT and the *lon* mutant in a *hrp*-inducing medium (HMM) using Western blot. The *lon* mutant accumulated about 3-and 2-fold more HrpS and HrpA proteins than those in the WT, respectively (Fig. 2.3A, B). The half-life of HrpS *in vivo* was increased to more than 45 min in the *lon* mutant from less than 15 min in the WT (Fig. 2.3C); whereas the half-life of HrpA was also increased from about 15 min to more than 45 min in the absence of Lon (Fig. 2.3D). These results indicate that HrpS and HrpA are directly targeted by Lon-dependent degradation.

2.4.3 Lon negatively regulates amylovoran by targeting RcsA, but not RcsB

In enterobacteria, previous reports showed that Lon negatively regulates EPS biosynthesis by degrading RcsA, an auxiliary protein of the Rcs system (Gottesman et al., 1985; Torres-Cabassa and Gottesman, 1987). Therefore, we examined the abundance and stability of RcsA as well as RcsB in the WT and the *lon* mutant grown in MBMA media using Western blot. As expected, the RcsA protein was 2.4-fold more abundant and exhibited longer half-life (> 45 min) in the *lon* mutant (Fig. 2.4A, C), indicating that RcsA is also negatively regulated by Lon-dependent degradation in *E. amylovora*. Interestingly, the RcsB protein was 1.6-fold more abundant in the *lon* mutant, but the RcsB protein stability was not significantly affected (Fig. 2.4B, D), suggesting that RcsB might not be directly targeted by Lon, but its expression might be subjected to feedback regulation of the Rcs system.

2.4.4 RcsA/RcsB accumulation suppresses motility and *flhD* transcription in the lon mutant

In addition, we found that the *lon* mutant was non-motile (Fig. 2.5A). Diameter of the WT on the motility plate was 9 mm at 24 h and 29.6 mm at 48 h, while no circular movement was observed in the *lon* mutant, which remained at about 6 mm (Fig. 2.5B). Complementation of the *lon* mutant restored the motile phenotype (Fig. 2.5A), indicating that Lon is essential for motility in *E. amylovora*.

In order to identify suppressors of the *lon* mutant in controlling motility, we performed a transposon mutagenesis screening in the *lon* mutant background and obtained nine mutants with partially restored motility (Table 2.3). Among them, transposon insertion in the *rcsA* gene recovered motility the most in the *lon* mutant (Table 2.3). In order to confirm this result, we

constructed the *lon*/*rcsA* as well as the *lon*/*rcsB* double deletion mutants. Interestingly, both the *lon*/*rcsA* and *lon*/*rcsB* double mutants partially recovered motility (Fig. 2.5B). Expression of the *flhD* gene, the master regulator of flagellar biosynthesis, was also recovered to the WT level in the *lon*/*rcsA* and *lon*/*rcsB* double mutants, whereas decreased 5-fold in the *lon* mutant (Fig. 2.5C). Transcript levels of the *flhD* gene increased slightly in the *rcsA* and *rcsB* single mutants, although they exhibited irregular and slightly decreased motility (Wang et al., 2009). These results indicate that accumulation of RcsA/RcsB negatively regulates *flhD* transcription, and thus suppresses motility in the *lon* mutant. In addition, other regulators, such as RNA chaperone Hfq and cholera toxin transcription activator YqeI, also contribute to suppression of motility in the *lon* mutant, but the functional relevance in these situations was not determined in this study (Table 2.3).

2.4.5 Expression of *hrpS* is transcriptionally activated by RcsA/RcsB

Previous microarray study showed that RcsB is required for full T3SS gene expression, but the mechanism remains uncertain (Wang et al., 2012). Bioinformatic analyses of promoters found a potential RcsAB box (TAGGA-N_4-TCTTA) located 350 bp upstream of the *hrpS* start site. Indeed, *hrpS* gene expression was down-regulated in both *rcsA* and *rcsB* mutants in HMM, whereas it was up-regulated about 2-fold in the *lon* mutant (Fig. 2.6A). Deletion of either *rcsA* or *rcsB* in the *lon* mutant diminished this up-regulation of *hrpS* gene expression in the *lon* mutant, suggesting that *hrpS* gene expression is transcriptionally activated by RcsA/RcsB. Binding of RcsA/RcsB to the *hrpS* upstream sequence was assessed by EMSA as described previously (Ancona et al., 2015a). A distinct band shift of the *hrpS* DNA probe was observed with RcsB and RcsA/RcsB proteins, but not with RcsA protein alone (Fig. 2.6B). Western blot analyses also

showed that the abundance of RcsA and RcsB proteins were increased in the *lon* mutant grown in HMM as compared to the WT (Fig. 2.6C). These results indicate that accumulation of the RcsA/RcsB proteins led to the up-regulation of *hrpS* transcription in the *lon* mutant.

2.4.6 Expression of the *csrB* sRNA is suppressed by RcsA/RcsB accumulation in the *lon* mutant

Virulence gene expression of the *lon* mutant observed in this study were very similar to those reported for the *gacS/gacA* and *csrB* mutants in *E. amylovora* (Ancona et al., 2016, Li et al., 2014). We hypothesized that a connection between Lon and the GacS/GacA-Csr regulatory system exists. It has also been proposed that the Rcs system negatively regulates expression of *rsmB*, a homologue of *csrB* sRNA, possibly by direct binding to its upstream sequence in *Pectobacterium* (Andresen et al., 2010). Bioinformatic analysis of the *csrB* gene indeed found a potential RcsA/RcsB box (TACGA-N_4-TCTTA), which is located 172 bp upstream of the start site and is close to the GacA-binding site (Fig. 2.7A) (Lee and Zhao, 2016). A shifted band of the *csrB* DNA probe was observed with RcsB and RcsA/RcsB proteins, but not with RcsA alone (Fig. 2.7B). Transcript levels of *csrB* decreased about 5-fold in the *lon* mutant, but increased 1.5-fold in the *rcsA* and *rcsB* mutants in MBMA (Fig. 2.7C). Deletion of the *rcsA/rcsB* gene in the *lon* mutant restored *csrB* expression to the WT level (Fig. 2.7C). However, *csrA* transcript levels were slightly increased in the five mutants tested as compared to the WT (Fig. 2.7C). Similar expression patterns for both *csrA* and *csrB* were observed in these mutants grown in HMM (Fig. 2.8A). These results indicated that RcsA/RcsB accumulation in the *lon* mutant led to the suppression of *csrB* transcription.

2.4.7 Transcription of *lon* is suppressed by CsrA

Given that mutations in *lon* and *csrA* caused the opposite virulence gene expression patterns in *E. amylovora* (Ancona et al., 2016), we further hypothesized that increased Lon activity might contribute to the diminution in T3SS and amylovoran production observed in the *csrA* mutant. Transcript levels of *lon* in the *csrA* mutant were about 2.5-fold up-regulated in both MBMA and HMM growth conditions, while no significant changes were observed in the *csrB* mutant (Fig. 2.7D, 2.8B), However, Western blot analyses showed slightly increased Lon protein levels in the *csrA* mutant, but not in the *csrB* mutant (Fig. 2.7E, 2.8C). These results suggest that CsrA might mainly regulate the expression of *lon* at the transcriptional level, but the possibility that CsrA post-transcriptionally affects *lon* translation could not be excluded.

To determine the effects of the increased Lon levels on the *csrA* mutant, we generated a *lon*/*csrA* double deletion mutant. The *lon*/*csrA* mutant still failed to cause disease on immature pears (Fig. 2.9A), but exhibited significantly increased amylovoran production (Fig. 2.9B). Western blot analyses showed that the *lon*/*csrA* mutant showed slightly increased HrpS protein expression as compared to the *csrA* mutant, but HrpA proteins were barely detected in both mutants (Fig. 2.9C, D). These results suggest that CsrA might positively control both T3SS and amylovoran production partially by suppressing Lon, whereas CsrA may also play a critical role in T3SS by affecting unknown targets.

2.5 Discussion

In bacteria, the abundance and quality of functional proteins are constantly monitored to meet the physiological needs of the cell by robust and highly selective post-translational

degradation and modification. As one of the major ATP-dependent proteases in bacteria, Lon has been found to influence diverse cellular processes. In this study, we not only corroborated that Lon directly degrades RcsA, but also demonstrated that HrpA and HrpS, an activator of RpoN-dependent transcription of the T3SS, are direct targets of Lon in *E. amylovora*. We further provided evidence that accumulation of RcsA/RcsB proteins in the *lon* mutant represses motility by inhibiting *flhD* expression, and promotes EPS production and T3SS gene expression by suppressing *csrB* sRNA expression and activating *hrpS* expression. Moreover, we documented that expression of *lon* is under the control of CsrA, possibly at both transcriptional and posttranscriptional levels. These results are novel and further suggest that CsrA contributes to the activation of both T3SS and amylovoran production partially by suppressing Lon.

The complex enterobacterial-specific Rcs system was originally identified as a primary activator of EPS biosynthesis in *E. coli* (Gottesman et al., 1985; Majdalani and Gottesman, 2005). It is also well-established that Lon negatively regulates the Rcs system by targeting RcsA, and thus inhibits EPS over-production (Torres-Cabassa and Gottesman, 1987). We validated that Lon also directly degrades RcsA in *E. amylovora*, the only plant-pathogen known to require a functional Rcs system for its pathogenesis (Ancona et al., 2015a; Wang et al., 2009; Wang et al., 2012; Zhao et al., 2009b). Here we also provided novel insights into the role of the Rcs system in the regulation of *E. amylovora* virulence through characterization of the *lon* mutant, which accumulates higher levels of RcsA/RcsB proteins.

Previous studies have reported that the Rcs system also negatively regulates motility through transcriptional repression of the flagellum master regulator *flhDC* (Francez-Charlot et al.,

2003; Wang et al., 2007). In *E. coli*, the *rcsB* mutant was hyper-motile, while the *rcsA* mutant exhibited WT-level of motility (Francez-Charlot et al., 2003; Fredericks et al., 2006). RcsA was shown to affect *E. coli* motility when expressed at high levels (Fredericks et al., 2006). The *rcsB* mutant of *Proteus mirabilis* also showed increased *flhDC* expression and motility (Clemmer and Rather, 2007). However, in *Salmonella*, RcsA was not involved in the regulation of *flhDC* expression, and thus mutation in *lon* had no effect on flagellum formation and motility (Takaya et al., 2002; Wang et al., 2007). In contrast, the *rcsB* mutant of *E. amylovora* was less motile than the WT despite increased *flhDC* promoter activity (Wang et al., 2009; Zhao et al., 2009b). Over-expression of $RcsB_{D56E}$, a phosphorylation mimic variant, significantly reduced motility in *E. amylovora* (Ancona et al., 2015a). This is consistent with our current observations that accumulation of RcsA/RcsB in the *lon* mutant led to decreased *flhD* expression and motility, suggesting that the Rcs system in *E. amylovora* indeed acts as a negative regulator of motility; and this is dependent upon its expression level.

HrpS in *E. amylovora* and HrpR/HrpS in *P. syringae* are bEBPs, critical for activating RpoN-dependent *hrpL* gene expression (Hutcheson et al., 2001; Lee et al., 2016; Wei et al., 2000). In general, bEBP is regulated through its N-terminal regulatory domain that interacts with various signal transduction intermediates, including phosphoryl groups, ligands and anti-activator proteins (Bush and Dixon, 2012). However, HrpR and HrpS in *P. syringae* and HrpS in *E. amylovora* lack this regulatory domain. In *P. syringae*, HrpR is subject to Lon-dependent degradation, whereas HrpS activity is suppressed by direct interaction with HrpV, which further interacts with a chaperone-like protein HrpG to relieve the suppression (Bretz et al., 2002; Jovanovic et al., 2011; Ortiz-Martín et al., 2010b; Preston et al., 1998; Wei et al., 2005). In *E.*

amylovora, HrpG and HrpV form a stable heterodimer complex *in vitro*, suggesting that similar regulation mechanism may exist (Gazi et al., 2015). In this study, we demonstrated that HrpS is regulated at least at two levels. Despite low amino acid identity with *P. syringae* HrpR and HrpS, *E. amylovora* HrpS is a direct Lon substrate, and *hrpS* gene expression is under positive regulation of the Rcs system. This is consistent with previous microarray analysis of the *rcsB* mutant, which showed that the Rcs system, especially RcsB, is required for full T3SS gene expression (Wang et al., 2012).

It was proposed that type III effector proteins in the cytoplasm are maintained in an unfolded state to pass through the narrow secretion machinery, and are generally associated with specific chaperone(s) to prevent premature folding and aggregation (Page and Parsot, 2002; Stebbins and Galan, 2001). Meanwhile, effector proteins could also be exposed to Lon degradation as features of unfolded proteins, such as hydrophobic peptides, can be easily recognized by Lon (Gur and Sauer, 2008). In *P. syringae*, Lon affects the stability of at least eight type III effector proteins, which becomes rate-limiting for effector secretion (Losada and Hutcheson, 2005). The Hrp pilus of *P. syringae* and *E. amylovora* consists of HrpA subunits and extends to the plant cell by addition of HrpA at the distal end (Jin and He, 2001; Li et al., 2002). We showed here that HrpA stability was greatly enhanced in the *lon* mutant, suggesting that HrpA protein is subject to Lon degradation, but we could not rule out the possibility that other T3SS proteins might also be targeted by Lon. Therefore, Lon, as a negative regulator of the T3SS in *E. amylovora*, could also function at multiple stages.

The wide-distributed GacS/GacA system is a conserved global dual regulatory system, which specifically activates the expression of the *csrB/rsmB* sRNAs and antagonizes the activity of the CsrA/RsmA proteins (Lapouge et al., 2008; Li et al., 2013; Remeo et al., 2013; Vakulskas et al., 2015). At the transcription level, expression of *csrB* also requires IHF, ppGpp and DksA in *E. coli* and *S. enterica* (Edwards et al., 2011; Martínez et al., 2014; Zere et al., 2015). In *E. amylovora*, expression of *csrB* is positively mediated by GacS/GacA and IHF (Lee and Zhao, 2016). Here we provided evidence that accumulation of RcsA/RcsB in the *lon* mutant inhibited *csrB* expression, suggesting that Lon indirectly activates *csrB* expression.

On the other hand, CsrA positively activates T3SS and amylovoran production in *E. amylovora*, but the molecular mechanisms of CsrA regulation remains enigmatic (Ancona et al., 2016). CsrA generally binds to GGA motifs in the 5' untranslated region of target transcripts and affects the translation rate or stability of target mRNAs either positively or negatively (Vakulskas et al., 2015). CsrA also promotes premature transcription termination by altering Rho-dependent transcript structure in *E. coli*, such as *pgaA* mRNA, which encodes a polysaccharide adhesin export protein (Figueroa-Bossi et al., 2014). Recent studies have shown that *lon* mRNA could be co-purified with CsrA protein in *E. coli*, and CLIP-seq data from *Salmonella* showed that CsrA binds to the coding region of *lon* mRNA, which is conserved in *E. amylovora* (Edwards et al., 2011; Holmqvist et al., 2016). Our results suggested that Lon is possibly under the control of CsrA at both transcriptional and posttranscriptional levels. It is reasonable to speculate that Lon might be a direct target of CsrA since deletion of *lon* in the *csrA* mutant background fully restored amylovoran production. On the other hand, although CsrA could indirectly promote HrpS stability and *hrpS* gene expression by suppressing Lon, deletion of *lon* in the *csrA* mutant

background failed to restore the T3SS and virulence, suggesting that CsrA might also target other unknown regulators besides Lon. Therefore, further studies are needed to determine the molecular targets of CsrA in regulating the T3SS in *E. amylovora*.

Based on our results, it is tempting to speculate that Lon-mediated suppression of RcsA and HrpS/HrpA activities could effectively block *E. amylovora* pathogenesis, allowing the bacteria to utilize cellular resources in other processes under non-pathogenic conditions. Increased motility might also enable the bacteria to reach infection sites. Several studies have shown that environmental stimuli such as phosphate molecules can regulate Lon activity. Inorganic phosphate (polyP) forms a complex with Lon and promotes the degradation of ribosomal proteins under nutrient starvation (Kuroda et al., 2001). Cardiolipin and lipopolysaccharide (LPS), respectively found in inner and outer membranes in gram negative bacteria, directly binds to Lon through their phosphate groups and inhibits Lon activity (Minami et al., 2011; Sugiyama et al., 2013). The Lon activity *in vitro* can be also inhibited by polyP, cyclic adenosine monophosphate (cAMP), (p)ppGpp, and c-di-GMP (Osbourne et al., 2014). In *E. amylovora*, (p)ppGpp and c-di-GMP have been shown to positively regulate T3SS and amylovoran production, respectively, suggesting potential involvement of the nucleotide second messengers in the post-translational regulation of virulence (Ancona et al., 2015b; Edmunds et al., 2013), which warrants further investigation.

In summary, we propose the following working model for Lon-mediated virulence regulation, and its interaction with Rcs and Gac-Csr regulatory systems in *E. amylovora* (Fig. 2.10). Lon broadly impacts *E. amylovora* virulence by negatively regulating amylovoran

production and T3SS, and positively affecting motility. These could mainly be achieved through directly targeting major regulators of amylovoran (RcsA) and the T3SS (HrpS/HrpA), and indirectly through suppressing the Rcs system. Over-activation of the Rcs system inhibits flagellar formation and *csrB* sRNA expression, and activates T3SS (*hrpS*) expression. On the other hand, CsrA protein positively regulates both amylovoran and T3SS, partially by suppressing Lon activity and other unknown regulators. The balance of CsrA and Lon activities is further monitored by the regulatory circuit between the Rcs and the Gac-Csr systems. Future research should focus on understanding the molecular mechanisms underlying regulation of Lon by CsrA and identifying other CsrA and Lon targets.

2.6 Tables

Table 2.1 Bacterial strains and plasmids used in this study

Strains, Plasmids	Description	Reference, Source
E. amylovora		
Ea1189	Wild type, isolated from apple	Wang et al., 2009
Δ*lon*	*lon*::Cm; Cm^R-insertional mutant of *lon* of Ea1189	This study
Δ*rcsA*	*rcsA*::Cm; Cm^R-insertional mutant of *rcsA* of Ea1189	Ancona et al., 2015a
Δ*rcsB*	*rcsB*::Km; Km^R-insertional mutant of *rcsB* of Ea1189	Wang et al., 2009
Δ*lon*/*rcsA*	*rcsA*::Cm, *lon*::Km; Km^R-insertional mutant of *lon* of Δ*rcsA*	This study
Δ*lon*/*rcsB*	*rcsB*::Km, *lon*::Cm; Cm^R-insertional mutant of *lon* of Δ*rcsB*	This study
Δ*csrA*	*csrA*::Cm; Cm^R-insertional mutant of *csrA* of Ea1189	Ancona et al., 2016
Δ*csrB*	*csrB*::Cm; Cm^R-insertional mutant of *csrB* of Ea1189	Ancona et al., 2016
Δlon/csrA	*csrA*::Km, *lon*::Cm; Km^R-insertional mutant of *csrA* of Δ*lon*	This study
E. coli		
DH10B	F– *mcr*A Δ(*mrr-hsd*RMS-*mcr*BC) Φ80*lac*ZΔM15 Δ*lac*X74 *rec*A1 *end*A1 *ara*D139 Δ(*ara leu*) 7697 *gal*U *gal*K *rps*L *nup*G λ-	Invitrogen
Plasmids		
pKD46	ApR, PBAD *gam bet exo* pSC101 oriTS	Datsenko and Wanner, 2000
pKD32	Cm^R, FRT *cat* FRT tL3 oriR6Kγ *bla rgnB*	Datsenko and Wanner, 2000
pKD13	Km^R, FRT *kan* FRT tL3 oriR6Kγ *bla rgnB*	Datsenko and Wanner, 2000
pWSK29	Ap^R, cloning vector, low copy number	Wang and Kushner, 1991
pLon	3077-bp DNA fragment containing promoter sequence of *lon* gene in pWSK29	This study
pHrpS-His6	1537-bp DNA fragment containing promoter sequence of *hrpS* gene and c-terminal His-tag in pWSK29	This study
pHrpA-His6	803-bp DNA fragment containing promoter sequence of *hrpA* gene and c-terminal His-tag in pWSK29	Ancona et al., 2015b
pRcsA-His6	1058-bp DNA fragment containing promoter sequence of *rcsA* gene and c-terminal His-tag in pWSK29	This study
pRcsB-His6	1142-bp DNA fragment containing promoter sequence of *rcsB* gene and c-terminal His-tag in pWSK29	This study
pLon-His6	2877-bp DNA fragment containing promoter sequence of *lon* gene and c-terminal His-tag in pWSK29	This study

Table 2.2 Primers used in this study

Primer	Sequences (5' to 3')
Primers for mutation	
lon-F	ATGAATCCTGAGCGTTCTGAACGCATTGAAATCCCTGTGTTGCCGTTGCGCGATTGTGT AGGCTGGAGCT
lon-R	CTATTTTACCGAGGCAACCTGCATGCCATAAGGTGCATTTTGCAGCGCCAATTCCGGGG ATCCGTCGACC
lon-C1	CAGCAGGTGTCTGGTGAATA
lon-C2	CGGCCTGCAAAGATTCTGTT
Cm1	TTATACGCAAGGCGACAAGG
Cm2	GATCTTCCGTCACAGGTAGG
Km1	CAGTCATAGCCGAATAGCCT
Km2	CGGTGCCCTGAATGAACTGC
Primers for qRT-PCR	
rpoD-rt1	ACATGCGTGAAATGGGTACGGT
rpoD-rt2	TTGATGCCGTCTTCGATGCGTT
hrpL-rt1	TTAAGGCAATGCCAAACACC
hrpL-rt2	GACGCGTGCATCATTTTATT
hrpA-rt1	GAGTCCATTTTGCCATCCAG
hrpA-rt2	TGGCAGGCAGTTCACTTACA
hrpS-rt1	AATGCTACGCGTGCTGGAAA
hrpS-rt2	AACAATGGCGTTTGCGTTGC
rcsA-rt1	TTAAACCTGTCTGTGCGTCA
rcsA-rt2	AGAAACCGTTTTGGCTTTGA
amsG-rt1	CAAAGAGGTGCTGGAAGAGG
amsG-rt2	GTTCCATAGTTGCGGCAGTT
flhD-rt1	TGGTTTGTCAGTTCCGCTTC
flhD-rt2	TTTTCGGCGTCTCTTGTTCT
csrA-rt1	TCATGATCGGTGATGAGGTG
csrA-rt2	ACTCGTTTGCTGCGTCTTTT
csrB-rt1	CCTGACGTCGATCCTTTGAC
csrB-rt2	GTAAGGGACATTCGGCAGTC
Primers for cloning	
hrpS-His6-F	AGTAGGTACCATGCATGAACGCCTGACG
hrpS-His6-R	AGTAGAATTCCTAGTGATGATGATGATGATGCTGAGCAATAACCCGACCGGTG
rcsA-His6-F	TCAGGGTACCTACTGGACTGTTTGCCTGAT
rcsA-His6-R	TCAGGAATTCCTAGTGATGATGATGATGATGTCTTTCGTTAACATAAATGCCG
rcsB-His6-F	TCAGGGTACCCGATGTTCTGATCACTGACC
rcsB-His6-R	TCAGGAATTCTTAGTGATGATGATGATGATGTTTATCTACCGGCGTCATGCTT
lon-His6-F	AGTACTCGAGTAAGCGAGCTAAGCGAGGAA
lon-His6-F	TCAGGAATTCCTAGTGATGATGATGATGATGTTTTACCGAGGCAACCTGCATG
Primers for inverse PCR	
PvuI-left	GAAAAACAGCATTCCAGGTATTAGA
PvuI-right	AAGTTTATGCATTTCTTTCCAGACT
KAN-2 FP-1	ACCTACAACAAAGCTCTCATCAACC
KAN-2 RP-1	GCAATGTAACATCAGAGATTTTGAG
Primers for EMSA	
EMSAcsrB F	CCGAATTAAGCCGCCTGCCCTGTACGAGATCTCTTACAGATTATGTAAGAGATCGCTT
EMSAcsrB R	AAGCGATCTCTTACATAATCTGTAAGAGATCTCGTACAGGGCAGGCGGCTTAATTCGG
EMSAhrpS-F	CATTAGTCATTGCCTGATAACTTAGGAATGCTCTTATATTTGTCTCTCGCCCTTCCCT
EMSAhrpS-R	AGGGAAGGGCGAGAGACAAATATAAGAGCATTCCTAAGTTATCAGGCAATGACTAATG

Table 2.3 Tn5 mutants with recovered motility in the *lon* mutant background

Accession	Gene	Description	Motility (24 h, mm)	Motility (48 h, mm)
EAM_0994	*lon*	Lon protease	6	7
EAM_1482	*rcsA*	Colanic acid capsular biosynthesis activation protein A	11.7 ± 0.58	16.3 ± 0.58
EAM_0427	*bspA*	Mechanosensitive ion channel protein	6.7 ± 0.58	11.7 ± 0.58
EAM_0436	*hfq*	RNA chaperone	8.7 ± 0.58	14
EAM_3422	*yqeI*	Cholera toxin transcription activator	7.3 ± 0.58	12.3 ± 0.58
EAM_3014		Hypothetical protein	6	10.7 ± 0.58
EAM_2896	*hrpI*	Type III secretion protein	5	9.3 ± 0.58
EAM_2178	*udk*	Uridine kinase	5	8
EAM_0009		Hypothetical protein	5	8
EAM_0609		Acetyltransferase	5.8 ± 0.58	9

2.7 Figures

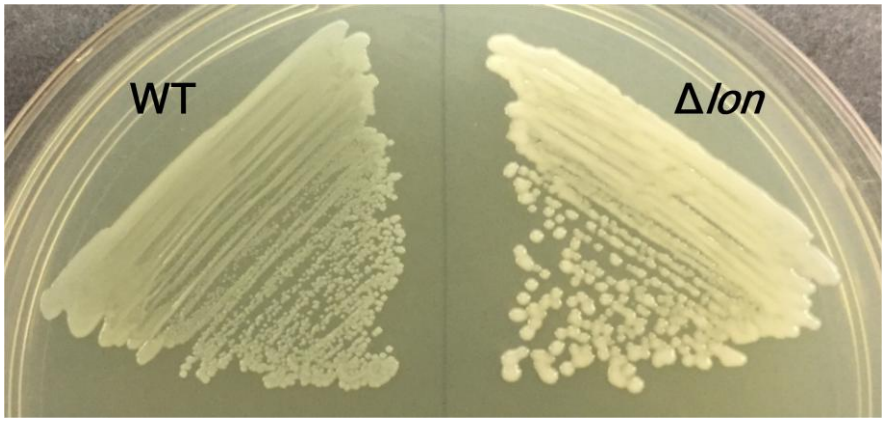

Figure 2.1 Mucoid colony morphology of the *lon* mutant. The WT and the *lon* mutant strains were grown in LB at 28 ℃. Pictures were taken at 48 h after incubation.

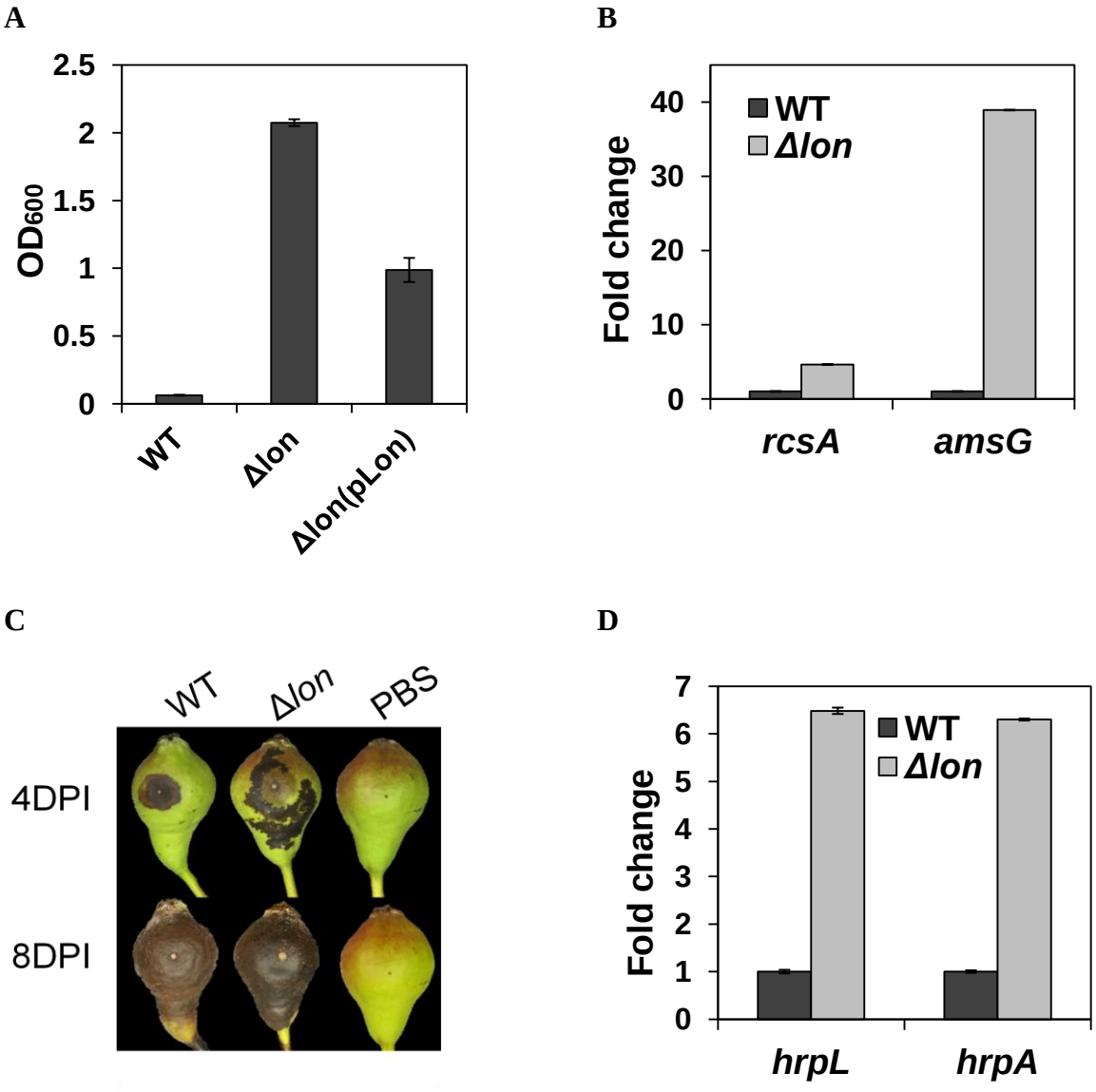

Figure 2.2 Characterization of the *lon* mutant. (A) Amylovoran production of the wild-type (WT), the *lon* mutant and its complementation strain grown in MBMA medium for 24 h at 28 ℃. (B) Relative gene expression of the *rcsA* and *amsG* genes in the *lon* mutant compared to the WT grown in MBMA medium for 18 h at 28 ℃. (C) Disease symptoms caused by the WT and the *lon* mutant on immature pear fruits at 4 and 8 days post-inoculation (DPI). (D) Relative gene expression of the *hrpL* and *hrpA* genes in the *lon* mutant compared to the WT grown in HMM for 6 h at 18 ℃. The values of OD_{600} (A) and the relative fold change (B, D) are the means of three replicates, and similar results were obtained from repeated experiments. A representative of three independent experiments is presented for virulence assay (C). Error bars indicate standard deviation.

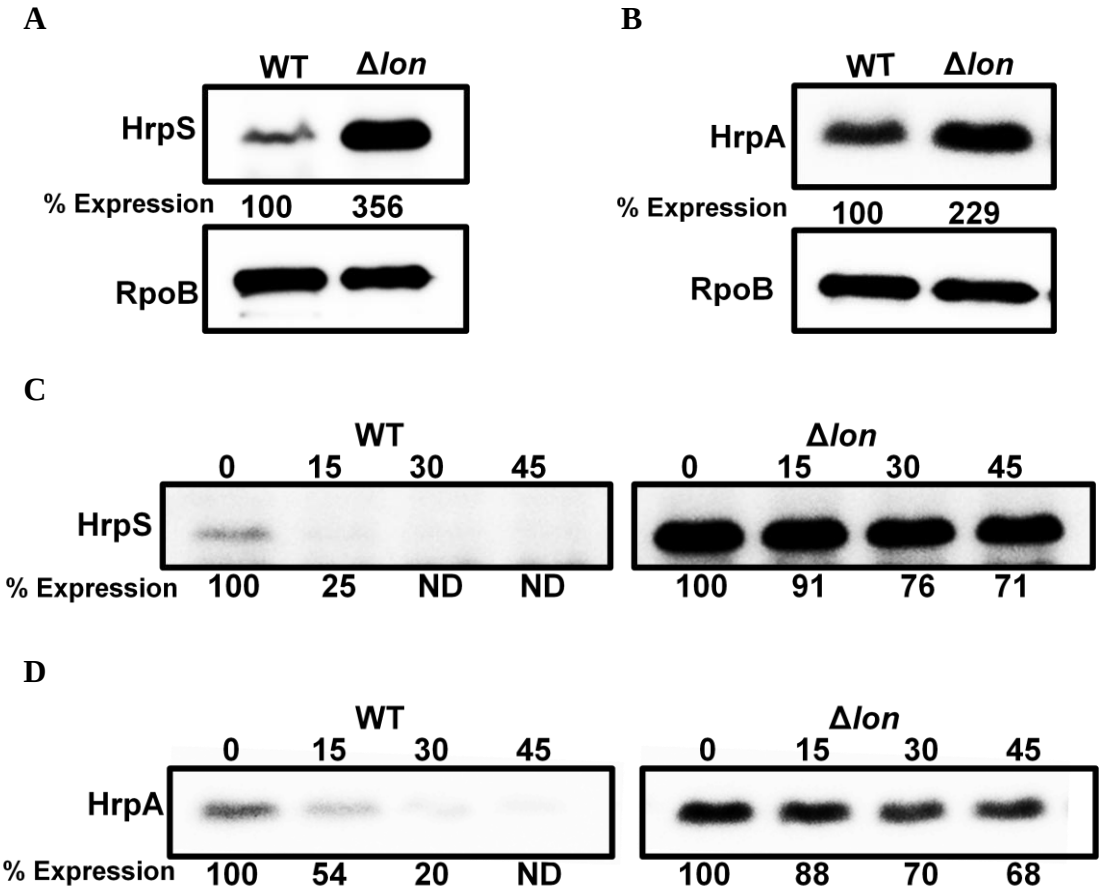

Figure 2.3 Lon-dependent degradation of HrpS/HrpA regulates T3SS gene expression in *Erwinia amylovora*. Abundance of HrpS-His6 (A) and HrpA-His6 (B) proteins in the wild-type (WT) and the *lon* mutant strains grown in HMM for 6 h at 18 ℃; abundance of the RpoB protein was used as a loading control. Half-life of HrpS-His6 (C) and HrpA-His6 (D) proteins in the WT and the *lon* mutant strains. For protein stability test, cells were grown in HMM for 6 h at 18 ℃. Translation was stopped by addition of tetracycline, and samples were taken at the indicated time points (min) on the top. Relative protein abundance at the bottom of each lane was calculated using ImageJ software. Cropped gel blots and % expression values are representatives of three independent experiments. ND: not detected.

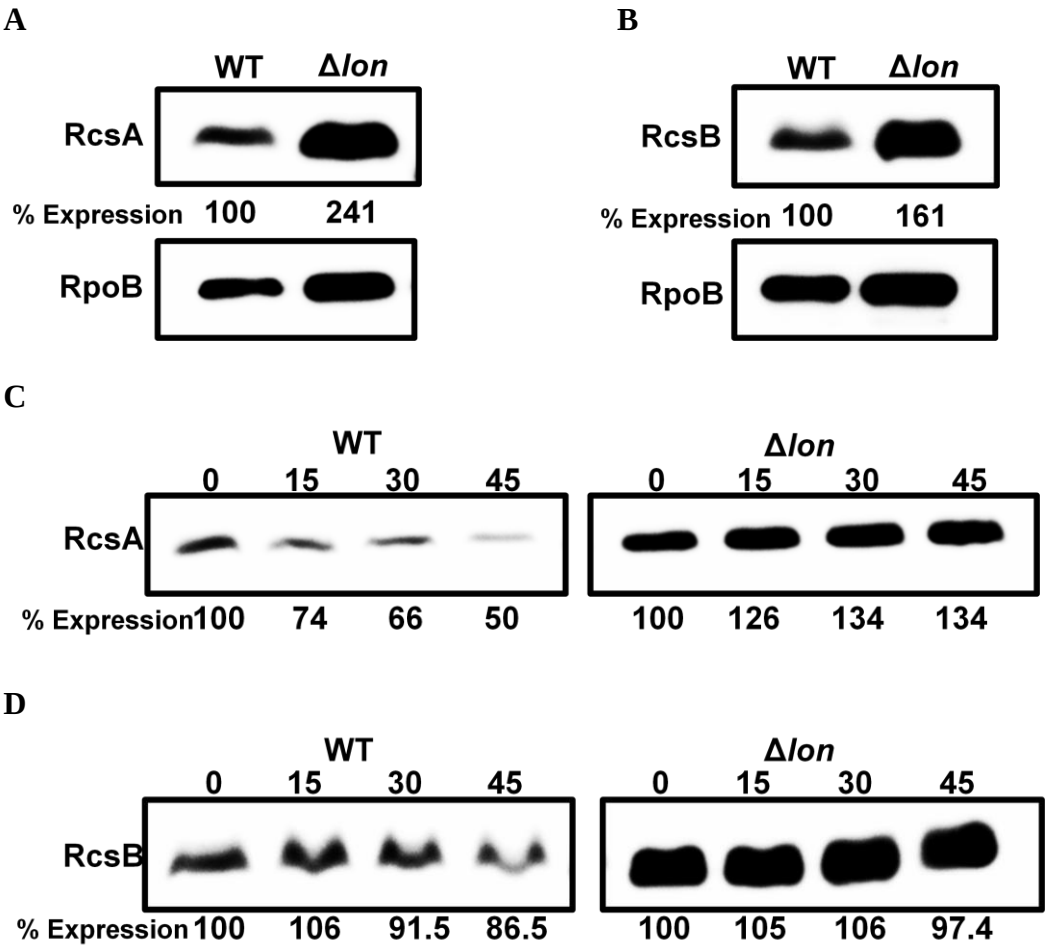

Figure 2.4 Lon-dependent degradation of RcsA regulates amylovoran production in *Erwinia amylovora*. Abundance of RcsA-His6 (A) and RcsB-His6 (B) proteins in the wild-type (WT) and the *lon* mutant strains grown in MBMA for 24 h at 28 ℃; abundance of the RpoB protein was used as a loading control. Half-life of RcsA-His6 (C) and RcsB-His6 (D) proteins in the WT and the *lon* mutant strains. For protein stability test, cells were grown in MBMA medium for 24 h at 28 ℃. Translation was stopped by addition of tetracycline, and samples were taken at the indicated time points (min) on the top. Relative protein abundance at the bottom of each lane was calculated using ImageJ software. Cropped gel blots and % expression values are representatives of three independent experiments.

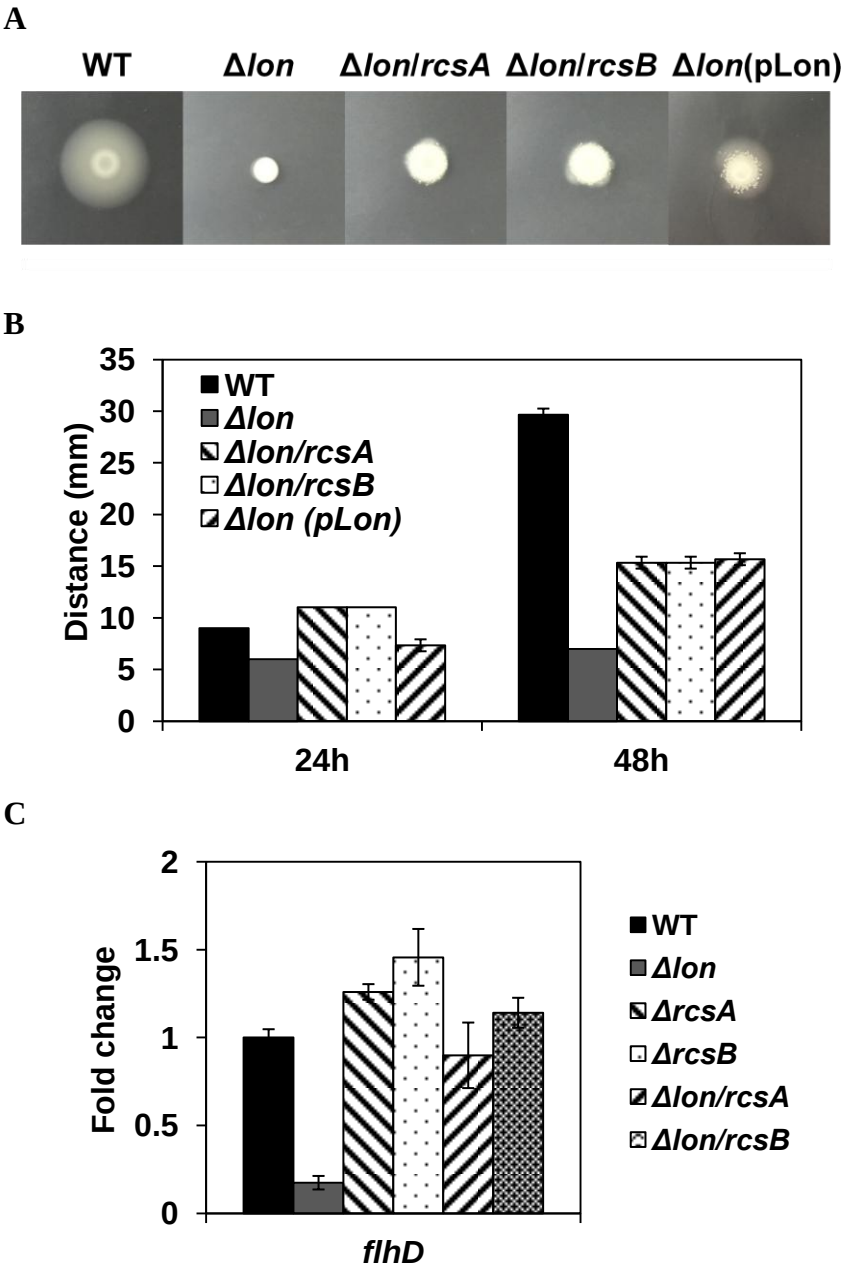

Figure 2.5 RcsA/RcsB accumulation suppresses motility and *flhD* transcription in the *lon* mutant. (A) Movement of the wild-type (WT), the *lon*, *rcsA*, *rcsB*, *lon*/*rcsA* and *lon*/*rcsB* mutants and the complementation strain of the *lon* mutant. Pictures were taken at 48 h post-incubation in motility agar plate. (B) The moving distance of the WT, the *lon*, *rcsA*, *rcsB*, *lon*/*rcsA* and *lon*/*rcsB* mutants and the complementation strain of the *lon* mutant. Diameters of the circle around the inoculation site (mm) were measured at 24 and 48 h post-inoculation. (C) Relative gene expression of *flhD* in the five mutant strains compared to the WT grown in MBMA medium for 18 h at 28 ℃. The values of the relative fold change are the means of three replicates and the experiment was repeated three times with similar results. Error bars indicate standard deviation.

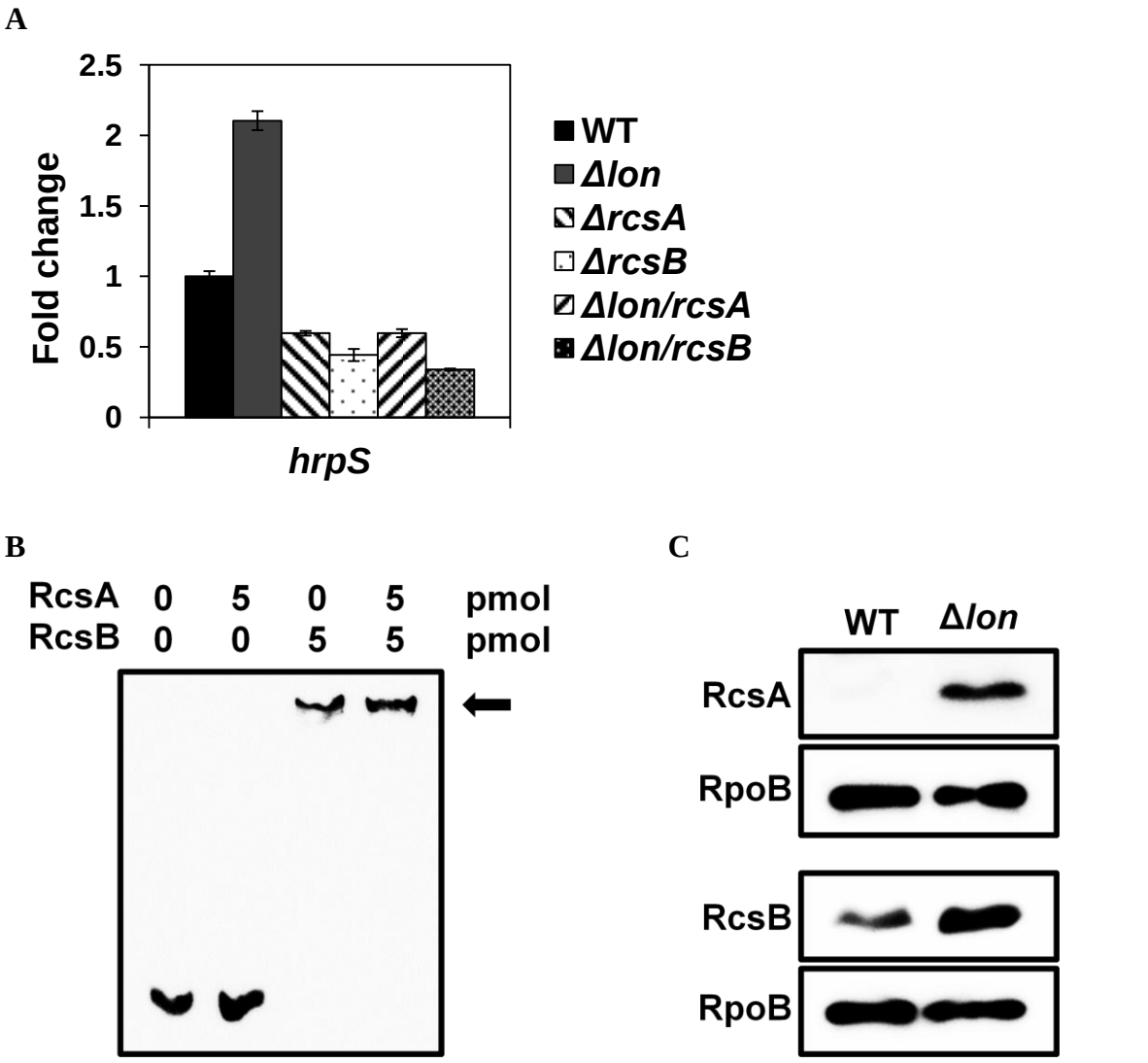

Figure 2.6 Lon-dependent degradation of RcsA regulates the expression of *hrpS* in *Erwinia amylovora*. (A) Relative gene expression of the *hrpS* gene in the WT, the *lon*, *rcsA*, *rcsB*, *lon*/*rcsA* and *lon*/*rcsB* mutants compared to the WT grown in HMM for 6 h at 18 ℃. The values of the relative fold change are the means of three replicates and the experiment was repeated three times with similar results. Error bars indicate standard deviation. (B) EMSA for a 58-bp fragment of the *hrpS* upstream region and RcsA/RcsB proteins. Black arrows at the bottom and top indicate the free probe and the protein-DNA complex, respectively. The concentration of RcsA and RcsB (pmol) is indicated above each lane. (C) Abundance of RcsA-His6 and RcsB-His6 proteins in the *lon* mutant strains compared to the WT grown in HMM for 6 h at 18 ℃. Abundance of the RpoB protein was used as a loading control. Cropped gel blots are representatives of three independent experiments.

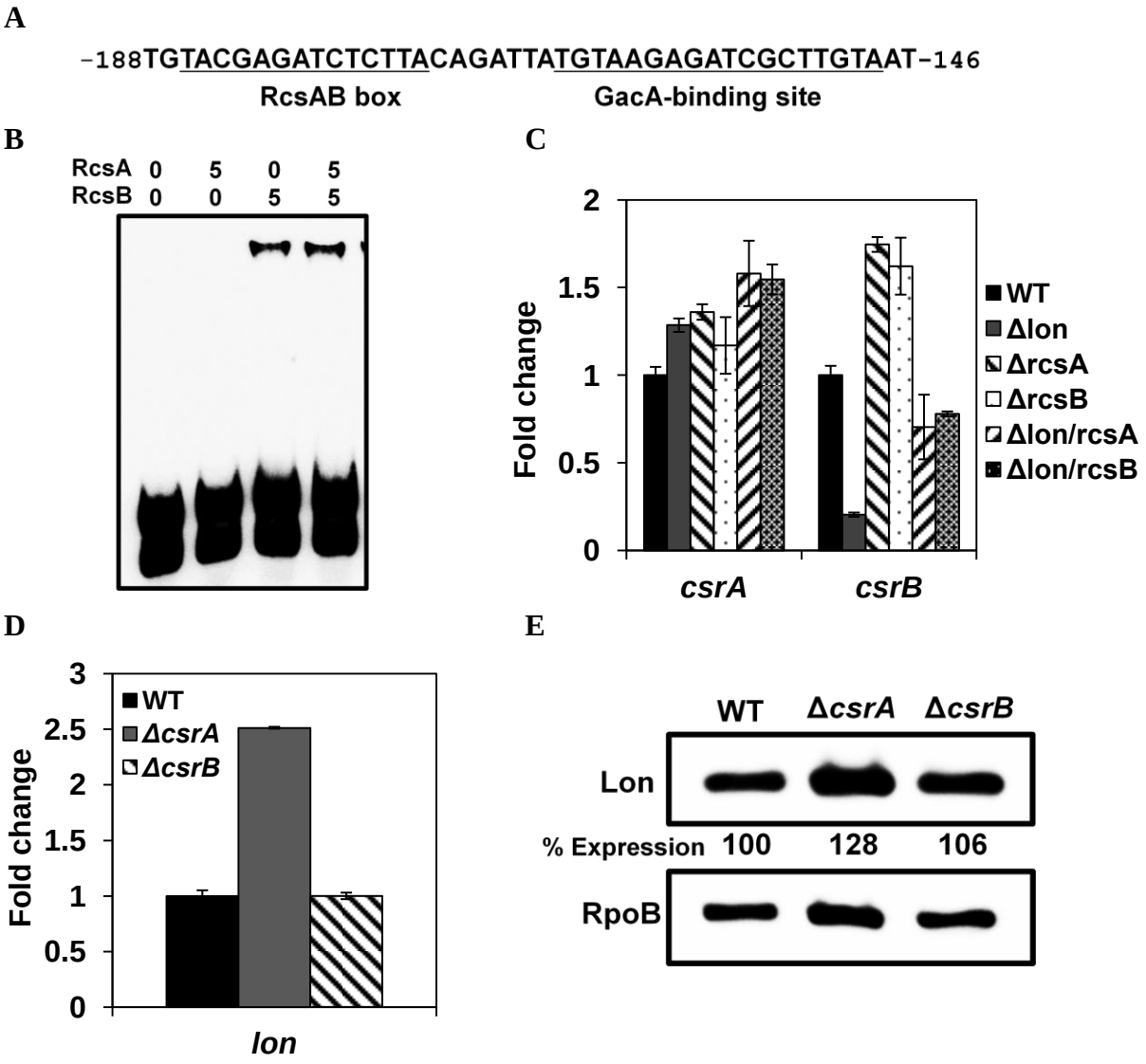

Figure 2.7 RcsA/RcsB accumulation suppresses *csrB* sRNA expression and the effect of *csrA* mutation on the *lon* gene under EPS-inducing condition. (A) The consensus RcsA/RcsB box and GacA-binding site on the *csrB* upstream region. Numbers refer to the nucleotide position relative to the start site of the *csrB* gene. (B) EMSA for a 58-bp fragment of the *csrB* upstream region and RcsA/RcsB proteins. Black arrows at the bottom and top indicate the free probe and the protein-DNA complex, respectively. The protein concentration (pmol) is indicated above each lane. (C) Relative gene expression of *csrA* and *csrB* in the *lon*, *rcsA*, *rcsB*, *lon*/*rcsA* and *lon*/*rcsB* mutants compared to the WT grown in MBMA medium for 18 h at 28 ℃. (D) Relative expression of *lon* in the *csrA* and *csrB* mutants compared to the WT grown in MBMA medium for 18 h at 28 ℃. The values of the relative fold change are the means of three replicates and the experiment was repeated twice with similar results. Error bars indicate standard deviation. (E) Abundance of Lon-His6 protein in the *csrA* and *csrB* mutant strains compared to the WT grown in MBMA for 18 h at 28 ℃. Abundance of the RpoB protein was used as a loading control. Relative protein abundance at the bottom of each lane was calculated using ImageJ software. Cropped gel blots and % expression values are representatives of three independent experiments.

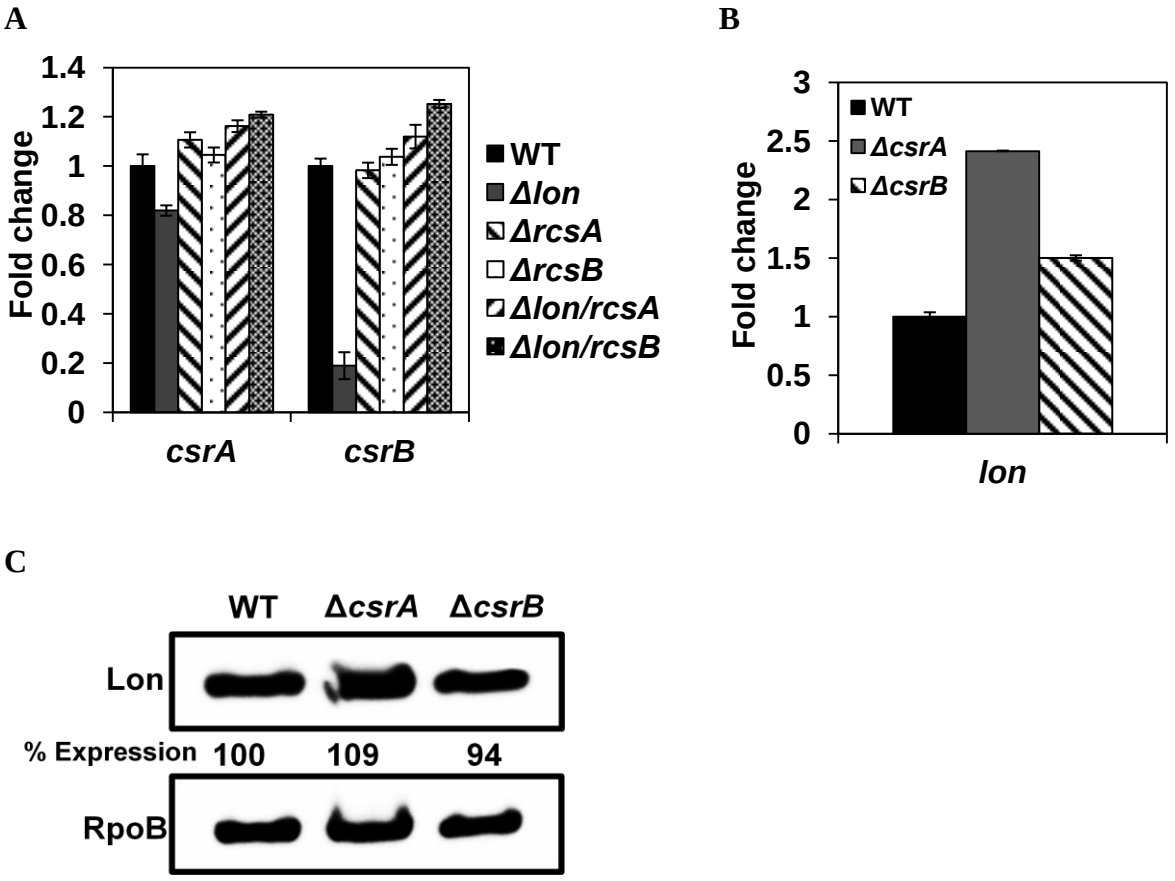

Figure 2.8 RcsA/RcsB accumulation suppresses *csrB* sRNA expression and the effect of *csrA* mutation on the *lon* gene under T3SS-inducing condition. (A) Relative gene expression of the *csrA* and *csrB* in the *lon* mutant compared to the WT grown in HMM for 6 h at 18 ℃. (B) Relative expression of *lon* in the *csrA* and *csrB* mutant compared to the WT grown in HMM for 6 h at 18 ℃. The values of the relative fold change were the means of three replicates and the experiment was repeated twice with similar results. Error bars indicate standard deviation. (C) Abundance of Lon-His6 protein in the *csrA* and *csrB* mutant strains compared to the WT grown in HMM for 6 h at 18 ℃. Abundance of the RpoB protein was used as a loading control. Relative protein abundance at the bottom of each lane was calculated using ImageJ software. Cropped gel blots and % expression values are representatives of three independent experiments.

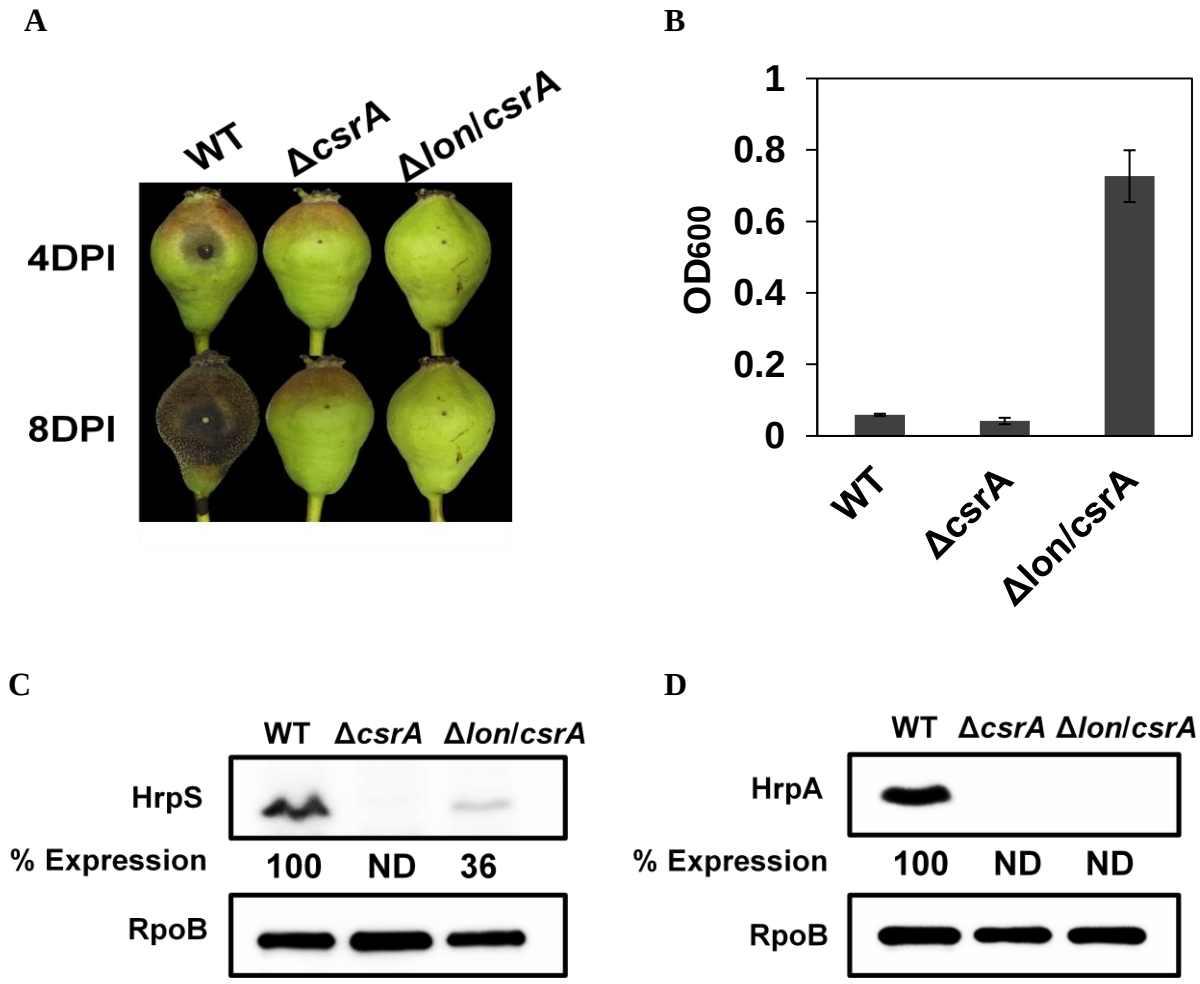

Figure 2.9 Effect of *lon* mutation in the *csrA* mutant. (A) Disease symptoms caused by the wild-type (WT), the *csrA* and *lon*/*csrA* mutant strains on immature pear fruits at 4 and 8 days post-inoculation (DPI). (B) Amylovoran production of the WT, the *csrA* and *lon*/*csrA* mutant strains grown in MBMA medium for 24 h at 28 ℃. The values of OD_{600} are the means of three replicates and the experiment was repeated three times with similar results. Error bars indicate standard deviation. (C) Abundance of HrpS-His6 protein in the *csrA* and *lon*/*csrA* mutant strains compared to the WT grown in HMM for 6 h at 18 ℃. (D) Abundance of HrpA-His6 protein in the *csrA* and *lon*/*csrA* mutant strains compared to the WT grown in HMM for 6 h at 18 ℃. Abundance of the RpoB protein was used as a loading control. Relative protein abundance at the bottom of each lane was calculated using ImageJ software. Cropped gel blots and % expression values are representatives of three independent experiments. ND: not detected.

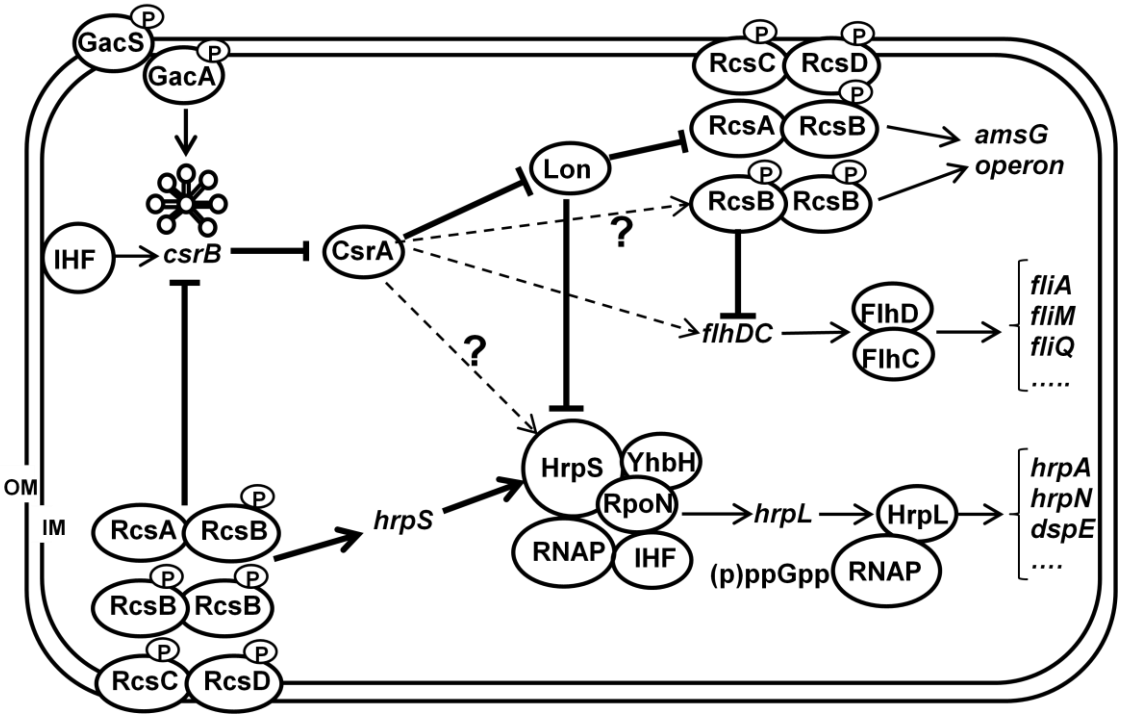

Figure 2.10 A working model illustrating Lon-mediated virulence regulation and its interaction with Rcs and Gac-Csr regulatory systems in *Erwinia amylovora*. This model is based on findings obtained in this study as well as those reported in previous studies (Ancona et al., 2014; 2015ab; 2016; Lee and Zhao, 2016; Lee et al., 2016; Li et al., 2014; Wang et al., 2009; 2012; Zhao et al., 2009b). FlhDC: master regulator of flagellar formation; HrpL: an ECF sigma factor and master regulator of T3SS; HrpS: a σ^{54}-dependent enhancer binding protein; IHF: integration host factor; RpoN: σ^{54} alternative sigma factor; YhbH: σ^{54} modulation protein (ribosome-associated protein); RNAP: RNA polymerase. (p)ppGpp: guanosine tetraphosphateand guanosine pentaphosphate; GacS/GacA and RcsABCD: two-component regulatory systems; *csrB*: small non-coding regulatory RNA; CsrA: RNA-binding protein; OM, outer membrane; IM, inner membrane; P, phosphorylation. Symbols: ↓, positive effect; ⊥, negative effect; dash line with/without ?: unknown mechanism.

CHAPTER 3

ClpXP-dependent RpoS degradation enables full activation of type III secretion system, amylovoran production, and motility in *Erwinia amylovora*

3.1 Abstract

Erwinia amylovora, the causal agent of fire blight disease of apples and pears, employs intracellular proteases, including Lon and ClpXP, for post-translational regulation of various cellular proteins. It has been shown that Lon plays a critical role in *E. amylovora* virulence by directly targeting type III secretion (T3SS) proteins and the Rcs phosphorelay system. In this study, we genetically examined the role of ClpXP and its potential interaction with Lon in *E. amylovora*. Mutation in *clpXP* diminished the expression of the T3SS, reduced exopolysaccharide amylovoran production and motility, and resulted in delayed disease progress. Western blot analyses showed highly accumulated RpoS proteins in the *clpXP* mutant. Moreover, mutation of *rpoS* in the *clpXP* mutant background rescued the expression of the T3SS and amylovoran production, suggesting that ClpXP-dependent RpoS degradation positively affects virulence traits. Interestingly, lack of both ClpXP and Lon resulted in significantly reduced virulence, but increased expression of the T3SS and amylovoran production. However, this phenomenon was independent of RpoS accumulation, suggesting that ClpXP and Lon are indispensable for full virulence in *E. amylovora*.

3.2 Introduction

Fire blight disease, caused by an enterobacterium *Erwinia amylovora*, is one of the most economically important diseases in the plant family Rosaceae. It has been demonstrated that *E. amylovora* utilizes two major virulence factors, the hypersensitive response and pathogenicity

(*hrp*)-type III secretion system (T3SS) and the exopolysaccharide (EPS) amylovoran (Khan et al., 2012; Oh and Beer, 2005). The *hrp*-T3SS directly injects virulence-associated proteins into host cells to overcome host defense response and promote disease development (Nissinen et al., 2007). The expression of *hrp*-T3SS genes is activated by the master regulator HrpL, a member of the ECF (extracytoplasmic functions) subfamily of sigma factors (McNally et al., 2012; Wei and Beer, 1995). Recent studies showed that the alternative sigma factor 54 (RpoN), its modulation protein YhbH, enhancer binding protein HrpS and the nucleoid-associated protein IHF are all essential for the expression of *hrpL* and other *hrp*-T3SS genes (Ancona et al., 2014; Lee and Zhao, 2016; Lee et al. 2016). Moreover, the RpoN-HrpL alternative sigma factor cascade is further activated by the bacterial alarmone (p)ppGpp-mediated stringent response under nutrient-limited conditions (Ancona et al., 2015b). On the other hand, the EPS amylovoran is a heteropolymer composed of pentasaccharide-repeating units and contributes to pathogenesis through biofilm formation and vessel blockage in plants (Koczan et al. 2009; Nimtz et al., 1996). Amylovoran biosynthesis genes are encoded by the 12-gene *ams* operon, which is positively regulated by the Rcs phosphorelay system (Bernhard et al., 1993; Wang et al., 2009, 2012).

ClpXP and Lon are two major proteases in bacteria, belonging to the AAA^+ (ATPase-associated with diverse cellular activities) family proteins, and control the abundance and quality of intracellular proteins in response to a wide variety of environments (Sauer and Baker, 2011). Previous studies have indicated that proteolytic activities from ClpXP and Lon are required during bacterial pathogenesis (Bretz et al., 2002; Iyoda and Watanabe, 2005; Losada and Hutcheson, 2005; Yamamoto et al., 2001). It was recently reported that Lon plays a major role in regulation of virulence in *E. amylovora* by directly targeting HrpS and HrpA T3SS proteins, as

well as RcsA, an auxiliary response regulator of the Rcs phosphorelay system (Lee et al., 2017). Furthermore, accumulation of RcsA/RcsB in the *lon* mutant led to up-regulation of *hrpS* and *amsG*, and down-regulation of *flhD* and small RNA *csrB*. Suppression of *csrB* expression indirectly enhanced the activity of the RNA-binding protein CsrA (carbon storage regulator A), which plays a central role in *E. amylovora* virulence (Ancona et al., 2016). However, the role of ClpXP in *E. amylovora* virulence remains unknown.

ClpXP is an ATP-dependent cytosolic protease, composed of AAA^+ ATPase (ClpX) and proteolytic chamber (ClpP). ClpP alone can degrade damaged or misfolded peptides, but its proteolytic activity becomes selective and tightly controlled only after association with ClpX (Frees et al., 2013). A number of proteins involved in diverse cellular processes, including metabolic enzymes and transcription factors, have been identified as ClpXP substrates (Flynn et al., 2003). Most importantly, ClpXP-mediated proteome changes are largely achieved by regulating RpoS activity (Schweder et al., 1996). RpoS is an alternative sigma factor induced during stationary phase and under stress conditions, and plays major roles in stress response and virulence regulation by altering stress sensitivity and virulence-associated phenotypes (Badger and Miller, 1995; Fang et al., 1992; Flavier et al., 1998; Solis et al., 2006). Recent study showed that the *rpoS* mutant of *E. amylovora* exhibited increased sensitivity to oxidative, osmotic, acid and heat stresses (Santander et al., 2014). On the other hand, RpoS activity is tightly controlled by multiple layers of regulatory elements, including ClpXP-dependent degradation, during favorable growth conditions (Battesti et al., 2011). The rate-limiting factor for RpoS degradation is the adaptor protein RssB, which facilitates RpoS recognition by ClpXP (Becker et al., 1999; Pruteanu and Hengge-Aronis, 2002). Under stress conditions or during stationary phase, RssB

inhibitors and low ATP levels release RpoS from degradation by ClpXP (Bougour et al., 2006, 2008; Peterson et al., 2012). This process leads to increased RpoS level and allows cells to activate genes involved in cell survival. A defect in controlling RpoS level has been reported to cause reduced virulence in enterohemorrhagic *Escherichia coli* (EHEC) and *Dickeya dadantii* (Iyoda and Watanabe, 2005; Li et al., 2010).

We aim to examine the role of ClpXP in *E. amylovora* virulence and its potential interaction with Lon. Our results showed that RpoS accumulation in the *clpXP* mutants contributed to the suppression of T3SS, amylovoran production and motility. Deletion of both *clpXP* and *lon* genes led to significantly reduced virulence independent of RpoS level and other virulence factors.

3.3 Materials and methods

3.3.1 Bacterial strains and growth conditions

Bacterial strains and plasmids used in this study are listed in Table 3.1. Luria-Bertani (LB) broth was used for routine growth of *E. amylovora* and *E. coli* strains. A *hrp*-inducing medium (HMM) (1g $(NH_4)_2SO_4$, 0.246 g $MgCl_2 \cdot 6H_2O$, 0.1 g NaCl, 8.708 g K_2HPO_4, 6.804 g KH_2PO_4) supplemented with 10 mM galactose as carbon source was used for T3SS gene expression, while a modified basal medium A (MBMA) (3 g KH_2PO_4, 7 g K_2HPO_4, 1g $(NH_4)_2SO_4$, 2 ml glycerol, 0.5 g citric acid, 0.03 g $MgSO_4$) supplemented with 1% sorbitol was used for amylovoran production (Wang et al., 2009; Ancona et al., 2014). When required, antibiotics were used at the following concentrations: 100 μg ml^{-1} ampicillin (Ap), 50 μg ml^{-1}

kanamaycin (Km), and 10 μg ml^{-1} chloramphenicol (Cm). Primer sequences used in this study for mutant construction, mutant confirmation and qRT-PCR are listed in Table 3.2.

3.3.2 Mutant generation by λ-Red recombinase cloning

To generate *E. amylovora* Ea1189 mutant strains, the Lambda-Red recombinase cloning method was performed as described previously (Zhao et al., 2009a). Briefly, competent cells of *E. amylovora* strain carrying pKD46 were prepared by subculturing in LB with 0.1 % arabinose to exponential phase (OD_{600} = 0.8, approximately 8 $x10^8$ CFU/ml) and washing with cold sterile water. These cells were transformed by electroporation with recombinant DNA fragments, which contain a selection marker (Cm^R or Km^R) flanked with a 50-nucleotide homology from the target gene or region. Plasmids pDK32 or pKD13 were used as a template. Double mutant strains were generated using single mutants as a background. For complementation, the genomic region containing the native promoter and coding sequence of the target gene was PCR-amplified and cloned into pWSK29. The resulting plasmids were verified by sequencing at the University of Illinois at Urbana-Champaign Core sequencing facility.

3.3.3 Virulence assay on immature pear

Overnight cultures of *E. amylovora* WT, mutant and complementation strains in LB were harvested and suspended in 0.5X PBS to OD_{600} = 0.1 and then diluted 100 times (approximately 10^6 CFU/ml) (Zhao et al. 2009b). Immature Bartlett pears (*Pyrus communis* L. cv. Bartlett) were surface-sterilized with 10% bleach for 10 min, rinsed with sterile distilled water and air-dried. Pears were pricked with a sterile needle, inoculated with 2 μl of bacterial suspension and incubated at 28 ℃ in a humidified chamber in dark. Disease symptoms were

recorded at 4 and 8 days post-inoculation. The experiments were repeated at least twice in triplicate.

3.3.4 Cetylpyrimidinium chloride assay

Amylovoran production was measured using cetylpyrimidinium chloride (CPC) as described previously (Bellemann et al., 1994, Zhao et al. 2009b). Overnight cultures of *E. amylovora* WT, mutant and complementation strains in LB were harvested, washed and inoculated into 5 ml MBMA medium to OD_{600} = 0.2 (approximately $2x10^8$ CFU/ml). After 24 h incubation at 28 ℃ with shaking, 1 ml of each culture was centrifuged at 4,500 g for 10 min, and 50 μl of 50 mg/ml CPC was added to the supernatant. After 10 min incubation, amylovoran production was quantified by measuring OD_{600} turbidity and normalized for a cell density of 1.0. Each experiment was performed in triplicate and repeated three times. Statistical analysis was performed using Student's t-test with $P < 0.05$ considered as statistically significant.

3.3.5 Motility assay

Overnight cultures of *E. amylovora* WT, mutant and complementation strains in LB were harvested, washed and suspended in 0.5X PBS to OD_{600} = 1 (approximately 10^9 CFU/ml). The bacterial suspensions were then plated onto the center of the motility plates (Zhao et al. 2009b)(10 g Bacto tryptone (BD, Sparks, MD, USA), 5 g NaCl and 2.5 g agar (plant tissue culture agar, PhytoTechnology Laboratories, Shawnee Mission, KS, USA) per liter) and incubated at 28 ℃. Diameters of movement were measured at 24 and 48 h post-inoculation, and the experiments were repeated three times with three replicates. Statistical analysis was performed using Student's t-test with $P < 0.05$ considered as statistically significant.

3.3.6 Western blot

Western blotting analyses of RpoS and HrpA proteins were performed as previously described (Ancona et al., 2016; Lee et al., 2017). Briefly, equal amount of cell lysates from *E. amylovora* cultures were separated by sodium dodecyl sulfate polyacrylamide gels followed by transfer to polyvinylidene fluoride membrane (Millipore, MA, USA). After blocking with 5% milk in PBS, membranes were incubated with 1.0 μg/ml rabbit anti-His antibodies (GeneScript, NJ, USA) or rabbit anti-RNA polymerase beta antibodies (1:2000 dilution; Abcam, MA, USA) and then horseradish peroxidase-linked antirabbit IgG antibodies (1:10,000 dilution; Amersham Bioscience, Uppsala, Sweden). Protein bands were detected using enhanced chemiluminescence reagents (Pierce, IL, USA) and ImageQuant LAS 4010 CCD camera (GE Healthcare, NJ, USA). This experiment was repeated three times with similar results.

3.3.7 Quantitative real-time PCR (qRT-PCR)

To isolate RNA, 2 ml of bacterial cell cultures grown under the indicated conditions were mixed with 4 ml of RNA protect reagent (Qiagen, Hilden, Germany) (Lee et al., 2016). RNA was extracted using RNeasy® mini kit (Qiagen) followed by DNaseI treatment and reverse transcription using TURBO DNA-free kit (Ambion, TX, USA) and Superscript III reverse transcriptase (Invitrogen, Carlsbad, CA), respectively, following the manufacturer's instructions. qRT-PCR were carried out by mixing cDNA samples, Power SYBR® Green PCR master mix (Applied Biosystems, CA, USA) and appropriate primers (Table 3.2) under the following conditions: 95 ℃ for 10 min, followed by 40 cycles of 95 ℃ for 15 s and 60 ℃ for 1 min in the StepOnePlus Real-Time PCR system (Applied Biosystems). The melting curves were measured to confirm primer specificity, and three replicates were performed for each biological sample.

3.4 Results

3.4.1 ClpXP positively contributes to virulence in *E. amylovora*

Based on published genome sequences (Blattner et al., 1997; Bell et al., 2004; Smits et al., 2010a, 2010b; Glasner et al., 2011), *E. amylovora* and its closely related species *Erwinia pyrifoliae* contain two sets of *clpXP* genes, while *E. coli* and two related enterobacterial plant pathogens, *Pectobacterium atrosepticum* and *D. dadantii*, contain only one set of *clpXP* genes (Fig. 3.1A). However, the location of the *clpXP* genes, i.e. between *tig*, encoding a chaperone protein, and *lon*, is conserved among these bacteria. The deduced amino acids of *E. amylovora* ClpP1, ClpX1 and ClpX2 share high identities and similarities with their homologues of *E. coli*, *P. atrosepticum* and *D. dadantii* (Table 3.3); whereas *E. amylovora* ClpP2 is less conserved in both length and deduced amino acid sequence, and the gene also lies in the opposite direction relative to other *clpXP* genes (Fig. 3.1A). Phylogenetic analysis also separated ClpP2 of *E. amylovora* and *E. pyrifoliae* from other ClpP homologues and clustered into another clad (Fig. 3.1B).

To determine the role of ClpXP in *E. amylovora* virulence, a *clpXP* mutant was generated by deleting all four genes (Fig. 3.1A). For complementation, each set of *clpXP* genes, i. e. *clpXP1* and *clpXP2*, were cloned and transformed into the mutant (Fig. 3.1A). Virulence assay on immature pears showed that the *clpXP* mutant caused slightly delayed disease progress as compared to the WT (Fig. 3.2A), indicating that ClpXP contributes to full virulence in *E. amylovora*. The complementation strain carrying pXP1 (containing the *clpXP1* genes), but not pXP2 (containing the *clpXP2* genes), completely restored disease symptoms comparable to the

WT (Fig. 3.2A), indicating that the first set of *clpXP* genes in *E. amylovora* is functional under tested conditions.

Our previous studies showed that Lon plays a major role in *E. amylovora* virulence by negatively regulating T3SS and amylovoran production (Lee et al., 2017). In order to determine the effect of lacking both Lon and ClpXP, a *clpXP*/*lon* mutant was generated. Interestingly, the mutant exhibited noticeable reduction of necrotic lesion on immature pears at 8 DPI, which could also be rescued by pXP1, but not pXP2 (Fig. 3.2B), further suggesting that ClpXP1 are functional under tested conditions and that lack of both ClpXP and Lon leads to noticeable delayed disease progress.

3.4.2 Accumulation of RpoS contributes to delayed disease progress in the *clpXP* mutant

RpoS has been regarded as one of the physiologically important ClpXP substrates (Battesti et al., 2011; Flynn et al., 2003). Under favorable growth conditions and at early growth stage, degradation of RpoS by ClpXP with the aid of RssB restricts its activity post-translationally (Schweder et al., 1996). To determine whether the lack of ClpXP led to RpoS accumulation and thus reduced virulence, deletion mutants of *rpoS* in the WT, *rssB*, *clpXP* and *clpXP*/*lon* mutant backgrounds were generated. Virulence assay showed that the *rpoS*, *rssB* and *rssB*/*rpoS* double mutants were as pathogenic as the WT (Fig. 3.2C). Interestingly, the *clpXP*/*rpoS* mutant exhibited a comparable disease progress as the WT, while deletion of *rpoS* in the *clpXP*/*lon* mutant did not change the *clpXP/lon* mutant in causing reduction of necrotic lesion at 8 DPI (Fig. 3.2C).

To verify whether RpoS is accumulated in *clpXP* mutant and contributes to disease progress, RpoS protein level at different time points in HMM was determined by Western blot. *E. amylovora* grew slowly at first 12 h of incubation (hoi) and reached the stationary phase at 24 hoi in HMM (Fig. 3.3A). Intracellular level of RpoS in *E. amylovora* was maintained at low level until 12 hoi and increased starting at 18 hoi around late exponential or at early stationary phase (Fig. 3.4A). Compared to the WT, RpoS accumulation was about 16- and 7- fold higher in the *clpXP* and *clpXP*/*lon* mutant, and *rssB* mutant at 6 hoi, respectively (Fig. 3.4B). These results indicate that RpoS accumulation is growth-dependent and under the control of RssB and ClpXP. These results also suggest that higher accumulation of RpoS in the *clpXP* mutant might influence its virulence. However, reduced virulence in the *clpXP*/*lon* and *clpXP*/*lon*/*rpoS* mutants might be caused by unknown factors independent of RpoS.

3.4.3 RpoS accumulation leads to reduced expression of the T3SS

In *E. amylovora,* T3SS is activated at early growth stages in nutrient-limited conditions (Ancona et al., 2015b; Wei et al., 2000). Expression of the T3SS genes, *hrpL* and *hrpA*, peaked at 6 hoi *in vitro*, and then the *hrpL* gene expression was reduced to basal level; whereas transcript of *hrpA* was maintained at relative high level until 24 hoi (Fig. 3.3B). To determine the effect of RpoS accumulation on T3SS in the *rssB*, *clpXP* and *clpXP*/*lon* mutants, Western blot analysis of HrpA protein was performed (Fig. 3.4C). The abundance of HrpA was reduced about 3-, 12- and 50-folds in the *rssB, clpXP* and *clpXP*/*lon* mutants, respectively, as compared to the WT. Deletion of *rpoS* in the *rssB* and *clpXP* mutant backgrounds rescued HrpA expression to comparable levels as in the *rpoS* mutant. Deletion of *rpoS* in the *clpXP*/*lon* mutant also increased HrpA protein level similar to that in the *lon* mutant, which is about 2-fold higher than that of the

WT (Lee et al. 2017). These results indicate that RpoS accumulation led to reduced expression of the T3SS.

3.4.4 RpoS suppresses amylovoran production

Previous characterization of the *rpoS* mutant in *E. amylovora* strain CFBP 1430 proposed the regulatory role of RpoS in EPS production and motility (Santander et al., 2014), we therefore determined EPS production in the *clpXP* mutant and its related mutant strains. Amylovoran production was barely detected in the *clpXP* mutant, but increased in its complementation strain with pXP1, indicating that ClpXP positively affects amylovoran production (Fig. 3.5A). Consistently, amylovoran production in the *clpXP*/*lon* mutant was lower than that in the *lon* mutant (Lee et al. 2017) and in the *clpXP*/*lon* complementation strain with pXP1. In contrast, amylovoran production was about 8-fold higher in the *rpoS* mutant as compared to that of the WT (Fig. 3.5B), indicating that RpoS negatively affects amylovoran production. Similar to the *clpXP* mutant, the *rssB* mutant also exhibited reduced amylovoran production, which could be rescued by deletion of *rpoS* in both mutant backgrounds. This further confirms that RpoS negatively affects amylovoran production. On the other hand, the *clpXP*/*lon*/*rpoS* mutant did not show any significant difference in amylovoran production as compared to the *clpXP*/*rpoS* mutant.

3.4.5 ClpXP is required for motility partially by inhibiting RpoS accumulation

Our recent study reported that the *lon* mutant is non-motile mainly due to the accumulation of RcsA/RcsB proteins (Lee et al. 2017). Interestingly, the *clpXP* mutant also exhibited non-motile phenotype, whereas the *clpXP*/*lon* mutant exhibited reduced motility as

compared to the WT (Fig. 3.6A, 3.7). Complementation of the *clpXP*/*lon* mutant with pXP1 returned to the non-motile phenotype like the *clpXP* or *lon* mutant, while the non-motile phenotype of the *clpXP* mutant could not be rescued by pXP1. On the other hand, the *rpoS*, *rssB* and *rpoS*/*rssB* mutants all exhibited reduced motility as compared to the WT (Fig. 3.6B, 3.7). Deletion of *rpoS* rendered the cell motile in the *clpXP* mutant, indicating that ClpXP positively affects motility in *E. amylovora* possibly by inhibiting RpoS accumulation. However, unexpectedly, the *clpXP*/*lon*/*rpoS* mutant also exhibited the non-motile phenotype (Fig. 3.6B, 3.7). Some of these results seemingly contradicted with each other, suggesting that explaining what controls motility might be difficult at this stage.

3.5 Discussion

Post-translational regulation effectively controls various metabolic enzymes and transcription factors under changing environmental conditions (Sauer and Baker, 2011). ClpXP, an intracellular protease belonging to the AAA^+ family protein, is known to be responsible for regulating more than 50 functional proteins (Flynn et al., 2003). One of its major substrates is RpoS sigma factor, which affects the expression of genes necessary for growth at stationary phase, stress responses and virulence (Patten et al., 2004; Battesti et al., 2011). In this study, we showed that ClpXP contributes to *E. amylovora* virulence by delaying RpoS accumulation. If accumulated at high level, RpoS suppresses T3SS gene expression, amylovoran production, and motility. In addition, *E. amylovora* lacking both ClpXP and Lon exhibited reduced virulence independent of RpoS, suggesting that ClpXP and/or Lon proteases are indispensable to maintain certain functions for *E. amylovora* virulence.

ClpXP has been shown to activate full T3SS gene expression in several enterobacterial pathogens. In EHEC, mutation in *clpXP* caused significantly reduced expression of the enterocyte effacement (LEE)-encoded T3SS genes due to accumulation of GrlR and RpoS (Iyoda and Watanabe, 2005). Increased levels of GrlR in *E. coli clpXP* mutant directly inhibit the activity of GrlA, which positively regulates Ler (LEE-encoded regulator), the master regulator of T3SS genes (Deng et al., 2004). *Yersinia pestis* utilizes both ClpXP and Lon to activate T3SS by degrading a small histone-like protein YmoA, which represses LcrF, the master regulator of T3SS genes (Hoe and Goguen, 1993; Jackson et al., 2004; Lambert de Rouvroit et al., 1992). In the soft rot plant pathogen *D. dadantii*, ClpXP-dependent RpoS degradation has been proposed to positively regulate T3SS by lowering the expression of an RNA-binding protein RsmA (repressor of secondary metabolites), a homologue of CsrA (Ancona et al. 2016; Li et al., 2010). Analysis of promoter sequence in *E. coli* showed that the *csrA* gene has two RpoS-dependent promoters (Yakhnin et al., 2011). In this study, we also found that excess accumulation of RpoS at early growth stage suppresses T3SS gene expression. However, in *E. amylovora*, CsrA positively regulates various virulence traits, including T3SS and amylovoran (Ancona et al., 2016).

Lon, AmyR (amylovoran repressor), and several two-component systems were previously identified as negative regulators of amylovoran production in *E. amylovora* (Lee et al., 2017; Li et al., 2014; Wang et al., 2012; Zhao et al., 2009b). In this study, we provided evidence that RpoS also acts as a negative regulator of amylovoran production as previously reported (Santander et al., 2014). This is also consistent with previous findings in *E. coli* that the *rpoS* mutant overproduces EPS (Ferrieres et al., 2009; Ionescu and Belkin, 2009). It has been

suggested that EPS overproduction in the *rpoS* mutant is an adaptive response, since both RpoS and EPS contribute to cell survival in stress conditions (Battesti et al., 2011; Flemming et al., 2007). Transcriptome analyses in *E. coli* revealed that the *rpoS* mutant exhibits increased transcript level of *rcsA*, which encodes RcsA, a rate-limiting factor in EPS production (Dong et al., 2010; Ionescu and Belkin, 2009). On the other hand, the Rcs phosphorelay system also activates small RNA RprA to promote translation initiation of *rpoS* (Majdalani et al., 2001, 2002), suggesting that RpoS might negatively regulate EPS production through the Rcs phosphorelay system.

In EHEC and *Salmonella*, ClpXP negatively regulates FlhDC, the master regulator of flagellar gene expression, at the post-translational levels, and the *clpXP* mutants are hyper-flagellated (Kitagawa et al., 2011; Tomoyasu et al., 2002, 2003). In contrast, the *clpXP* mutant of *E. amylovora* exhibited the non-motile phenotype, which could be partially rescued by deletion of *rpoS*. Previously, we have demonstrated that accumulation of RcsA/RcsB in the *lon* mutant causes the non-motile phenotype (Lee et al., 2017). In *E. amylovora*, RcsA/RcsB binds to the promoter of *flhDC*, and its accumulation negatively regulates motility by inhibiting transcription initiation of *flhDC*. Interestingly, the *clpXP*/*lon* mutant recovered motility, while the *clpXP*/*lon*/*rpoS* mutant exhibited the non-motile phenotype. Since mutation in the *rpoS* gene in the *clpXP* mutant rescued the amylovoran production, the *clpXP*/*lon*/*rpoS* might have increased levels of RcsA/B, which would block motility. However, the effect of *lon* deletion on motility of the *clpXP* mutant remains unexplained.

Taken together, we provided evidence that ClpXP-dependent degradation of RpoS contributes to *E. amylovora* virulence. As a sixth dissociable subunit of RNAP, sigma factor plays a critical role in the regulation of transcription initiation in bacteria. RpoD (sigma factor 70) acts as a primary sigma factor responsible for the expression of essential genes, while alternative sigma factors such as RpoN and RpoS activate expression of the subset of genes implicated in diverse cellular functions, including virulence and stress responses (Gruber and Gross, 2003). The RpoN-HrpL alternative sigma factor cascade directs the expression of all T3SS genes in *E. amylovora* (Ancona et al., 2014; McNally et al., 2012; Wei and Beer, 1995). Transcription of structural components of flagella apparatus is also activated by FliA (sigma factor 28) (Liu and Matsumura, 1995). Since the total level of sigma factors in the cell exceeds that of core-RNAP, competition between sigma factors occurs and leads to antagonistic effects on gene expression (Grigorova et al., 2006; Piper et al., 2009; Ö sterberg et al., 2011). RpoS accumulation during stationary phase down-regulates the expression of several genes under control of RpoD and FliA (Patten et al., 2004; Weber et al., 2005). Mutation in *rpoS* also up-regulates about 60% of RpoN-dependent genes (Dong et al., 2011; Patten et al., 2004). Therefore, it is reasonable to assume that higher levels of RpoS in the *rssB*, *clpXP* and *clpXP*/*lon* mutants might outcompete other sigma factors, resulting in over-expression of RpoS regulon and suppression of virulence genes.

In summary, our results showed that ClpXP positively contributes to *E. amylovora* virulence by maintaining certain levels of RpoS in the cell. However, reduced virulence of the *clpXP/lon* double mutant might be independent of RpoS. Future research should focus on understanding genes under control of RpoS, ClpXP and Lon that affect *E. amylovora* virulence.

3.6 Tables

Table 3.1 Bacterial strains and plasmids used in this study

Strains, Plasmids	Description	Reference, Source
E. amylovora		
Ea1189	Wild type, isolated from apple	Wang et al., 2009
Δ*lon*	*lon*::Cm; Cm^R-insertional mutant of *lon* of Ea1189	Lee et al., 2017
Δ*clpXP*	*clpP1*,*clpX1*,*clpP2*,*clpX2*::Cm; Cm^R-insertional mutant of *clpXP* of Ea1189	This study
Δ*clpXP*/*lon*	*clpP1*,*clpX1*,*clpP2*,*clpX2*,*lon*::Cm; Cm^R-insertional mutant of *clpXP*/*lon* of Ea1189	This study
Δ*rpoS*	*rpoS*::Cm; Cm^R-insertional mutant of *rpoS* of Ea1189	This study
Δ*rssB*	*rssB*::Cm; Cm^R-insertional mutant of *rssB* of Ea1189	This study
Δ*clpXP*/*rpoS*	*rpoS*::Cm, *clpP1*,*clpX1*,*clpP2*,*clpX2*::Km; Km^R-insertional mutant of *clpXP* of Δ*rpoS*	This study
Δ*clpXP*/*lon*/*rpoS*	*rpoS*::Cm, *clpP1*,*clpX1*,*clpP2*,*clpX2*,*lon*::Km; Km^R-insertional mutant of *clpXP*/*lon* of Δ*rpoS*	This study
Δ*rssB*/*rpoS*	*rpoS*::Cm, *rssB*::Km; Km^R-insertional mutant of *rssB* of Δ*rpoS*	This study
E. coli		
DH10B	F– *mcr*A Δ(*mrr-hsd*RMS-*mcr*BC) Φ80*lac*ZΔM15 Δ*lac*X74 *rec*A1 *end*A1 *ara*D139 Δ(*ara leu*) 7697 *gal*U *gal*K *rps*L *nup*G λ-	Invitrogen
Plasmids		
pKD46	ApR, PBAD *gam bet exo* pSC101 oriTS	Datsenko and Wanner, 2000
pKD32	Cm^R, FRT *cat* FRT tL3 oriR6Kγ *bla rgnB*	Datsenko and Wanner, 2000
pKD13	Km^R, FRT *kan* FRT tL3 oriR6Kγ *bla rgnB*	Datsenko and Wanner, 2000
pWSK29	Ap^R, cloning vector, low copy number	Wang and Kushner, 1991
pXP1	2848-bp DNA fragment containing promoter sequence of *clpP1* and *clpX1* genes in pWSK29	This study
pXP2	2618-bp DNA fragment containing promoter sequence of *clpP2* and *clpX2* genes in pWSK29	This study
pRpoS-His6	1893-bp DNA fragment containing promoter and coding sequence of *rpoS* gene and c-terminal His-tag in pWSK29	This study
pHrpA-His6	803-bp DNA fragment containing promoter and coding sequence of *hrpA* gene and c-terminal His-tag in pWSK29	Ancona et al., 2015b

Table 3.2 Primers used in this study

Primer	Sequences (5' to 3')
Primers for mutation	
clpXP-F	ATGTCATACAGTGGCGAACGTGAATTAACTGCACCTCATATGGCCTTGGTCGATTG TGTAGGCTGGAGCT
clpXP-R	TTATTCACCAGACACCTGCTGAACGTCCGATTTACCATAAATTAGCAGCGATTCCG GGGATCCGTCGACC
lon-R	CTATTTTACCGAGGCAACCTGCATGCCATAAGGTGCATTTTGCAGCGCCAATTCCG GGGATCCGTCGACC
rpoS-F	ATGAGCCAGAATACGCTGAAAGTTAACGAGTTAAATGAAGACGCGGAATTGTGTA GGCTGGAGCTGCTTC
rpoS-R	TCATTCACGGAAGAGTGCTTCAATACTCAATCCCTGCCCCTGCAGTATTTCATATGA ATATCCTCCTTA
rssB-F	ATGGAAAAGCCATTAACAGGAAAACATATTCTCATCGTTGAGGACGAAGTCGATT GTGTAGGCTGGAGCT
rssB-R	CTATAATGTAGACAGCATGAGGCGCAAACGACCACCCGCCCCCCAGACCTATTCC GGGGATCCGTCGACC
clpXP-C1	CCTGGTTAGCAGTTGATAAAAA
clpXP-C2	GCTCAGGATTCATAGAGCTCTC
lon-C2	CGGCCTGCAAAGATTCTGTT
rpoS-C1	CAGCAGGTGTCTGGTGAATA
rpoS-C2	CGGCCTGCAAAGATTCTGTT
rssB-C1	CAGACTGTTCTGCCAGCGGC
rssB-C2	AGACATCAAAATACCTCTCT
Cm1	TTATACGCAAGGCGACAAGG
Cm2	GATCTTCCGTCACAGGTAGG
Km1	CAGTCATAGCCGAATAGCCT
Km2	CGGTGCCCTGAATGAACTGC
Primers for cloning	
ClpXP1-F	AGTAGGTACCAGAGATGGCTTCCGCATATGA
ClpXP1-R	AGTAGGATCCCGCTGCCTAATACCCGCTTTA
ClpXP2-F	AGTAGGTACCACAGCAAGGGAGATACCCAG
ClpXP2-R	AGTAGGATCCGATCCATGGCGGCTTCAAGGC
RpoS-His-F	AGTAGGTACCTGCCGGCACGCAGATGAA
RpoS-His-R	TCAGGAGCTCTCAGTGATGATGATGATGATGTTCACGGAAGAGTGCTTCAATA

Table 3.3 Percentage of identity and similarity of deduced amino acid sequences for ClpXP in *Erwinia amylovora* and related enterobacterial species

Protein	Length	Identity	Similarity	Protein	Length	Identity	Similarity
Ea ClpP1	207	-	-	Ea ClpX1	424	-	
Ea ClpP2	198	36.4	68.2	Ea ClpX2	424	98.3	99.1
Ep ClpP1	207	99	99	Ep ClpX1	424	98.8	99.8
Ep ClpP2	198	36.4	68.9	Ep ClpX2	424	97.2	98.6
Ec ClpP	207	87.4	96.6	Ec ClpX	424	91.5	97.6
Pa ClpP	207	88.4	96.1	Pa ClpX	424	90.3	97.2
Dd ClpP	207	87.9	96.6	Dd ClpX	424	89.2	96.5

Ea, *Erwinia amylovora*; Ep, *Erwinia pyrifoliae*; Ec, *Escherichia coli*; Pa, *Pectobacterium atrosepticum*; Dd, *Dickeya dadantii*.

3.7 Figures

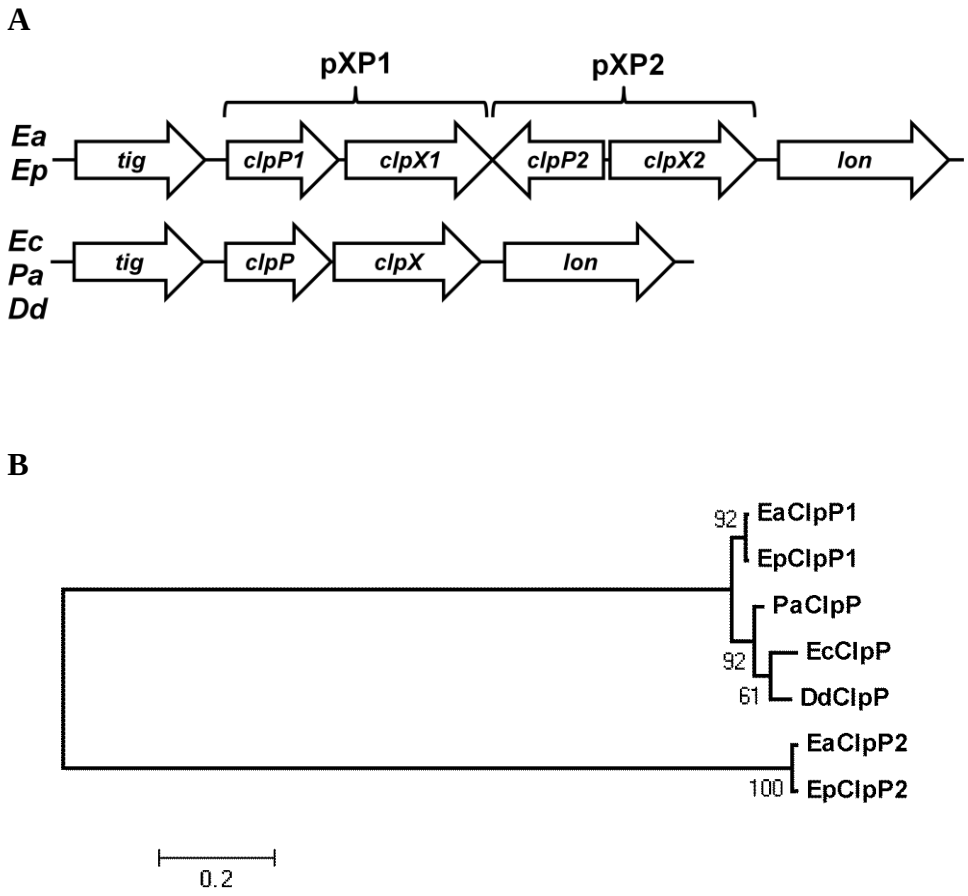

Figure 3.1 Comparison of ClpXP in *Erwinia amylovora* and other related species. (A) Schematic maps of the *clpP* and *clpX* genes. For complementation of the mutant strains, plasmids pXP1, containing *clpP1* and *clpX1*, and pXP2, containing *clpP2* and *clpX2*, were constructed. (B) Phylogenetic tree of ClpP proteins. Based on deduced amino acid sequences, a phylogenetic neighbor-joining tree was generated using MEGA 5.0, and bootstrap values were indicated at each node. Ea, *Erwinia amylovora*; Ep, *Erwinia pyrifoliae*; Ec, *Escherichia coli*; Pa, *Pectobacterium atrosepticum*; Dd, *Dickeya dadantii*

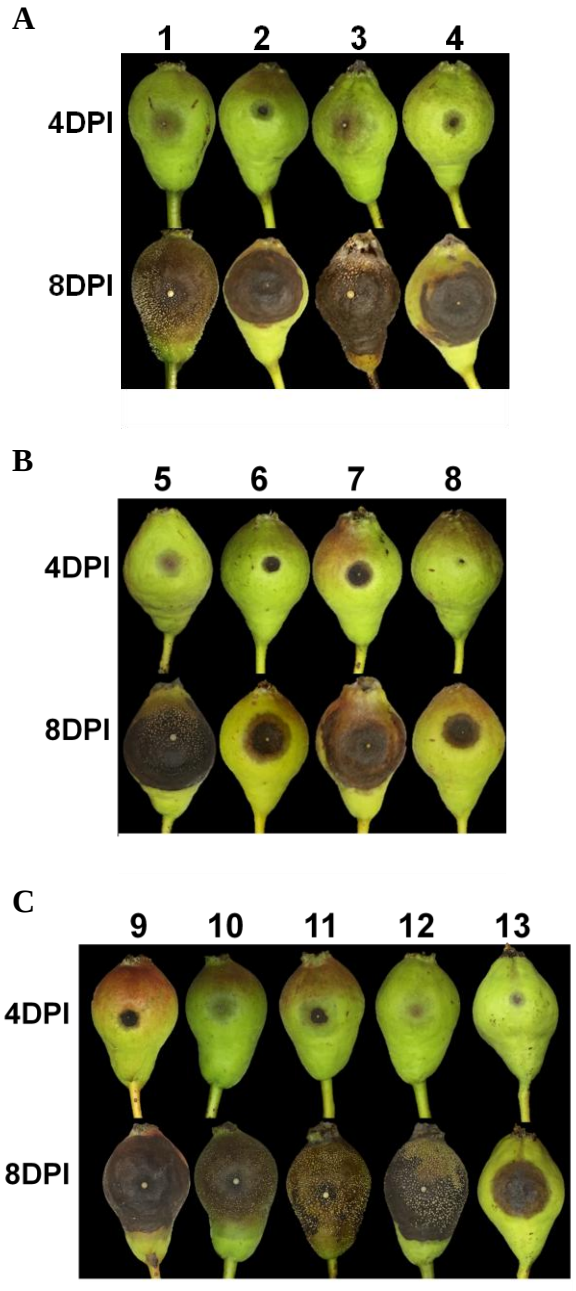

Figure 3.2 ClpXP contributes to virulence in *Erwinia amylovora* possibly by affecting RpoS accumulation. (A, B, C) Disease symptoms caused by the wilt-type (WT), mutants and complementation strains on immature pear fruits at 4 and 8 days post-inoculation (DPI). 1, Ea1189 WT; 2, *clpXP*; 3, *clpXP* (pXP1); 4, *clpXP* (pXP2); 5, *lon*; 6, *clpXP*/*lon*; 7, *clpXP*/*lon* (pXP1); 8, *clpXP*/*lon* (pXP2); 9, *rpoS*; 10, *rssB*; 11, *rssB*/*rpoS*; 12, *clpXP*/*rpoS*; 13, *clpXP*/*lon*/*rpoS*.

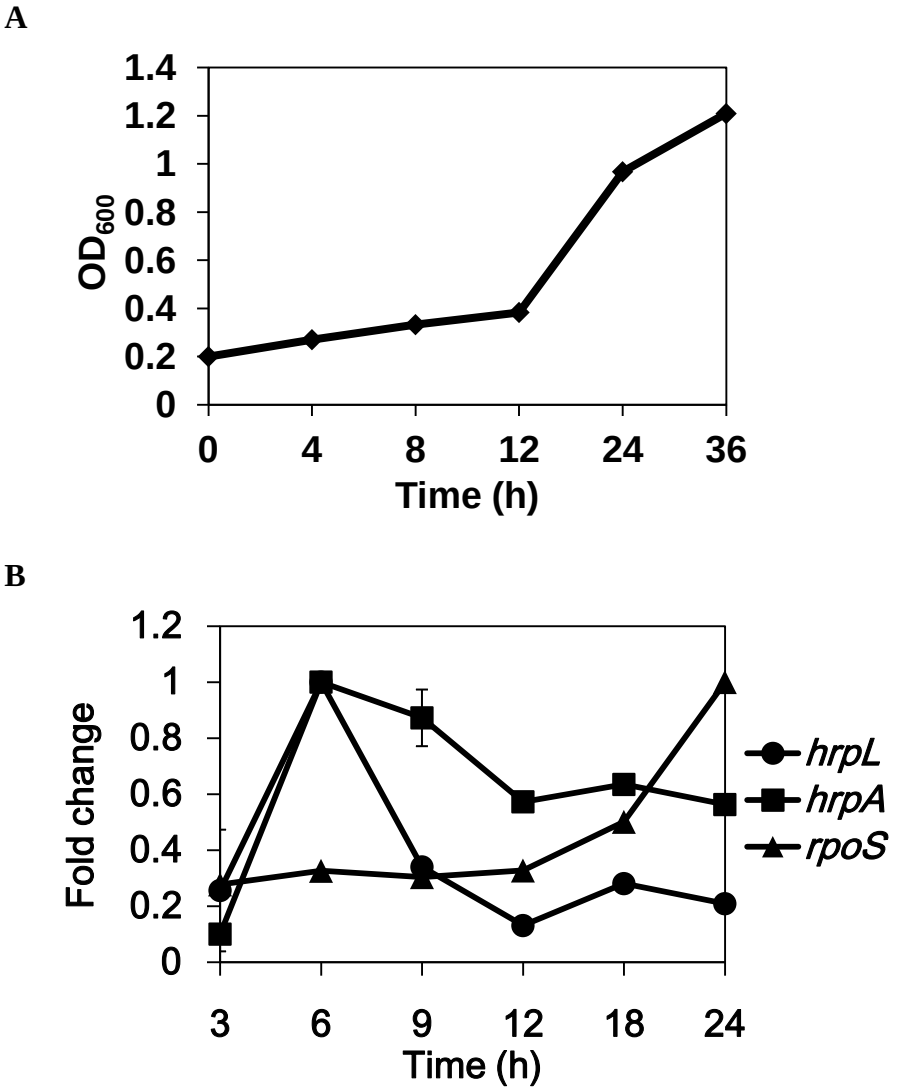

Figure 3.3 Time course analysis of *rpoS*, *hrpL* and *hrpA* transcription in *Erwinia amylovora*. (A) Growth curve of *E. amylovora* wild-type (WT) in *hrp*-inducing minimal medium (HMM) at 18 ℃. (B) Relative gene expression of *rpoS*, *hrpL* and *hrpA* genes in the WT grown in HMM at different time points at 18 ℃. Three replicates were performed for each biological sample and the experiment was repeated. The *rpoD* gene was used as an endogenous control to calculate relative gene expression. The values of fold changes are the means of three replicates. Error bars indicate standard deviation.

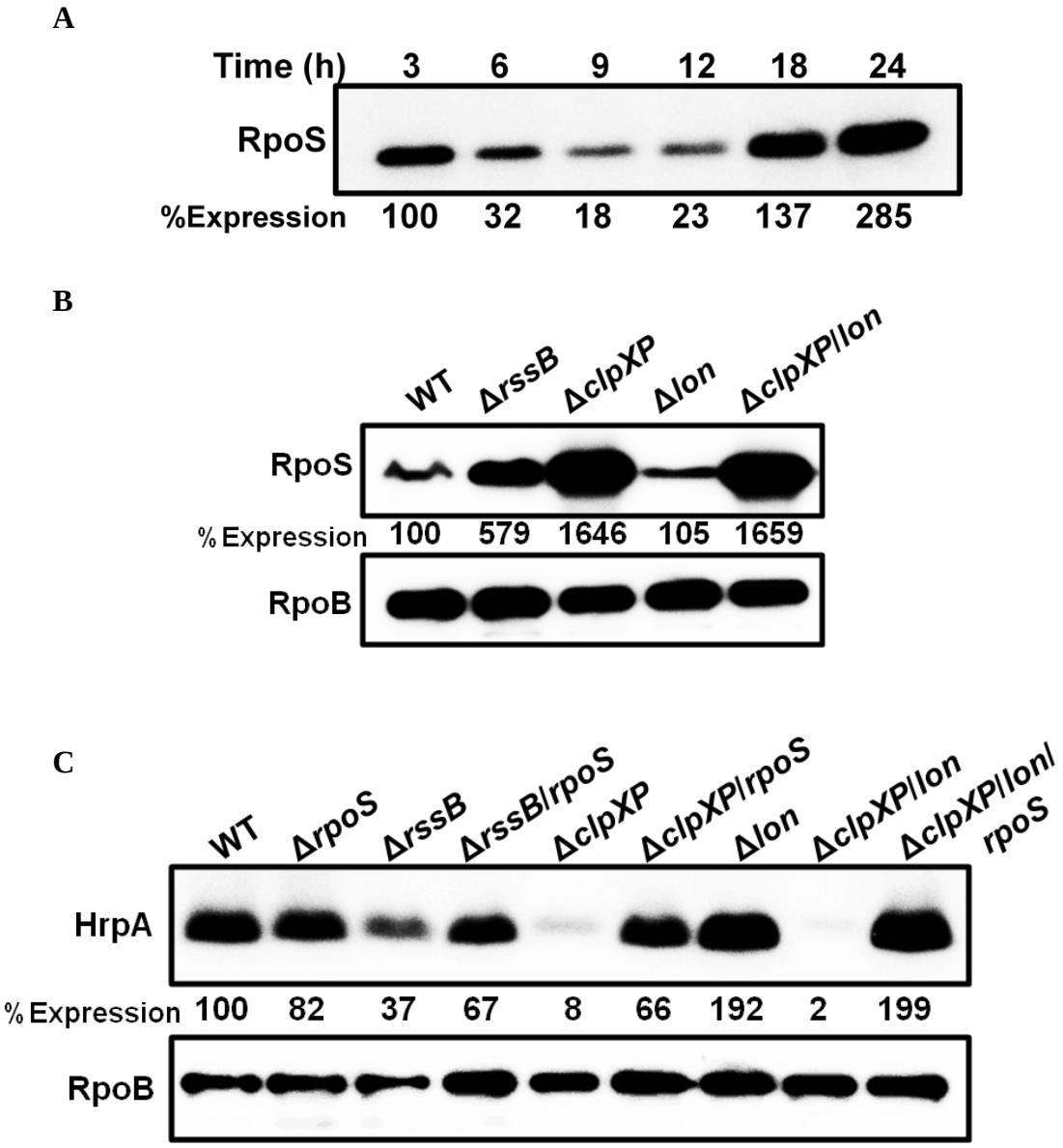

Figure 3.4 ClpXP/RssB-dependent RpoS degradation contributes to T3SS gene expression. (A) Abundance of RpoS-His6 protein in the wild-type (WT) grown in *hrp*-inducing minimal medium (HMM) at different hours of inoculation at 18 ℃. (B) Abundance of RpoS-His6 protein in the WT and mutant strains grown in HMM at 18 ℃ for 6 h. (C) Abundance of HrpA-His6 protein in the WT and mutant strains grown in HMM at 18 ℃ for 6 h. Abundance of the RpoB protein was used as a loading control, and relative protein abundance (% expression) was calculated using ImageJ software. These experiments were repeated three times with similar results.

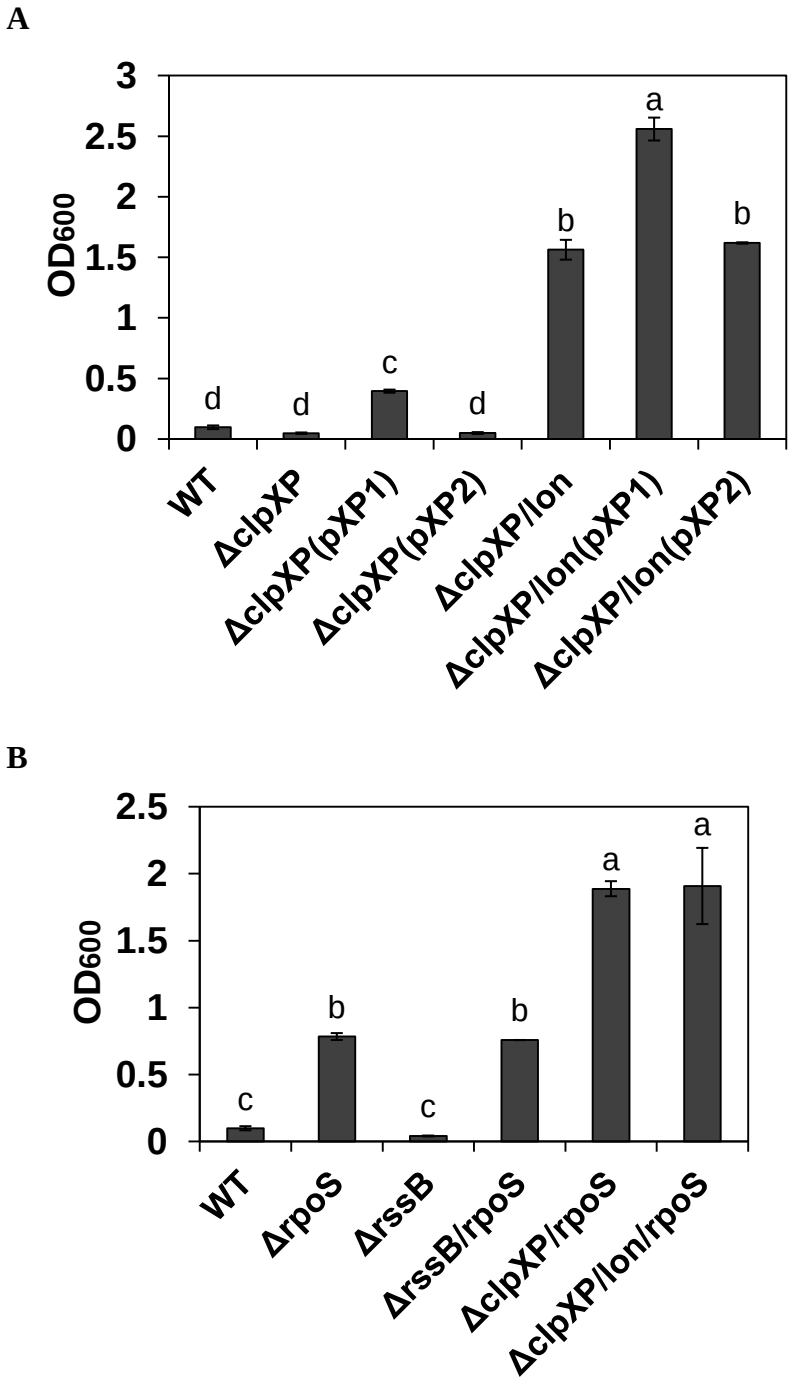

Figure 3.5 ClpXP affects amylovoran production by inhibiting RpoS accumulation. (A, B) Amylovoran production of the wild-type (WT), mutants and complementation strains grown in MBMA medium at 28 ℃ for 24 h. Presented values are representative of three independent experiments with similar results. Error bars indicate standard deviation of three replicates. The values marked with the same letter do not differ significantly ($P < 0.05$).

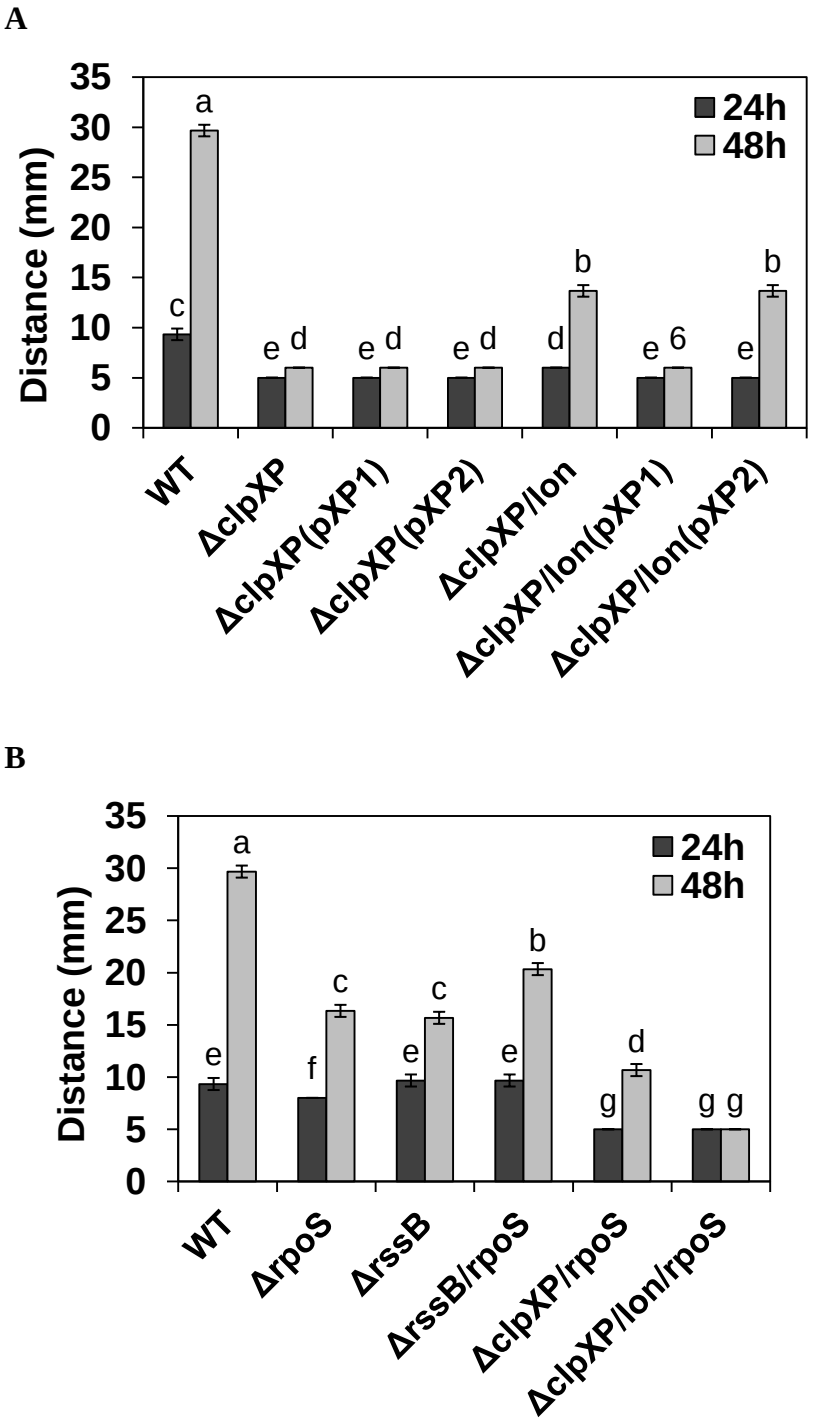

Figure 3.6 ClpXP affects motility partially by inhibiting RpoS accumulation. (A, B) The moving distance of the WT and mutant strains on the motility plate. Diameters of the circle around the inoculation site (mm) were measured at 24 and 48 h of inoculation. Presented values are representative of three independent experiments with similar results. Error bars indicate standard deviation of three replicates. The values marked with the same letter do not differ significantly ($P < 0.05$).

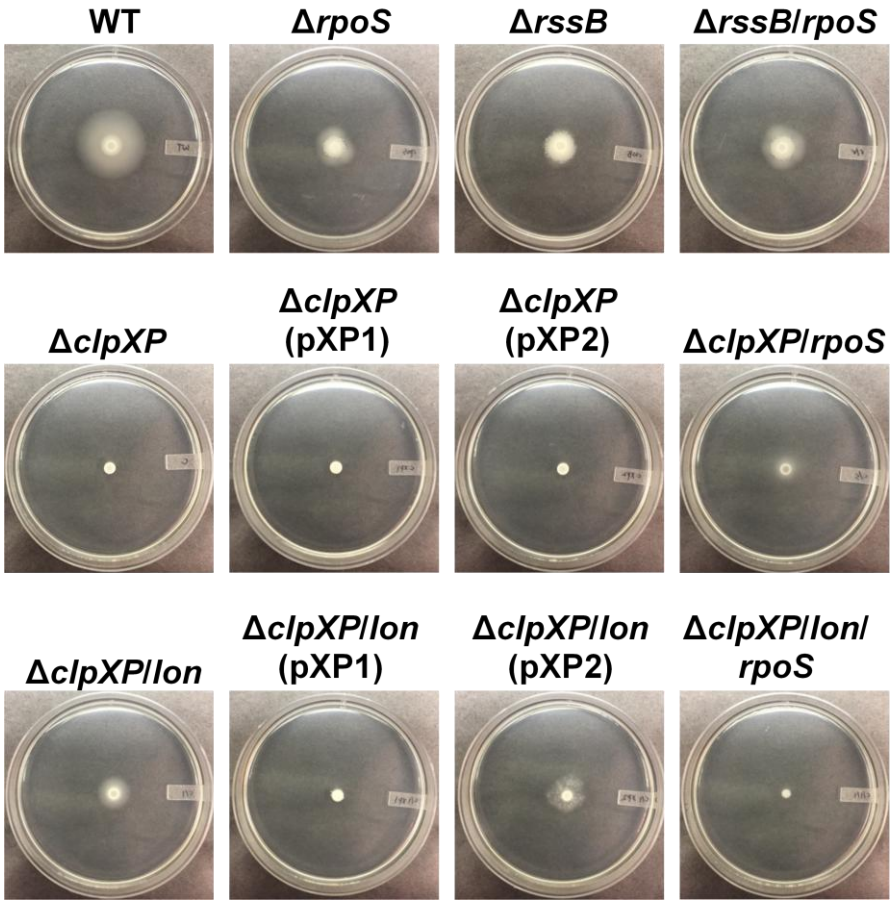

Figure 3.7 Movement of the WT, mutant and complementation strains on the motility plates. Pictures were taken at 48 h of inoculation.

CHAPTER 4

Integration of multiple stimuli-sensing systems to regulate HrpS and type III secretion system in *Erwinia amylovora*

4.1 Abstract

The bacterial enhancer binding protein (bEBP) HrpS is essential for *Erwinia amylovora* virulence by activating the type III secretion system (T3SS). However, how the *hrpS* gene is regulated remains poorly understood in *E. amylovora*. In this study, 5' rapid amplification of cDNA ends and promoter deletion analyses showed that the *hrpS* gene contains two promoters driven by HrpX/HrpY and the Rcs phosphorelay system, respectively. Electrophoretic mobility shift and gene expression assays demonstrated that integration host factor IHF positively regulates *hrpS* expression through directly binding the *hrpX* promoter and positively regulating *hrpX/hrpY* expression. Moreover, *hrpX* expression was down-regulated in the *relA*/*spoT* ((p)ppGpp-deficient) mutant and the *dksA* mutant, but up-regulated when the wild-type strain was treated with serine hydroxamate, which induced (p)ppGpp-mediated stringent response. Furthermore, the *csrA* mutant showed significantly reduced transcripts of major *hrpS* activators, including the *hrpX*/*hrpY*, *rcsA* and *rcsB* genes, indicating that CsrA is required for full *hrpS* expression. On the other hand, the *csrB* mutant exhibited up-regulation of the *rcsA* and *rcsB* genes, and *hrpS* expression was largely diminished in the *csrB*/*rcsB* mutant, indicating that the Rcs system is mainly responsible for the increased *hrpS* expression in the *csrB* mutant. These findings suggest that *E. amylovora* recruits multiple stimuli-sensing systems, including HrpX/HrpY, the Rcs phosphorelay system and the Gac-Csr system, to regulate *hrpS* and T3SS gene expression.

4.2 Introduction

Erwinia amylovora, the causal agent of fire blight on apple and pear trees, utilizes the hypersensitive response and pathogenicity (*hrp*)-type III secretion system (T3SS) as an essential virulence factor. The *hrp*-T3SS is believed to contribute to the early stages of infection by suppressing host defense responses and promoting bacterial growth (Büttner 2012; Zhao 2014). In *E. amylovora*, structural and functional components of the *hrp*-T3SS are encoded in the *hrp*-pathogenicity island (PAI), and their expression is under control of the master regulator HrpL (Wei and Beer 1995; Oh and Beer 2005; McNally et al. 2012). HrpL belongs to the extracytoplasmic function (ECF) sigma factor, which generally responds to external stimuli by regulating its activity through interaction with an anti-sigma factor (Mascher 2013). However, in *E. amylovora*, no anti-sigma factor has been reported for HrpL, and its activity is regulated at the transcription level by sigma factor 54 (RpoN), bacterial enhancer binding protein (bEBP) HrpS, integration host factor IHF, and RpoN-modulation protein YhbH (Ancona et al. 2014; Lee and Zhao 2016; Wei et al. 2000). In contrast to sigma factor 70-family members, the RpoN-RNA polymerase (RNAP) holoenzyme forms transcriptionally silent closed complex, which is hardly converted to an open complex without energy input (Guo et al. 2000). To initiate transcription, bEBP must bind to DNA and remodel the holoenzyme-DNA complex (Bush and Dixon 2012). Since the HrpS-binding site on the *hrpL* promoter region is relatively far upstream of the transcription start site, IHF is required to allow interaction between the holoenzyme and HrpS by bending DNA (Lee et al. 2016; Lee and Zhao 2016). YhbH, also known as hibernation promoting factor, is deemed as an essential factor for *hrpL* transcription, but its exact role remains unclear (Ancona et al. 2014; Ueta et al. 2005).

The *hrp*-T3SS gene expression of *E. amylovora* is induced at early growth stages in the apoplast-like conditions, such as low pH and low available nutrients (Wei et al. 1992; Yang et al. 2014). The RelA-SpoT homologue (RSH) proteins detect various nutrient-limiting conditions and control levels of linear nucleotide second messengers, guanosine tetraphosphate (ppGpp) and guanosine pentaphosphate (pppGpp), collectively referred to (p)ppGpp (Dalebroux and Swanson 2012; Potrykus and Cashel 2008). Stress responses coordinated by (p)ppGpp ultimately redirect the global transcriptional capacity of the cell from genes for growth and reproduction towards those for survival and thus, is referred to as the ‘‘stringent response’’(Kalia et al. 2013**).** Accumulation of (p)ppGpp leads to global transcriptional reprogramming by interacting with RNAP and its cofactor DksA and increasing interaction between RNAP and alternative sigma factors (Kalia et al. 2013). Both (p)ppGpp and DksA are essential for the activation of the RpoN-HrpL alternative sigma factor cascade during T3SS gene expression and virulence in *E. amylovora* (Ancona et al. 2015b).

Two component signal transduction systems (TCSTs) also play a major role in T3SS regulation in *E. amylovora*. The HrpX/HrpY system, conserved in enterobacterial plant pathogens, activates the T3SS through *hrpS* expression, where HrpX senses environmental /intracellular signals to phosphorylate HrpY (response regulator) (Wei et al. 2000; Zhao et al. 2009b), while the GacS/GacA and EnvZ/OmpR systems act as negative regulators of the T3SS (Li et al. 2014). In particular, GacS/GacA is closely associated with the Csr post-transcriptional regulatory system through the small regulatory RNA *csrB*, which negatively affects the RNA-binding protein CsrA activities (Ancona et al. 2016; Zere et al. 2015). Although the exact molecular details of CsrA action remain to be determined, its pleiotropic effects on diverse

cellular processes are believed to be critical for the T3SS (Ancona et al. 2016; Lee et al. 2017). Recent studies showed that the enterobacterial-specific Rcs phosphorelay system is also involved in T3SS regulation by activating *hrpS* expression and suppressing *csrB* expression (Lee et al. 2017). The Rcs system is an unusual complex TCST, comprised of three core proteins RcsBCD and one auxiliary protein RcsA without the phosphorylation site. RcsB homodimer or RcsA/RcsB heterodimer binds to conserved RcsAB box to regulate gene expression (Ancona et al. 2015a; Lee and Zhao 2017). In addition to TCSTs, Lon protease, small RNA chaperone Hfq, base-pairing sRNAs and cyclic di-GMP are also reported to contribute to T3SS regulation in *E. amylovora* (Edmunds et al. 2013; Lee et al. 2017; Zeng et al. 2013).

It has been revealed that HrpS is likely to serve only as an activator for *hrpL* transcription in *E. amylovora* based on the HrpS-binding sequence analysis (Lee et al. 2016). In general, bEBPs respond to environmental signals through the N-terminal sensory domain; however, in *E. amylovora*, HrpS contains no such domain, and no alternative regulatory mechanism besides Lon-dependent degradation is currently known at the protein level (Lee et al. 2017). In the closely related plant pathogens, such as *Dickeya* and *Pantoea*, HrpX/HrpY is critical for the expression of *hrpS* and thus downstream T3SS genes (Merighi et al. 2003; Yap et al. 2005), while *E. amylovora* HrpX/HrpY is dispensable for the T3SS and virulence (Zhao et al. 2009b). Therefore, we hypothesized that novel regulatory network of T3SS gene expression may exist in *E. amylovora*. In this study, we showed that transcription of the *hrpS* gene is directly driven by two TCSTs, the HrpX/HrpY and the Rcs phosphorelay systems, both of which are positively regulated by CsrA. Our results further demonstrated that IHF and (p)ppGpp are required for *hrpS* transcription by activating *hrpX*/*hrpY* expression.

4.3 Materials and methods

4.3.1 Bacterial strains and growth conditions

Bacterial strains and plasmids used in this study are listed in Table 4.1. LB broth was used for routine culture of *E. amylovora* and *Escherichia coli* strains, and a *hrp*-inducing medium (HMM) (1g $(NH_4)_2SO_4$, 0.246 g $MgCl_2 \cdot 6H_2O$, 0.1 g NaCl, 8.708 g K_2HPO_4, 6.804 g KH_2PO_4) was used for T3SS gene expression. When required, antibiotics were used at the following concentrations: 100 μg ml^{-1} ampicillin (Ap), 50 μg ml^{-1} kanamaycin (Km), 10 μg ml^{-1} chloramphenicol (Cm) and gentamicin (Gen) 10 μg ml^{-1}. Primers used for 5' rapid amplification of cDNA ends (5' RACE), construction of the *lacZ* transcriptional fusions, real-time quantitative reverse transcription PCR **(**qRT-PCR) and electrophoretic mobility shift assay (EMSA) are listed in Table 4.2.

4.3.2 5' rapid amplification of cDNA ends (5' RACE)

5' RACE analysis was performed using the 5'/3' RACE kit (Roche, Mannheim, Germany) according to the manufacturer's instruction. Briefly, total RNA isolated from cell cultures grown in HMM for 6 h at 18 ℃ was reverse-transcribed using HrpS-SP1 primer. The resulting cDNA was purified using a QIAquick PCR purification kit (Qiagen, Hilden, Germany) and poly A-tailed at the 3' end. The resulting product was PCR-amplified using oligo dT-anchor primer, HrpS-SP2 and HrpS-SP3 primers and cloned into the pGEM-T Easy vector (Promega, Madison, WI). DNA sequencing was performed at the Keck center for functional and comparative genomics at the University of Illinois at Urbana-Champaign (UIUC). The experiment was repeated three times.

4.3.3 β-galactosidase assay

β-galactosidase assay was performed using a microtiter plate as described previously (Slauch and Silhavy 1991). Briefly, cell cultures grown in HMM for 6 h at 18 ℃ were collected and resuspended in Z-buffer (Miller 1972). After measuring OD_{600}, cell suspensions were treated with 1% SDS and chloroform, and reaction was initiated by adding 10 mg/ml *o*-nitrophenyl galactoside (ONPG). Units for β-galactosidase assay are defined as (μmol of ONP formed per minute) x 10^6/(OD_{600} x ml of cell suspension) and reported as means ± standard deviation. Constructs of four *hrpS-lacZ* (Fig. 4.1) and *hrpX-lacZ* transcriptional fusions were generated using vector pHRP309 (Parales and Harwood 1993), and cloned inserts were confirmed by sequencing at the Keck center at UIUC. The assay was repeated three times, and statistical analysis was performed using Student's *t*-test with $P < 0.05$ considered as statistically significant.

4.3.4 Quantitative real-time PCR (qRT-PCR)

RNA was isolated from cell cultures grown in HMM for 6 h at 18 ℃ using RNeasy® mini kit (Qiagen, Hilden, Germany) according to the manufacturer's instruction. For inducing (p)ppGpp-mediated stringent response, cells were treated with serine hydroxamate (SHX) at final concentration of 250 μg/ml for 30 min before RNA isolation. DNaseI treatment and reverse transcription were performed using TURBO DNA-free kit (Ambion, TX, USA) and Superscript III reverse transcriptase (Invitrogen, Carlsbad, CA). RNA quality and quantity was determined using Nano-Drop ND100 spectrophotometer (Nano-Drop Technologies, Wilmington, DE, USA).

qRT-PCR reaction mixtures were prepared by adding cDNA samples, Power SYBR® Green PCR master mix (Applied Biosystems, CA, USA) and appropriate primers, and incubated

under the following conditions: 95 ℃ for 10 min, followed by 40 cycles of 95 ℃ for 15 s and 60 ℃ for 1 min in the StepOnePlus Real-Time PCR system (Applied Biosystems). Primer specificities were evaluated by measuring the melting curves after the cycles. The *rpoD* gene was used as an endogenous control to calculate relative quantification (ΔΔCt). The experiment was repeated three times, and statistical analysis was performed using Student's *t*-test with $P < 0.05$ considered as statistically significant.

4.3.5 Electrophoretic mobility shift assay (EMSA)

EMSA using *E. coli* IHFαβ (a gift from Professor J. Gardner at UIUC) was performed as described previously (Lee and Zhao 2016). Briefly, two complementary oligonucleotides (Table 4.2) containing the target region of *E. amylovora* genome were 3' biotinylated using the biotin 3' end DNA labeling kit (Pierce) and mixed together for annealing according to the manufacturer's instruction. Reaction mixtures were prepared using lightshift® chemiluminescent EMSA kit (Pierce) in volumes of 10 µl, containing 20 fmol of labeled oligonucleotides, different amounts of protein, 1X binding buffer, 50 ng/µl Poly(dI·dC), 0.5mM MgCl2, 0.1% Nonidet P-40, 0.05 mg/ml BSA and 5% glycerol. After incubation at room temperature for 20 min, reaction mixtures were mixed with 5X loading buffer and loaded on a 6% native polyacrylamide gel in 0.5X TBE buffer (44.5 mM Tris-base, 44.5 mM Boric acid and 1 mM EDTA). DNA-protein complexes were then UV cross-linked to a positively charged nylon membrane, and the chemiluminescent signals were detected using ImageQuant LAS 4010 CCD camera (GE Healthcare). The experiment was repeated three times.

4.4 Results

4.4.1 Transcription of the *hrpS* gene is activated by two promoters dependent upon HrpX/HrpY and the Rcs phosphorelay system

In order to determine how the *hrpS* gene is transcriptionally activated, 5' RACE was performed to identify *hrpS* transcription start sites (TSSs) under the *hrp*-inducing condition. Two TSSs were detected at -227 and -129 bp relative to the *hrpS* start codon. Close to each TSS, putative σ^{70}-binding sites located at -235 and -137 bp were identified and named P1 (TTGTGG-N_{16}-TTTAT) and P2 (TGGTTT-N_{17}-TATTTC), respectively (Fig. 4.1). Besides the RcsB-binding site (RcsAB box) at -350 bp (Lee et al. 2017), a putative HrpY-binding site at -187 bp with direct repeats (TAATCCCTAC-N_{13}-GATTCCTTAC) was also identified (Fig. 4.1). This putative HrpY-binding site is similar to that reported in *P. stewartii*, and both are located about 30 bp upstream of a putative σ^{70}-binding site (Merighi et al. 2006; Yap et al. 2005).

Based on these results, four *lacZ* transcriptional fusion constructs were generated, where placZS1 contains full-length *hrpS* upstream sequence; placZS2 and placZS3 contain *hrpS* P2 with and without the HrpY-binding site, respectively; and placZS4 contains *hrpS* P1 with the RcsAB box and the HrpY-binding site without P2 (Fig. 4.1). Their LacZ activities in the WT and the *hrpXY* and *rcsB* mutants were then determined using β-galactosidase assay (Fig. 4.2A; Table 4.1). LacZ activities in both mutant strains carrying placZS1 were about 1.5-fold lower than that in the WT, indicating that both HrpX/HrpY and the Rcs system positively affect *hrpS* gene expression. The *hrpXY* mutant carrying placZS2 and placZS3 exhibited similar LacZ activities, while LacZ activities were slightly higher in the WT and the *rcsB* mutant carrying placZS2 than those carrying placZS3. In addition, all three strains carrying placZS3 exhibited higher levels of

LacZ activities compared to empty vector controls, indicating that *hrpS* P2 is dependent on HrpX/HrpY and it has a basal activity in the absence of HrpX/HrpY. On the other hand, LacZ activity of the *rcsB* mutant carrying placZS4 decreased to the level of the vector control, indicating that RcsB is essential for *hrpS* P1 activation. Furthermore, LacZ activity of the *rcsB* mutant carrying placZS1 was higher than that of the *hrpXY* mutant carrying placZS1, and higher in the WT carrying placZS3 than carrying placZS4, indicating that HrpY-dependent *hrpS* P2 activity is slightly stronger than RcsB-dependent *hrpS* P1 activity.

To confirm these results, qRT-PCR was performed to determine the transcripts of the *hrpS* and other T3SS genes in the *hrpXY* and *rcsB* mutants (Fig. 4.2B). Expression of the *hrpS* gene was about 5- and 2.5-fold down-regulated in the *hrpXY* and *rcsB* mutants, respectively, as compared to the WT. Expression of the *hrpL* and *hrpA* genes was barely detectable in the *hrpXY* mutant and about 3-fold decreased in the *rcsB* mutant as compared to the WT. These results are consistent with previous findings that HrpX/HrpY acts as a primary activator of *hrpS* expression in plant enterobacterial pathogens (Merighi et al. 2003) and also indicate that the Rcs system is another major activator of *hrpS* gene expression in *E. amylovora*.

4.4.2 IHF positively regulates *hrpX*/*hrpY* gene expression

Our previous study showed that the nucleoid-associated protein IHF not only plays an essential role in the σ^{54}-dependent *hrpL* transcription, but also acts as a positive regulator of *hrpS* expression (Lee and Zhao 2016). It was also reported that in *P. stewartii*, the IHF-binding site is located in the *hrpS* upstream sequence, and IHF is critical for *hrpS* expression (Merighi et al. 2006). In *E. amylovora*, a putative IHF-binding site (GAGCAG-N_4-TTA) was found at -312 bp

relative to the *hrpS* start codon, but no band shift was detected in EMSA (data not shown). However, qRT-PCR results showed that expression of the *hrpX*/*hrpY* genes is down-regulated 2- to 5-fold in the *ihfA* mutant (Fig. 4.3A; Table 4.1), indicating that IHF positively regulates *hrpX*/*hrpY* expression. Indeed, EMSA result showed that IHF binds to a well-conserved IHF-binding site (TATCAG-N_4-TTG) at -232 bp relative to the *hrpX* start codon (Fig. 4.3B). These results suggest that IHF directly binds to the *hrpX* upstream sequence and activates the expression of *hrpX*/*hrpY*, and thus *hrpS*.

4.4.3 (p)ppGpp-mediated stringent response activates *hrpX*/*hrpY* gene expression

Given that (p)ppGpp and its co-factor DksA are required for T3SS gene expression in *E. amylovora* by activating the RpoN-HrpL alternative sigma factor cascade (Ancona et al. 2015b), we examined their impact on *hrpS* expression (Fig. 4.4A). LacZ activities in the *relA*/*spoT* (ppGpp-deficient) and *dksA* mutants carrying placZS1 were about 1.5- to 2-fold lower than that in the WT, but similar to those in the *hrpXY* and *hrpXY*/*relA*/*spoT* mutants, indicating that (p)ppGpp and DksA positively regulate *hrpS* expression. These results further suggest that HrpX/HrpY and (p)ppGpp/DksA might not act in a synergistic way, but may share the same pathway(s) for *hrpS* regulation. To confirm this hypothesis, *hrpX* promoter activities were determined in the WT and the *dksA* and *relA*/*spoT* mutants carrying the *lacZ* transcriptional fusion construct under full-length *hrpX* upstream sequence (placZX). As expected, LacZ activities in the two mutants were about 2-fold less than that in the WT (Fig. 4.4B), indicating that (p)ppGpp/DksA are required for full *hrpX*/*hrpY* expression.

To further examine how ppGpp/DksA-mediated stringent response affects *hrpX* and *hrpS* gene expression, cells of the WT and the *dksA* and *hrpXY* mutants were treated with SHX and compared to the WT and corresponding mutants without SHX treatment by qRT-PCR (Fig. 4.4C). Consistent with a previous report (Ancona et al. 2015b), the *hrpL* and *hrpA* transcripts were 1.5- to 2.5-fold increased after SHX treatment in the WT and the *hrpXY* mutant, but no change was observed in the *dksA* mutant. Interestingly, expression of *hrpX*, but not *hrpS*, was increased about 1.5-fold in the WT, but not in the *dksA* mutant (Fig. 4.4C). These results suggest that (p)ppGpp/DksA-mediated stringent response may directly activate *hrpX*/*hrpY* expression, which in turn regulates *hrpS* expression.

4.4.4 RcsB is responsible for the increased *hrpS* expression in the *csrB* mutant

Recent studies have shown that the RNA-binding protein CsrA and its antagonist sRNA *csrB* act as a positive and negative regulator of *hrpS* expression, respectively (Ancona et al. 2016; Lee et al. 2017). Interestingly, expressions of the *hrpX*, *hrpY*, *rcsA* and *rcsB* genes were significantly reduced in the *csrA* mutant, but only slightly higher in the *csrB* mutant (though statistically significant), except that the *rcsA* transcript was increased about 10-fold as compared to the WT (Fig. 4.5A). These results suggest that CsrA positively regulates expression of major *hrpS* activators, and its increased activity might lead to up-regulation of *hrpS* expression.

Previously, we showed that in the *lon* mutant, accumulation of RcsA and RcsB proteins leads to the activation of *hrpS* expression and suppression of *csrB* expression (Lee et al. 2017). To further confirm this, LacZ activities of the WT and the *csrB*, *rcsB* and *csrB*/*rcsB* mutants carrying the placZS1 or placZS4 constructs were determined using β-galactosidase assay (Fig.

4.5B). As expected, LacZ activity was increased approximately 2-fold in the *csrB* mutant, but decreased about 2-fold in the *rcsB* mutant as compared to that of the WT, all carrying placZS1. Interestingly, the *csrB*/*rcsB* double mutant carrying placZS1 exhibited a slightly decreased (though statistically significant) LacZ activity as compared to the WT (Fig. 4.5B). Similarly, LacZ activity was also higher in the *csrB* mutant and significantly decreased in the *rcsB* and *csrB*/*rcsB* mutants as compared to the WT, all carrying placZS4 (Fig. 4.5B). These results indicate that increased *hrpS* expression in the *csrB* mutant is mainly driven by RcsB, but also possibly by other factor(s), such as HrpX/HrpY.

4.5 Discussion

Numerous studies on the T3SS have led to significant advances in our knowledge of plant-microbe interaction and bacterial pathogenesis. In *E. amylovora*, the T3SS is essential for virulence and found to be governed by complex regulatory networks. Current model of T3SS regulation in *E. amylovora* involves the RpoN-HrpL alternative sigma factor cascade mediated by various regulators, including the bacterial alarmone (p)ppGpp-mediated stringent response, the Gac-Csr post-transcriptional system, proteases and TCSTs (Ancona et al. 2016; Lee et al. 2017; Li et al. 2014). In this study, we further demonstrated that *E. amylovora* recruits multiple stimuli-sensing systems, including HrpX/HrpY, the Rcs phosphorelay system, and the Gac-Csr system, as well as IHF and (p)ppGpp/DksA-mediated stringent response, to regulate *hrpS* and T3SS gene expression. These novel findings also indicate that the *hrpS* promoter might serve as an important converging point for regulation of *E. amylovora* virulence by subsequently activating *hrpL* and its downstream genes.

The bEBP HrpS is an essential virulence activator in *E. amylovora* by allowing the initiation of σ^{54}-dependent *hrpL* transcription via its conserved AAA^+ (ATPases-associated with various cellular activities) domain (Ancona et al. 2014; Lee et al. 2016; Wei et al. 2000). In general, activity of bEBPs is dependent on environmental stimuli through sensory domains at the N-terminal region. Signaling intermediates, such as phosphates and small molecules, interact with sensory domain and alter the activity of AAA^+ domain (Bush and Dixon 2012). However, some bEBPs, such as HrpS, contain no typical sensory domain. In *P. syringae* pathovars, formation of functional HrpR/HrpS complex is negatively regulated by Lon-dependent degradation of HrpR and sequestration of HrpS by HrpV (Bretz et al. 2002; Preston et al. 1998; Wei et al. 2005). Under the T3SS-inducing conditions, these can be relieved by up-regulation of *hrpR*/*hrpS* gene expression and inactivation of HrpV by a chaperone-like protein HrpG (Jovanovic et al. 2011; Ortiz-Martín et al. 2010b). Furthermore, HrpG directly interacts with HrpF, possibly contributing to the regulation of free HrpS level and activity (Huang et al. 2016). Similar regulatory mechanism through protein-protein interactions for bEBPs has also been reported in the phage shock protein PspF and the transcriptional activator NifA of nitrogen fixation genes (Dixon 1998; Elderkin et al. 2002).

On the other hand, HrpS activity in many related enterobacterial pathogens has been reported to be mainly determined at the transcription level by HrpX/HrpY (Merighi et al. 2003; Yap et al. 2005; Wei et al. 2000). Bioinformatics analysis showed that the sensor kinase HrpX contains repeats of Per-Arnt-Sim (PAS) domain that is capable of sensing various internal stimuli, including small molecules, gases and redox potential (Henry and Crosson 2011); however, stimuli for HrpX remain unknown. The cognate response regulator HrpY can be activated by

alternative phosphate sources, such as acetyl phosphate, and its over-expression can bypass T3SS repression caused by organic acids and nitrogen compounds (Merighi et al. 2003, 2005). These observations suggest that sensing environmental stimuli to activate T3SS could be mediated by HrpX/HrpY. In *Dickeya* and *Pantoea*, HrpY directly activates *hrpS* expression and thus is essential for T3SS activation and virulence (Merighi et al. 2003; Yap et al. 2005). In contrast, the *hrpXY* mutant of *E. amylovora* was fully virulent, suggesting additional *hrpS* activator(s) exist in *E. amylovora* (Zhao et al. 2009b). In this study, we provided evidence that, unlike other enterobacterial plant pathogens, the *E. amylovora hrpS* gene contains two promoters, which depend on HrpX/HrpY and the Rcs phosphorelay system, respectively.

Furthermore, characterization of the *hrpS* promoters revealed that the Rcs system-dependent promoter was driven independently of HrpX/HrpY, and lack of RcsB caused more than 50% reduction in the transcripts of the *hrpS* and T3SS genes. In *E. amylovora*, the Rcs system is generally believed to be important for the late stage of infection by activating amylovoran biosynthesis and inducing the characteristic wilting symptoms (Koczan et al. 2009; Wang et al. 2009). Our recent study showed that in addition to the T3SS, the Rcs system also regulates other early stage-virulence factors, including motility and the *csrB* sRNA (Lee et al. 2017). These findings suggest that the Rcs system might play a critical role in sensing environmental signals and mediating cross-talks between different virulence factors during *E. amylovora* pathogenesis.

It has been previously reported that the *hrpX*/*hrpY* promoter has a high basal activity and is strongly induced in the apoplast-like conditions (Wei et al. 2000). During plant infection,

bacteria are under nutrient stress, which promotes the synthesis and transient accumulation of (p)ppGpp in the cell, leading to extensive transcriptional reprogramming (Hauryliuk et al. 2015). In *E. amylovora*, it has been proven that (p)ppGpp serves as a major internal signal for T3SS activation (Ancona et al. 2015b). In this study, we showed that *hrpX*/*hrpY* is positively controlled by (p)ppGpp/DksA-mediated stringent response, suggesting that HrpX/HrpY could directly respond to (p)ppGpp, or HrpX might sense (p)ppGpp as its internal signal. In addition, *hrpX*/*hrpY* expression is found to be activated by IHF. Given that both (p)ppGpp and IHF allow the initiation of σ^{54}-dependent *hrpL* transcription (Ancona et al. 2015b; Lee and Zhao 2016), full *hrpX*/*hrpY* expression might be an important step to activate the downstream regulatory cascade. It is interesting to note that IHF has been reported to directly activate *hrpS* in *P. stewartii* and *D. dadantii* (Merighi et al. 2006; Yap et al. 2008), suggesting different adaptations of HrpX/HrpY-*hrpS* regulatory pathway in plant enterobacterial pathogens.

The RNA binding protein CsrA is essential for *E. amylovora* virulence by activating various traits, including the T3SS (Ancona et al. 2016). In the absence of CsrA, transcripts of major regulatory genes for *hrpL* expression were all down-regulated, and *hrpS* expression appeared to have the most dramatic effect (Ancona et al. 2016). This study revealed that expression of two major *hrpS* activators, HrpX/HrpY and the Rcs system, was also significantly down-regulated in the *csrA* mutant, indicating that CsrA functions at the top of the T3SS activation pathways. On the other hand, mutation in *csrB* promotes expression of the *hrpS* and the Rcs regulon, including *amsG* and *rcsA* (Ancona et al. 2016), suggesting that increased activity of the Rcs system might render the *csrB* mutant more virulent. Future studies are warranted to define targets of CsrA during T3SS activation.

In summary, we propose the following model for the regulatory network of the T3SS through *hrpS* gene expression in *E. amylovora* (Fig. 4.6). Multiple pathways, including HrpX/HrpY, the Rcs phosphorelay, and the Gac-Csr systems, which sense environmental or metabolic (internal) signals, are integrated to regulate *hrpS* expression and thus reflected in T3SS activation through the RpoN-HrpL alternative sigma factor cascade (Ancona et al. 2015b, 2016; Lee and Zhao 2016; Lee et al. 2016; 2017; Li et al. 2014). These findings corroborate the *hrpS* promoter as a converging point in responding to environmental signals for T3SS activation and also provide an insight into unique regulatory pathways of bEBP activity at the transcription level. Future researches should identify specific stimuli for those sensing systems in activating the T3SS.

4.6 Tables

Table 4.1 Bacterial strains and plasmids used in this study

Strains, Plasmids	Description	Reference, Source
E. amylovora		
Ea1189	Wild type, isolated from apple	Wang et al. 2009
Δ*hrpXY*	*hrpX*,*hrpY*::Km; Km^R-insertional mutant of *hrpXY* of Ea1189, Km^R	Zhao et al. 2009b
Δ*rcsB*	*rcsB*::Km; Km^R-insertional mutant of *rcsB* of Ea1189, Km^R	Wang et al. 2009
Δ*ihfA*	*ihfA*::Cm; Cm^R-insertional mutant of *ihfA* of Ea1189, Cm^R	Lee and Zhao 2016
Δ*dksA*	*dksA*::Cm; Cm^R-insertional mutant of *dksA* of Ea1189, Cm^R	Ancona et al. 2015b
Δ*relA*/*spoT*	*relA*::Cm *spoT*::Km; Km^R-insertional mutant of *spoT* of Δ*relA*	Ancona et al. 2015b
Δ*hrpXY*/*relA*/ *spoT*	*relA*::Cm *spoT*::Km; Cm^R-, Km^R-insertional mutant of *relA*, *spoT* of Δ*hrpXY*	This study
Δ*csrA*	*csrA*::Cm; Cm^R-insertional mutant of *csrA* of Ea1189, Cm^R	Ancona et al. 2016
Δ*csrB*	*csrB*::Cm; Cm^R-insertional mutant of *csrB* of Ea1189, Cm^R	Ancona et al. 2016
Δ*csrB*/*rcsB*	*rcsB*::Km *csrB*::Cm; Cm^R-insertional mutant of *csrB* of Δ*rcsB*	This study
E. coli		
DH10B	F– *mcr*A Δ(*mrr-hsd*RMS-*mcr*BC) Φ80*lac*ZΔM15 Δ*lac*X74 *rec*A1 *end*A1 *ara*D139 Δ(*ara leu*) 7697 *gal*U *gal*K *rps*L *nup*G λ-	Invitrogen
Plasmids		
pHRP309	Broad-host-range *lacZ* transcriptional fusion vector, Gm^R	Parales and Harwood 1993
placZS1	502-bp fragment containing *hrpS* gene (-404-+98) in pHRP309	This study
placZS2	332-bp fragment containing *hrpS* gene (-234-+98) in pHRP309	This study
placZS3	277-bp fragment containing *hrpS* gene (-179-+98) in pHRP309	This study
placZS4	234-bp fragment containing *hrpS* gene (-404--171) in pHRP309	This study
placZX	698-bp fragment containing *hrpX* gene (-600-+98) in pHRP309	This study

Table 4.2 Primers used in this study

Primer	Sequences (5' to 3')
Primers for 5'RACE	
HrpS-SP1	GGATCGCCGCGCAGTTAACCGC
HrpS-SP2	CGTGCCAGCGTGTCTTTTCCGG
HrpS-SP3	GCCAATGTGTCGTGGATATCGA
Primers for qRT-PCR	
rpoD-rt1	CCTCCAAGTCGACATCGTTT
rpoD-rt2	TGTAGCGGTGAAATGCGTAG
hrpL-rt1	TTAAGGCAATGCCAAACACC
hrpL-rt2	GACGCGTGCATCATTTTATT
hrpS-rt1	AATGCTACGCGTGCTGGAAA
hrpS-rt2	AACAATGGCGTTTGCGTTGC
hrpA-rt1	GAGTCCATTTTGCCATCCAG
hrpA-rt2	TGGCAGGCAGTTCACTTACA
hrpX-rt1	ACAGTATGTGCGTAGTAAGG
hrpX-rt2	GGATCCGTCTCCCTCTGAGC
hrpY-rt1	GAGCATGCCGGGAGTTTGTG
hrpY-rt2	GTTGACCACGCGCCACGCGG
rcsA-rt1	TTAAACCTGTCTGTGCGTCA
rcsA-rt2	AGAAACCGTTTTGGCTTTGA
rcsB-rt1	GTGGTTGGCGAGTTTGAAGA
rcsB-rt2	GGTCAGGATAATGGCGTTTG
Primers for cloning	
placZS1-F	ACTGTCTAGAGGACATCGTGAAATACGCCAT
placZS2-F	ACTGTCTAGACCCCCGAATGTAGGGTAATCC
placZS3-F	ACTGTCTAGATCAGCATAAGACGATGGTTTC
placZS-R	TCAGGAATTCGTGTCGTGGATATCGATGGGT
placZS12-R	TCAGGAATTCTTATGCTGAACATTAAGTAAG
placZX-F	ACTGTCTAGAGGCGACGCGTGCATCATTTT
placZX-R	TCAGGAATTCTCAACCAGATAGACGGCGTC
Primers for EMSA	
hrpX-IHF-F	CTGGTCGAGAAAGACGGCAGTTATCAGGCTATTGCAGCACATTTGAATATCCCGA
hrpX-IHF-R	TCGGGATATTCAAATGTGCTGCAATAGCCTGATAACTGCCGTCTTTCTCGACCAG

4.7 Figures

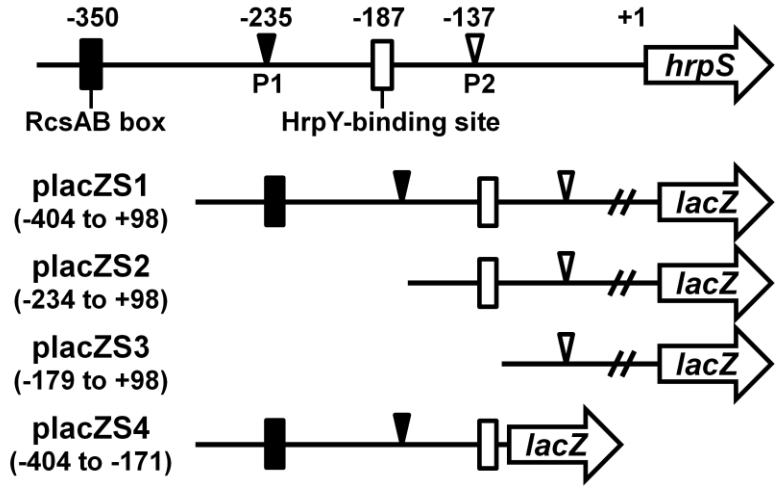

Figure 4.1 Schematic diagram showing the *hrpS* promoters and the *hrpS-lacZ* transcriptional fusion constructs. Two putative σ^{70}-dependent promoters were identified in the *hrpS* upstream sequence by 5' RACE and named P1 and P2. The RcsAB box and the putative HrpY-binding site are located upstream of P1 and P2, respectively. Numbers are relative to the start codon of the *hrpS* gene. For verification of promoters, four *lacZ* transcriptional fusion constructs were generated in pHRP309 and introduced into *E. amylovora* wild type (WT) strain Ea1189 and derived mutants. Filled rectangle, RcsAB box; filled triangle, P1; open rectangle, putative HrpY-binding site; open triangle, P2.

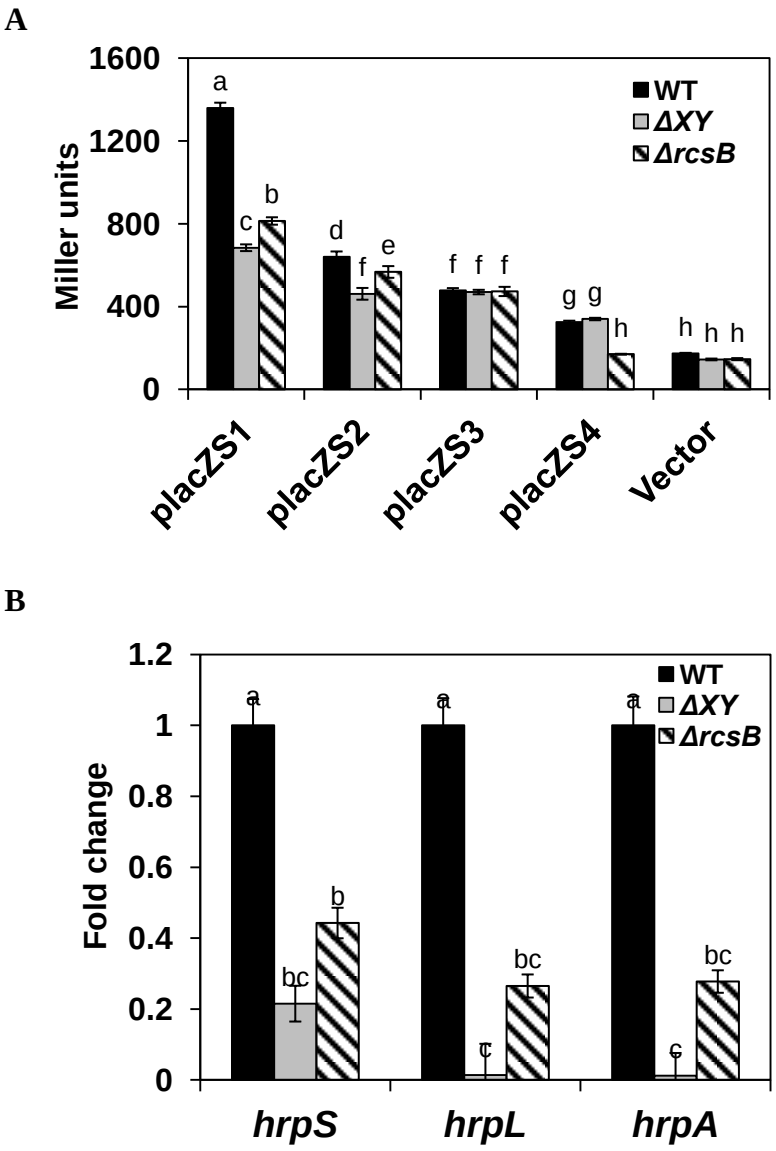

Figure 4.2 Transcription of *hrpS*, driven by two promoters, is under the control of HrpX/HrpY and the Rcs phosphorelay system. (A) LacZ activities of four transcriptional fusion constructs in the wild-type (WT) and the *hrpXY* and *rcsB* mutant strains grown in HMM for 6 h at 18 ℃. The values of miller units were the means of four replicates, and empty vector was used as a control. (B) Relative expression of the *hrpS*, *hrpL* and *hrpA* genes in the *hrpXY* and *rcsB* mutants compared with the WT grown in HMM for 6 h at 18 ℃. The *rpoD* gene was used as an endogenous control. The values of the relative fold change were the means of three replicates. Both experiments were repeated three times with similar results, and error bars indicate standard deviation. The Miller unit values and fold changes marked with the same letter do not differ significantly ($P < 0.05$). ΔXY, the *hrpXY* mutant; *ΔrcsB*, the *rcsB* mutant.

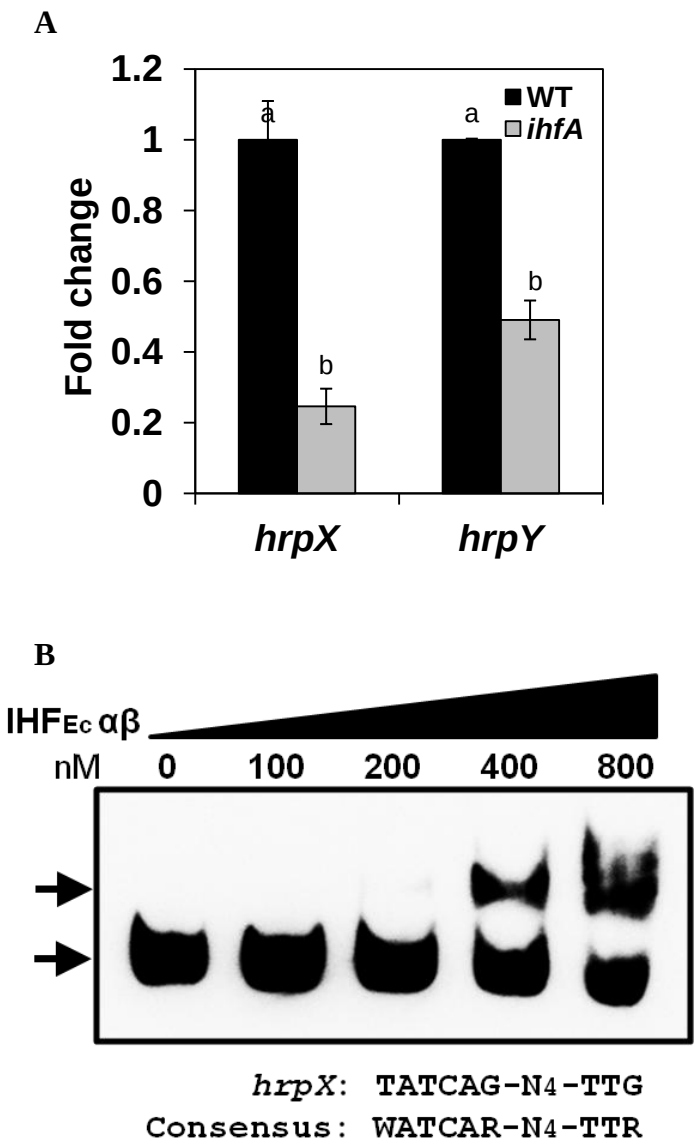

Figure 4.3 IHF positively regulates *hrpX*/*hrpY* expression by binding to the *hrpX* promoter. (A) Relative expression of the *hrpX* and *hrpY* genes in the *ihfA* mutant compared with the wild-type (WT) grown in HMM for 6 h at 18 ℃. The *rpoD* gene was used as an endogenous control. The values of the relative fold change were the means of three replicates. Error bars indicate standard deviation, and the fold changes with the same letter do not differ significantly ($P < 0.05$). *ΔihfA*, the *ihfA* mutant. (B) Electrophoretic mobility shift assay (EMSA) for a 55-bp fragment of the *hrpX* upstream sequence was carried out for binding to *Escherichia coli* IHF_{Ec} proteins, as described previously (Lee and Zhao 2016). Black arrows at the bottom and top indicate free probe and the protein-DNA complex, respectively. The concentration of protein (nM) is indicated above each lane. Both experiments were repeated three times with similar results.

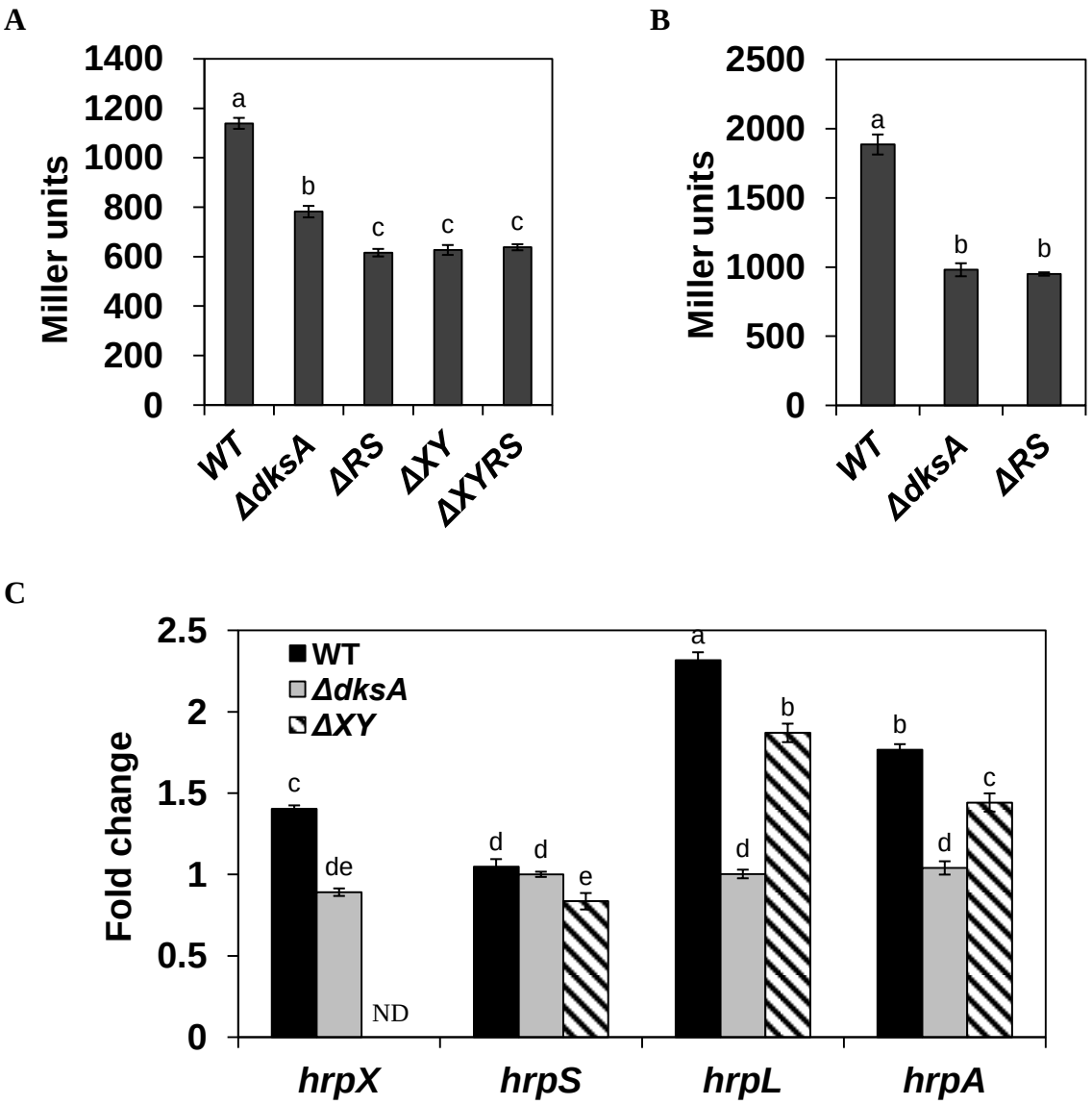

Figure 4.4 (p)ppGpp/DksA-mediated stringent response positively regulates *hrpX*/*hrpY* expression. (A) LacZ activities of the placZS1 transcriptional fusion construct in the wild-type (WT) and the *dksA*, *relA*/*spoT*, *hrpXY* and *hrpXY*/*relA*/*spoT* mutants grown in HMM for 6 h at 18 ℃. (B) LacZ activities of the placZX transcriptional fusion construct in the WT and the *dksA* and *relA*/*spoT* mutants grown in HMM for 6 h at 18 ℃. The values of Miller units were the means of four replicates. (C) Relative expression of the *hrpX*, *hrpS*, *hrpL* and *hrpA* genes in the WT and the *dksA* and *hrpXY* mutants grown in HMM for 6 h at 18 ℃ with and without SHX treatment (final concentration at 250 μg/ml for 30 min to induce stringent response). The *rpoD* gene was used as an endogenous control. The values of the relative fold change were the means of three replicates, and ND indicates not determined. Both experiments were repeated three times with similar results, and error bars indicate standard deviation. The Miller unit values and fold changes with the same letter do not differ significantly ($P < 0.05$). *ΔdksA*, the *dksA* mutant; ΔRS, the *relA*/*spoT* mutant; ΔXY, the *hrpXY* mutant; ΔXYRS, the *hrpXY*/*relA*/*spoT* mutant.

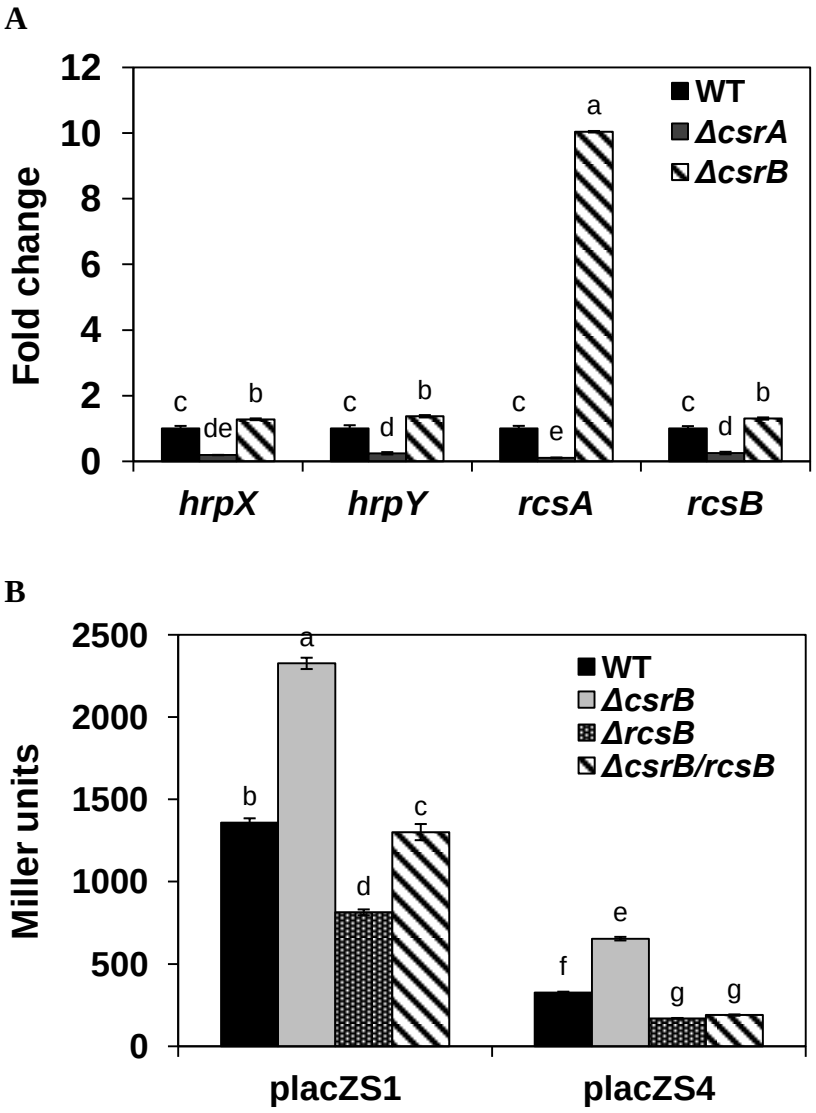

Figure 4.5 Up-regulation of *hrpS* in the *csrB* mutant could be through the Rcs phosphorelay system. (A) Relative expression of the *hrpX*, *hrpY, rcsA* and *rcsB* genes in the *csrA* and *csrB* mutants compared with the wild-type (WT) grown in HMM for 6 h at 18 ℃. The *rpoD* gene was used as an endogenous control. The values of the relative fold change were the means of three replicates. (B) LacZ activities of two *hrpS* transcriptional fusion constructs in the WT and the *csrB, rcsB*, and *csrB*/*rcsB* mutant strains grown in HMM for 6 h at 18 ℃. The values of miller units were the means of four replicates. Both experiments were repeated three times with similar results, and error bars indicate standard deviation. The fold changes and Miller unit values with the same letter do not differ significantly ($P < 0.05$). *ΔcsrA*, the csrA mutant; *ΔcsrB*, the *csrB* mutant; *ΔrcsB*, the *rcsB* mutant; *ΔcsrB/rcsB*, the csrB/*rcsB* mutant.

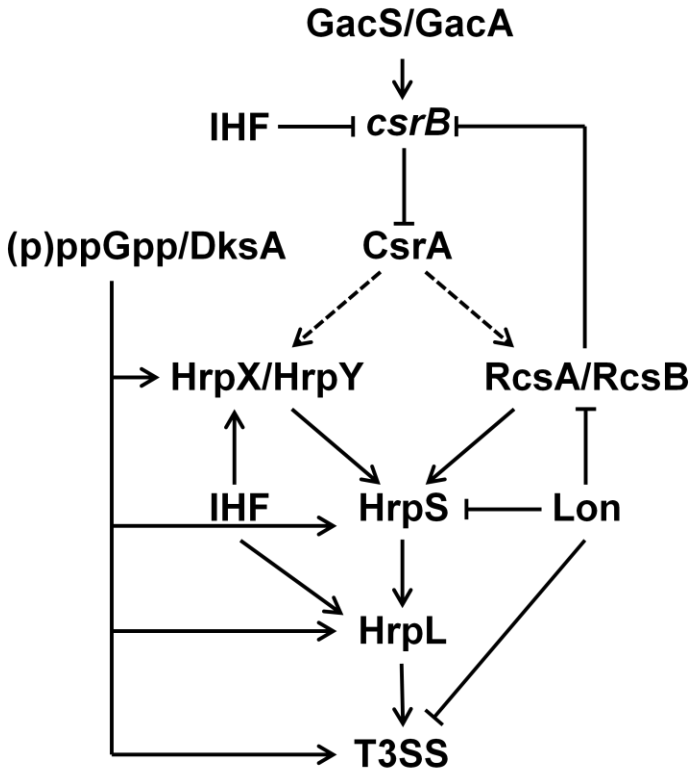

Figure 4.6 A working model for the regulatory network of the T3SS through *hrpS* gene expression in *Erwinia amylovora*. This model is based on findings obtained in this study as well as those reported in previous studies (Ancona et al. 2014, 2015b, 2016; Lee and Zhao 2016; Lee et al. 2016; 2017; Li et al. 2014). HrpX/HrpY; GacS/GacA; RcsA/RcsB: two-component signal transduction systems; CsrA: RNA-binding protein; *csrB*: small non-coding regulatory RNA; IHF: integration host factor; (p)ppGpp: guanosine tetraphosphate and guanosine pentaphosphate; DksA: transcription factor; Lon: protease; HrpS: a σ^{54}-dependent enhancer binding protein; HrpL: an ECF sigma factor and master regulator of T3SS; Symbols: ↓, positive effect; ⊥, negative effect; dash line: unknown mechanism.

CHAPTER 5

Posttranscriptional regulation of virulence by RNA-binding protein CsrA in *Erwinia amylovora*

5.1 Abstract

CsrA is a posttranscriptional regulatory RNA-binding protein that binds to target transcripts and alters translation rate. Previously, we reported that CsrA is an essential regulator of virulence in *Erwinia amylovora* by positively regulating the expression of major virulence factors, including type III secretion system (T3SS), exopolysaccharide (EPS) amylovoran and motility. In this study, we examined the global effect of CsrA and determined potential molecular mechanisms of CsrA-dependent virulence regulation in *E. amylovora*. Using RNA electrophoretic mobility shift assay (REMSA), direct interaction between CsrA protein and *csrB* sRNA was confirmed, while CsrA did not bind to the transcripts of T3SS activators, *hrpL* and *hrpS*. Transcriptomic analyses under the T3SS-inducing condition revealed that mutation in *csrA* led to differential expression in more than 20% genes in the genome. Of these, T3SS genes and those required for cell growth and viability were significantly down-regulated, explaining the pleiotropic effects of the *csrA* mutation. On the other hand, the *csrB* mutant exhibited significant up-regulation of the major virulence genes, further suggesting antagonistic effects of *csrB* on CsrA, which acts as a positive regulator of *E. amylovora* virulence. Through REMSA combined with site-directed mutagenesis and LacZ reporter gene assay, three CsrA targets (*flhD*, *rcsB* and *relA*) were identified that positively regulate *E. amylovora* virulence.

5.2 Introduction

Erwinia amylovora, a Gram-negative bacterium belonging to the *Enterobacteriaceae* family, is the causal agent of fire blight disease in apple and pear trees. It utilizes two pathogenicity factors, a *hypersensitive response and pathogenicity* (*hrp*)-type III secretion system (T3SS) and the exopolysaccharide (EPS) amylovoran (Khan et al., 2012; Zhao et al., 2009a; Zhao, 2014). The *hrp*-T3SS that translocates effector proteins directly into host cells contributes to interfering plant immunity (Buttner 2012; Zhao 2014). The expression of *hrp*-T3SS genes clustered in the *hrp*-pathogenicity island is activated by the master regulator HrpL (McNally et al., 2012; Wei and Beer, 1995). Since the *hrpL* gene contains the RpoN-dependent promoter, other transcription factors, including YhbH, HrpS, IHF, (p)ppGpp and DksA, are also indispensably required for transcription initiation and control the HrpL activity (Ancona et al., 2014; Ancona et al., 2015b; Lee and Zhao, 2016). On the other hand, the EPS amylovoran plays a role in biofilm formation and cell survival during late stages of infection process (Koczan et al., 2009; Nimtz et al., 1996). Genes encoding EPS amylovoran biosynthesis components are clustered in the *ams* operon and primarily activated by the Rcs phosphorelay system (Berhnhard et al., 1993; Wang et al., 2009, 2012).

The Csr system, which was first reported in *Escherichia coli* as a regulator of glycogen biosynthesis, is one of the major posttranscriptional regulators in bacteria. It consists of CsrA (or its homologs RsmA and RsmE) and its regulatory non-coding small RNAs (sRNAs). CsrA predominantly binds to GGA motif in a hairpin structure at the 5’ untranslated region (5’ UTR) of mRNA, leading to RNA stabilization or destabilization, translation activation or translation repression (Vakulskas et al., 2015). Recently, changes in RNA secondary structures caused by

CsrA binding are also found to affect Rho-dependent termination and riboswitch confirmation, suggesting diverse regulatory action of CsrA at the posttranscriptional level (Figueroa-Bossi et al., 2014; Patterson-Fortin et al., 2013). On the other hand, small non-coding regulatory RNAs, such as *csrB* in *E. amylovora*, *rsmB* in *Pecobacterium carotovorum* and *Dickeya dadantii*, and *csrB* and *csrC* in *E. coli* and *Salmonella enterica*, contain a number of GGA motifs, which sequester CsrA and inhibit its activity. In Gamma-proteobacteria, expression of Csr sRNAs is specifically dependent on the BarA/UvrY two component system or its homologs, such as GrrS/GrrA of *E. amylovora* (Suzuki et al., 2002; Zere et al., 2015). Other regulators, such as RNA helicases, CsrD, (p)ppGpp and DksA, have also been reported to play a role in regulating Csr sRNAs (Edwards et al., 2011; Suzuki et al., 2006; Vakulskas et al., 2014).

There is accumulating evidence that the Csr system greatly impacts virulence gene regulation in pathogenic bacteria. In *Salmonella*, CsrA suppresses the expression of HilD, which acts as a central regulator in the activation of *Salmonella* pathogenicity island-1 (SPI-1) and SPI-2 (Martinez et al., 2011). In *Legionella pneumophila*, CsrA negatively regulates the expression of flagellar biosynthesis activator FleQ and quorum sensing component LqsR. It also directly interacts with transcripts of Dot/Icm type IV secretion system effectors (Sahr et al., 2017). RsmA of *Xanthomonas citri* subsp. *citri* protects *hrpG* transcript, encoding the master regulator of T3SS, from RNase E cleavage and allows T3SS gene expression (Andrade et al., 2014). In *E. amylovora*, the Csr system is a key virulence regulator activating T3SS and amylovoran production, while the *grrS*/*grrA*, *ihf* and *csrB* mutants also exhibited increased T3SS gene expression, amylovoran production and motility (Li et al., 2014; Ancona et al., 2016; Lee et al., 2017). However, target transcripts of CsrA remain unknown.

In *E. amylovora*, the Csr system has been shown to be closely associated with other important virulence regulators. It was reported that expression of *csrB* is under the control of IHF and the Rcs system (Lee and Zhao, 2016; Lee et al., 2017). The nucleoid-associated protein IHF is involved in various DNA-dependent processes, including cell division, transcription and site-specific recombination, via DNA remodeling, and its intracellular abundance varies with growth phase (Azam et al., 1999; Dillon and Dorman, 2010). Transcriptional initiation of *hrpL* also requires IHF to enable interaction between transcription activators, such as RpoN and HrpS (Lee and Zhao, 2016; Lee et al, 2016). The Rcs system acts as a central two-component system that regulates major virulence factors of *E. amylovora*, including the T3SS, amylovoran production and motility (Ancona et al., 2015a; Lee et al., 2017; Wang et al., 2012). Furthermore, Lon, an ATP-dependent protease, is also reported to be linked to the Csr system. Absence of Lon resulted in the accumulation of the RcsA/RcsB proteins, which suppress *csrB* expression, while absence of CsrA resulted in differential expression of *lon* at both transcriptional and posttranscriptional levels (Lee et al., 2017). These findings suggest that *E. amylovora* CsrA could respond to both internal and external stimuli and act as a key component in the regulatory networks that coordinate the expression of different virulence factors.

In this study, we examined the molecular mechanisms of CsrA-dependent virulence regulation in *E. amylovora*. Transcriptomic analysis under the T3SS-inducing condition revealed that altered activity of CsrA resulted in differential expression of hundreds of genes, including those involved in virulence and important physiological processes, further supporting its role as a global regulator. A direct physical interaction between CsrA protein and *csrB* regulatory sRNA

was confirmed, and several CsrA target transcripts that are responsible for the regulation of T3SS, amylovoran production and motility were determined.

5.3 Materials and methods

5.3.1 Bacterial strains and growth conditions

Bacterial strains and plasmids used in this study are listed in Table 5.1. LB was used routinely to culture *E. amylovora* and *E. coli* strains, and the *hrp*-inducing medium (HMM) (1 g (NH4)2SO4, 0.246 g MgCl2·6H2O, 0.1 g NaCl, 8.708 g K2HPO4, 6.804 g KH2PO4) was used to determine gene expression. Tryptone broth (10 g tryptone, 5 g NaCl per 1 Liter) was used to measure flagellar gene expression. When required, antibiotics were added at the following concentrations: 100 μg ml^{-1} ampicillin (Ap), 50 μg ml^{-1} kanamaycin (Km), 10 μg ml^{-1} chloramphenicol (Cm) and 10 μg ml^{-1} gentamicin (Gen). Primers used in this study are listed in Table 5.2.

5.3.2 RNA isolation, RNA-seq, real-time quantitative reverse transcription PCR (qRT-PCR)

RNA was isolated from cell cultures grown in HMM for 6 h at 18 ℃ using RNeasy ® mini kit (Qiagen, Hilden, Germany), followed by DNae I treatment using TURBO DNA free kit (Thermo Fisher Scientific, Waltham, MA, USA), according to the manufacturer's instruction. The quantity and quality of RNA samples were assessed using either Nano-Drop ND-100 spectrophotometer (Nano-Drop Technologies, Wilmington, DE, USA) or Agilent RNA 6000 Nano chip Bioanalyzer (Agilent, Santa Clara, CA, USA). For RNA-seq analysis, library construction and sequencing using Illumina HiSeq 4000 (Illumina, San Diego, CA, USA) were performed on three biological samples for the WT and the mutants by the Keck Center at the

UIUC. The sequence reads were aligned to the genome of *E. amylovora* CFBP1430 (Smits et al., 2010a). To perform normalization and statistical analysis on the raw read counts, the R package DESeq2 was used as described previously (Love et al., 2014). Differentially expressed genes (DEGs) were defined as genes with a $|\log_2(\text{fold change; FC})|$ value ≥ 1 and a corrected p value < 0.05 from three independent biological replicates.

For qRT-PCR, reverse transcription was performed using Superscript III reverse transcriptase (Invitrogen, Carlsbad, CA, USA), and cDNA samples were mixed with Power SYBR ® Green PCR master mix (Applied Biosystems, CA, USA) and appropriate primers. StepOnePlus Real-Time PCR system (Applied Biosystems) was used for qRT-PCR reaction under the following conditions: 95 ℃ for 10 min, followed by 40 cycles of 95 ℃ for 15 s and 60 ℃ for 1 min in the. Primer specificities were assessed using melting curves. The *rpoD* gene was used as an endogenous control to calculate relative quantification ($\Delta\Delta Ct$). The experiment was repeated three times, and statistical analysis was performed using Student's *t*-test with $p < 0.05$.

5.3.3 CsrA protein purification

The coding sequence of the *csrA* gene was cloned into pET28a expression vector (Novagen, Madison, WI, USA), and after confirmation by sequencing at the Keck center of UIUC, final plasmid was introduced into *E. coli* BL21 (DE3) strain. Overnight culture of the CsrA-overexpressing strain was inoculated into 500 ml of fresh LB media containing 50 μg/ml of Km. After 2-3 h growth, bacteria culture was treated with 0.1 mM of IPTG to induce protein expression and incubated overnight at 18 ℃. Cells were harvested, washed with cell wash buffer

(50 mM MOPS, 150 mM NaCl), and resuspended [1:10 ratio (w/v)] in cell wash buffer. Cell suspension was treated with 250 μg/ml lysozyme (Promega, Madison, WI, USA) for 30 min, cooled on ice for 30 min, and mixed with Halt™ protease inhibitor (1x, Thermo Fisher Scientific), NaCl (300 mM) and imidazole (60 mM). After sonication, cell lysates were removed by centrifugation at 35,000 g for 20 min. The supernatant was treated with Ni-NTA agarose resin (Qiagen) at 4 ℃ for 30 min with gentle rocking to collect His-tagged CsrA proteins. Ni-NTA resins were then washed with equilibration/wash buffer (50 mM MOPS, 300 mM NaCl, 60 mM imidazole), and proteins were eluted with elution buffer (50 mM MOPS, 300 mM NaCl, 500 mM imidazole). Proteins were dialyzed overnight against buffer containing 20 mM MOPS and 1 mM DTT, and protein concentration was measured using Invitrogen Qubit protein assay.

5.3.4 RNA electrophoretic mobility shift assay (REMSA)

Leader sequences of genes of interest were transcribed *in vitro* using MEGAshortscript™ kit (Thermo Fisher Scientific) and labeled with biotin using Pierce™ RNA 3' end biotinylation kit (Thermo Fisher Scientific), according to the manufacturer's instruction. Reaction mixtures were prepared using Lightshift® chemiluminescent RNA EMSA kit (Thermo Fisher Scientific) in volumes of 10 μl, containing 2 nM of biotin-labeled target RNA, different amounts of CsrA protein, 1X binding buffer, 5% glycerol and 0.4 unit RNase inhibitor, incubated at room temperature for 20 min, and mixed with 5× loading buffer. For competition assays, 2 nM of unlabeled *csrB* RNA was additionally added to the reaction mixture. CsrA-RNA complexes were separated on a 6% native polyacrylamide gel in 0.5X TBE buffer (44.5 mM Tris-base, 44.5 mM Boric acid and 1 mM EDTA), followed by UV-light crosslinking to a positively charged nylon membrane. Chemiluminescent signals were then detected using ImageQuant LAS 4010 CCD camera (GE Healthcare, Piscataway, NJ, USA).

5.3.5 β-Galactosidase assay

β-Galactosidase assay was performed using a microtiter plate as described previously (Slauch and Silhavy 1991). Cell cultures grown in HMM for 6 h at 18 ℃ were collected and resuspended in Z-buffer (Miller 1972). After measuring OD_{600}, cell suspensions were treated with 1% SDS and chloroform, and then mixed with 10 mg/ml *o*-nitrophenyl galactoside (ONPG) to initiate the reaction. Units for β-galactosidase assay are defined as (μmol of ONP formed per minute) × 10^6/(OD_{600} × ml of cell suspension) and reported as mean ± standard deviation. Constructs of transcriptional and translational fusions were generated using vector pHRP309 and pZLac29, respectively, and confirmed by sequencing at the Keck center at UIUC. The vector pZLac29 was generated by transferring multiple cloning site and *lacZ* reporter gene from pRS552 into pWSK29. The assay was repeated three times, and statistical analysis was performed using Student's *t*-test with $p < 0.05$.

5.4 Results

5.4.1 CsrA does not directly interact with *hrpL* and *hrpS* transcripts.

It is assumed that *csrB* regulatory sRNA acts antagonistically to regulate CsrA in *E. amylovora*, however, their direct interaction was not experimentally confirmed (Ancona et al., 2016). REMSA analysis showed that *csrB* RNA caused a band shift with as low as 10 nM of CsrA protein (Fig. 5.1A), indicating high binding affinity between *csrB* sRNA and CsrA.

Our previous studies have shown that both *hrpL* and *hrpS*, are barely expressed in the *csrA* mutant, but are significantly up-regulated in the *csrB* mutant, indicating that *hrpL* and/or *hrpS* transcripts might be the direct targets of CsrA (Ancona et al., 2016; Lee and Zhao, 2017b).

Unexpectedly, REMSA showed no interaction between CsrA protein and both *hrpL* and *hrpS* RNA probes (Fig. 5.1B, C), suggesting that CsrA does not directly target *hrpL* and *hrpS* transcripts and might target other regulatory genes involved in the regulation of T3SS gene expression.

5.4.2 CsrA acts as a global regulator under the T3SS-inducing condition

In order to further determine potential CsrA targets, we performed RNA-seq on the wild-type (WT) and the *csrA* and *csrB* mutants grown under the T3SS-inducing condition. In total, 13,370,077 to 18030556 reads from each biological sample were generated, and the percentage of reads mapped to *E. amylovora* genome ranged from 71 to 92 %. MA plots (M: $\log_2$FC, A: mean of normalized counts) were generated to visualize expression pattern of individual genes (Fig. 5.2). DEGs, which exhibited a $|\log_2 FC| \geq 1$ and a corrected p value < 0.05 between the WT and the mutants, were also functionally categorized based on the clusters of orthologous groups (COGs) in Fig. 5.3 and 5.4.

A total of 804 of DEGs were found in the *csrA* mutant, including 317 up-regulated genes and 487 down-regulated genes, indicating that more than 20% of genes in *E. amylovora* genome was directly or indirectly affected in the absence of CsrA (Fig. 5.2A, 5.3; Table A.1, A.2). Besides the functional and regulatory components of T3SS, other virulence genes, including those encoding motility and type VI secretion system (T6SS), were rarely expressed in the *csrA* mutant (Table 5.3), further indicating that CsrA is critical for virulence activation in *E. amylovora*. Moreover, many genes responsible for important cellular processes, including nucleotide biosynthesis, electron transport chain and ribosomal biosynthesis, were also

significantly down-regulated, while heat shock response and sulfur metabolism genes were up-regulated in the *csrA* mutant (Table A.1, A.2). These dramatic physiological perturbations seem to contribute to non-pathogenic phenotype, no motility and slow growth in the *csrA* mutant (Ancona et al., 2016).

On the other hand, 379 DEGs (171 up-regulated genes, 208 down-regulated genes) were found in the *csrB* mutant (Table A.3, A.4). Compared to those observed in the *csrA* mutant, DEGs of the *csrB* mutant exhibited relatively less fluctuation in transcription levels across the genome, including metabolic and stress responsive genes (Fig. 5.2B, 5.4). The expression of genes responsible for all the major virulence factors, including T3SS, EPS amylovoran and motility, was significantly increased in the *csrB* mutant (Table A.3, A.4). This is consistent with the results from phenotypic data of our previous studies (Li et al., 2014; Ancona et al., 2016).

Though large number of DEGs in both the *csrA* and *csrB* mutants was annotated as hypothetical protein (Table A.1, A.2, A.3, A.4), Venn diagrams (Fig. 5.5) identified four groups of genes whose expression might be closely associated with the Csr system. Group I included 68 genes that were down-regulated in the *csrA* mutant but up-regulated in the *csrB* mutant, including mostly T3SS and flagellar genes (Table 5.3). Expression of the *rcsA* gene also exhibited the same trend, while expression of the *rcsB*, *rcsC* and *rcsD* genes in the Rcs system was not significantly changed in both mutants (Table 5.3), suggesting that CsrA might positively regulate the Rcs system at the posttranscriptional level.

Group II contained 33 genes that were up-regulated in the *csrA* mutant but down-regulated in the *csrB* mutant, including *rcsV* (LuxR-family transcriptional regulator), *narPQ* (two-component system), *ompT* (outer membrane protease) and CRISPR (clustered regularly interspaced short palindromic repeats)-associated (Cas) protein genes (Table 5.4). Interestingly, the *rcsV* gene was about 60-fold up-regulated and the most differentially expressed in the *csrA* mutant, while it was 3-fold down-regulated in the *csrB* mutant. However, due to lack of functional characterization of RcsV, further studies are needed to clarify its role in *E. amylovora* virulence.

Group III and IV included 20 and 97 genes that were significantly up-regulated or down-regulated in both mutants, respectively. Posttranslational regulators, such as ATP-dependent protease *hslUV* genes and molecular chaperone *groEL*, *htpG* genes, and sulfur transport systems, including *tauABCD* (EAMY_3404 to EAMY_3407) and *ssuEADC* (EAMY_1370 to EAMY_1373) gene clusters were all up-regulated (Table 5.5), whereas genes encoding glycosyltransferase, lipoproteins and membrane-associated proteins were all down-regulated (Table 5.6).

To validate RNA-seq data, nine representative DEGs of the *csrA* or *csrB* mutant were selected, and their expression was determined in HMM using qRT-PCR (Fig. 5.6). Although different magnitude of the fold change was observed in the T3SS genes, such as *hrpL* and *hsvA*, all genes tested showed similar trends between qRT-PCR and RNA-seq results, suggesting that our results are reliable and reproducible.

5.4.3 CsrA positively regulates motility through *flhD* at the posttranscriptional level

One of the well-studied CsrA target transcript in *E. coli* is *flhD*, encoding the master regulator of flagellar gene expression. It has been shown that CsrA binds to the leader sequence of *flhD* and increases its translation by protecting the transcript from RNase E-mediated cleavage (Wei et al., 2001; Yakhnin et al., 2013). Although the leader sequences of *flhD* in *E. coli* and *E. amylovora* are not homologous, genetic analyses suggested that CsrA positively regulates motility in *E. amylovora* possibly through *flhD* (Ancona et al., 2016; Lee and Zhao, 2016; Li et al., 2014). To determine its underlying mechanism, expression of different classes of flagellar gene using transcriptional fusion constructs in the *csrB* mutant was measured (Fig. 5.7A). Compared to the WT, expression of class II and class III flagellar genes (*fliL*, *fliA*, *flgM*, *fliD*) increased about 3-fold, while expression of class I flagellar gene (*flhD*) was not significantly changed, suggesting that posttranscriptional regulation might occur in the *flhD* gene. REMSA showed that CsrA directly and specifically bind to *flhD* RNA (Fig. 5.7B, C). Translational fusion reporter gene assay showed that expression of *flhD* increased about 2-fold in the *csrB* mutant as compared to that of the WT (Fig. 5.7D), indicating that CsrA positively regulates *flhD* expression at the posttranscriptional level in *E. amylovora*.

To further characterize CsrA-dependent *flhD* up-regulation, each of four putative CsrA-binding sites (named GGA1 to GGA4) on the leader sequence of *flhD* was deleted, and differential expression using translational fusion constructs was compared (Fig. 5.8A). In the WT, deletion of each GGA motif did not significantly affect *flhD* expression; whereas, in the *csrB* mutant, *flhD* expression was not affected after deletion of GGA2, but reduced after deletion of GGA1, GGA3 and GGA4 (Fig. 5.8B). This suggests that binding of CsrA on multiple sites of the

flhD leader sequence increases the translation rate of *flhD* and thus other flagellar gene expression in *E. amylovora*.

5.4.4 CsrA positively regulates *rcsB* expression at the posttranscriptional level

Previous genetic studies and transcriptomic analysis showed increased expression of many Rcs-dependent genes in the *csrB* mutant, including *rcsA*, *hrpS* and *ams* operon genes, we thus hypothesized that the activity of the Rcs system might be positively regulated by CsrA (Lee et al., 2017; Lee and Zhao, 2017b). REMSA analyses showed that CsrA specifically binds to the leader sequence of *rcsB* (Fig. 5.9A, B). Under the T3SS-inducing condition, transcript level of the *rcsB* gene was not changed in the *csrB* mutant (Lee et al., 2017b), however, expression of *rcsB* from the translational fusion construct increased about 1.5-fold. No increase was observed for the *rcsD* gene, which is in the same operon as *rcsB* (Fig. 5.9C). These results suggest that binding of CsrA to the *rcsB* transcript positively regulates *rcsB* expression at the posttranscriptional level. However, since our transcriptomic analysis of the *csrB* mutant also showed differential gene expression of many lipoproteins and membrane-associated proteins (Table A.3, A.4), we cannot rule out the possibility that altered membrane composition following increased CsrA activity might also increase RcsB phosphorylation.

5.4.5 CsrA is required for full translation of *relA*

In *E. amylovora*, the nucleotide second messenger (p)ppGpp is a key activator of T3SS gene expression by activating the RpoN-HrpL alternative sigma factor cascade as well as *hrpS* expression through HrpX/HrpY (Ancona et al., 2016; Lee and Zhao, 2017b). Since our transcriptomic analysis showed that major T3SS regulators under (p)ppGpp control are

significantly down-regulated in the *csrA* mutant (Ancona et al., 2015b; Lee and Zhao, 2017b), we hypothesized that CsrA might be involved in the regulation of the (p)ppGpp biosynthesis genes, *relA* and *spoT*. REMSA showed a direct interaction between CsrA and *relA* and *spoT* RNA probes (Fig. 5.10), however, expression of both genes from the translational fusion construct was not significantly changed in the *csrB* mutant (Fig. 5.11A). Secondary structure analysis showed two hairpin loop structures containing the putative CsrA-binding sites in the *relA* leader sequence (Fig. 5.11B). To further examine the role of CsrA on the *relA* translation, the putative CsrA-binding site near the putative Shine-Dalgarno sequence was mutated from GGA to GGG to eliminate CsrA-binding effect without affecting RNA secondary structure (Fig. 5.11B). Translation of *relA* was decreased about 80% after mutation in the GGA motif (Fig. 5.11C), indicating that CsrA binding contributes to full *relA* expression. However, further evidence is needed to demonstrate whether *spoT* is also a target of CsrA.

5.5 Discussion

The RNA-binding protein CsrA is indispensable for virulence in *E. amylovora*. Previous studies showed that the *csrA* mutation greatly diminished the level of two pathogenicity factors, T3SS and amylovoran, resulting in the non-pathogenic phenotype (Ancona et al., 2016). To expand our knowledge of CsrA-dependent regulation, we examined the transcriptomic changes upon the altered CsrA activity under the T3SS-inducing condition. We found that CsrA is a global regulator of not only virulence gene expression, but also of diverse cellular processes required for cell growth and viability. We also demonstrated that CsrA directly binds to *flhD*, *rcsB* and *relA* transcripts and positively regulates their expression, thus contributing to virulence in *E. amylovora*.

The global regulatory roles of CsrA have been studied in several species using deep sequencing. In transcriptomic analysis of *S. typhimurium* and *Pseudomonas aeruginosa*, a mutation in *csrA* led to 375 and 506 DEGs, respectively, compared to the WT, which are about 10 % of total genes in each species (Burrowes et al., 2006; Lawhon et al., 2003). Recent studies using CsrA-RNA complex immunoprecipitation combined with deep sequencing approach (CLIP-seq) also revealed that in *S. typhimurium*, *L. pneumophila* and *Campylobacter jujuni*, CsrA directly interacts with about 10 % of their total gene transcripts (Dugar et al., 2016; Holmqvist et al., 2016; Sahr et al., 2017). On the other hand, integration of different transcriptomic approaches in *E. coli* revealed that about 25 % and 12.5 % of total gene transcripts were differentially expressed in the *csrA* mutant and directly bound by CsrA *in vivo*, respectively (Potts et al., 2017). These reports collectively indicate that CsrA acts as a major posttranscriptional regulator in bacteria under different experimental conditions.

In this study, transcriptomic analysis of *E. amylovora* showed that about 20 % of its genes were differentially expressed in the absence of CsrA. In addition, unlike other species examined, the DEGs included not only virulence genes, but also many physiologically important genes. The *csrA* mutant exhibited a significant down-regulation of nucleotide biosynthesis, electron transport chain and ribosomal biosynthesis (Table A.2), suggesting its incapability to maintain cell integrity. The *csrA* mutant also exhibited a significant up-regulation of heat-shock genes (Table A.1). Given that transcription of heat-shock genes are triggered in response to various stress conditions, including temperature variations, toxic chemicals, desiccation and viral infections, to protect intracellular proteins from denaturation and aggregation (Morimoto, 1993), up-regulation of these genes in the *csrA* mutant indicates unstable intracellular states.

Consistently, it was reported in *E. coli* that cells under heat-shock stress exhibited a down-regulation of genes involved in ribosome assembly and energy metabolism (Murata et al., 2011), suggesting that a mutation in the *csrA* gene results in severe cellular stress. These results together showed that gene regulation and cell physiology in *E. amylovora* is highly dependent on CsrA, and thus, its absence causes pleiotropic defects, including slow growth and non-pathogenic phenotype.

Interestingly, 5 heat-shock genes (*groE*, *groL*, *hslU*, *hslV* and *htpG*) were up-regulated in both the *csrA* and *csrB* mutants. Since the *csrB* mutant did not exhibit any notable defects in growth and virulence, increased expression of heat shock genes in the *csrB* mutant appears to be caused by different source of stress. Extrapolating from the function of heat shock proteins, one possibility is that heat-shock gene expression might be induced in response to significantly increased levels of T3SS and flagellar proteins in the cell. Transcriptomic analysis in this study was performed in the condition when T3SS transcript levels reaching a peak in the WT (Lee and Zhao, 2017). The *csrB* mutant exhibited up to 11-fold up-regulation of T3SS and flagellar proteins, and also up to 6-fold up-regulation of proteins for amylovoran production (Table A.3), possibly resulting in sudden increased demand for molecular chaperones. Several studies have reported a similar induction pattern of heat shock genes during overproduction of recombinant proteins in *E. coli* to ensure correct protein folding (Hoffmann et al., 2000; Jurgen et al., 2000; Li et al., 2017). Up-regulation of heat shock genes in the *csrB* mutant might be also associated with the function of T3SS and/or flagellar motor. It was reported in *E. coli* that HtpG is required for the production of virulence-associated secondary metabolites, colibactin and yersiniabactin, and the activity of CRISPR/Cas system (Yosef et al., 2011; Garcie et al., 2016). HtpG of *E. coli* also

can directly interact with cytoplasmic flagellar motor components, FliN and FliI (Li and Sourjik, 2011). Moreover, heat-shock proteins in eukaryotes are widely observed in the assembly process of oligomers and protein complexes (Haslbeck and Vierling, 2015), suggesting that bacterial heat-shock proteins might be also capable of promoting the assembly of T3SS and/or flagellar motor apparatus.

In addition, the *tau* and *ssu* gene clusters, encoding ABC-type sulfur transporters and sulfur metabolism-related products, were also up-regulated in both *csrA* and *csrB* mutants. Expression of both gene clusters is reported to be positively regulated by Cbl transcription factor in *E. coli* (van der Ploeg et al., 1997; van der Ploeg et al., 1999). In our transcriptomic data, the *csrA* mutant showed about 12-fold increased expression of *cbl* as compared to the WT, and accordingly, showed a significant up-regulation of 13 sulfur metabolism genes known to contain Cbl-dependent promoter, including *tauABCD*, *ssuEADC*, *cysK*, *cysHIJ* and *sbp* (Table A.1; van der Ploeg et al., 2001). Other sulfur metabolism genes, such as *cysP* and *cysCND*, were also up-regulated in the *csrA* mutant. It has been reported that sulfur metabolism is highly associated with methionine and cysteine biosynthesis as well as oxidative stress response (Gyaneshwar et al., 2005), further suggesting unstable intracellular states in the *csrA* mutant. However, no significant changes in transcript levels of *cbl* and other sulfur metabolism genes were observed in the *csrB* mutant, and thus up-regulation of the *tau* and *ssu* genes might be mediated by yet unknown regulatory factors.

Transcriptomic analyses also revealed possible CsrA-dependent gene regulations by identifying DEGs with opposite trends. Expression of 33 genes were negatively regulated by

CsrA, and of these, the *rcsV* gene was the most strongly induced in the absence of CsrA (Table 5.4). The *rcsV* gene of *E. amylovora* was first identified that can recover EPS production in the *rcsA* mutant of *Pantoea stewartii* (Aldridge et al., 1998). However, it was reported that the *rcsV* mutant of *E. amylovora* caused no phenotypic differences, and its expression was not induced even under the strong *lac* promoter by unknown mechanism (Aldridge et al., 1998). Our transcriptomic analysis showed that *rcsV* expression was highly enhanced in the *csrA* mutant, but suppressed in the *csrB* mutant, suggesting that the Csr system might be responsible for the suppression of *rcsV* expression under normal conditions. A gene cluster (EAMY_2813 to EAMY_2820), encoding Cas proteins, was also negatively regulated by CsrA. Consistent with its primary role as a defense mechanism against foreign nucleic acids, *cas* gene expression has been reported to be induced against viral infection and regulated by various transcription factors and signaling molecules (Patterson et al., 2017); whereas a role of the Csr system in the CRISPR/Cas system regulation was not reported. Since the CRISPR/Cas system utilizes guide RNAs to target invading genetic elements, it may also contribute to posttranscriptional regulation through RNA interference-like system (Bhaya et al., 2011). In *E. amylovora*, studies of the CRISPR/Cas system have been focused on genetic diversity of short DNA repeat sequences from different isolates (McGhee and Sundin, 2012; Rezzonico et al., 2011), and thus our knowledge of its function and gene regulation is still incomplete. Further studies are warranted to assess interaction of the Csr system with the CRISPR/Cas system.

On the other hand, distinct subsets of genes, which were positively regulated by CsrA, provided insights into how the increased activity of CsrA positively regulates virulence gene expression in *E. amylovora*. In *E. coli*, it is well established that CsrA-binding of *flhD* inhibits

RNase E-mediated cleavage and enhances the translation rate (Wei et al., 2001; Yakhnin et al., 2013). Consistently, CsrA of *E. amylovora* also binds to multiple sites on the *flhD* transcript, resulting in enhanced translation (Fig. 5.7, 5.8). This finding reinforces our previous observations that mutant strains with increased CsrA activity, such as the *csrB*, *grrS*/*grrA*, and *ihf* mutants, were hypermotile (Li et al., 2014; Ancona et al., 2016; Lee and Zhao, 2016). Although it was not detected from the *lacZ* reporter fusion assays under the flagellar gene-inducing condition, transcriptome analysis under the T3SS-inducing condition showed that flagellar class 3 genes (*fliA*, *flgM*, *fliD*) were about 3-fold up-regulated as compared to flagellar class 2 genes (*fliL*, *fliP*) in the *csrB* mutant (Table 5.3). This suggests that CsrA-dependent flagellar gene regulation might also be mediated through the class 3 gene regulators, *fliA* and *flgM*.

The Rcs phosphorelay system is widely found in enterobacterial pathogens and is well known as a regulator of EPS production and biofilm formation (Ferrieres and Clarke, 2003; Erickson and Detweiler, 2006). In *E. amylovora*, the Rcs system acts as an essential virulence regulator by activating T3SS and amylovoran production, and also contributes to the regulation of motility, *csrB* sRNA expression and antibiotic resistance (Ancona et al., 2015a; Ge et al., 2018; Lee et al., 2017; Wang et al., 2009; Wang et al., 2012). Given that RcsB-dependent genes, including *hrpS* and *rcsA*, were differentially expressed in the *csrB* mutant without changes in *rcsB* transcript level (Lee and Zhao, 2018), we assumed that increased activity of CsrA might elevate the activity of the Rcs system. In *E. amylovora*, since *rcsB* expression was stable in different conditions, phosphorylation status of RcsB was thought to be a major determinant of the Rcs system activity (Wang et al., 2012). However, this study showed that CsrA can directly

interact with the leader sequence of *rcsB* and positively regulate its translation (Fig. 5.9), proposing a novel mechanism that affects the Rcs system activity through posttranscriptional regulation.

The Rcs system is composed of the complex and non-canonical signaling pathway. Several factors have been identified to affect its activity, and among them, perturbations in the outer and inner membranes have been shown as the major source of input signals (Majdalani and Gottesman, 2006). Differential gene expression of a number of membrane components, including glycosyltransferases, lipoproteins and other membrane-associated proteins, was observed in both the *csrA* and *csrB* mutants (Table A.1, A.2, A.3, A.4). The resulting altered membrane composition might also increase the Rcs system activity in the *csrB* mutant. In *E. coli*, CsrA was proposed to affect membrane integrity by suppressing the expression of extracytoplasmic stress response sigma factor RpoE and its anti-sigma factor RseA (Potts et al., 2017). The same study also showed positive regulation of *rcsA* expression by CsrA, although a direct relationship between the altered RpoE activity and the Rcs system was not examined (Potts et al., 2017). In addition, histidine kinase of two component systems utilizes γ-phosphoryl group of ATP as the major source for autophosphorylation (Stock et al., 2000). Significant down-regulation of genes encoding the electron transport chain and nucleotide biosynthesis was observed in the *csrA* mutant of *E. amylovora* (Table 5.3, A.1, A.2). This might also cause insufficient levels of ATP in the cell to activate signal transduction, and thus reduce the Rcs system activity in the absence of CsrA.

The nucleotide second messenger (p)ppGpp is another major global regulatory systems in bacteria. Under starvation conditions, bacteria produce high levels of (p)ppGpp, which induces massive transcriptional reprogramming to adjust various stress responses (Dalebroux and Swanson, 2012). During early stages of infection processes, *E. amylovora* undergoes the nutrient-limited conditions. The subsequent accumulation of (p)ppGpp plays an essential role in virulence activation by reducing cell size to increase resistance to abiotic stresses and activating the RpoN-HrpL alternative sigma factor cascade for T3SS gene expression (Khakimova et al., 2013; Ancona et al., 2015b). Since the presence of both (p)ppGpp and CsrA is essential for the T3SS, codependence of two global regulators was of particular interests in our studies. In *E. coli*, (p)ppGpp and DksA positively regulates the expression of CsrA and *csrB*/*csrC* sRNAs, while CsrA suppresses (p)ppGpp accumulation by inhibiting *relA* translation, forming a reciprocal regulatory circuit (Edwards et al., 2011). In contrast, in *E. amylovora*, the absence in *dksA* resulted in about 2-fold decrease in *csrA* transcription, but no significant effects by (p)ppGpp were observed on *csrB* expression under the T3SS-inducing condition (unpublished data). *E. amylovora* CsrA is also required for full translation of *relA*, although it binds to the region near the ribosome-binding site and the start codon (Fig. 5.11). Similar observation was reported in *L. pneumophila*, but the exact molecular mechanisms underlying this auxiliary effect of CsrA binding remain unclear (Sahr et al., 2017). Taken together, CsrA enables *E. amylovora* to induce higher levels of (p)ppGpp by maintaining cellular nucleotide pool and also activating full *relA* translation.

In summary, our results showed that CsrA is a key component coordinating a number of cellular processes in *E. amylovora*. Major CsrA targets responsible for the regulation of

virulence, including T3SS, EPS amylovoran and motility, were characterized, while our understanding of how the Csr system monitors cellular homeostasis is still incomplete. Future direction of this study might include identification of additional CsrA target genes that are associated with the regulation of physiologically important processes.

5.6 Tables

Table 5.1 Bacterial strains and plasmids used in this study

Strains, Plasmids	Description	Reference, Source
E. amylovora		
Ea1189	Wild type, isolated from apple	Wang et al., 2009
Δ*csrA*	*csrA*::Cm; Cm^R-insertional mutant of *csrA* of Ea1189	Ancona et al. 2016
Δ*csrB*	*csrB*::Cm; Cm^R-insertional mutant of *csrB* of Ea1189	Ancona et al. 2016
E. coli		
DH10B	F– *mcr*A Δ(*mrr-hsd*RMS-*mcr*BC) Φ80*lacZ*ΔM15 Δ*lac*X74 *rec*A1 *end*A1 *ara*D139 Δ(*ara leu*) 7697 *gal*U *gal*K *rps*L *nup*G λ-	Invitrogen
BL21 (DE3)	F^- *ompT hsdS*$_B$ (r_B^- m_B^-) *gal dcm* (DE3)	Novagen, CA
XL10-Gold	Tet^R Δ(*mcrA*)*183* Δ(*mcrCB-hsdSMR-mrr*)*173 endA1 supE44 thi-1 recA1 gyrA96 relA1 lac* Hte	Stratagene, CA
Plasmids		
pWSK29	Ap^R, cloning vector, low copy number	Wang and Kushner, 1991
pET28a	Km^R, T7 expression vector carrying an N-terminal His-Tag/thrombin/T7 Tag coniguration plus an optional C-terminal His-Tag sequence	Novagen, CA
pCsrA-His	183-bp DNA fragment containing *csrA* gene in pET28a	This study
pRS552	Translation fusion vector containing the MCS, *Eco*RI-*Sma*I-*Bam*HI-*lacZYA′*	Simons et al., 1987
pHRP309	Broad-host-range *lacZ* transcriptional fusion vector, Gm^R	Parales and Harwood
pZLac29	pWSK29 containing the MCS, *Eco*RI-*Sma*I-*Bam*HI-*lacZ*	This study
pFlhD309	626-bp fragment containing *flhD* gene (-600-+26) in pHRP309	This study
pFliL309	626-bp fragment containing *fliL* gene (-600-+26) in pHRP309	This study
pFliA309	626-bp fragment containing *fliA* gene (-600-+26) in pHRP309	This study
pFlgM309	626-bp fragment containing *flgM* gene (-600-+26) in pHRP309	This study
pFliD309	626-bp fragment containing *fliD* gene (-600-+26) in pHRP309	This study
pFlhD29	626-bp fragment containing *flhD* gene (-600-+26) in pZLac29	This study
pFlhD29-Mut1	626-bp fragment containing *flhD* gene (-600-+26) with a mutation at position -253 to -251 in pZLac29	This study
pFlhD29-Mut2	626-bp fragment containing *flhD* gene (-600-+26) with a mutation at position -216 to -214 in pZLac29	This study
pFlhD29-Mut3	626-bp fragment containing *flhD* gene (-600-+26) with a mutation at position -204 to -202 in pZLac29	This study
pFlhD29-Mut4	626-bp fragment containing *flhD* gene (-600-+26) with a mutation at position -189 to -187 in pZLac29	This study
pRelA29	626-bp fragment containing *relA* gene (-600-+26) in pZLac29	This study
pRelA29-Mut	626-bp fragment containing *flhD* gene (-600-+26) with a mutation at position -20 to -18 in pZLac29	This study
pSpoT29	626-bp fragment containing *spoT* gene (-600-+26) in pZLac29	This study
pRcsD29	626-bp fragment containing *rcsD* gene (-600-+26) in pZLac29	This study
pRcsB29	626-bp fragment containing *rcsB* gene (-600-+26) in pZLac29	This study

Table 5.2 Primers used in this study

Primer	Sequences (5'- 3')
Cloning of *lacZ* reporter gene fusion constructs	
FlhDlac-F	AGTCGAATTCTCTAGACACCGTGAGTGATTAATTCAT
FlhDlac-R	AGTCGGATCCTGTTTGAGTAATTCTGATGT
FliLlac-F	AGTCGAATTCTCTAGAACCGCTACTCAACGCCCAGC
FliLlac-R	AGTCGGATCCCTCTTGGCTTTCGCGCTATT
FliAlac-F	AGTCGAATTCTCTAGAGTTGCCGCAGCCTGGCGGCG
FliAlac-R	AGTCGGATCCCGCTGCCACAGCGAATGTTT
FlgMlac-F	AGTCGAATTCTCTAGACTGTGACAACCCGCAATTCC
FlgMlac-R	AGTCGGATCCATGGGCTGAGTTCTGTCGAT
FliDlac-F	AGTCGAATTCTCTAGATCGGAATCAGAGTTAGTGCC
FliDlac-R	AGTCGGATCCATGCCTAAAGTAGAAATACT
RelAlac-F	AGTCGAATTCTCTAGAGACTCGCTGGAGCAGGTTAG
RelAlac-R	AGTCGGATCCAGATGTGCACTTCTTACCGC
SpoTlac-F	AGTCGAATTCTCTAGATCACCAAACGTATGGCTCAG
SpoTlac-R	AGTCGGATCCTGATTGAGGCTTTCAAACAG
RcsDlac-F	AGTCGAATTCTCTAGATCCGATAAACAAGAGGAATT
RcsDlac-R	AGTCGGATCCGTTAGCGGAAATTTATATGG
RcsBlac-F	AGTCGAATTCTCTAGATGATTGATATTACCGTTGAG
RcsBlac-R	AGTCGGATCCGCAATAATGACATTCAGATT
qRT-PCR	
purF-rt1	AATTACCCTTGCCCATAACG
purF-rt2	GCGGCGAAGATGTTATCCGC
pyrB-rt1	GGCGTCGGTGGTGGGCTTTG
pyrB-rt1	TTCAGTACCGGCACGCCGCC
atpB-rt1	CGAAATCAGCAACCAGCGGC
atpB-rt1	AGCAAATCGATAGGCAGCAG
cydA-rt1	CACTGTTGACTTACGAAGTG
cydA-rt1	CTGCGGGGTTTGCATCCAGC
celB-rt1	TCGCTGCCGCTATCGCCTAC
celB-rt1	AGCTCGGTGGAATAAAGGCT
bioB-rt1	GCATGACGCTGGGTTCGCTC
bioB-rt1	GAACAGACCTTGATGCCGGC
hrpL-rt1	TTAAGGCAATGCCAAACACC
hrpL-rt1	GACGCGTGCATCATTTTATT
hsvA-rt1	AACGCTTCCCGGAAGAACTG
hsvA-rt1	GCAAAAAGACAGTCCCTTGG
narP-rt1	CGGGACTTGAAACCCTAAAG
narP-rt1	ACTCTACCTTCAGCCACCTC
Site-directed mutagenesis	
flhD-GGA1-F	GATAGAGTTGCCTTGCTTTAATAGTCCTGGTAGAGTGCAA
flhD-GGA1-R	TTGCACTCTACCAGGACTATTAAAGCAAGGCAACTCTATC
flhD-GGA2-F	GTGCAACAAGAAGTCATAAAAGAAGTCAGGGAAGAAGAGG
flhD-GGA2-R	CCTCTTCTTCCCTGACTTCTTTTATGACTTCTTGTTGCAC
flhD-GGA3-F	GTCATAAAGGAAGAAGTCAGAGAAGAGGCTCAGGAATAGC
flhD-GGA3-R	GCTATTCCTGAGCCTCTTCTCTGACTTCTTCCTTTATGAC
flhD-GGA4-F	GTCAGGGAAGAAGAGGCTCAATAGCCGCTGGCAAAACGAG
flhD-GGA4-R	CTCGTTTTGCCAGCGGCTATTGAGCCTCTTCTTCCCTGAC

Table 5.2 (cont.)

Primer	Sequences (5'- 3')
Site-directed mutagenesis	
relA-GGA-F	TAGCTCCCTGAACGGGGGCAATGCCTGGAGGGCAT
relA-GGA-R	ATGCCCTCCAGGCATTGCCCCCGTTCAGGGAGCTA
Cloning of protein expression constructs	
csrAhis-F	CAGCCATATGATGCTTATTCTAACTCGTCG
csrAhis-R	GATCCTCGAGTTAGTAACTCGTTTGCTGCG
RNA EMSA	
csrB-F-T7	TAATACGACTCACTATGGGCGTTGCGAAGGAACAGCATGAT
csrB-R-T7	TGAGCAGACATCTTCCTGACGT
hrpL-F-T7	TAATACGACTCACTATGGGTCATCAGCCGCATTTATCGCGA
hrpL-R-T7	TTCTGTCATGGCTTGCTCCGTT
hrpS-F-T7	TAATACGACTCACTATGGGAAACACCATTAAAAACAATTGG
hrpS-R-T7	TGCTCTCTCCGTCCCGGCCATG
flhD-F-T7	TAATACGACTCACTATGGGAACAAGAAGTCATAAAGGAAGA
flhD-R-T7	TTTCCATCCTGACTAGCACTGC
rcsB-F-T7	TAATACGACTCACTATGGGACTGACCAACCAGAACATTTAG
rcsB-R-T7	CAGATTATTCATATTATTGGTT
relA-F-T7	TAATACGACTCACTATGGGCAATAAAGTATTACTTGATCCT
relA-R-T7	TACCGCAACCATATGCCCTCCA

Table 5.3 Differentially expressed group I genes[a] in HMM medium

Gene ID	Gene description	log_2FC Δ*csrA*/WT	log_2FC Δ*csrB*/WT
EAMY_0491	*lidJ*, disulphide bond formation protein	-1.31	2.84
EAMY_0492	phytochelatin synthase	-1.09	3.41
EAMY_0519	*hrpK*, T3SS, pathogenicity locus protein	-2.39	2.07
EAMY_0520	*hsvA*, T3SS, Hrp-associated systemic virulence protein	-2.52	3.47
EAMY_0521	*hsvB*, T3SS, Hrp-associated systemic virulence protein	-1.47	3.40
EAMY_0522	*hsvC*, T3SS, Hrp-associated systemic virulence protein	-1.10	2.52
EAMY_0524	biphenyl 2,3-dioxygenase	-4.40	1.80
EAMY_0525	*hrcU*, T3SS, type III secretion protein	-3.17	1.71
EAMY_0526	*hrcT*, T3SS, type III secretion apparatus protein	-2.66	1.90
EAMY_0527	*hrcS*, T3SS, type III secretion protein	-4.29	1.89
EAMY_0528	*hrcR*, T3SS, type III secretion apparatus protein	-3.76	1.93
EAMY_0529	*hrcQ*, T3SS, type III secretion system apparatus protein	-3.12	1.80
EAMY_0530	*hrpP*, T3SS, type III secretion protein	-4.35	1.80
EAMY_0531	*hrpO*, T3SS, type III secretion protein	-5.30	1.81
EAMY_0532	*hrcN*, T3SS, type III secretion system ATPase	-4.90	1.78
EAMY_0533	*hrpQ*, T3SS, type III secretion system protein	-5.79	1.83
EAMY_0534	*hrcV*, T3SS, type III secretion inner-membrane protein	-5.45	1.78
EAMY_0535	*hrpJ*, T3SS, type III secretion system protein	-5.59	1.73
EAMY_0536	*hrpL*, T3SS, RNA polymerase sigma factor	-5.58	1.68
EAMY_0542	*hrpA*, T3SS, Hrp pili protein	-6.87	1.72
EAMY_0543	*hrpB*, T3SS, type III secretion system protein	-6.20	1.67
EAMY_0544	*hrcJ*, T3SS, type III secretion inner-membrane protein	-5.78	1.66
EAMY_0545	*hrpD*, T3SS, type III secretion protein	-5.43	1.73
EAMY_0546	*hrpE*, T3SS, type III secretion apparatus protein	-3.94	1.81
EAMY_0547	*hrpF*, T3SS, type III secretion protein	-5.67	1.73
EAMY_0548	*hrpG*, T3SS, type III secretion protein	-5.57	1.73
EAMY_0549	*hrcC*, T3SS, type III secretion system outer membrane pore	-5.07	1.78
EAMY_0550	*hrpT*, T3SS, type III secretion lipoprotein	-4.71	1.79
EAMY_0551	*hrpV*, T3SS, type III secretion protein	-4.75	1.75
EAMY_0552	*hrpN*, T3SS, harpin protein	-6.50	1.98
EAMY_0553	*orfA*, T3SS, Tir chaperone family protein	-4.81	1.79
EAMY_0554	*orfB*, T3SS, avirulence protein	-3.78	1.71
EAMY_0555	*orfC*, T3SS, HrpW-specific chaperone	-5.28	1.80
EAMY_0556	*hrpW*, T3SS, harpin protein	-5.82	1.90
EAMY_0557	*dspE*, T3SS, Hrp secreted pathogenicity-like protein	-5.20	1.58
EAMY_0558	*dspF*, T3SS, Hrp secreted pathogenicity-like protein	-5.20	1.57
EAMY_0653	*eop2*, T3SS, type III effector	-3.62	1.85
EAMY_1450	*flgN*, motility, flagella synthesis protein	-1.77	1.64
EAMY_1451	*flgM*, motility, negative regulator of flagellin synthesis	-2.16	1.70
EAMY_1462	*flgK*, motility, flagellar hook-associated protein	-1.83	1.65
EAMY_1463	*flgL*, motility, flagellar hook-associated protein	-1.92	1.75
EAMY_1498	*rcsA*, colanic acid capsular biosynthesis activation protein	-1.42	2.73

Table 5.3 (cont.)

Gene ID	Gene description	log_2FC Δ*csrA*/WT	log_2FC Δ*csrB*/WT
EAMY_2094	*cheW*, motility, chemotaxis signal transduction protein	-2.07	1.33
EAMY_2095	*cheA*, motility, chemotactic sensory histidine kinase	-2.21	1.44
EAMY_2096	*motB*, motility, flagellar motor protein	-2.25	1.57
EAMY_2097	*motA*, motility, flagellar motor protein	-2.96	1.46
EAMY_2134	*yedO*, 1-aminocyclopropane-1-carboxylate deaminase	-1.83	1.48
EAMY_2135	*D*-cysteine desulfhydrase	-1.45	1.41
EAMY_2139	*fliA*, motility, RNA polymerase sigma factor	-5.35	1.09
EAMY_2141	*fliC*, motility, filament structural protein	-3.22	3.42
EAMY_2142	*fliD*, motility, flagellar capping protein	-2.71	1.62
EAMY_2143	*fliS*, motility, flagellin-specific chaperone	-2.72	1.26
EAMY_2144	*fliT*, motility, flagellar export chaperone	-1.85	1.23
EAMY_2218	*yeeF*, putrescine transporter	-1.16	1.03
EAMY_2275	*aroQ*, chorismate mutase	-1.42	1.43
EAMY_2945	acyltransferase	-1.16	1.79
EAMY_3175	*avrRpt2*, T3SS, cysteine protease avirulence protein	-1.61	1.54

[a] Group I genes were down-regulated in the *csrA* mutant but up-regulated in the *csrB* mutnat with $|log_2FC|$ value ≥ 1 and a corrected p value < 0.05 between the WT and the mutants.

Table 5.4 Differentially expressed group II genes[a] in HMM medium

Gene ID	Gene description	log_2FC Δ*csrA*/WT	log_2FC Δ*csrB*/WT
EAMY_0054	LuxR-family transcriptional regulator	2.22	-1.47722
EAMY_0249	*ompT*, outer membrane protease	1.13	-1.01609
EAMY_0441	creatininase	2.41	-2.6658
EAMY_0442	dihydroorotate dehydrogenase	2.51	-2.74218
EAMY_0444	*mcyE*, Glutamate-1-semialdehyde aminotransferase	2.84	-2.9406
EAMY_0445	*mcyE*, beta-ketoacyl synthase	2.18	-2.36154
EAMY_0446	*irp*, polyketide synthase	2.38	-2.78833
EAMY_0447	*sypC*, gramicidin S synthetase II	2.50	-2.96328
EAMY_0448	*ppsD*, polyketide synthase	2.41	-2.81697
EAMY_0449	polyketide synthase	1.84	-2.13904
EAMY_1738	*ynfM*, major facilitator superfamily transporter	1.80	-1.03952
EAMY_2423	*fabB*, 3-oxoacyl-(acyl-carrier-protein) synthase	2.87	-1.15477
EAMY_2475	hypothetical protein	1.44	-1.81294
EAMY_2506	*narQ*, two-component system histidine kinase	1.15	-1.44746
EAMY_2552	major facilitator superfamily transporter	3.62	-1.22834
EAMY_2800	*rcsV*, LuxR-family transcriptional regulator	5.85	-1.68411
EAMY_2813	*ygbF*, CRISPR-associated protein Cas2	1.32	-1.70694
EAMY_2814	*ygbT*, CRISPR-associated protein Cas1	1.29	-2.01252
EAMY_2815	*ygcH*, Cse3-family CRISPR-associated protein	1.12	-2.10032
EAMY_2816	*ygcI*, CRISPR-associated protein Cas5	1.21	-2.21313
EAMY_2817	*ygcJ*, Cse4-family CRISPR-associated protein	1.39	-2.2221
EAMY_2818	*ygcK*, Cse2-family CRISPR-associated protein	1.61	-2.25029
EAMY_2819	*ygcL*, Cse1-family CRISPR-associated protein	1.90	-2.20392
EAMY_2820	*ygcB*, CRISPR-associated helicase Cas3	1.68	-1.68656

[a] Group II genes were up-regulated in the *csrA* mutant but down-regulated in the *csrB* mutnat with $|log_2FC|$ value ≥ 1 and a corrected *p* value < 0.05 between the WT and the mutants.

Table 5.5 Differentially expressed group III genes[a] in HMM medium

Gene ID	Gene description	log_2FC Δ*csrA*/WT	log_2FC Δ*csrB*/WT
EAMY_0110	*cdh*, CDP-diacylglycerol pyrophosphatase	2.76	1.10
EAMY_0131	*hslU*, ATP-dependent protease	1.04	1.26
EAMY_0132	*hslV*, ATP-dependent protease	1.13	1.17
EAMY_0658	*prfB*, peptide chain release factor I	1.10	1.43
EAMY_0826	*aroF*, phospho-2-dehydro-3-deoxyheptonate aldolase	3.91	4.12
EAMY_0827	*tyrA*, prephenate dehydrogenase	2.63	2.79
EAMY_1019	*htpG*, molecular chaperone	2.38	1.17
EAMY_1371	*ssuD*, alkanesulfonate monooxygenase	3.98	1.03
EAMY_1373	*ssuE*, NAD(P)H-dependent FMN reductase	5.72	1.88
EAMY_1548	*mltE*, membrane-bound lytic murein transglycosylase E	1.30	1.50
EAMY_1749	*dcp*, dipeptidyl carboxypeptidase II	1.79	1.99
EAMY_1987	*wbaP*, undecaprenyl-phosphate galactose phosphotransferase	3.89	1.26
EAMY_3179	*groL*, molecular chaperone	2.61	1.57
EAMY_3180	*groE*, molecular chaperone	2.69	1.58
EAMY_3405	*tauC*, taurine ABC transporter permease	4.06	1.02
EAMY_3566	*gnl*, gluconolactonase	1.75	1.47

[a] Group III genes were up-regulated in both the *csrA* and *csrB* mutnats with $|log_2FC|$ value ≥ 1 and a corrected *p* value < 0.05 between the WT and the mutants.

Table 5.6 Differentially expressed group IV genes[a] in HMM medium

Gene ID	Gene description	log_2FC Δ*csrA*/WT	log_2FC Δ*csrB*/WT
EAMY_0148	*oxyR*, hydrogen peroxide-inducible genes activator	-2.11	-2.66
EAMY_0463	*yqhE*, 2,5-diketo-*D*-gluconate reductase	-1.39	-1.27
EAMY_0472	*yghA*, oxidoreductase	-1.96	-1.29
EAMY_0622	acyltransferase	-1.57	-1.33
EAMY_0720	lipoprotein	-2.19	-1.36
EAMY_0914	*psiF*, phosphate starvation-inducible protein	-1.66	-1.69
EAMY_0956	lipoprotein	-1.89	-1.75
EAMY_0957	*ygaU*, peptidoglycan-binding protein	-1.93	-1.80
EAMY_0999	*ybaY*, lipoprotein	-1.30	-1.19
EAMY_1068	*osmC*, peroxiredoxin	-1.94	-1.75
EAMY_1181	*nadA*, Quinolinate synthetase	-2.44	-2.73
EAMY_1182	*pnuC*, nicotinamide mononucleotide transporter	-2.17	-2.12
EAMY_1183	*ybgR*, zinc transporter	-1.05	-1.28
EAMY_1184	*ybgS*, homeobox protein	-2.29	-1.11
EAMY_1204	*yncB*, NADP-dependent oxidoreductases	-1.96	-1.12
EAMY_1230	*yohC*, YIP1 family protein	-2.29	-2.19
EAMY_1239	glycosyltransferase	-1.76	-1.52
EAMY_1262	aspartate/glutamate/hydantoin racemase	-1.16	-1.03
EAMY_1275	*dps*, DNA-binding ferritin-like protein	-1.39	-1.65
EAMY_1403	*agp*, glucose-1-phosphatase	-1.28	-1.25
EAMY_1420	*marR*, transcriptional regulator	-1.43	-1.14
EAMY_1427	*ymdC*, phospholipase D family protein	-1.44	-1.27
EAMY_1445	*grxB*, glutaredoxin II	-1.43	-1.11
EAMY_1551	*yeaQ*, membrane protein	-1.07	-1.49
EAMY_1566	lipoprotein	-2.29	-1.45
EAMY_1567	*ygdR*, lipoprotein	-2.50	-1.57
EAMY_1628	*astC*, succinylornithine transaminase	-1.95	-1.07
EAMY_1629	*astA*, arginine *N*-succinyltransferase	-1.51	-1.00
EAMY_1644	*yniA*, fructosamine kinase	-1.73	-1.43
EAMY_1645	*ydiZ*, hypothetical protein	-1.33	-1.41
EAMY_1686	*cfa*, cyclopropane-fatty-acyl-phospholipid synthase	-1.38	-1.09
EAMY_1786	*yhjG*, FAD monooxygenase	-1.14	-1.87
EAMY_1787	*pvcB*, pyoverdine biosynthesis protein	-1.09	-4.12
EAMY_1841	acid-shock protein	-2.09	-1.46
EAMY_1895	lipoprotein	-1.68	-1.70
EAMY_1905	*acnA*, aconitate hydratase	-1.77	-1.37
EAMY_2034	methyl-accepting chemotaxis protein	-2.51	-1.35
EAMY_2099	*flhC*, flagellar transcriptional activator	-4.10	-1.13
EAMY_2100	*flhD*, flagellar transcriptional activator	-4.29	-1.24
EAMY_2176	*sqdD*, glycosyltransferase	-1.90	-1.73
EAMY_2212	*yeeO*, Na^+-driven multidrug efflux pump	-1.34	-1.34

Table 5.6 (cont.)

Gene ID	Gene description	log_2FC Δ*csrA*/WT	log_2FC Δ*csrB*/WT
EAMY_2326	helicase	-3.42	-2.02
EAMY_2327	endonuclease	-3.14	-2.01
EAMY_2498	*amiA*, *N*-acetylmuramoyl-*L*-alanine amidase	-1.15	-1.15
EAMY_2570	*prt*, metalloprotease	-1.48	-1.54
EAMY_2602	*csiE*, transcriptional anti-terminator	-1.24	-1.20
EAMY_2970	nuclear pore complex protein	-1.05	-1.03
EAMY_3103	*yqjC*, hypothetical protein	-1.26	-1.40
EAMY_3104	*yqjD*, membrane protein	-1.43	-1.21
EAMY_3105	*yqjE*, membrane protein	-1.44	-1.18
EAMY_3245	*gdh*, glucose 1-dehydrogenase	-1.61	-1.02
EAMY_3249	*yedU*, intracellular protease/amidase	-1.34	-1.18
EAMY_3254	*treF*, cytoplasmic trehalase	-1.80	-1.15
EAMY_3325	*yjbJ*, CsbD family protein	-4.52	-2.90
EAMY_3533	*uspB*, universal stress protein	-1.02	-1.12
EAMY_3665	*kdgK*, 2-dehydro-3-deoxygluconokinase	-1.42	-1.58
EAMY_3693	*pstC*, phosphate ABC transporter	-1.25	-1.01
EAMY_3694	*pstS*, phosphate ABC transporter substrate-binding protein	-1.24	-1.14
EAMY_3695	*lscC*, levansucrase	-1.39	-4.06
EAMY_3696	bacteriophage protein	-2.16	-4.29

[a] Group IV genes were down-regulated in both the *csrA* and *csrB* mutnats with $|log_2FC|$ value ≥ 1 and a corrected *p* value < 0.05 between the WT and the mutants.

5.7 Figures

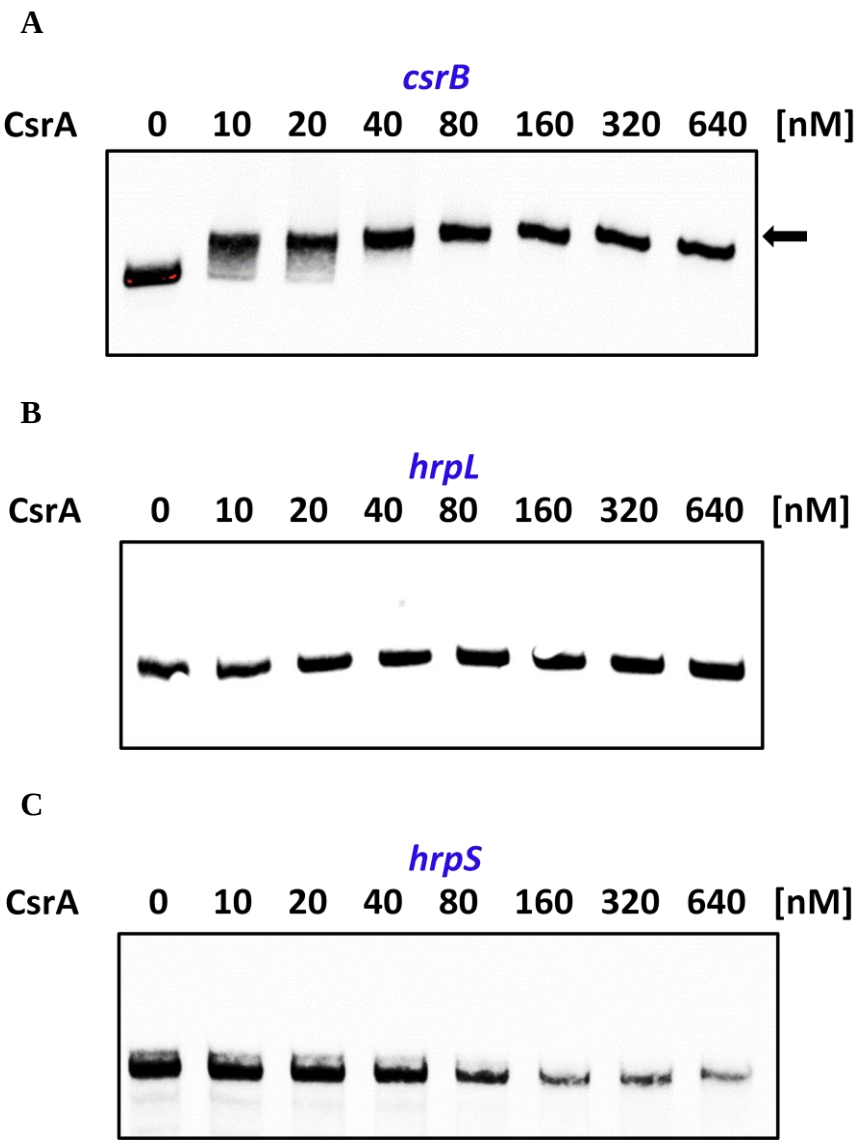

Figure 5.1 Gel shift assays (REMSA) of CsrA binding to the leader sequences of (A) *csrB*, (B) *hrpL*, (C) *hrpS*. Black arrows at the bottom and top indicate free probe and the protein-RNA complex, respectively. The concentration of protein (nM) is indicated above each lane. Experiments were repeated three times with similar results.

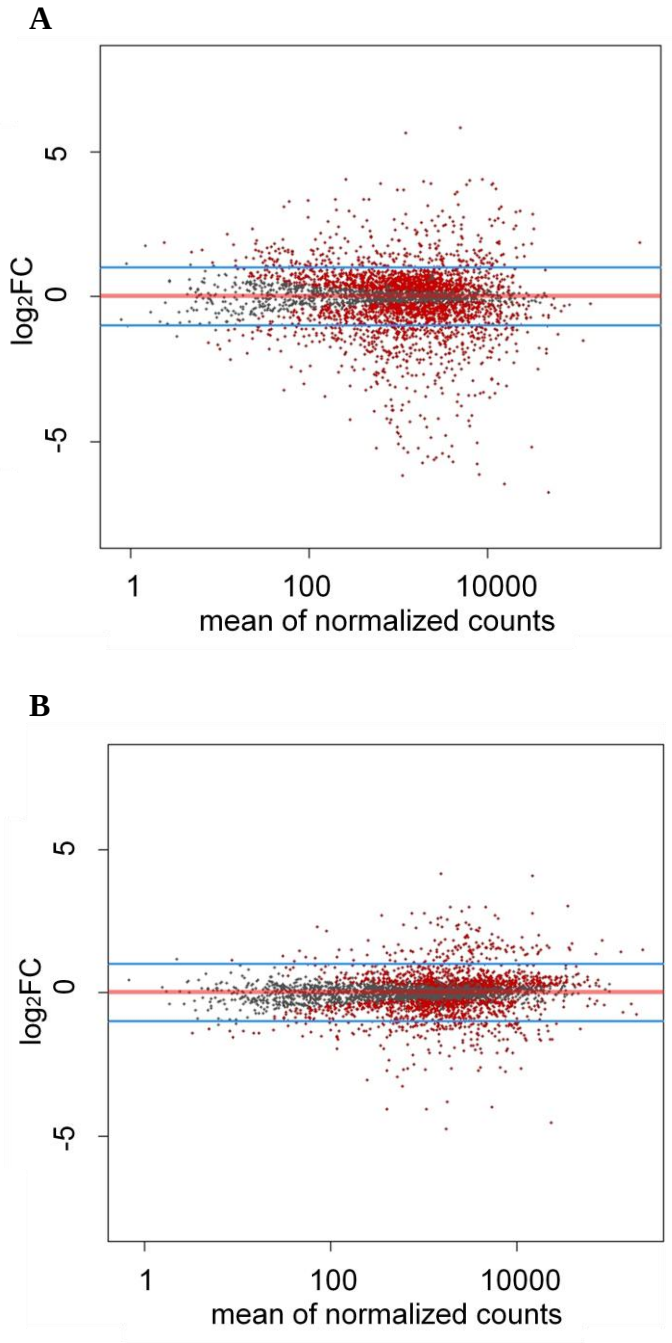

Figure 5.2 MA plots showing transcriptome changes of the mutants compared to the WT under the T3SS-inducing condition. (A) the *csrA* mutant. (B) the *csrB* mutant. The y-axis represents $\log_2$FC between the mutant and the WT, and the x-axis represents mean of normalized counts. Each dot indicates an individual gene; red dots indicate genes with a corrected *p* value < 0.05, while grey dots indicate genes with a corrected *p* value ≥ 0.05. Blue lines indicate $|\log_2 FC| = 1$.

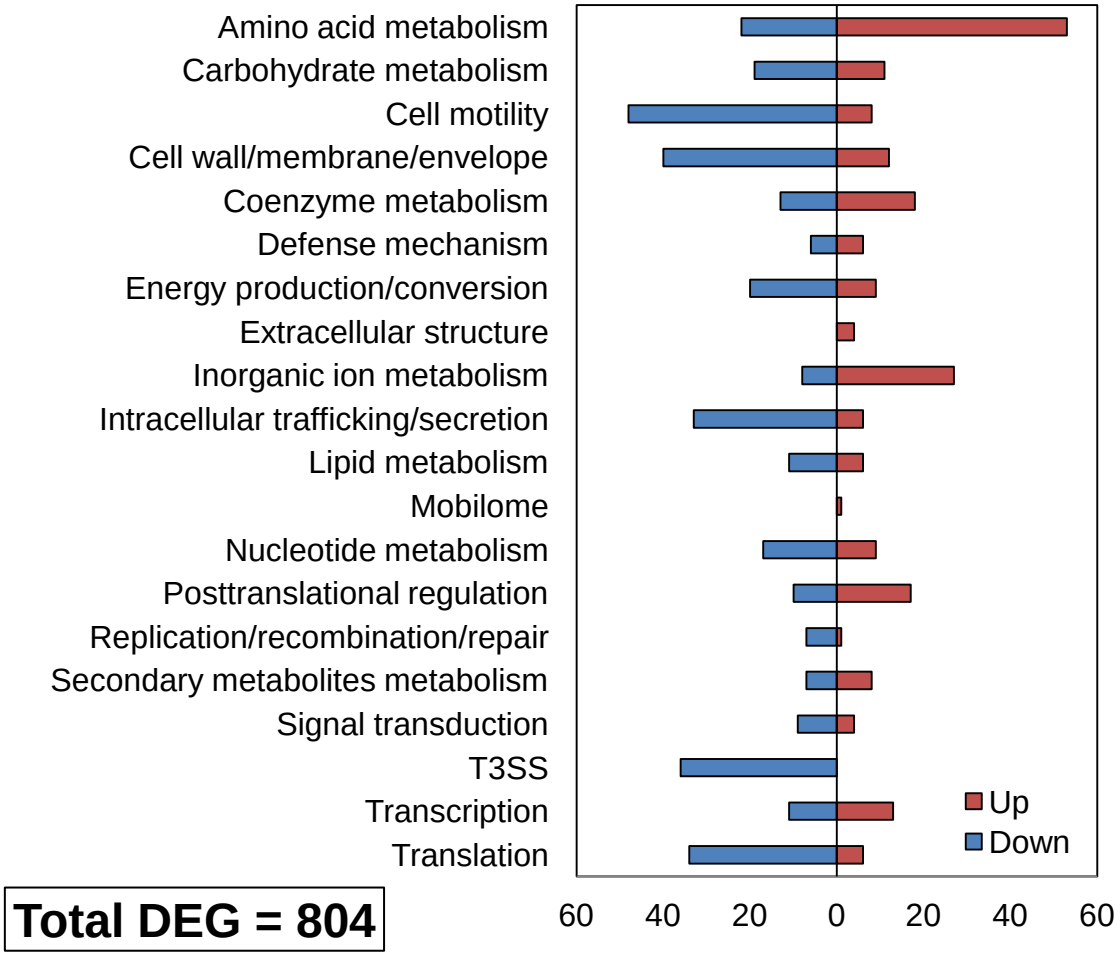

Figure 5.3 Differential gene expression of the *csrA* mutant compared to the WT under the T3SS-inducing condition. Functional classification of differentially expressed genes (DEGs) based on the clusters of orthologous groups (COGs). DEGs were defined as genes with a $|\log_2 FC|$ value ≥ 1 and a corrected p value < 0.05 from three independent biological replicates.

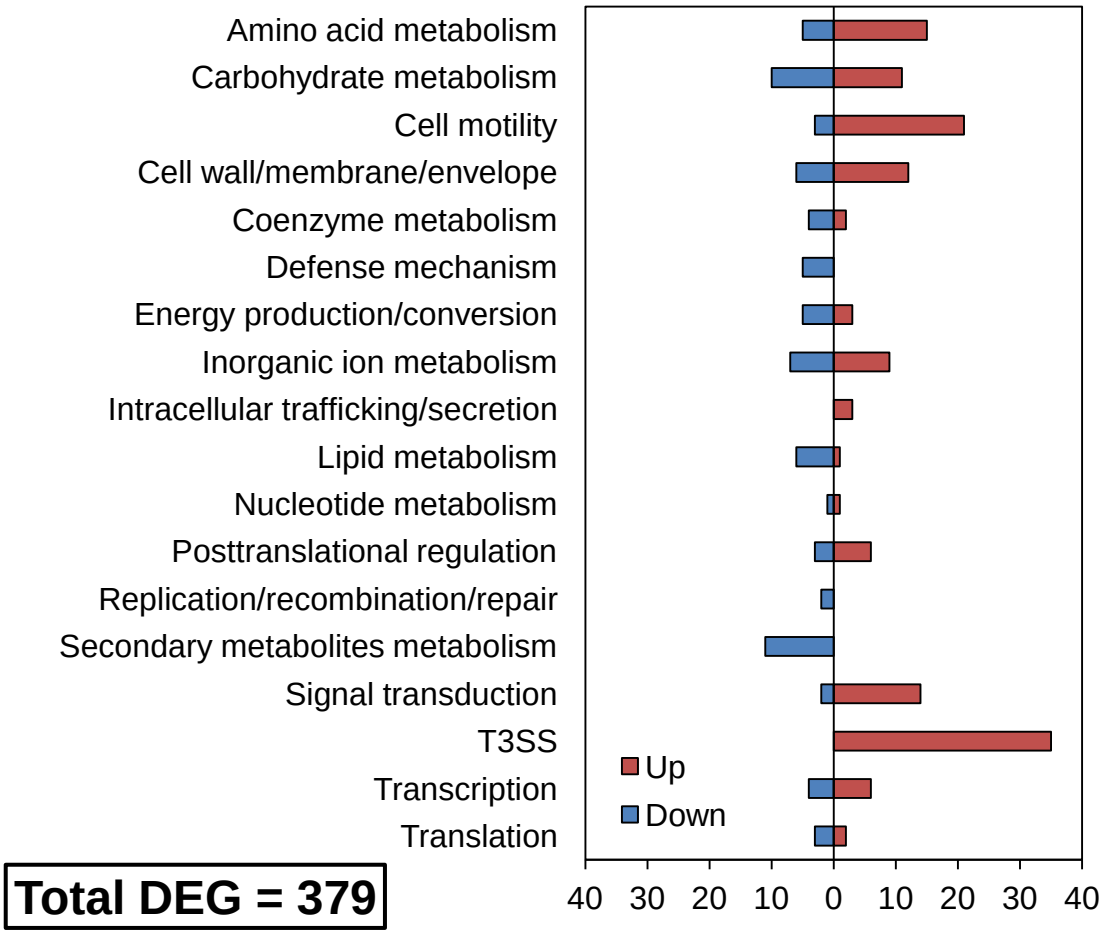

Figure 5.4 Differential gene expression of the *csrB* mutant compared to the WT under the T3SS-inducing condition. Functional classification of differentially expressed genes (DEGs) based on the clusters of orthologous groups (COGs). DEGs were defined as genes with a $|\log_2 FC|$ value ≥ 1 and a corrected p value < 0.05 from three independent biological replicates.

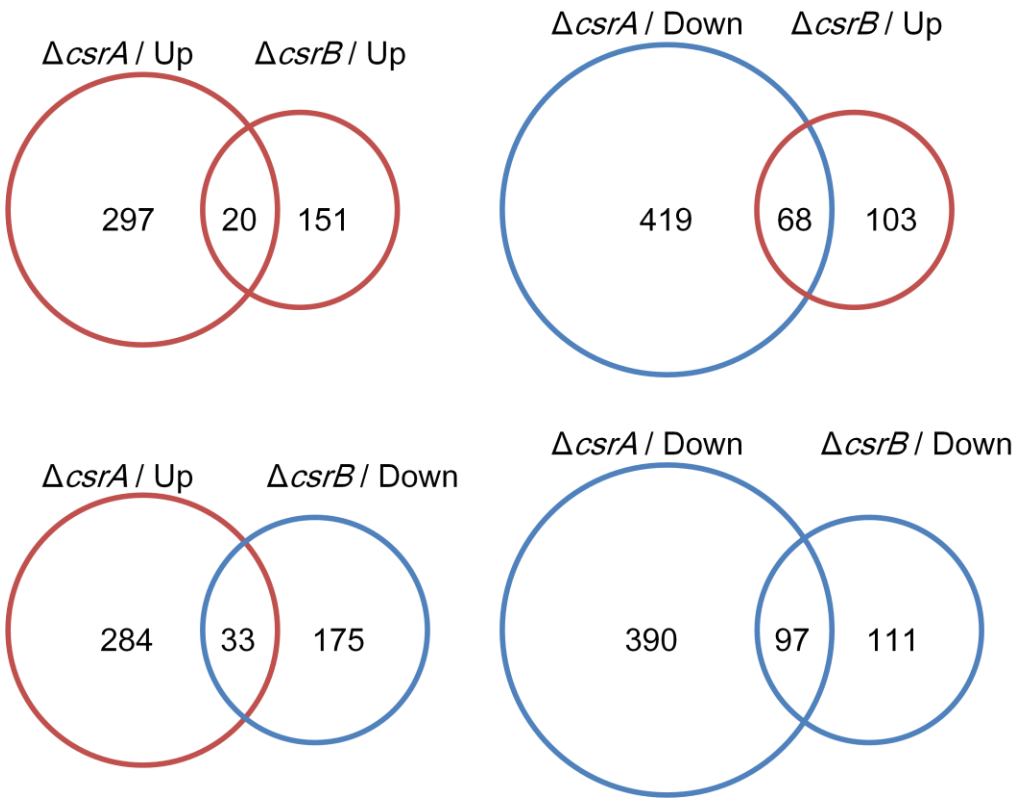

Figure 5.5 Venn diagrams of overlapping and unique differentially expressed genes (DEGs) between the *csrA* and *csrB* mutants. DEGs were defined as genes with a $|\log_2 FC|$ value ≥ 1 and a corrected p value < 0.05 from three independent biological replicates.

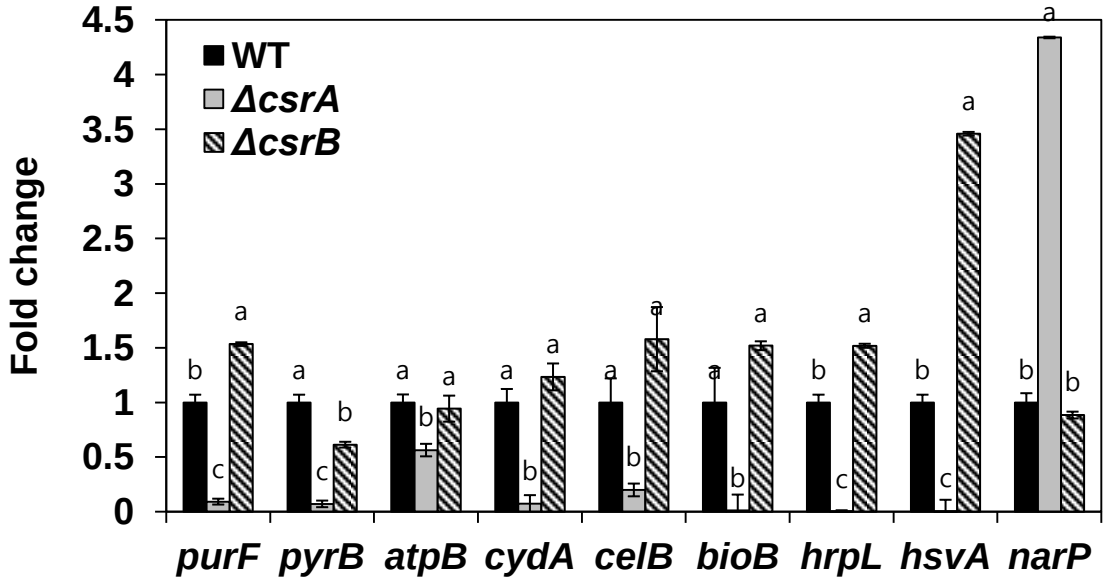

Figure 5.6 Validation of RNA-seq results. Relative gene expression of the selected genes in the *csrA* and *csrB* mutants compared to the WT grown in HMM at 18 ℃ for 6 h. The *rpoD* gene was used as an endogenous control. The values of the relative fold change were the means of three replicates, and the values with the same letter in each gene do not differ significantly ($p < 0.05$). Error bars indicate standard deviation.

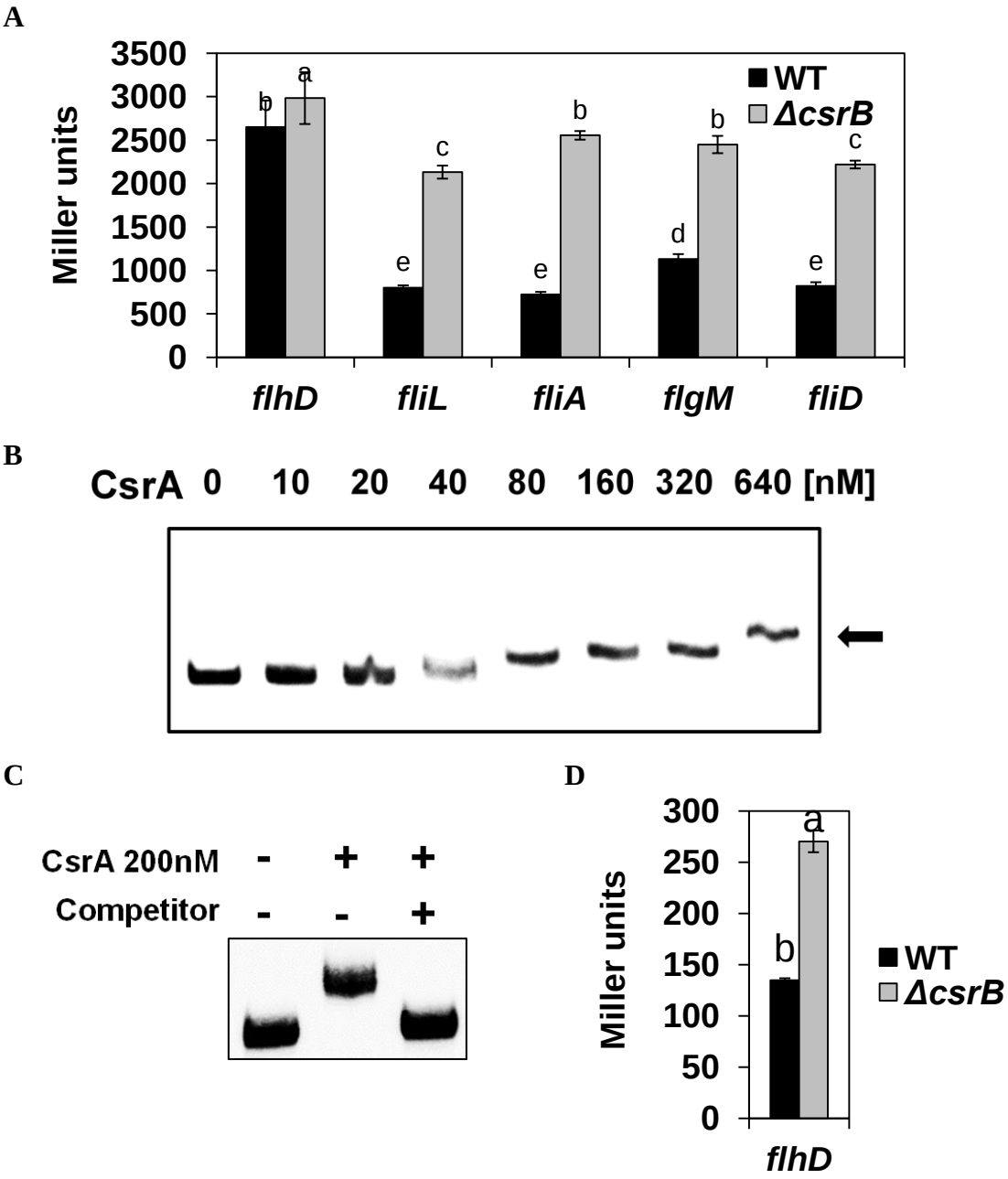

Figure 5.7 CsrA positively regulates *flhD* expression at the posttranscriptional level. (A) LacZ activities of transcriptional fusion constructs carrying upstream sequences of five different flagellar genes (*flhD*, *fliL*, *fliA*, *flgM*, *fliD*) in the WT and the *csrB* mutant grown in TB at 28 ℃ for 6 h. The values of Miller units were the means of four replicates. (B) REMSA for CsrA binding to the leader sequence of *flhD*. (C) Competition assay of interaction between CsrA and *flhD* RNA by adding unlabeled *csrB* RNA. Black arrows at the bottom and top indicate free probe and the protein-RNA complex, respectively. The concentration of protein (nM) is indicated above each lane. (D) LacZ activities of translational fusion constructs carrying upstream sequences of the *flhD* gene in the WT and the *csrB* mutant grown in TB at 28 ℃ for 6 h. The values of Miller units were the means of four replicates, and the values with the same letter do not differ significantly ($p < 0.05$). Experiments were repeated three times with similar results.

A

GCTTTAGGAATAGTCCTGGTAGAGTGCAACAAGAAGTC
TSS (1)
ATAAAGGAAGAAGTCAGGGAAGAAGAGGCTCAGGAATA
(2) (3) (4)
GCCGCTGGCAAAACGAGTCTATAATTATCTCTGGCTTA

GTTTCTCGAACTAAGAAATAAGCCAGCTTTAGCTCATC

TTTGGCTCCTGCCACTAAATATTTTGCCATCTTTAGAT

CTACCAACCAGCAACCAGGTAGCGGTATCCACCGCGCA

CGTTAAAAGCAGTGCTAGTCAGGATGGAAAAATG
start codon

B

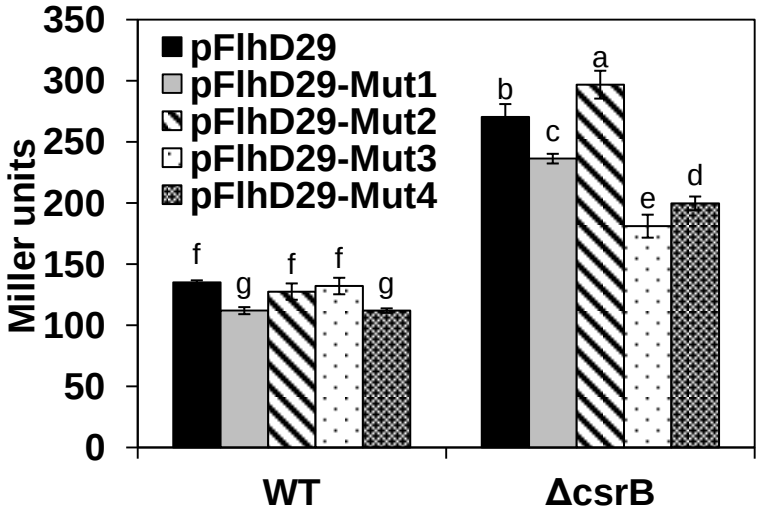

Figure 5.8 Binding of CsrA to the leader sequence of *flhD* enhances translation. (A) The leader sequence of the *flhD* gene. Transcription start site (TSS), four putative CsrA-binding sites and ATG start codon are underlined. Each GGA motif was deleted using site-directed mutagenesis, and the four different mutated sequences were cloned into pZLac29. The plasmids were designated as pFlhD29-Mut1 to pFlhD29-Mut4 and introduced into the WT and the *csrB* mutant. (B) LacZ activities of translational fusion constructs carrying different upstream sequences of the *flhD* gene in the WT and the *csrB* mutant grown in TB at 28 ℃ for 6 h. The values of Miller units were the means of four replicates, and the values with the same letter do not differ significantly ($p < 0.05$). Experiments were repeated three times with similar results.

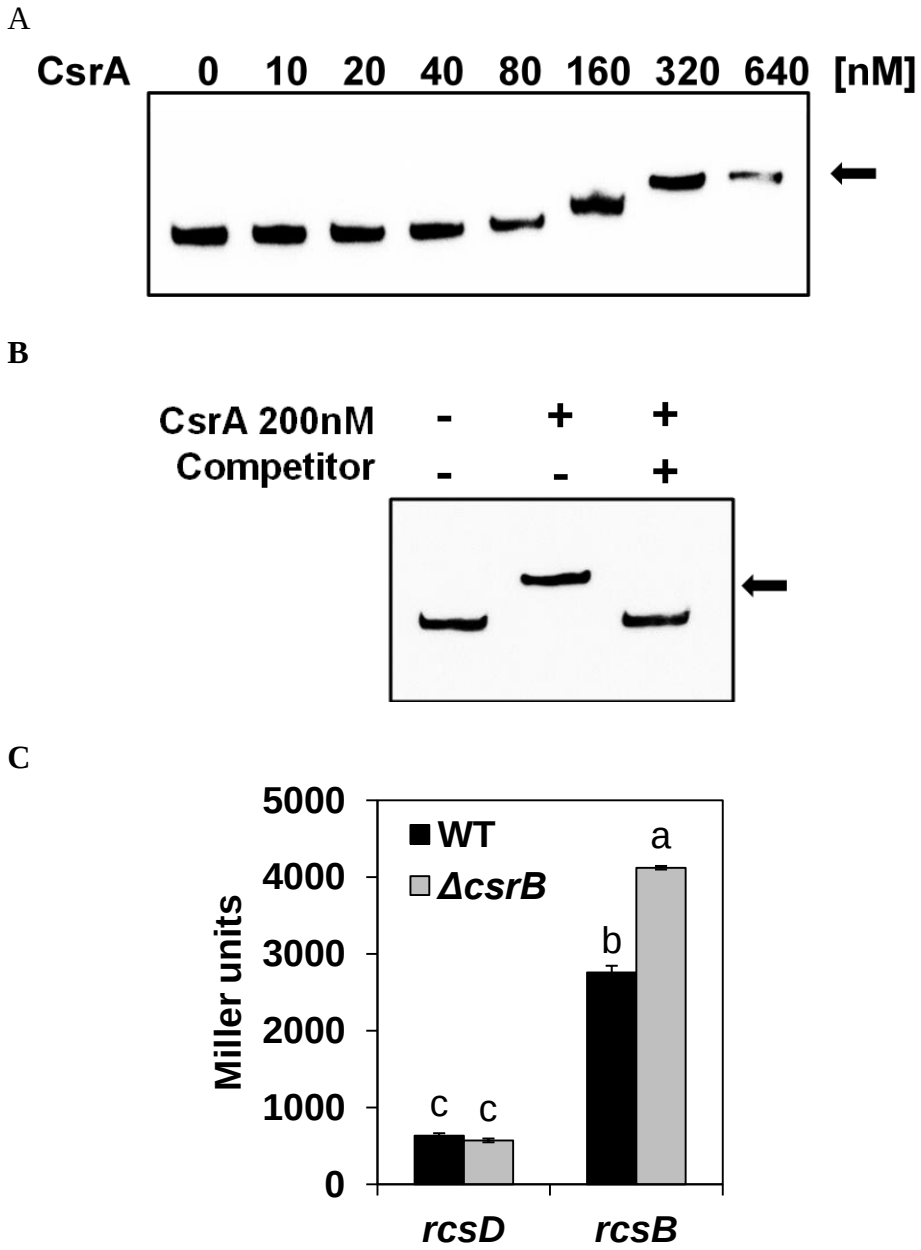

Figure 5.9 CsrA positively regulates *rcsB* expression at the posttranslational level. (A) REMSA for CsrA binding to the leader sequence of *rcsB*. (B) Competition assay of interaction between CsrA and *rcsB* RNA by adding unlabeled *csrB* RNA. Black arrows at the bottom and top indicate free probe and the protein-RNA complex, respectively. The concentration of protein (nM) is indicated above each lane. (C) LacZ activities of translational fusion constructs carrying upstream sequences of the *rcsD* and *rcsB* genes in the WT and the *csrB* mutant grown in HMM at 18 ℃ for 6 h. The values of Miller units were the means of four replicates, and the values with the same letter do not differ significantly ($p < 0.05$). Experiments were repeated three times with similar results.

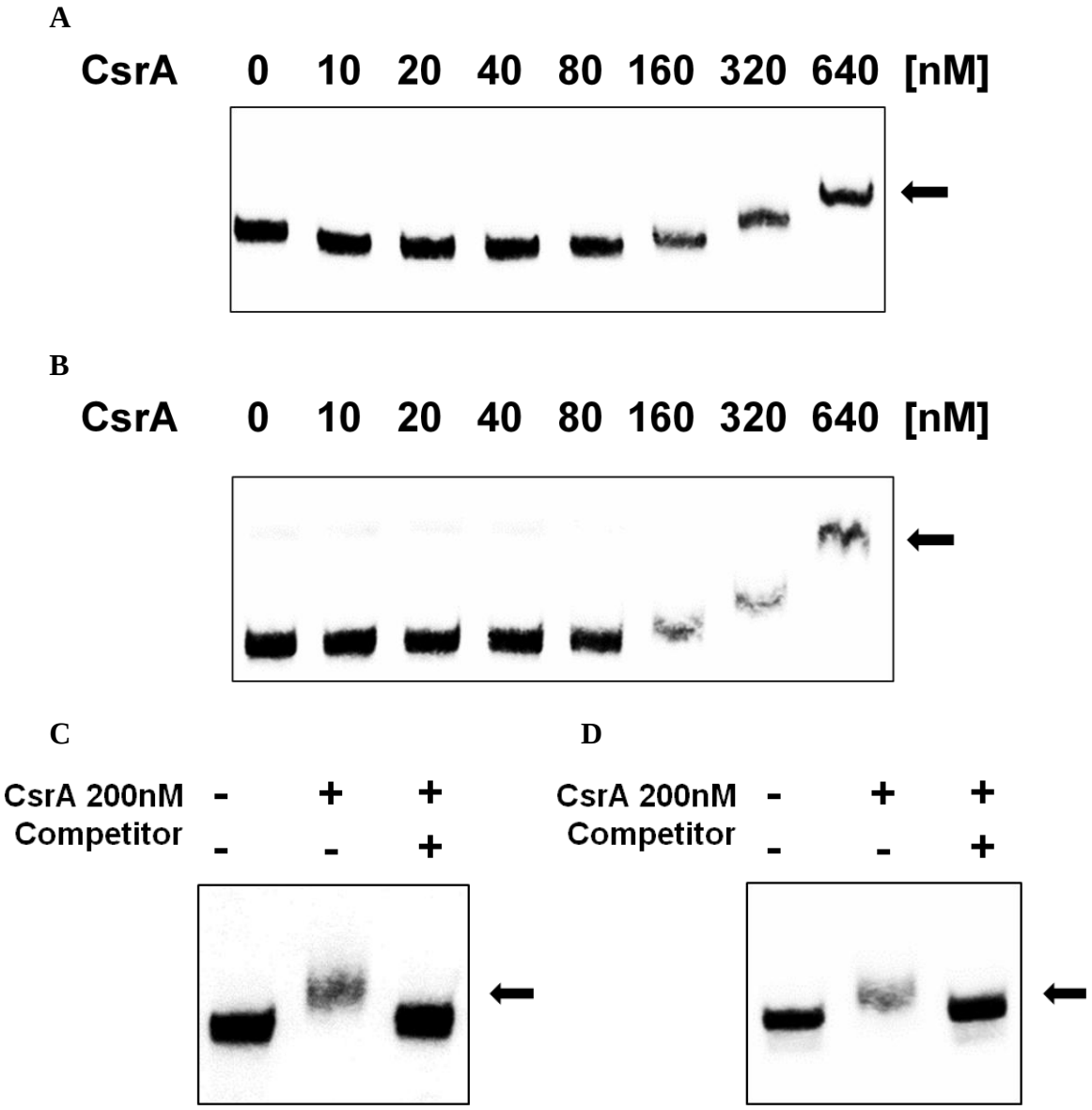

Figure 5.10 CsrA can interact with the leader sequence of *relA* and *spoT*. REMSA for CsrA binding to the leader sequence of (A) *relA* and (B) *spoT*. Competition assays of interaction between CsrA and (C) *relA* (D) *spoT* RNA probes by adding unlabeled *csrB* RNA. Black arrows at the bottom and top indicate free probe and the protein-RNA complex, respectively. The concentration of protein (nM) is indicated above each lane. Experiments were repeated three times with similar results.

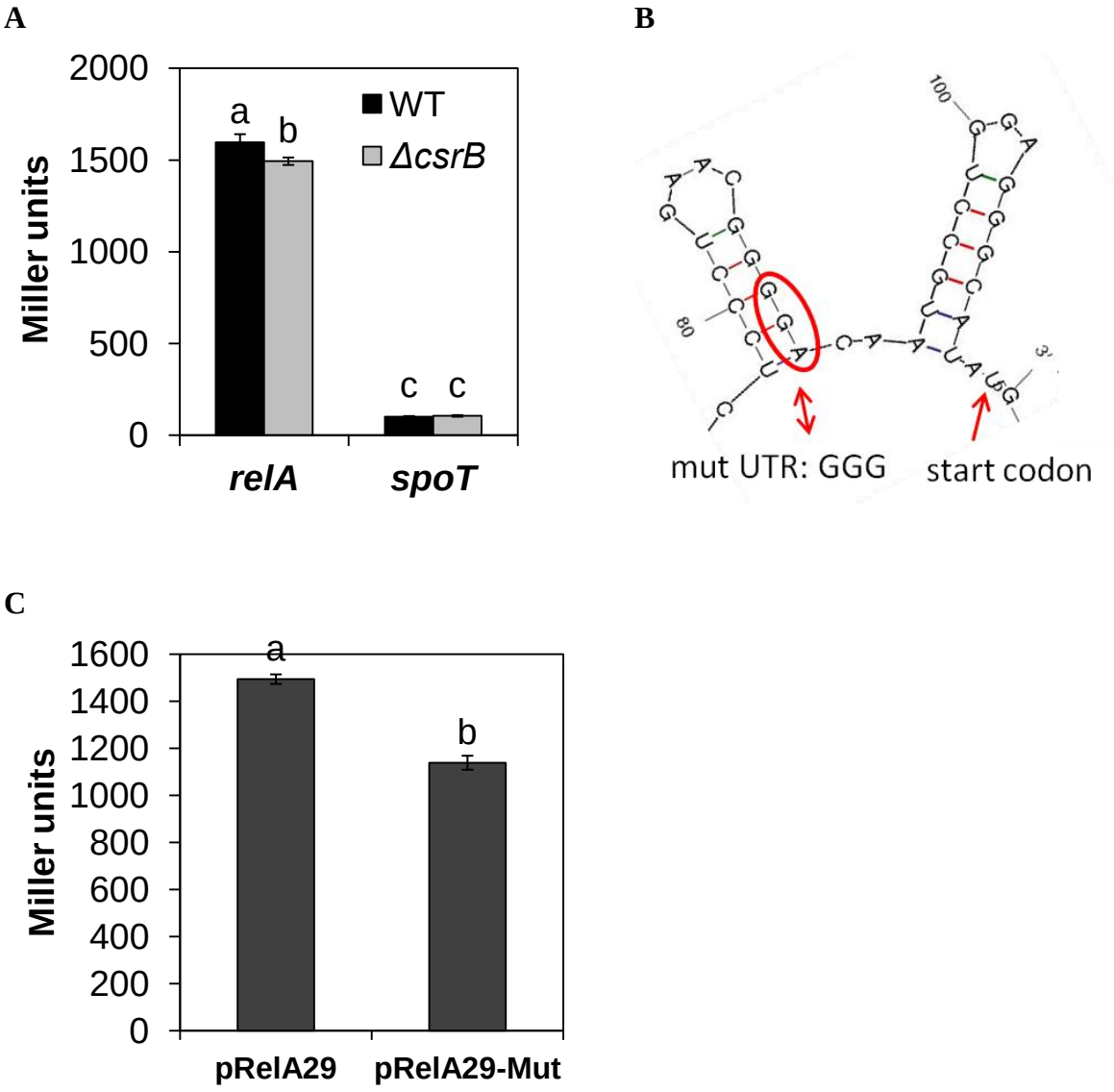

Figure 5.11 CsrA is required for full translation of *relA*. (A) LacZ activities of translational fusion constructs carrying upstream sequences of the *relA* and *spoT* genes in the WT and the *csrB* mutant grown in HMM at 18 ℃ for 6 h. The values of Miller units were the means of four replicates. (B) The predicted secondary structure of the *relA* leader sequence. The putative CsrA-binding site and the start codon are indicated with red circle and arrow, respectively. (C) LacZ activities of translational fusion constructs carrying different upstream sequences of the *relA* genes in the WT grown in HMM at 18 ℃ for 6 h. The values of Miller units were the means of four replicates, and the values with the same letter do not differ significantly ($p < 0.05$). Experiments were repeated three times with similar results.

REFERENCES

Aldridge P, Bernhard F, Bugert P, Coplin DL, Geider K (1998) Characterization of a gene locus from *Erwinia amylovora* with regulatory functions in exopolysaccharide synthesis of *Erwinia* spp. Can. J. Microbiol. 44: 657-666

Alfano JR, Collmer A (1997) The type III (Hrp) secretion pathway of plant pathogenic bacteria: trafficking harpins, Avr proteins, and death. J. Bacteriol. 179: 5655-5662

Amerik A, Antonov VK, Ostroumova NI, Rotanova TV, Chistiakova LG (1990) Cloning, structure and expression of the full-size *lon* gene in *Escherichia coli* coding for ATP-dependent La-proteinase. Bioor. Khim. 16: 869-880

Amerik A, Antonov VK, Gorbalenya AE, Kotova SA., Rotanova TV, Shimbarevich EV (1991). Site-directed mutagenesis of La protease. FEBS Lett. 287: 211-214

Ancona V, Zhao Y (2013) The GrrSA-Csr global regulatory system plays a critical role in *Erwinia amylovora* virulence. XIII Int. Work Fire Blight 1056: 207-212

Ancona V, Li W, Zhao Y (2014) Alternative sigma factor RpoN and its modulation protein YhbH are indispensable for *Erwinia amylovora* virulence. Mol. Plant. Pathol. 15: 58-66

Ancona V, Chatnaparat T, Zhao Y. (2015a) Conserved aspartate and lysine residues of RcsB are required for amylovoran biosynthesis, virulence, and DNA binding in *Erwinia amylovora*. Mol. Genet. Genomics 290**:** 1265-1276

Ancona V, Lee JH, Chatnaparat T, Oh J, Hong JI, Zhao Y. (2015b) The bacterial alarmone (p)ppGpp activates the type III secretion system in *Erwinia amylovora*. J. Bacteriol. 197: 1433-1443

Ancona V, Lee JH, Zhao Y (2016) The RNA-binding protein CsrA plays a central role in positively regulating virulence factors in *Erwinia amylovora*. Sci. Rep. 6: 37195

Anderson HW (1952) Maintaining virulent cultures of *Erwinia amylovora* and suggestion of overwinter survival in mummied fruit. Plant Dis. Rep. 36: 301-302

Andrade MO, Farah CS, Wang N (2014) The post-transcriptional regulator rsmA/csrA activates T3SS by stabilizing the 5' UTR of *hrpG*, the master regulator of *hrp*/*hrc* genes in *Xanthomonas*. PLoS Pathog. 10: e1003945

Andresen L, Sala E, Koiv V, Mäe A (2010) A role for the Rcs phosphorelay in regulating expression of plant cell wall degrading enzymes in *Pectobacterium carotovorum* subsp. *carotovorum*. Microbiol. 156: 1323-1334

Azam TA, Iwata A, Nishimura A, Ueda S, Ishihama A (1999) Growth phase dependent variation in protein composition of the *Escherichia coli* nucleoid. J. Bacteriol. 181: 6361-6370

Bachman MA, Swanson MS (2004) Genetic evidence that *Legionella pneumophila* RpoS modulates expression of the transmission phenotype in both the exponential phase and the stationary phase. Infect. Immun. 72: 2468-2476

Badger JL, Miller VL (1995) Role of RpoS in survival of *Yersinia enterocolitica* to a variety of environmental stresses. J. Bacteriol. 177: 5370-5373

Baker CS, Morozov I, Suzuki K, Romeo T, Babitzke P (2002) CsrA regulates glycogen biosynthesis by preventing translation of *glgC* in *Escherichia coli*. Mol. Microbiol. 44: 1599-1610

Baldwin C, Goodman RN (1962) Prevalence of *Erwinia amylovora* in apple buds as detected by phage. Phytopathol. 52: 724

Barembruch C, Hengge R (2007) Cellular levels and activity of the flagellar sigma factor FliA of *Escherichia coli* are controlled by FlgM-modulated proteolysis. Mol. Microbiol. 65: 76-89

Barkow SR, Levchenko I, Baker TA, Sauer RT (2009) Polypeptide translocation by the AAA^+ ClpXP protease machine. Chem. Biol. 16: 605-612

Battesti A, Majdalani N, Gottesman S (2011) The RpoS-mediated general stress response in *Escherichia coli**. Annu. Rev. Microbiol. 65: 189-213

Becker G, Klauck E, Hengge-Aronis R (1999) Regulation of RpoS proteolysis in *Escherichia coli*: the response regulator RssB is a recognition factor that interacts with the turnover element in RpoS. Proc. Natl. Acad. Sci. USA 96: 6439-6444

Becker G, Klauck E, Hengge‐Aronis R (2000) The response regulator RssB, a recognition factor for σ^S proteolysis in *Escherichia coli*, can act like an anti‐σ^S factor. Mol. Microbiol. 35: 657-666

Bell KS, Sebaihia M, Pritchard L, Holden MTG, Hyman LJ, Holeva MC, Thomson NR, Bentley SD, Churcher LJC, Mungall K, Atkin R (2004) Genome sequence of the enterobacterial phytopathogen *Erwinia carotovora* subsp. *atroseptica* and characterization of virulence factors. Proc. Natl. Acad. Sci. USA 101: 11105-11110

Bellemann P, Bereswill S, Berger S, Geider K (1994) Visualization of capsule formation by *Erwinia amylovora* and assays to determine amylovoran synthesis. Int. J. Biol. Macromol. 16: 290–296

Bentley SD, Chater KF, Cerdeño-Tárraga AM, Challis GL, Thomson NR, James KD, Harris DE, Quail MA, Kieser H, Harper D, et al (2002) Complete genome sequence of the model actinomycete *Streptomyces coelicolor A3(2)*. Nature 417: 141-147

Bereswill S, Geider K (1997) Characterization of the *rcsB* gene from *Erwinia amylovora* and its influence on exoploysaccharide synthesis and virulence of the fire blight pathogen. J. Bacteriol. 179: 1354–1361

Berger C, Robin GP, Bonas U, Koebnik R (2010) Membrane topology of conserved components of the type III secretion system from the plant pathogen *Xanthomonas campestris* pv. vesicatoria. Microbiol. 156: 1963-1974

Bernhard F, Coplin DL, Geider K (1993) A gene cluster for amylovoran synthesis in *Erwinia amylovora*: characterization and relationship to *cps* genes in *Erwinia stewartii*. Mol. Gen. Genet. 239: 158–168

Bernhard F, Poetter K, Geider K, Coplin DL (1990) The *rcsA* gene from *Erwinia amylovora*: identification, nucleotide sequence, and regulation. Mol. Plant-Microbe Interact. 3: 429-437

Bhaya D, Davisons M, Barrangou R (2011) CRISPR-Cas systems in bacteria and archaea: versatile small RNAs for adaptive defense and regulation. Annu. Rev. Genet. 45*:* 273–297

Biggs AR, Turechek WW, Gottwald, TR (2008) Analysis of fire blight shoot infection epidemics on apple. Plant Dis. 92: 1349-1356

Billing E (1974) The effect of temperature on the growth of the fire blight pathogen, *Erwinia amylovora*. J. Appl. Bacteriol. 37: 643-648

Bissonnette SA, Rivera-Rivera I, Sauer RT, Baker TA (2010) The IbpA and IbpB small heat-shock proteins are substrates of the AAA^+ Lon protease. Mol. Microbiol. 75: 1539-1549

Blattner, F.R., Plunkett, G., Bloch, C.A., Perna, N.T., Burland, V., Riley, M., Collado-Vides, J., Glasner, J.D., Rode, C.K., Mayhew, G.F. and Gregor, J. 1997. The complete genome sequence of *Escherichia coli K-12*. Science 277: 1453-1462

Bocsanczy AM, Nissinen RM, Oh CS, Beer SV (2008) HrpN of *Erwinia amylovora* functions in the translocation of DspA/E into plant cells. Mol. Plant Pathol. 9: 425-434

Bogdanove AJ, Bauer DW, Beer SV (1998) *Erwinia amylovora* secretes DspE, a pathogenicity factor and functional AvrE homolog, through the Hrp (type III secretion) pathway. J. Bacteriol. 180: 2244-2247

Bogdanove AJ, Beer SV, Bonas U, Boucher CA, Collmer A, Coplin DL, Cornelis GR, Huang HC, Hutcheson SW, Panopoulos NJ, Van Gijsegem F (1996) Unified nomenclature for broadly conserved *hrp* genes of phytopathogenic bacteria. Mol. Microbiol. 20: 681-683

Bolon DN, Wah DA, Hersch GL, Baker TA, Sauer RT (2004) Bivalent tethering of SspB to ClpXP is required for efficient substrate delivery: a protein-design study. Mol. Cell 13: 443-449

Bonasera JM, Meng X, Beer SV, Owens T, Kim WS (2004) Interaction of DspE/A, a pathogenicity/avirulence protein of *Erwinia amylovora*, with pre-ferredoxin from apple and its relationship to photosynthetic efficiency. X Int. Work Fire Blight 704: 473-478

Bonn WG (1999) Opening address. Acta. Hortic. 489: 27-28

Bougdour A, Cunning C, Baptiste PJ, Elliott T, Gottesman S (2008) Multiple pathways for regulation of σ^S (RpoS) stability in *Escherichia coli* via the action of multiple anti‐adaptors. Mol. Microbiol. 68: 298-313

Bougdour A, Wickner S, Gottesman S (2006) Modulating RssB activity: IraP, a novel regulator of σ^S stability in *Escherichia coli*. Genes Dev. 20: 884-897

Bougdour A, Cunning C, Baptiste PJ, Elliott T, Gottesman S (2008) Multiple pathways for regulation of σ^S (RpoS) stability in *Escherichia coli* via the action of multiple anti-adaptors. Mol. Microbiol. 68: 298-313

Boureau T, ElMaarouf-Bouteau H, Garnier A, Brisset MN, Perino C, Pucheu I, Barny MA (2006) DspA/E, a type III effector essential for *Erwinia amylovora* pathogenicity and growth *in planta*, induces cell death in host apple and nonhost tobacco plants. Mol. Plant-Microbe Interact. 19: 16-24

Braun PG, Hildebrand PD (2005) Infection, carbohydrate utilization, and protein profiles of apple, pear, and raspberry isolates of *Erwinia amylovora*. Can. J. Plant Pathol. 27: 338–346

Brennan MA, Cookson BT (2000) *Salmonella* induces macrophage death by caspase-1-dependent necrosis. Mol. Microbiol. 38: 31-40

Brenner, DJ (1984) Bergey's manual of systematic bacteriology, family I *Enterobacteriaceae*. 1: 408–420

Bretz J, Losada L, Lisboa K, Hutcheson SW (2002) Lon protease functions as a negative regulator of type III protein secretion in *Pseudomonas syringae*. Mol. Microbiol. 45: 397-409

Brill JA, Quinlan-Walshe C, Gottesman S (1988). Fine-structure mapping and identification of two regulators of capsule synthesis in *Escherichia coli* K-12. J. Bacteriol. 170: 2599-2611

Broich M, Rydzewski K, McNealy TL, Marre R, Flieger A (2006) The global regulatory proteins LetA and RpoS control phospholipase A, lysophospholipase A, acyltransferase, and other hydrolytic activities of *Legionella pneumophila* JR32. J. Bacteriol. 188: 1218-1226

Burrowes E, Baysse C, Adams C, O'Gara F (2006) Influence of the regulatory protein RsmA on cellular functions in *Pseudomonas aeruginosa* PAO1, as revealed by transcriptome analysis. Microbiol. 152: 405-418

Bush M, Dixon R (2012) The role of bacterial enhancer binding proteins as specialized activators of σ^{54}-dependent transcription. Microbiol. Mol. Biol. Rev. 76: 497–529

Büttner D (2012) Protein export according to schedule: architecture, assembly, and regulation of type III secretion systems from plant-and animal-pathogenic bacteria. Microbiol. Mol. Biol. Rev. 76: 262-310

Büttner D, He SY (2009) Type III protein secretion in plant pathogenic bacteria. Plant Physiol. 150: 1656-1664

Bzymek KP, Hamaoka BY, Ghosh P (2012) Two translation products of *Yersinia* yscQ assemble to form a complex essential to type III secretion. Biochem. 51: 1669-1677

Camacho MI, Alvarez AF, Chavez RG, Romeo T, Merino E, Georgellis D (2015) Effects of the global regulator CsrA on the BarA/UvrY two-component signaling system. J. Bacteriol. 197: 983-991

Chaba R, Grigorova IL, Flynn JM, Baker TA, Gross CA (2007) Design principles of the proteolytic cascade governing the σ^E-mediated envelope stress response in *Escherichia coli*: keys to graded, buffered, and rapid signal transduction. Genes Dev. 21: 124-136

Chao NX, Wei K, Chen Q, Meng QL, Tang DJ, He YQ, Lu GT, Jiang BL, Liang XX, Feng JX, Chen B, Tang JL (2008) The *rsmA*-like gene $rsmA_{Xcc}$ of *Xanthomonas campestris* pv. *campestris* is involved in the control of various cellular processes, including pathogenesis. Mol. Plant-Microbe Interact. 21: 411-423

Chatterjee A, Cui Y, Liu Y, Dumenyo CK, Chatterjee AK (1995) Inactivation of *rsmA* leads to overproduction of extracellular pectinases, cellulases, and proteases in *Erwinia carotovora* subsp. *carotovora* in the absence of the starvation/cell densitity-sensing signal, N-(3-oxohexanoyl)-L-homoserine lactone. Appl. Environ. Microb. 61: 1959-1967

Chatterjee A, Cui Y, Yang H, Collmer A, Alfano JR, Chatterjee AK (2003) GacA, the response regulator of a two-component system, acts as a master regulator in *Pseudomonas syringae* pv. *tomato* DC3000 by controlling regulatory RNA, transcriptional activators, and alternate sigma factors. Mol. Plant-Microbe Interact. 16: 1106-1117

Chavez RG, Alvarez AF, Romeo T, Georgellis D (2010) The physiological stimulus for the BarA sensor kinase. J. Bacteriol. 192: 2009–2012

Choi KH, Licht S (2005) Control of peptide product sizes by the energy-dependent protease ClpAP. Biochem. 44: 13921-13931

Chung CH, Goldberg AL (1981) The product of the *lon* (*capR*) gene in *Escherichia coli* is the ATP-dependent protease, protease La. Proc. Natl. Acad. Sci. USA 78: 4931-4935

Claret L, Hughes C (2000) Rapid turnover of FlhD and FlhC, the flagellar regulon transcriptional activator proteins, during *Proteus* swarming. J. Bacteriol. 182: 833-836

Clemmer, K.M., and Rather, P.N. (2007) Regulation of *flhDC* expression in *Proteus mirabilis*. Res. Micribiol. 158: 295-302

Costa A, Hood IV, Berger JM (2013) Mechanisms for initiating cellular DNA replication. Annu. Rev. Biochem. 82: 25-54

Cui Y, Chatterjee A, Chatterjee AK (2001) Effects of the two-component system comprising GacA and GacS of *Erwinia carotovora* subsp. *carotovora* on the production of global regulatory *rsmB* RNA, extracellular enzymes, and $harpin_{Ecc}$. Mol. Plant-Microbe Interact. 14: 516-526

Dalebroux ZD, Swanson MS (2012) ppGpp: magic beyond RNA polymerase. Nat. Rev. Microbiol. 10: 203–212

Damerau K, St John AC (1993) Role of Clp protease subunits in degradation of carbon starvation proteins in *Escherichia coli*. J. Bacteriol. 175: 53-63

Datsenko KA, Wanner BL (2000) One-step inactivation of chromosomal genes in *Escherichia coli* K-12 using PCR products. Proc. Natl. Acad. Sci. USA 97: 6640-6645

DebRoy S, Thilmony R, Kwack Y-B, Nomura K, He SY (2004) A family of conserved bacterial effectors inhibits salicylic acid-mediated basal immunity and promotes disease necrosis in plants. Proc. Natl. Acad. Sci. USA 101: 9927-9932

Degrave A, Fagard M, Perino C, Brisset MN, Gaubert S, Laroche S, Patrit O, Barny MA (2008) *Erwinia amylovora* type three-secreted proteins trigger cell death and defense responses in *Arabidopsis thaliana*. Mol. Plant-Microbe Interact. 21: 1076-1086

Deng W, Puente JL, Gruenheid S, Li Y, Vallance BA, Vázquez A, Barba J, Ibarra JA, O'Donnell P, Ashman K (2004) Dissecting virulence: systematic and functional analyses of a pathogenicity island. Proc. Natl. Acad. Sci. USA 101:3597-3602

Dillon SC, Dorman CJ (2010) Bacterial nucleoid-associated proteins, nucleoid structure and gene expression. Nat. Rev. Microbiol. 8: 185–195

Dixon R (1998) The oxygen-responsive NIFL-NIFA complex: a novel two-component regulatory system controlling nitrogenase synthesis in γ-proteobacteria. Arch. Microbiol. 169: 371-380

Dong T, Joyce C. Schellhorn HE (2008) The role of RpoS in bacterial adaptation. Bacterial physiology, Springer Berlin Heidelberg 313–337

Dong T, Schellhorn HE (2010) Role of RpoS in virulence of pathogens. Infect. Immun. 78: 887-897

Dong T, Yu R, Schellhorn H (2011) Antagonistic regulation of motility and transcriptome expression by RpoN and RpoS in *Escherichia coli*. Mol. Microbiol. 79:375-386

Dubey AK, Baker CS, Romeo T, Babitzke, P (2005) RNA sequence and secondary structure participate in high-affinity CsrA-RNA interaction. RNA 11: 1579–1587

Dugar G, Svensson SL, Bischler T, Wäldchen S, Reinhardt R, Sauer M, Sharma CM (2016) The CsrA-FliW network controls polar localization of the dual-function flagellin mRNA in *Campylobacter jejuni*. Nat. Commun. 7: 11667

Duss O, Michel E, Yulikov M, Schubert M, Jeschke G, Allain FHT (2014) Structural basis of the non-coding RNA RsmZ acting as a protein sponge. Nature 509: 588-592

Eastgate JA, Taylor N, Coleman MJ, Healy B, Thompson L, Roberts IS (1995) Cloning, expression, and characterization of *lon* gene of *Erwinia amylovora*: evidence for a heat shock response. J. Bacteriol. 177: 932-937

Ebel W, Skinner MM, Dierksen KP, Scott JM, Trempy JE (1999) A conserved domain in *Escherichia coli* Lon protease is involved in substrate discriminator activity. J. Bacteriol. 181: 2236-2243

Edmunds AC, Castiblanco LF, Sundin GW, Waters CM (2013) Cyclic Di-GMP modulates the disease progression of *Erwinia amylovora*. J. Bacteriol. 195: 2155-2165

Edwards AN, Patterson-Fortin LM, Vakulskas CA, Mercante JW, Potrykus K, Vinella D, Camacho MI, Fields JA, Thompsom SA, Georgellis D, Cashel M, Babitzke P, Romeo T (2011) Circulatory linking the Csr and stringent response global regulatory systems. Mol. Microbiol. 80: 1561-1580

Elderkin S, Jones S, Schumacher J, Studholme D, Buck M (2002) Mechanism of action of the *Escherichia coli* phage shock protein PspA in repression of the AAA family transcription factor PspF. J. Mol. Biol. 320: 23-37

Erickson KD, Detweiler CS (2006) The Rcs phosphorelay system is specific to enteric pathogens/commensals and activates *ydeI*, a gene important for persistent *Salmonella* infection of mice. Mol. Microbiol. 62: 883-894

Erzberger JP, Berger JM (2006) Evolutionary relationships and structural mechanisms of AAA^+ proteins. Annu. Rev. Biophys. Biomol. Struct. 35: 93-114

Fang FC, Libby SJ, Buchmeier NA, Loewen PC, Switala J, Harwood J, Guiney DG (1992) The alternative sigma factor katF (rpoS) regulates Salmonella virulence. Proc. Natl. Acad. Sci. USA 89: 11978-11982

Feklístov A, Sharon BD, Darst SA, Gross CA (2014) Bacterial sigma factors: a historical, structural, and genomic perspective. Annu. Rev. Microbiol. 68: 357-376

Ferrières L, Clarke DJ (2003) The RcsC sensor kinase is required for normal biofilm formation in *Escherichia coli* K-12 and controls the expression of a regulon in response to growth on a solid surface. Mol. Microbiol. 50: 1665-1682

Ferrieres L, Thompson A, Clarke DJ (2009) Elevated levels of σ^S inhibit biofilm formation in *Escherichia coli*: a role for the Rcs phosphorelay. Microbiol. 155:3544-3553

Figueroa-Bossi N, Schwartz A, Guillemardet B, D'Heygère F, Bossi L, Boudvillain M (2014) RNA remodeling by bacterial global regulator CsrA promotes Rho-dependent transcription termination. Genes Dev. 28: 1239-1251

Figueroa-Bossi N, Schwartz A, Guillemardet B, D'Heygère F, Bossi L, Boudvillain M (2014) RNA remodeling by bacterial global regulator CsrA promotes Rho-dependent transcription termination. Genes Dev. 28: 1239-1251

Flavier AB, Schell MA, Denny TP (1998) An RpoS (σ^S) homologue regulates acylhomoserine lactone-dependent autoinduction in *Ralstonia solanacearum*. Mol. Microbiol. 28: 475-486

Flemming HC, Neu TR, Wozniak DJ (2007) The EPS matrix: the "house of biofilm cells". J. Bacteriol. 189:7945-7947

Flynn JM, Levchenko I, Sauer RT, Baker TA (2004) Modulating substrate choice: the SspB adaptor delivers a regulator of the extracytoplasmic-stress response to the AAA^+ protease ClpXP for degradation. Genes Dev. 18: 2292-2301

Flynn JM, Neher SB, Kim YI, Sauer RT, Baker TA (2003) Proteomic discovery of cellular substrates of the ClpXP protease reveals five classes of ClpX-recognition signals. Mol. Cell 11: 671-683

Francez-Charlot A, Laugel B, Van Gemert A, Dubarry N, Wiorowski F, Castanié-Cornet MP, Gutierrez C, Cam K (2003) RcsCDB His-Asp phosphorelay system negatively regulates the *flhDC* operon in *Escherichia coli*. Mol. Microbiol. 49: 823-832

Fraser CM, Gocayne JD, White O, Adams MD, Clayton RA, Fleischmann RD, Bult CJ, Kerlavage AR, Sutton G, Kelley JM, et al (1995) The minimal gene complement of *Mycoplasma genitalium*. Science 270: 397-403

Fredericks CE, Shibata S, Aizawa SI, Reimann SA, Wolfe AJ (2006) Acetyl phosphate-sensitive regulation of flagellar biogenesis and capsular biosynthesis depends on the Rcs phosphorelay. Mol. Microbiol. 61: 734-747

Frees D, Brøndsted L, Ingmer H (2013) Bacterial proteases and virulence. Regulated proteolysis in microorganisms, Springer Netherlands 161-192

Frees D, Savijoki K, Varmanen P, Ingmer H (2007) Clp ATPases and ClpP proteolytic complexes regulate vital biological processes in low GC, Gram-positive bacteria. Mol. Microbiol. 63: 1285-1295

Garcie C, Tronnet S, Garénaux A, McCarthy AJ, Brachmann AO, Pénary M, Houle S, Nougayrede J, Piel J, Taylor PW, Dozois CM, Genevaux P, Oswald E, Martin P (2016) The bacterial stress-responsive Hsp90 chaperone (htpG) is required for the production of the genotoxin colibactin and the siderophore yersiniabactin in *Escherichia coli*. J. Infect. Dis. 214: 916-924

Gaudriault S, Malandrin L, Paulin JP, Barny MA (1997) DspA, an essential pathogenicity factor of *Erwinia amylovora* showing homology with AvrE of *Pseudomonas syringae*, is secreted via the Hrp secretion pathway in a DspB-dependent way. Mol. Microbiol. 26: 1057-1069

Gaudriault S, Paulin JP, Barny MA (2002) The DspB/F protein of *Erwinia amylovora* is a type III secretion chaperone ensuring efficient intrabacterial production of the Hrp‑secreted DspA/E pathogenicity factor. Mol. Plant Pathol. 3: 313-320

Gazi AD, Charova S, Aivaliotis M, Panopoulos NJ, Kokkinidis M (2015) HrpG and HrpV proteins from the Type III secretion system of *Erwinia amylovora* form a stable heterodimer. FEMS Microbiol. Lett. 36: 1–8

Ge Y, Lee JH, Hu B, Zhao YF (2018) Loss-of-function mutations in the Dpp and Opp permeases render *Erwinia amylovora* resistant to kasugamycin and blasticidin S. Mol. Plant-Microbe Interact. DOI: 10.1094/MPMI-01-18-0007-R

Glasner JD, Yang CH, Reverchon S, Hugouvieux-Cotte-Pattat N, Condemine G, Bohin JP, Gijsegem F, Yang S, Franza T, Expert D, Plunkett G (2011) Genome sequence of the plant pathogenic bacterium *Dickeya dadantii* 3937. J. Bacteriol. 193: 2076-2077

Gonzalez M, Frank EG, Levine AS, Woodgate R (1998) Lon-mediated proteolysis of the *Escherichia coli* UmuD mutagenesis protein: *in vitro* degradation and identification of residues required for proteolysis. Genes Dev. 12: 3889-3899

Goodman R (1954) Apple fruits a source of overwintering fire blight inoculum. Plant Dis. Rep. 38: 414

Gottesman S (2005) Micros for microbes: non-coding regulatory RNAs in bacteria. Trends Genet. 21: 399-404

Gottesman S, Clark WP, de Crecy-Lagard V, Maurizi MR (1993) ClpX, an alternative subunit for the ATP-dependent Clp protease of *Escherichia coli*. Sequence and *in vivo* activities. J. Biol. Chem. 268: 22618-22626

Gottesman S, Roche E, Zhou Y, Sauer RT (1998) The ClpXP and ClpAP proteases degrade proteins with carboxy-terminal peptide tails added by the SsrA-tagging system. Genes Dev. 12: 1338-1347

Gottesman S, Halpern E, Trisler P (1981) Role of sulA and sulB in filamentation by lon mutants of *Escherichia coli* K-12. J. Bacteriol. 148: 265-273

Gottesman S, Trisler P, Torres-Cabassa A (1985) Regulation of capsular polysaccharide synthesis in *Escherichia coli* K-12: characterization of three regulatory genes. J. Bacteriol. 162: 1111-1119

Gouk SC, Bedford RJ, Hutchins SO (1996) Effect of apple flower phenology on growth of *Erwinia amylovora*. Phytopathol. 86: S42

Grainger DC, Goldberg MD, Lee DJ, Busby SJ (2008) Selective repression by Fis and H-NS at the *Escherichia coli dps* promoter. Mol. Microbiol. 68: 1366-1377

Grigorova IL, Phleger NJ, Mutalik VK, Gross CA (2006) Insights into transcriptional regulation and sigma competition from an equilibrium model of RNA polymerase binding to DNA. Proc. Natl. Acad. Sci. USA 103:5332–5337

Grimaud R, Kessel M, Beuron F, Steven AC, Maurizi MR (1998) Enzymatic and Structural Similarities between the *Escherichia coli* ATP-dependent Proteases, ClpXP and ClpAP. J. Biol. Chem. 273: 12476-12481

Gross CA, Chan C, Dombroski A, Gruber T, Sharp M, Tupy J, Young B (1998) The functional and regulatory roles of sigma factors in transcription. Cold Spring Harb. Symp. Quant. Biol. 63: 141-156

Gruber TM, Gross CA (2003) Multiple sigma subunits and the partitioning of bacterial transcription space. Annu. Rev. Microbiol. 57:441-466

Guo Y, Lew CM, Gralla JD (2000) Promoter opening by σ^{54} and σ^{70} RNA polymerases: σ factor-directed alterations in the mechanism and tightness of control. Genes Dev. 14: 2242-2255

Gur E, Ottofueling R, Dougan DA (2013) Machines of destruction–AAA^+ proteases and the adaptors that control them. Regulated proteolysis in microorganisms, Springer Netherlands 3-33

Gur E, Sauer RT (2008) Recognition of misfolded proteins by Lon, a AAA^+ protease. Genes Dev. 22: 2267-2277

Gutierrez P, Li Y, Osborne MJ, Pomerantseva E, Liu Q, Gehring K (2005) Solution structure of the carbon storage regulator protein CsrA from *Escherichia coli*. J. Bacteriol. 187: 3496–3501

Gyaneshwar P, Paliy O, McAuliffe J, Popham DL, Jordan MI, Kustu S (2005) Sulfur and nitrogen limitation in *Escherichia coli* K-12: specific homeostatic responses. J. Bacteriol. 187: 1074-1090

Hanson PI, Whiteheart SW (2005) AAA^+ proteins: have engine, will work. Nat. Rev. Mol. Cell Biol. 6: 519-529

Haslbeck M, Vierling E (2015) A first line of stress defense: small heat shock proteins and their function in protein homeostasis. J. Mol. Biol. 427: 1537-1548

Haugen SP, Ross W, Gourse RL (2008) Advances in bacterial promoter recognition and its control by factors that do not bind DNA. Nat. Rev. Microbiol. 6: 507-519

Hauryliuk V, Atkinson GC, Murakami KS, Tenson T, Gerdes K (2015) Recent functional insights into the role of (p)ppGpp in bacterial physiology. Nat. Rev. Microbiol. 13: 298-309

He SY, Nomura K, Whittam TS (2004) Type III protein secretion mechanism in mammalian and plant pathogens. Biochem. Biophys. Acta. 1694: 181-206

Heeb S, Kuehne SA, Bycroft M, Crivii S, Allen MD, Haas D, Camara M, Williams P (2006) Functional analysis of the post-transcriptional regulator RsmA reveals a novel RNA-binding site. J. Mol. Biol. 355: 1026-1036

Heimann MF, Worf GL (1985) Fire blight of raspberry caused by *Erwinia amylovora* in Wisconsin. Plant Dis. 69: 360

Hendrickson EL, Guevera P, Ausubel FM (2000) The alternative sigma factor RpoN is required for hrp activity in *Pseudomonas syringae* pv. *maculicola* and acts at the level of *hrpL* transcription. J. Bacteriol. 182: 3508-3516

Hengge R (2009) Principles of c-di-GMP signalling in bacteria. Nat. Rev. Microbiol. 7: 263-273

Henry JT, Crosson S (2011) Ligand-binding PAS domains in a genomic, cellular, and structural context. Annu. Rev. Microbiol. 65: 261-286

Hinnerwisch J, Fenton WA, Furtak KJ, Farr GW, Horwich AL (2005) Loops in the central channel of ClpA chaperone mediate protein binding, unfolding, and translocation. Cell 121: 1029-1041

Hoe NP, Goguen JD (1993) Temperature sensing in *Yersinia pestis*: translation of the LcrF activator protein is thermally regulated. J. Bacteriol. 175*:*7901–7909
Hoffmann F, Rinas U (2000) Kinetics of heat-shock response and inclusion body formation during temperature-induced production of basic fibroblast growth factor in high-cell-density cultures of recombinant *Escherichia coli*. Biotechnol. Prog. 16: 1000-1007
Holmqvist E, Wright PR, Li L, Bischler T, Barquist L, Reinhardt R, Backofen R, Vogel J (2016) Global RNA recognition patterns of post-transcriptional regulators Hfq and CsrA revealed by UV crosslinking *in vivo*. EMBO J. e201593360
Holt JG, Krieg NR, Sneath PHA, Staley JT, Williams ST (1994) Bergey's Manual of Determinative Bacteriology. 9: 787
Huang YC, Lin YC, Wei CF, Deng WL, Huang HC (2016) The pathogenicity factor HrpF interacts with HrpA and HrpG to modulate type III secretion system (T3SS) function and t3ss expression in *Pseudomonas syringae* pv. *averrhoi*. Mol. Plant Pathol. 17: 1080-1094
Huisman O, D'Ari R (1981) An inducible DNA replication-cell division coupling mechanism in *E. coli*. Nature 290: 797-799
Hutcheson SW, Bretz J, Sussan T, Jin S, Pak K (2001) Enhancer-binding proteins HrpR and HrpS interact to regulate *hrp*-encoded type III protein secretion in *Pseudomonas syringae* strains. J. Bacteriol. 183: 5589-5598
Ionescu, M., and Belkin, S. 2009. Overproduction of exopolysaccharides by an *Escherichia coli* K-12 *rpoS* mutant in response to osmotic stress. Appl. Environ. Microbiol. 75:483-492
Irie Y, Starkey M, Edwards AN, Wozniak DJ, Romeo T, Parsek MR (2010) *Pseudomonas aeruginosa* biofilm matrix polysaccharide Psl is regulated transcriptionally by RpoS and post-transcriptionally by RsmA. Mol. Microbiol. 78: 158-172
Iyoda S, Watanabe H (2005) ClpXP protease controls expression of the type III protein secretion system through regulation of RpoS and GrlR levels in enterohemorrhagic *Escherichia coli*. J. Bacteriol. 187: 4086-4094
Jackson MW, Silva-Herzog E, Plano GV (2004) The ATP-dependent ClpXP and Lon proteases regulate expression of the *Yersinia pestis* type III secretion system via regulated proteolysis of YmoA, a small histone-like protein. Mol. Microbiol. 54: 1364-1378
Jennings LD, Lun DS, Médard M, Licht S (2008) ClpP hydrolyzes a protein substrate processively in the absence of the ClpA ATPase: mechanistic studies of ATP-independent proteolysis. Biochem. 47: 11536-11546
Jin Q, He SY (2001) Role of the Hrp pilus in type III protein secretion in *Pseudomonas syringae*. Science 294: 2556-2558
Jishage M, Ishihama A (1998) A stationary phase protein in *Escherichia coli* with binding activity to the major σ subunit of RNA polymerase. Proc. Natl. Acad. Sci. USA 95: 4953-4958
Jovanovic M, James EH, Burrows PC, Rego FG, Buck M, Schumacher J (2011) Regulation of the co-evolved HrpR and HrpS AAA^+ proteins required for *Pseudomonas syringae* pathogenicity. Nat. Commun. 2: 177
Jurgen B, Lin HY, Riemschneider S, Scharf C, Neubauer P, Schmid R, Hecker M, Schweder, T (2000) Monitoring of genes that respond to overproduction of an insoluble recombinant protein in Escherichia coli glucose-limited fed-batch fermentations. Biotechnol. Bioeng. 70: 217-224

Kalia D, Merey G, Nakayama S, Zheng Y, Zhou J, Luo Y, Guo M, Roembke BT, Sintim, HO (2013) Nucleotide, c-di-GMP, c-di-AMP, cGMP, cAMP, (p)ppGpp signaling in bacteria and implications in pathogenesis. Chem. Soc. Rev. 42: 305–341

Keil HL, Zwet, T (1972) Recovery of *Erwinia amylovora* from symptomless stems and shoots of *Jonathan* apple and *Bartlett* pear trees. Phytopathol. 62: 39-42

Khakimova M, Ahlgren HG, Harrison JJ, English AM, Nguyen D (2013) The stringent response controls catalases in *Pseudomonas aeruginosa* and is required for hydrogen peroxide and antibiotic tolerance. J. Bacteriol. 195: 2011-2020

Khan MA, Zhao YF, Korban SS (2012) Molecular mechanisms of pathogenesis and resistance to the bacterial pathogen *Erwinia amylovora*, causal agent of fire blight disease in Rosaceae. Plant Mol. Biol. Rep. 30: 247–260

Kim JF, Beer SV (1998) HrpW of *Erwinia amylovora*, a new harpin that contains a domain homologous to pectate lyases of a distinct class. J. Bacteriol. 180: 5203-5210

Kitagawa R, Takaya A, Yamamoto T (2011) Dual regulatory pathways of flagellar gene expression by ClpXP protease in enterohaemorrhagic *Escherichia coli*. Microbiol. 157:3094-3103

Koczan JM, McGrath MJ, Zhao Y, Sundin GW (2009) Contribution of *Erwinia amylovora* exopolysaccharides amylovoran and levan to biofilm formation: implications in pathogenicity. Phytopathol. 99: 1237-1244

Koiv V, Andresen L, Broberg M, Frolova J, Somervuo P, Auvinen P, Pirhonen M, Tenson T, Mae A (2013) Lack of RsmA-mediated control results in constant hypervirulence, cell elongation, and hyperflagellation in Pectobacterium wasabiae. PLoS one 8: e5428

Kong HS, Roberts DP, Patterson CD, Kuehne SA, Heeb S, Lakshman DK, Lydon J (2012) Effect of overexpressing rsmA from Pseudomonas aeruginosa on virulence of select phytotoxin-producing strains of P. syringae. Phytopathol. 102: 575-587

Kress W, Maglica Ž, Weber-Ban E (2009) Clp chaperone-proteases: structure and function. Res. Microbiol. 160: 618-628

Kuroda A, Nomura K, Ohtomo R, Kato J, Ikeda T, Takiguchi N, Ohtake H, Kornberg A (2001) Role of inorganic polyphosphate in promoting ribosomal protein degradation by the Lon protease in *E. coli*. Science 293: 705-708

Lacour S, Landini P (2004) σ^S-dependent gene expression at the onset of stationary phase in *Escherichia coli*: function of σ^S-dependent genes and identification of their promoter sequences. J. Bacteriol. 186: 7186-7195

Lai YC, Peng HL, Chang HY (2003) RmpA2, an activator of capsule biosynthesis in *Klebsiella pneumoniae* CG43, regulates K2 *cps* gene expression at the transcriptional level. J. Bacteriol. 185: 788-800

Lambert de Rouvroit C, Sluiters C, Cornelis GR (1992) Role of the transcriptional activator, VirF, and temperature in the expression of the pYV plasmid genes of *Yersinia enterocolitica*. Mol. Microbiol. 6*:*395–409

Lapouge K, Schubert M, Allain FHT, Haas D (2008) Gac/Rsm signal transduction pathway of γ-proteobacteria: from RNA recognition to regulation of social behaviour. Mol. Microbiol. 67: 241-253

Lawhon SD, Frye JG, Suyemoto M, Porwollik S, McClelland M, Altier C (2003) Global regulation by CsrA in *Salmonella typhimurium*. Mol. Microbiol. 48: 1633-1645

Lee C, Schwartz MP, Prakash S, Iwakura M, Matouschek A (2001) ATP-dependent proteases degrade their substrates by processively unraveling them from the degradation signal. Mol. Cell 7: 627-637

Lee JH, Ancona V, Zhao Y (2017) Lon protease modulates virulence traits in *Erwinia amylovora* by directly monitoring major regulators and indirectly through the Rcs and Gac‑Csr regulatory systems. Mol. Plant Pathol. DOI: 10.1111/mpp.12566

Lee JH, Sundin GW, Zhao Y (2016) Identification of the HrpS binding site in the *hrpL* promoter and effect of the RpoN binding site of HrpS on the regulation of the type III secretion system in *Erwinia amylovora*. Mol. Plant Pathol. 17: 691-702

Lee JH, Zhao Y (2016) Integration host factor is required for RpoN-dependent *hrpL* gene expression and controls motility by positively regulating *rsmB* sRNA in *Erwinia amylovora*. Phytopathol. 106: 29-36

Lee JH, Zhao Y (2017) Integration of multiple stimuli-sensing systems to regulate HrpS and type III secretion system in *Erwinia amylovora*. Mol. Genet. Genomics 293: 187-196

Leng Y, Vakulskas CA, Zere TR, Pickering BS, Watnick PI, Babitzke P, Romeo T (2016) Regulation of CsrB/C sRNA decay by $EIIA_{Glc}$ of the phosphoenolpyruvate: carbohydrate phosphotransferase system. Mol. Microbiol. 99: 627-639

Li W, Ancona V, Zhao Y (2014) Co-regulation of polysaccharide production, motility, and expression of type III secretion genes by EnvZ/OmpR and GrrS/GrrA systems in *Erwinia amylovora*. Mol. Genet. Genomics, 289: 63–75

Li Y, Yamazaki A, Zou L, Biddle E, Zeng Q, Wang Y, Lin H, Wang Q, Yang CH (2010) ClpXP protease regulates the type III secretion system of *Dickeya dadantii* 3937 and is essential for the bacterial virulence. Mol. Plant-Microbe Interact. 23: 871-878

Li Z, Nimtz M, Rinas U (2017) Global proteome response of *Escherichia coli* BL21 to production of human basic fibroblast growth factor in complex and defined medium. Eng. Life Sci. 17: 881-891

Li CM, Brown I, Mansfield J, Stevens C, Boureau T, Romantschuk M, Taira S (2002) The Hrp pilus of *Pseudomonas syringae* elongates from its tip and acts as a conduit for translocation of the effector protein HrpZ. EMBO J. 21: 1909-1915

Lindeberg M (2012) Genome-enabled perspectives on the composition, evolution, and expression of virulence determinants in bacterial plant pathogens. Annu. Rev. Phytopathol. 50: 111-132

Liu X, Matsumura P (1995) An alternative sigma factor controls transcription of flagellar class-III operons in *Escherichia coli*: gene sequence, overproduction, purification and characterization. Gene 164:81-84

Losada LC, Hutcheson SW (2005) Type III secretion chaperones of *Pseudomonas syringae* protect effectors from Lon-associated degradation. Mol. Microbiol. 55: 941-953

Love MI, Huber W, Anders S (2014) Moderated estimation of fold change and dispersion for RNA-seq data with DESeq2. Genome Biol. 15: 550

Majdalani N, Gottesman S (2005) The Rcs phosphorelay: a complex signal transduction system. Annu. Rev. Microbiol. 59: 379–405

Majdalani N, Chen S, Murrow J, St John K, Gottesman S (2001) Regulation of RpoS by a novel small RNA: the characterization of RprA. Mol. Microbiol. 39: 1382-1394

Majdalani N, Hernandez D, Gottesman S (2002) Regulation and mode of action of the second small RNA activator of RpoS translation, RprA. Mol. Microbiol. 46:813-826

Malnoy M, Martens S, Norelli JL, Barny, MA, Sundin, GW, Smits TH, Duffy, B (2012) Fire blight: applied genomic insights of the pathogen and host. Annu. Rev. Phytopathol. 50: 475-494

Martin A, Baker TA, Sauer RT (2008) Protein unfolding by a AAA^+ protease is dependent on ATP-hydrolysis rates and substrate energy landscapes. Nat. Struct. Mol. Biol. 15: 139-145

Martin VJ, Mohn WW (1999) An alternative inverse PCR (IPCR) method to amplify DNA sequences flanking Tn5 transposon insertions. J. Microbiol. Meth. 35: 163-166

Martínez LC, Yakhnin H, Camacho MI, Georgellis D, Babitzke P, Puente JL, Bustamante VH (2011) Integration of a complex regulatory cascade involving the SirA/BarA and Csr global regulatory systems that controls expression of the Salmonella SPI-1 and SPI-2 virulence regulons through HilD. Mol. Microbiol. 80: 1637-1656

Martínez LC, Martínez-Flores I, Salgado H, Fernández-Mora M, Medina-Rivera A, Puente JL, Collado-Vides J, Bustamante VH (2014) *In silico* identification and experimental characterization of regulatory elements controlling the expression of the *Salmonella csrB* and *csrC* genes. J. Bacteriol. 196: 325-336

Mascher T (2013) Signaling diversity and evolution of extracytoplasmic function (ECF) σ factors. Curr. Opin. Microbiol. 16: 148-155

McGhee GC, Jones, AL (2000) Complete nucleotide sequence of ubiquitous plasmid pEA29 from *Erwinia amylovora* strain Ea88: gene organization and intraspecies variation. Appl. Environ. Microbiol. 66: 4897-4907

McGhee GC, Sundin GW (2012) *Erwinia amylovora* CRISPR elements provide new tools for evaluating strain diversity and for microbial source tracking. PLoS One 7: e41706

McNally R, Toth IK, Cock PJA, Pritchard L, Hedley PE, Morris JA, Zhao YF, Sundin GW (2012) Genetic characterization of the HrpL regulon of the fire blight pathogen *Erwinia amylovora* reveals novel virulence factors. Mol. Plant Pathol. 13: 160-173

Melnikov EE, Andrianova AG, Morozkin AD, Stepnov AA, Makhovskaya OV, Botos I, Gustchina A, Wlodawer A, Rotanova TV (2008) Limited proteolysis of *E. coli* ATP-dependent protease Lon-a unified view of the subunit architecture and characterization of isolated enzyme fragments. Acta Biochim. Pol. 55: 281-296

Mercante J, Suzuki K, Cheng X, Babitzke P, Romeo T (2006) Comprehensive alanine-scanning mutagenesis of *Escherichia coli* CsrA defines two subdomains of critical functional importance. J. Biol. Chem. 281: 31832–31842

Merighi M, Majerczak DR, Stover EH, Coplin DL (2003) The HrpX/HrpY two-component system activates *hrpS* expression, the first step in the regulatory cascade controlling the Hrp regulon in *Pantoea stewartii* subsp. *stewartii*. Mol. Plant-Microbe Interact. 16: 238–248

Merighi M, Majerczak DR, Zianni M, Tessanne K, Coplin DL (2006) Molecular characterization of *Pantoea stewartii* subsp. *stewartii* HrpY, a conserved response regulator of the Hrp type III secretion system, and its interaction with the *hrpS* promoter. J. Bacteriol. 188: 5089-5100

Merrikh H, Ferrazzoli AE, Bougdour A, Olivier-Mason A, Lovett ST (2009) A DNA damage response in *Escherichia coli* involving the alternative sigma factor, RpoS. Proc. Natl. Acad. Sci. USA 106: 611-616

Metzger M, Bellemann P, Bugert P, Geider K (1994) Genetics of galactose metabolism of *Erwinia amylovora* and its influence on polysaccharide synthesis and virulence of the fire blight pathogen. J. Bacteriol. 176: 450-459

Michiels T, Cornelis GR (1991) Secretion of hybrid proteins by the *Yersinia* Yop export system. J. Bacteriol. 173: 1677-1685

Miller JH (1972) Assay of β-galactosidase. Exp Mol Genet 352-355
Minami N, Yasuda T, Ishii Y, Fujimori K, Amano F (2011) Regulatory role of cardiolipin in the activity of an ATP-dependent protease, Lon, from *Escherichia coli*. J. Biochem. 149: 519-527
Mittenhuber G (2002) An inventory of genes encoding RNA polymerase sigma factors in 31 completely sequenced eubacterial genomes. J. Mol. Microbiol. Biotechnol. 4: 77-91
Mizusawa S, Gottesman S (1983) Protein degradation in *Escherichia coli*: the *lon* gene controls the stability of sulA protein. Proc. Natl. Acad. Sci. USA 80: 358-362
Momol MT, Norelli JL, Aldwinckle HS, Breth DI (1998) Internal movement of *Erwinia amylovora* from infection in the scion and economic loss estimates due to the rootstock phase of fire blight of apple. VIII Int. Work Fireblight 489: 505-508
Moore SD, Sauer RT (2007) The tmRNA system for translational surveillance and ribosome rescue. Annu. Rev. Biochem. 76: 101-124
Morimoto RI (1993) Cells in stress: transcriptional activation of heat shock genes. Science 259: 1409-1409
Morita-Ishihara T, Ogawa M, Sagara H, Yoshida M, Katayama E, Sasakawa C (2006) *Shigella* Spa33 is an essential C-ring component of type III secretion machinery. J. Biol. Chem. 281: 599-607
Muffler A, Fischer D, Altuvia S, Storz G, Hengge-Aronis R (1996) The response regulator RssB controls stability of the sigma (S) subunit of RNA polymerase in *Escherichia coli*. EMBO J. 15: 1333
Murakami KS, Darst, SA (2003) Bacterial RNA polymerases: the whole story. Curr. Opin. Struct. Biol. 13: 31-39
Murata M, Fujimoto H, Nishimura K, Charoensuk K, Nagamitsu H, Raina S, Kosaka T, Oshima T, Ogasawara N, Yamada M (2011) Molecular strategy for survival at a critical high temperature in *Eschierichia coli*. PLoS One 6: e20063
Neher SB, Sauer RT, Baker TA (2003) Distinct peptide signals in the UmuD and UmuD′ subunits of UmuD/D′ mediate tethering and substrate processing by the ClpXP protease. Proc. Natl. Acad. Sci. USA 100: 13219-13224
Neuwald AF, Aravind L, Spouge JL, Koonin EV (1999) AAA^{+}: A class of chaperone-like ATPases associated with the assembly, operation, and disassembly of protein complexes. Genome Res. 9: 27-43
Nimtz M, Mort A, Domke T, Wray V, Zhang Y, Qiu F, Coplin D, Geider K (1996) Structure of amylovoran, the capsular exopolysaccharide from the fire blight pathogen *Erwinia amylovora*. Carbohydr. Res. 287: 59-76
Nishii W, Suzuki T, Nakada M, Kim YT, Muramatsu T, Takahashi K (2005) Cleavage mechanism of ATP-dependent Lon protease toward ribosomal S2 protein. FEBS Lett. 579: 6846-6850
Nishii W, Takahashi K (2003) Determination of the cleavage sites in SulA, a cell division inhibitor, by the ATP-dependent HslVU protease from *Escherichia coli*. FEBS Lett. 553: 351-354
Nissinen RM, Ytterberg AJ, Bogdanove AJ, van Wijk K, Beer SV (2007) Analyses of the secretomes of *Erwinia amylovora* and selected *hrp* mutants reveal novel type III secreted proteins and an effect of HrpJ on extracellular harpin levels. Mol. Plant Pathol. 8:55–67

Nizan-Koren R, Manulis S, Mor H, Iraki NM, Barash I (2003) The regulatory cascade that activates the Hrp regulon in *Erwinia herbicola* pv. *gypsophilae*. Mol. Plant-Microbe Interact. 16: 249-260

Norel F, Robbe-Saule V, Popoff MY, Coynault C (1992) The putative sigma factor KatF (RpoS) is required for the transcription of the *Salmonella typhimurium* virulence gene *spvB* in *Escherichia coli*. FEMS Microbiol. Lett. 99: 271-276

Norelli JL, Jones AL, Aldwinckle HS (2003) Fire blight management in the twenty-first century: using new technologies that enhance host resistance in apple. Plant Dis. 87: 756-765

Ogura T, Whiteheart SW, Wilkinson AJ (2004) Conserved arginine residues implicated in ATP hydrolysis, nucleotide-sensing, and inter-subunit interactions in AAA and AAA^{+} ATPases. J. Struct. Biol. 146: 106-112

Oh CS, Beer SV (2005) Molecular genetics of *Erwinia amylovora* involved in the development of fire blight. FEMS Microbiol. Lett. 253: 185-192

Oh CS, Kim JF, Beer SV (2005) The Hrp pathogenicity island of *Erwinia amylovora* and identification of three novel genes required for systemic infection. Mol. Plant Pathol. 6: 125-138

Oh CS, Beer SV (2005) Molecular genetics of *Erwinia amylovora* involved in the development of fire blight. FEMS Microbiol. Lett. 253:185–192

Ortiz-Martín I, Thwaites R, Macho AP, Mansfield JW, Beuzón CR (2010a) Positive regulation of the Hrp type III secretion system in *Pseudomonas syringae* pv. *phaseolicola.* Mol. Plant-Microbe Interact. 23: 665-681

Ortiz-Martín I, Thwaites R, Mansfield JW, Beuzón CR (2010b) Negative regulation of the Hrp type III secretion system in *Pseudomonas syringae* pv. *phaseolicola*. Mol. Plant-Microbe Interact. 23: 682-701

Osbourne DO, Soo VW, Konieczny I, Wood TK (2014) Polyphosphate, cyclic AMP, guanosine tetraphosphate, and c-di-GMP reduce *in vitro* Lon activity. Bioengineered 5: 264-268

Ö sterberg S, Peso-Santos TD, Shingler V (2011) Regulation of alternative sigma factor use. Annu. Rev. Microbiol. 65:37-55

Page AL, Parsot C (2002) Chaperones of the type III secretion pathway: jacks of all trades. Mol. Microbiol. 46: 1-11

Paget MS, Helmann JD (2003) The sigma70 family of sigma factors. Genome Biol. 4: 203

Parales RE, Harwood CS (1993) Construction and use of a new broad-host-range *lacZ* transcriptional fusion vector, pHRP309, for $Gram^{-}$ bacteria. Gene 133: 23-30

Patten CL, Kirchhof MG, Schertzberg MR, Morton RA, Schellhorn HE (2004) Microarray analysis of RpoS-mediated gene expression in *Escherichia coli* K-12. Mol. Genet. Genomics 272: 580-591

Patterson AG, Yevstigneyeva MS, Fineran PC (2017) Regulation of CRISPR–Cas adaptive immune systems. Curr. Opin. Microbiol. 37: 1-7

Patterson-Fortin LM, Vakulskas CA, Yakhnin H, Babitzke P, Romeo T (2013) Dual posttranscriptional regulation via a cofactor-responsive mRNA leader. J. Mol. Biol. 425: 3662-3677

Perino C, Gaudriault S, Vian B, Barny M (1999) Visualization of harpin secretion *in planta* during infection of apple seedlings by *Erwinia amylovora*. Cell Microbiol. 1: 131-141

Peterson CN, Levchenko I, Rabinowitz JD, Baker TA, Silhavy TJ (2012) RpoS proteolysis is controlled directly by ATP levels in *Escherichia coli*. Genes Dev. 26: 548-553

Petnicki-Ocwieja T, Schneider DJ, Tam VC, Chancey ST, Shan L, Jamir Y, Schechter LM, Janes MD, Buell CR, Tang X, Collmer A (2002) Genomewide identification of proteins secreted by the Hrp type III protein secretion system of *Pseudomonas syringae* pv. *tomato* DC3000. Proc. Natl. Acad. Sci. USA 99: 7652-7657

Phillips TA, VanBogelen RA, Neidhardt FC (1984) *lon* gene product of *Escherichia coli* is a heat-shock protein. J. Bacteriol. 159: 283-287

Pickering BS, Smith DR, Watnick PI (2012) Glucose-specific enzyme IIA has unique binding partners in the *Vibrio cholerae* biofilm. MBio 3: e00228-12

Piper SE, Mitchell JE, Lee DJ, Busby SJ (2009) A global view of *Escherichia coli* Rsd protein and its interactions. Mol. Biosyst. 5:1943–1947

Potrykus K, Cashel M (2008) (p)ppGpp: still magical? Annu. Rev. Microbiol. 62: 35–51.

Potts AH, Vakulskas CA, Pannuri A, Yakhnin H, Babitzke P, Romeo T (2017) Global role of the bacterial post-transcriptional regulator CsrA revealed by integrated transcriptomics. Nat. Commun. 8: 1596

Preston G, Deng WL, Huang HC, Collmer A (1998) Negative regulation of *hrp* genes in *Pseudomonas syringae* by HrpV. J. Bacteriol. 180: 4532–4537

Pruteanu M, Hengge-Aronis R (2002) The cellular level of the recognition factor RssB is rate-limiting for σ^S proteolysis: implications for RssB regulation and signal transduction in σ^S turnover in *Escherichia coli*. Mol. Microbiol. 45: 1701-1713

Ratajczak E, Ziętkiewicz S, Liberek K (2009) Distinct activities of *Escherichia coli* small heat shock proteins IbpA and IbpB promote efficient protein disaggregation. J. Mol. Biol. 386: 178-189

Ren B, Shen H, Lu ZJ, Liu H, Xu Y (2014) The *phzA2-G2* transcript exhibits direct RsmA-mediated activation in *Pseudomonas aeruginosa* M18. PloS one 9: e89653

Rezzonico F, Smits TH, Duffy B (2011) Diversity, evolution and functionality of CRISPR regions in the fire blight pathogen *Erwinia amylovora*. Appl. Environ. Microb.

Romeo T, Gong M, Liu MY, Brun-Zinkernagel AM (1993) Identification and molecular characterization of *csrA*, a pleiotropic gene from *Escherichia coli* that affects glycogen biosynthesis, gluconeogenesis, cell size, and surface properties. J. Bacteriol. 175: 4744-4755

Romeo T, Vakulskas CA, Babitzke P (2013) Post-transcriptional regulation on a global scale: form and function of Csr/Rsm systems. Environ. Mirobiol. 15: 313-324

Rosen R, Biran D, Gur E, Becher D, Hecker M, Ron EZ (2002) Protein aggregation in *Escherichia coli*: role of proteases. FEMS Microbiol. Lett. 207: 9-12

Rotanova TV, Melnikov EE, Khalatova AG, Makhovskaya OV, Botos I, Wlodawer A, Gustchina A (2004) Classification of ATP-dependent proteases Lon and comparison of the active sites of their proteolytic domains. Eur. J. Biochem. 271: 4865-4871

Sahr T, Rusniok C, Impens F, Oliva G, Sismeiro O, Coppée JY, Buchrieser C (2017) The *Legionella pneumophila* genome evolved to accommodate multiple regulatory mechanisms controlled by the CsrA-system. PLoS genet. 13: e1006629

Santander RD, Monte-Serrano M, Rodríguez-Herva JJ, López-Solanilla E, Rodríguez-Palenzuela P, Biosca EG (2014) Exploring new roles for the *rpoS* gene in the survival and virulence of the fire blight pathogen *Erwinia amylovora*. FEMS Microbiol. Ecol. 90: 895-907

Sauer RT, Baker TA (2011) AAA^+ proteases: ATP-fueled machines of protein destruction. Annu. Rev. Biochem. 80: 587-612

Schesser K, Frithz-Lindsten E, Wolf-Watz H (1996) Delineation and mutational analysis of the *Yersinia pseudotuberculosis* YopE domains which mediate translocation across bacterial and eukaryotic cellular membranes. J. Bacteriol. 178: 7227-7233

Schmöe K, Rogov VV, Rogova NY, Löhr F, Güntert P, Bernhard F, Dötsch V (2011) Structural insights into Rcs phosphotransfer: the newly identified RcsD-ABL domain enhances interaction with the response regulator RcsB. Structure 19: 577-587

Schoemaker JM, Gayda RC, Markovitz A (1984) Regulation of cell division in *Escherichia coli*: SOS induction and cellular location of the sulA protein, a key to lon-associated filamentation and death. J. Bacteriol. 158: 551-561

Schroth MN, Thomson SV, Hildebrand DC, Moller WJ (1974). Epidemiology and control of fire blight. Annu. Rev. Phytopathol. 12: 389-412

Schweder T, Lee KH, Lomovskaya O, Matin A (1996) Regulation of *Escherichia coli* starvation sigma factor (sigma s) by ClpXP protease. J. Bacteriol. 178: 470-476

Sebaihia M, Bocsanczy AM, Biehl BS, Quail MA, Perna NT, Glasner JD, DeClerck GA, Cartinhour S, Schneider DJ, Bentley SD, Parkhill J (2010) Complete genome sequence of the plant pathogen *Erwinia amylovora* strain ATCC 49946. J. Bacteriol. 192: 2020-2021

Shin M, Song M, Rhee JH, Hong Y, Kim YJ, Seok YJ, Ha KS, Jung SH, Choy HE (2005) DNA looping-mediated repression by histone-like protein H-NS: specific requirement of $E\sigma^{70}$ as a cofactor for looping. Genes Dev. 19: 2388-2398

Simons RW, F Houman, N Kleckner (1987) Improved single and multicopy lac-based cloning vectors for protein and operon fusions. Gene 53: 85-96

Sjulin TM, Beer SV (1978) Mechanism of wilt induction by amylovoran in cotoneaster shoots and its relation to wilting of shoots infected by *Erwinia amylovora*. Phytopathol. 68: 89-94

Slauch JM, Silhavy TJ (1991) *cis*-acting *ompF* mutations that result in OmpR-dependent constitutive expression. J. Bacteriol. 173: 4039-4048

Sledjeski D, Gottesman S (1995) A small RNA acts as an antisilencer of the H-NS-silenced *rcsA* gene of *Escherichia coli*. Proc. Natl. Acad. Sci. USA 92: 2003-2007

Smits THM, Rezzonico F, Kamber T, Blom J, Goesmann A, Frey JE, Duffy B (2010a) Complete genome sequence of the fire blight pathogen *Erwinia amylovora* CFBP 1430 and comparison to other *Erwinia* spp. Mol. Plant-Microbe Interact. 23: 384-393

Smits TH, Jaenicke S, Rezzonico F, Kamber T, Goesmann A, Frey JE, Duffy B (2010b) Complete genome sequence of the fire blight pathogen *Erwinia pyrifoliae* DSM 12163 T and comparative genomic insights into plant pathogenicity. BMC genomics 11: 2

Solis R, Bertani I, Degrassi G, Devescovi G, Venturi V (2006) Involvement of quorum sensing and RpoS in rice seedling blight caused by *Burkholderia plantarii*. FEMS Microbiol. Lett. 259: 106-112

Sory MP, Boland A, Lambermont I, Cornelis GR (1995) Identification of the YopE and YopH domains required for secretion and internalization into the cytosol of macrophages, using the *cyaA* gene fusion approach. Proc. Natl. Acad. Sci. USA 92: 11998-12002

Stebbins CE, Galán JE (2001) Maintenance of an unfolded polypeptide by a cognate chaperone in bacterial type III secretion. Nature 414: 77-81

Stock AM, Robinson VL, Goudreau PN (2000) Two-component signal transduction. Annu. Rev. Biochem. 69: 183-215

Storz G, Vogel J, Wassarman KM (2011) Regulation by small RNAs in Bacteria: expanding frontiers. Mol. Cell 43: 880-891

Sugiyama N, Minami N, Ishii Y, Amano F (2013) Inhibition of Lon protease by bacterial lipopolysaccharide (LPS) though inhibition of ATPase. Adv. Biosci. Biotechnol. 4: 590-598
Suzuki K, Babitzke P, Kushner SR, Romeo T (2006) Identification of a novel regulatory protein (CsrD) that targets the global regulatory RNAs CsrB and CsrC for degradation by RNase E. Genes Dev. 20: 2605-2617
Suzuki K, Wang X, Weilbacher T, Pernestig AK, Melefors O, Georgellis D, Babitzke P, Romeo T (2002) Regulatory circuitry of the CsrA/CsrB and BarA/UvrY systems of *Escherichia coli*. J. Bacteriol. 184: 5130–5140
Takaya A, Kubota Y, Isogai E, Yamamoto T (2005) Degradation of the HilC and HilD regulator proteins by ATP-dependent Lon protease leads to downregulation of *Salmonella* pathogenicity island 1 gene expression. Mol. Microbiol. 55: 839-852
Takaya A, Tomoyasu T, Tokumitsu A, Morioka M, Yamamoto T (2002) The ATP-dependent lon protease of *Salmonella enterica* serovar Typhimurium regulates invasion and expression of genes carried on *Salmonella* pathogenicity island 1. J. Bacteriol. 184: 224-232
Tampakaki AP, Skandalis N, Gazi AD, Bastaki MN, Panagiotis FS, Charova SN, Kokkinidis M, Panopoulos NJ (2010) Playing the "Harp": Evolution of our understanding of *hrp*/*hrc* genes 1. Annu. Rev. Phytopathol. 48: 347-370
Thomsen LE, Olsen JE, Foster JW, Ingmer H (2002) ClpP is involved in the stress response and degradation of misfolded proteins in *Salmonella enterica* serovar *Typhimurium*. Microbiol. 148: 2727-2733
Thomson SV (1986) The role of the stigma in fire blight infections. Phytopathol. 76: 476-482
Tomoyasu T, Ohkishi T, Ukyo Y, Tokumitsu A, Takaya A, Suzuki M, Sekiya K, Matsui H, Kutsukake K, Yamamoto T (2002) The ClpXP ATP-dependent protease regulates flagellum synthesis in *Salmonella enterica* serovar Typhimurium. J. Bacteriol. 184:645-653
Tomoyasu T, Takaya A, Isogai E, Yamamoto T (2003) Turnover of FlhD and FlhC, master regulator proteins for *Salmonella* flagellum biogenesis, by the ATP-dependent ClpXP protease. Mol. Microbiol. 48:443-452
Torres-Cabassa AS, Gottesman S (1987) Capsule synthesis in *Escherichia coli* K-12 is regulated by proteolysis. J. Bacteriol. 169, 981-989
Tucker PA, Sallai L (2007) The AAA^+ superfamily-a myriad of motions. Curr. Opin. Struct. Biol. 17: 641-652
Turgay K, Hahn J, Burghoorn J, Dubnau D (1998) Competence in *Bacillus subtilis* is controlled by regulated proteolysis of a transcription factor. EMBO J. 17: 6730-6738
Ueta M, Yoshida H, Wada C, Baba T, Mori H, Wada A (2005) Ribosome binding proteins YhbH and YfiA have opposite functions during 100S formation in the stationary phase of *Escherichia coli*. Genes Cells 10: 1103-1112
Vakulskas CA, Leng Y, Abe H, Amaki T, Okayama A, Babitzke P, Suzuki K, Romeo T (2016) Antagonistic control of the turnover pathway for the global regulatory sRNA CsrB by the CsrA and CsrD proteins. Nucleic Acids Res. 44: 7896-7910
Vakulskas CA, Pannuri A, Cortés‐Selva D, Zere TR, Ahmer BM, Babitzke P, Romeo T (2014) Global effects of the DEAD‐box RNA helicase DeaD (CsdA) on gene expression over a broad range of temperatures. Mol. Microbiol. 92: 945-958
Vakulskas CA, Potts AH, Babitzke P, Ahmer BM, Romeo T (2015) Regulation of bacterial virulence by Csr (Rsm) systems. Microbiol. Mol. Biol. Rev. 79: 193-224
van der Ploeg JR, Eichhorn E, Leisinger T (2001) Sulfonate-sulfur metabolism and its regulation in *Escherichia coli*. Arch. Microbiol. 176: 1-8

van der Ploeg JR, Iwanicka-Nowicka R, Bykowski T, Hryniewicz MM, Leisinger T (1999) The *Escherichia coli ssuEADCB* gene cluster is required for the utilization of sulfur from aliphatic sulfonates and is regulated by the transcriptional activator Cbl. J. Biol. Chem. 274: 29358-29365

van der Ploeg JR, Iwanicka-Nowicka R, Kertesz MA, Leisinger T, Hryniewicz MM (1997) Involvement of CysB and Cbl regulatory proteins in expression of the *tauABCD* operon and other sulfate starvation-inducible genes in *Escherichia coli*. J. Bacteriol. 179: 7671-7678

Vanneste, JL (2000) Fire blight: the disease and its causative agent, *Erwinia amylovora*. CABI.

Venisse JS, Barny MA, Paulin JP, Brisset MN (2003) Involvement of three pathogenicity factors of *Erwinia amylovora* in the oxidative stress associated with compatible interaction in pear. FEBS Lett. 537: 198-202

Venisse JS, Gullner G, Brisset MN (2001) Evidence for the involvement of an oxidative stress in the initiation of infection of pear by *Erwinia amylovora*. Plant Physiol. 125: 2164-2172

Vieux EF, Wohlever ML, Chen JZ, Sauer RT, Baker TA (2013) Distinct quaternary structures of the AAA^+ Lon protease control substrate degradation. Proc. Natl. Acad. Sci. USA 110: E2002-E2008

Wang D, Korban SS, Zhao Y (2009) The Rcs phosphorelay system is essential for pathogenicity in *Erwinia amylovora*. Mol. Plant Pathol. 10: 277-290

Wang D, Qi M, Calla B, Korban SS, Clough SJ, Cock PJ, Sundin GW, Toth I, Zhao Y (2012) Genome-wide identification of genes regulated by the Rcs phosphorelay system in *Erwinia amylovora*. Mol. Plant-Microbe Interact. 25: 6-17

Wang J, Hartling JA, Flanagan JM (1997) The structure of ClpP at 2.3 Å resolution suggests a model for ATP-dependent proteolysis. Cell 91: 447-456

Wang D, Korban SS, Zhao Y (2009) The Rcs phosphorelay system is essential for pathogenicity in *Erwinia amylovora*. Mol. Plant Pathol. 10: 277-290

Wang D, Qi M, Calla B, Korban SS, Clough SJ, Cock PJ, Sundin GW, Toth I, Zhao YF (2012) Genome-wide identification of genes regulated by the Rcs phosphorelay system in *Erwinia amylovora*. Mol. Plant-Microbe Interact. 25: 6-17

Wang Q, Zhao Y, McClelland M, Harshey RM (2007) The RcsCDB signaling system and swarming motility in *Salmonella enterica* serovar Typhimurium: dual regulation of flagellar and SPI-2 virulence genes. J. Bacteriol. 189: 8447-8457

Wang RF, Kushner SR (1991) Construction of versatile low-copy-number vectors for cloning, sequencing and gene expression in *Escherichia coli*. Gene 100: 195-199

Webb C, Moreno M, Wilmes-Riesenberg M, Curtiss Iii R, Foster JW (1999) Effects of DksA and ClpP protease on sigma S production and virulence in *Salmonella typhimurium*. Mol. Microbiol. 34: 112-123

Weber H, Polen T, Heuveling J, Wendisch VF, Hengge R (2005) Genome-wide analysis of the general stress response network in *Escherichia coli*: σ^S-dependent genes, promoters, and sigma factor selectivity. J. Bacteriol. 187: 1591-1603

Wehland M, Bernhard F (2000) The RcsAB box characterization of a new operator essential for the regulation of expolysaccharide biosynthesis in *Enterica* bacteria. J. Biol. Chem. 275: 7013-7020

Wehland M, Kiecker C, Coplin DL, Kelm O, Saenger W, Bernhard F (1999) Identification of an RcsA/RcsB recognition motif in the promoters of exopolysaccharide biosynthetic operons from *Erwinia amylovora* and *Pantoea stewartii* subspecies *stewartii*. J. Biol. Chem. 274: 3300–3307

Wei BL, Brun-Zinkernagel AM, Simecka JW, Prüß BM, Babitzke P, Romeo T (2001) Positive regulation of motility and *flhDC* expression by the RNA‐binding protein CsrA of *Escherichia coli*. Mol. Microbiol. 40: 245-256

Wei CF, Deng WL, Huang HC (2005) A chaperone-like HrpG protein acts as a suppressor of HrpV in regulation of the *Pseudomonas syringae* pv. *syringae* type III secretion system. Mol. Microbiol. 57: 520–536

Wei Z, Kim JF, Beer SV (2000) Regulation of *hrp* genes and type III protein secretion in *Erwinia amylovora* by HrpX/HrpY, a novel two-component system, and HrpS. Mol. Plant–Microbe Interact. 13: 1251–1262

Wei ZM, Beer SV (1995) HrpL activates *Erwinia amylovora hrp* gene transcription and is a member of the ECF subfamily of s factors. J. Bacteriol. 177: 6201-6210

Wei ZM, Laby RJ, Zumoff CH, Bauer DW, He SY, Collmer A, Beer SV (1992b) Harpin, elicitor of the hypersensitive response produced by the plant pathogen *Erwinia amylovora*. Science 257: 85-88

Wei ZM, Sneath BJ, Beer SV (1992a) Expression of *Erwinia amylovora hrp* genes in response to environmental stimuli. J. Bacteriol. 174: 1875-1882

Wei CF, Deng WL, Huang HC (2005) A chaperone-like HrpG protein acts as a suppressor of HrpV in regulation of the Pseudomonas syringae pv. syringae type III secretion system. Mol. Microbiol. 57: 520–536

Wei Z, Kim JF, Beer SV (2000) Regulation of hrp genes and type III protein secretion in *Erwinia amylovora* by HrpX/HrpY, a novel two-component system, and HrpS. Mol. Plant-Microbe Interact. 13:1251–1262

Wei ZM, Beer SV (1995) *hrpL* activates *Erwinia amylovora hrp* gene transcription and is a member of the ECF subfamily of sigma factors. J. Bacteriol. 177:6201–6210

Wohlever ML, Baker TA, Sauer RT (2014) Roles of the N domain of the AAA^+ Lon protease in substrate recognition, allosteric regulation and chaperone activity. Mol. Microbiol. 91: 66-78

Wojtkowiak D, Georgopoulos C, Zylicz M (1993) Isolation and characterization of ClpX, a new ATP-dependent specificity component of the Clp protease of *Escherichia coli*. J. Biol. Chem. 268: 22609-22617

Xiao Y, Hutcheson SW (1994) A single promoter sequence recognized by a newly identified alternate sigma factor directs expression of pathogenicity and host range determinants in *Pseudomonas syringae*. J. Bacteriol. 176: 3089-3091

Xiao Y, Lan L, Yin C, Deng X, Baker D, Zhou JM, Tang X (2007) Two-component sensor RhpS promotes induction of *Pseudomonas syringae* type III secretion system by repressing negative regulator RhpR. Mol. Plant-Microbe Interact. 20: 223-234

Yakhnin AV, Baker CS, Vakulskas CA, Yakhnin H, Berezin I, Romeo T, Babitzke P (2013) CsrA activates *flhDC* expression by protecting *flhDC* mRNA from RNase E‐mediated cleavage. Mol. Microbiol. 87: 851-866

Yakhnin H, Yakhnin AV, Baker CS, Sineva E, Berezin I, Romeo T, Babitzke P (2011) Complex regulation of the global regulatory gene *csrA*: CsrA-mediated translational repression, transcription from five promoters by $E\sigma^{70}$ and $E\sigma^{S}$, and indirect transcriptional activation by CsrA. Mol. Microbiol. 81:689-704

Yamamoto T, Sashinami H, Takaya A, Tomoyasu T, Matsui H, Kikuchi Y, Hanawa T, Kamiya S, Nakane A (2001) Disruption of the genes for ClpXP protease in *Salmonella enterica* serovar *Typhimurium* results in persistent infection in mice, and development of persistence requires

endogenous gamma interferon and tumor necrosis factor alpha. Infect. Immun. 69: 3164-3174

Yang F, Korban SS, Pusey PL, Elofsson M, Sundin GW, Zhao Y (2014) Small-molecule inhibitors suppress the expression of both type III secretion and amylovoran biosynthesis genes in *Erwinia amylovora*. Mol. Plant Pathol. 15: 44-57

Yang S, Peng Q, Zhang Q, Yi X, Choi CJ, Reedy RM, Charkowski AO, Yang CH (2008) Dynamic regulation of GacA in type III secretion, pectinase gene expression, pellicle formation, and pathogenicity of *Dickeya dadantii* (*Erwinia chrysanthemi 3937*). Mol. Plant-Microbe Interact. 21: 133-142

Yap MN, Yang CH, Barak JD, Jahn CE, Charkowski AO (2005) The *Erwinia chrysanthemi* type III secretion system is required for multicellular behavior. J. Bacteriol. 18: 639-648

Yap MN, Yang CH, Charkowski AO (2008) The response regulator HrpY of *Dickeya dadantii 3937* regulates virulence genes not linked to the *hrp* cluster. Mol. Plant Microbe Interact. 21: 304-314

Yi X, Yamazaki A, Biddle E, Zeng Q, Yang CH (2010) Genetic analysis of two phosphodiesterases reveals cyclic diguanylate regulation of virulence factors in *Dickeya dadantii*. Mol. Microbiol. 77: 787-800

Yosef I, Goren MG, Kiro R, Edgar R, Qimron U (2011) High-temperature protein G is essential for activity of the *Escherichia coli* clustered regularly interspaced short palindromic repeats (CRISPR)/Cas system. Proc. Natl. Acad. Sci. USA 108: 20136-20141

Yu AYH, Houry WA (2007) ClpP: a distinctive family of cylindrical energy-dependent serine proteases. FEBS Lett. 581: 3749-3757

Zeng Q, McNally RR, Sundin GW (2013) Global small RNA chaperone Hfq and regulatory small RNAs are important virulence regulators in *Erwinia amylovora*. J. Bacteriol. 195: 1706-1717

Zere TR, Vakulskas CA, Leng Y, Pannuri A, Potts AH, Dias R, Tang D, Kolaczkowski B, Georgellis D, Ahmer BM, Romeo T (2015) Genomic targets and features of BarA-UvrY (-SirA) signal transduction systems. PloS one 10: e0145035

Zhao Y, Sundin GW, Wang D (2009a) Construction and analysis of pathogenicity island deletion mutants of *Erwinia amylovora*. Can. J. Microbiol. 55: 457-464

Zhao YF (2014) Genomics of *Erwinia amylovora* and related species associated with pome fruit trees. In: Genomics of Plant-Associated Bacteria (Gross, D., Lichens-Park, A. and Kole, C., eds). Berlin: Springer-Verlag. 1–36

Zhao Y, Wang D, Nakka S, Sundin GW, Korban SS (2009b) Systems level analysis of two-component signal transduction systems in *Erwinia amylovora*: role in virulence, regulation of amylovoran biosynthesis and swarming motility. BMC Genomics 10:1

Zhou Y, Gottesman S, Hoskins JR, Maurizi MR, Wickner S (2001). The RssB response regulator directly targets σ^S for degradation by ClpXP. Genes Dev. 15: 627-637

Zhu PL, Zhao S, Tang JL, Feng JX (2011) The *rsmA*-like gene $rsmA_{Xoo}$ of *Xanthomonas oryzae* pv. *oryzae* regulates bacterial virulence and production of diffusible signal factor. Mol. Plant Pathol. 12: 227-237

APPENDIX A: Supplementary file

The supplementary file includes tables of differentially expressed genes from RNA seq analyses of the *csrA* and *csrB* mutants compared to the WT after 6 h incubation in the *hrp*-inducing medium. Genes are grouped into functional categories according to the clusters of orthologous group (COG) database: FC, fold changes

Table A.1 Up-regulated genes in the *csrA* mutant (adjusted *P*-value < 0.05)

Locus tag	Gene description	log_2FC
Amino acid transport and metabolism		
EAMY_0826	*aroF*, phospho-2-dehydro-3-deoxyheptonate aldolase	3.91
EAMY_0162	*ilvA*, threoninedeaminase	3.15
EAMY_0158	*ilvG*, acetolactate synthase isozyme III large subunit	3.08
EAMY_0827	*tyrA*, prephenate dehydrogenase	2.63
EAMY_2184	*rhtB*, RhtB-family transporter	2.39
EAMY_1990	*dadA*, D-amino acid dehydrogenase subunit	2.32
EAMY_0138	*metB*, cystathionine gamma-synthase	2.03
EAMY_3228	type VI secretion system core protein	2.01
EAMY_2951	*thrA*, homoserine dehydrogenase	1.92
EAMY_0877	*mtnK*, 5-methylthioribose kinase	1.91
EAMY_0139	*metL*, bifunctional aspartokinase	1.85
EAMY_1749	*dcp*, dipeptidyl carboxypeptidase II	1.79
EAMY_1255	*hutH*, histidine ammonia-lyase	1.69
EAMY_2594	*yveA*, AGT-family transporter	1.66
EAMY_0907	beta-galactosidase	1.64
EAMY_0743	ABC transporter	1.63
EAMY_2950	homoserine kinase	1.57
EAMY_1260	*hutG*, *N*-formylglutamate amidohydrolase	1.51
EAMY_0468	*metC*, cystathionine beta-lyase	1.51
EAMY_0874	*masA*, enolase-phosphatase	1.47
EAMY_3527	*ocd*, ornithine cyclodeaminase	1.45
EAMY_2613	hypothetical protein	1.44
EAMY_0876	*eif*, translation initiation factor EIF-2B	1.44
EAMY_2591	proline racemase	1.43
EAMY_2484	*cysK*, cysteine synthase A	1.42
EAMY_0742	ABC transporter ATP-binding protein	1.39
EAMY_2590	FAD-dependent oxidoreductase	1.39
EAMY_1071	homocysteine *S*-methyltransferase family protein	1.32
EAMY_2392	ABC transporter substrate-binding protein	1.26
EAMY_2728	*metN*, methionine ABC transporter ATP-binding protein	1.24
EAMY_1917	*trpD*, anthranilate phosphoribosyltransferase	1.24
EAMY_1072	*ophA*, ABC transporter substrate-binding protein	1.24
EAMY_3342	*metA*, homoserine transsuccinylase	1.19

Table A.1 (cont.)

Locus tag	Gene description	log_2FC
Amino acid transport and metabolism		
EAMY_2393	ABC transporter	1.18
EAMY_2949	*thrC*, threonine synthase	1.09
EAMY_2391	*goaG*, 4-aminobutyrate aminotransferase	1.08
EAMY_0875	dioxygenase	1.08
EAMY_1918	*trpC*, indole-3-glycerol phosphate synthase	1.05
EAMY_1288	*ybiK*, asparaginase	1.04
EAMY_3536	*prlC*, Zn-dependent oligopeptidase	1.04
EAMY_0714	*argA*, acetylglutamate kinase	1.02
EAMY_0161	*ilvD*, dihydroxy-acid dehydratase	2.98
EAMY_0160	*ilvE*, branched-chain amino acidaminotransferase	2.68
EAMY_0749	*cysH*, 3'-phosphoadenosine 5'-phosphosulfate reductase	1.22
EAMY_1916	*trpG*, anthranilate synthase component II	1.21
EAMY_1915	*trpE*, anthranilate synthase component I	1.18
EAMY_0753	*cysD*, sulfate adenylyltransferase subunit II	1.12
EAMY_2593	dihydrodipicolinate synthetase	2.27
EAMY_0906	*dppB*, peptide ABC transporter permease	1.72
EAMY_0905	*dppC*, peptide ABC transporter permease	1.45
EAMY_0904	*dppD*, peptide ABC transporter permease	1.42
EAMY_1074	*ophC*, ABC transporter permease	1.32
EAMY_1073	*ophB*, ABC transporter	1.28
Carbohydrate transport and metabolism		
EAMY_2552	major facilitator superfamily transporter	3.62
EAMY_0161	*ilvD*, dihydroxy-acid dehydratase	2.98
EAMY_3649	ABC transporter ATP-binding protein	2.76
EAMY_3648	ABC transporter permease component	2.45
EAMY_3647	ABC transporter substrate-binding protein	2.23
EAMY_1738	*ynfM*, major facilitator superfamily transporter	1.80
EAMY_3566	*gnl*, gluconolactonase	1.75
EAMY_0873	methylthioribulose-1-phosphate dehydratase	1.53
EAMY_1988	major facilitator superfamily transporter	1.47
EAMY_3482	*ugpE*, Sn-glycerol-3-phosphate ABC transporter	1.22
EAMY_2716	*ygaY*, major facilitator superfamily permease	1.13
Coenzyme transport and metabolism		
EAMY_0444	*mcyE*, Glutamate-1-semialdehyde aminotransferase	2.84
EAMY_0160	*ilvE*, branched-chain amino acidaminotransferase	2.68
EAMY_0752	*cysG*, uroporphyrin-III C-methyltransferase	1.47
EAMY_0038	*yihX*, acyl-CoA dehydrogenase	1.29
EAMY_0429	*ribB*, 3,4-dihydroxy-2-butanone 4-phosphate synthase	1.22
EAMY_1750	flavoprotein monooxygenase	1.58
EAMY_3667	*yiaE*, lactate dehydrogenase	1.05
EAMY_0158	*ilvG*, acetolactate synthase isozyme III large subunit	3.08

Table A.1 (cont.)

Locus tag	Gene description	log_2FC
Coenzyme transport and metabolism		
EAMY_0441	creatininase	2.41
EAMY_1371	*ssuD*, alkanesulfonate monooxygenase	3.98
EAMY_1802	alkanesulfonate monooxygenase	1.59
EAMY_1803	*msuD*, alkanesulfonate monooxygenase	1.47
EAMY_1800	hypothetical protein	1.37
EAMY_0749	*cysH*, 3'-phosphoadenosine 5'-phosphosulfate reductase	1.22
EAMY_1916	*trpG*, anthranilate synthase component II	1.21
EAMY_1915	*trpE*, anthranilate synthase component I	1.18
EAMY_0753	*cysD*, sulfate adenylyltransferase subunit II	1.12
EAMY_0356	*yhbW*, alkanal monooxygenase subunit alpha	1.07
Cell motility		
EAMY_2665	*flgE*, flagellar hook protein	1.56
EAMY_2664	*flgF*, flagellar basal-body rod protein	1.25
EAMY_2661	*flgI*, flagellar P-ring protein	1.20
EAMY_2660	*flgJ*, flagellar rod assembly protein	1.25
EAMY_3147	*tar*, methyl-accepting chemotaxis serine transducer	1.05
EAMY_2856	*ppdD*, fimbrial protein	1.24
EAMY_2857	*gspE*, general secretion pathway protein E	1.49
EAMY_2867	*gspE*, general secretion pathway protein E	1.03
Cell wall/membrane/envelope biogenesis		
EAMY_1987	*wbaP*, undecaprenyl-phosphate galactose phosphotransferase	3.89
EAMY_2553	nucleoside-diphosphate-sugar epimerases	2.80
EAMY_2593	dihydrodipicolinate synthetase	2.27
EAMY_1844	*ybjR*, *N*-acetylmuramoyl-*L*-alanine amidase	2.11
EAMY_2614	*N*-acetylmuramic acid 6-phosphate etherase	2.07
EAMY_0669	*pagC*, virulence-related outer membrane protein	2.04
EAMY_3279	*ywgG*, Holin-like protein	1.70
EAMY_1962	*galU*, UDP-glucose pyrophosphorylase	1.31
EAMY_2005	*yeaY*, membrane protein	1.28
EAMY_2660	*flgJ*, flagellar rod assembly protein	1.25
EAMY_1961	*ugd*, nucleotide sugar dehydrogenase	1.14
EAMY_0249	*ompT*, outer membrane protease	1.13
Defense mechanisms		
EAMY_2820	*ygcB*, CRISPR-associated helicase Cas3	1.68
EAMY_0292	*aaeA*, *p*-hydroxybenzoic acid efflux pump subunit	1.37
EAMY_2814	*ygbT*, CRISPR-associated protein Cas1	1.29
EAMY_2508	*cmeB*, HAE1 family transporter	1.26
EAMY_2263	*yegN*, multidrug transporter subunit	1.09
EAMY_0508	*mdtJ*, spermidine export protein	1.04
Energy production and conversion		
EAMY_1373	*ssuE*, NAD(P)H-dependent FMN reductase	5.72

Table A.1 (cont.)

Locus tag	Gene description	log_2FC
Energy production and conversion		
EAMY_0159	*ilvM*, acetolactate synthase isozyme II small subunit	3.18
EAMY_1163	*gltA*, citrate synthase	1.79
EAMY_2587	NAD-dependent aldehyde dehydrogenases	1.78
EAMY_2586	malate/*L*-lactate dehydrogenases	1.68
EAMY_1750	flavoprotein monooxygenase	1.58
EAMY_3667	*yiaE*, lactate dehydrogenase	1.05
EAMY_2385	*ackA*, acetate kinase	1.02
EAMY_2387	*pta*, phosphate acetyltransferase	1.01
Extracellular structures		
EAMY_1862	*yhcA*, fimbrial chaperone	1.51
EAMY_2857	*gspE*, general secretion pathway protein E	1.49
EAMY_2856	*ppdD*, fimbrial protein	1.24
EAMY_2867	*gspE*, general secretion pathway protein E	1.03
General function prediction only		
EAMY_1371	*ssuD*, alkanesulfonate monooxygenase	3.98
EAMY_1748	*ygfP*, guanine deaminase	1.67
EAMY_1801	FAD-dependent oxidoreductase	1.66
EAMY_1802	alkanesulfonate monooxygenase	1.59
EAMY_1803	*msuD*, alkanesulfonate monooxygenase	1.47
EAMY_1800	hypothetical protein	1.37
EAMY_3549	*vanA*, vanillate *O*-demethylase oxygenase	1.29
EAMY_1913	*yciV*, phosphatase	1.29
EAMY_2546	*pstC*, phosphate ABC transporter permease	1.26
EAMY_1258	*hutF*, formiminoglutamate deiminase	1.09
EAMY_3280	*lrgA*, effector of murein hydrolase	1.09
EAMY_0356	*yhbW*, alkanal monooxygenase subunit alpha	1.07
EAMY_2120	*phoA*, alkaline phosphatase	1.05
EAMY_3667	*yiaE*, lactate dehydrogenase	1.05
EAMY_1298	membrane protein	1.02
EAMY_1160	*ybgL*, LamB/YcsF family protein	1.01
Inorganic ion transport and metabolism		
EAMY_3406	*tauB*, taurine ABC transporter ATP-binding protein	4.11
EAMY_3405	*tauC*, taurine ABC transporter permease	4.06
EAMY_1372	*ssuA*, aliphatic sulfonate ABC transporter substrate-binding protein	3.92
EAMY_3407	*tauA*, taurine ABC transporter substrate-binding protein	3.77
EAMY_1370	*ssuC*, sulfonate ABC transporter	3.70
EAMY_0109	*sbp*, sulphate-binding protein	2.95
EAMY_1369	*ssuB*, aliphatic sulfonate ABC transporter ATP-binding protein	2.56
EAMY_1666	*hmuS*, iron chelate transport protein	2.32
EAMY_1665	*hmuT*, iron ABC transporter substrate-binding protein	2.31
EAMY_1664	*hmuU*, iron chelate ABC transporter	1.98

Table A.1 (cont.)

Locus tag	Gene description	log_2FC
Inorganic ion transport and metabolism		
EAMY_0486	*yiuA*, ABC transporter substrate-binding protein	1.95
EAMY_3097	*ygjT*, TerC-family transporter	1.81
EAMY_0906	*dppB*, peptide ABC transporter permease	1.72
EAMY_0747	*cysJ*, sulfite reductase subunit alpha	1.52
EAMY_0408	*nlpA*, *D*-methionine-binding lipoprotein	1.49
EAMY_0748	*cysI*, sulfite reductase	1.45
EAMY_0905	*dppC*, peptide ABC transporter permease	1.45
EAMY_2585	*sseA*, thiosulfate sulfur transferase	1.44
EAMY_0904	*dppD*, peptide ABC transporter permease	1.42
EAMY_1074	*ophC*, ABC transporter permease	1.32
EAMY_3549	*vanA*, vanillate *O*-demethylase oxygenase	1.29
EAMY_1073	*ophB*, ABC transporter	1.28
EAMY_2158	*katG*, catalase	1.23
EAMY_2494	*cysP*, sulfate ABC transporter substrate-binding protein	1.13
EAMY_0754	*cysN*, sulfate adenylyltransferase subunit I	1.10
EAMY_0755	*cysC*, adenosine 5'-phosphosulfate kinase	1.09
EAMY_2120	*phoA*, alkaline phosphatase	1.05
Intracellular trafficking, secretion and vesicular transport		
EAMY_3295	*hecB*, activator or transporter protein of haemolysin-like protein	3.14
EAMY_3228	type VI secretion system core protein	2.01
EAMY_0706	*gspJ*, general secretion pathway protein J	1.63
EAMY_2857	*gspE*, general secretion pathway protein E	1.49
EAMY_0646	*yqfA*, HlyIII family-channel protein	1.41
EAMY_2867	*gspE*, general secretion pathway protein E	1.03
Lipid transport and metabolism		
EAMY_2423	*fabB*, 3-oxoacyl-(acyl-carrier-protein) synthase	2.87
EAMY_0110	*cdh*, CDP-diacylglycerol pyrophosphatase	2.76
EAMY_2588	opine oxidase subunit A	1.49
EAMY_1952	*fldX*, 3-hydroxyisobutyrate dehydrogenase	1.20
EAMY_0948	*yajB*, acyl carrier protein phosphodiesterase	1.17
EAMY_2755	*ispC*, 1-deoxy-*D*-xylulose 5-phosphate reductoisomerase	1.04
Nucleotide transport and metabolism		
EAMY_0442	dihydroorotate dehydrogenase	2.51
EAMY_2710	*nrdI*, ribonucleotide reductase	2.08
EAMY_2711	*nrdE*, ribonucleoside-diphosphate reductase subunit	1.82
EAMY_0361	*nrdD*, anaerobic ribonucleoside-triphosphate reductase	1.75
EAMY_1748	*ygfP*, guanine deaminase	1.67
EAMY_2712	*nrdF*, ribonucleotide reductase beta subunit	1.37
EAMY_2584	hypothetical protein	1.15
EAMY_1258	*hutF*, formiminoglutamate deiminase	1.09
EAMY_0500	*codB*, purine-cytosine permease	1.03

Table A.1 (cont.)

Locus tag	Gene description	log_2FC
Post-translational modification, protein turnover and chaperones		
EAMY_3180	*groE*, molecular chaperone	2.69
EAMY_3179	*groL*, molecular chaperone	2.61
EAMY_1633	*spy*, spheroplast protein Y	2.49
EAMY_2944	*dnaK*, molecular chaperone	2.46
EAMY_2709	*nrdH*, glutaredoxin	2.43
EAMY_1019	*htpG*, molecular chaperone	2.38
EAMY_2943	*dnaJ*, molecular chaperone	2.15
EAMY_1040	hypothetical protein	1.44
EAMY_3477	*yhhY*, acetyltransferase	1.40
EAMY_1396	hypothetical protein	1.34
EAMY_0985	*lon*, ATP-dependent protease	1.33
EAMY_0147	peroxiredoxin	1.31
EAMY_0835	*clpB*, ATP-dependent Clp protease ATP-binding subunit	1.25
EAMY_0106	*cpxP*, periplasmic protein	1.24
EAMY_0132	*hslV*, ATP-dependent protease	1.13
EAMY_0131	*hslU*, ATP-dependent protease	1.04
EAMY_1075	*ophD*, ABC transporter ATP-binding protein	1.01
Replication, recombination and repair		
EAMY_1152	*seqA*, replication initiation regulator	1.07
Secondary metabolites biosynthesis, transport and catabolism		
EAMY_3404	*tauD*, taurine dioxygenase	3.92
EAMY_2423	*fabB*, 3-oxoacyl-(acyl-carrier-protein) synthase	2.87
EAMY_0447	*sypC*, gramicidin S synthetase II	2.50
EAMY_0441	creatininase	2.41
EAMY_0448	*ppsD*, polyketide synthase	2.41
EAMY_1259	*hutI*, imidazolonepropionase	2.02
EAMY_0439	*S*-acyl fatty acid synthase thioesterase	1.54
EAMY_0430	hypothetical protein	1.22
Signal transduction mechanisms		
EAMY_2507	*narP*, two-component system response regulator	2.60
EAMY_0054	LuxR-family transcriptional regulator	2.22
EAMY_1531	*phoP*, two-component system response regulator	1.08
EAMY_3147	*tar*, methyl-accepting chemotaxis serine transducer	1.05
Transcription		
EAMY_2185	*cbl*, Cys-regulon transcriptional activator	3.59
EAMY_0163	*ilvY*, transcriptional regulator	2.85
EAMY_0394	Rha-family transcriptional regulator	2.77
EAMY_3646	*yqeI*, Transcriptional regulator	2.77
EAMY_2507	*narP*, two-component system response regulator	2.60
EAMY_0207	*metR*, transcriptional regulator	2.46
EAMY_0054	LuxR-family transcriptional regulator	2.22

Table A.1 (cont.)

Locus tag	Gene description	log_2FC
Transcription		
EAMY_1795	*rob*, AraC-family transcriptional regulator	1.74
EAMY_2592	GntR family transcriptional regulator	1.49
EAMY_1739	*ynfL*, LysR family transcriptional regulator	1.33
EAMY_1887	LysR family transcriptional regulator	1.24
EAMY_3528	AraC family transcriptional regulator	1.16
EAMY_1531	*phoP*, two-component system response regulator	1.08
Translation, ribosomal structure and biogenesis		
EAMY_2497	*ypeA*, acetyltransferase	1.47
EAMY_3477	*yhhY*, acetyltransferase	1.40
EAMY_2612	*yfhC*, tRNA-specific adenosine deaminase	1.31
EAMY_0040	*dtd*, *D*-tyrosyl-tRNA deacylase	1.11
EAMY_0658	*prfB*, peptide chain release factor I	1.10
EAMY_1225	*yohI*, tRNA-dihydrouridine synthase	1.07
Uncharacterized/functional unknown proteins		
EAMY_2800	*rcsV*, LuxR-family transcriptional regulator	5.85
EAMY_3645	hypothetical protein	4.94
EAMY_0944	hypothetical protein	3.92
EAMY_0657	hypothetical protein	3.70
EAMY_2422	hypothetical protein	3.41
EAMY_2801	hypothetical protein	3.40
EAMY_3293	hypothetical protein	3.39
EAMY_3294	hypothetical protein	3.36
EAMY_2380	hypothetical protein	3.35
EAMY_3644	Transcriptional regulator	3.22
EAMY_1861	*yhcF*, fimbrial protein	3.07
EAMY_1804	ABC transporter substrate-binding protein	3.00
EAMY_2381	hypothetical protein	2.99
EAMY_3567	hypothetical protein	2.79
EAMY_0440	hypothetical protein	2.74
EAMY_2435	hypothetical protein	2.62
EAMY_0443	hypothetical protein	2.55
EAMY_2505	hypothetical protein	2.54
EAMY_1186	hypothetical protein	2.49
EAMY_2802	hypothetical protein	2.45
EAMY_1195	hypothetical protein	2.38
EAMY_0446	*irp*, polyketide synthase	2.38
EAMY_0206	hypothetical protein	2.28
EAMY_2421	hypothetical protein	2.22
EAMY_2436	hypothetical protein	2.18
EAMY_0445	*mcyE*, beta-ketoacyl synthase	2.18
EAMY_1045	hypothetical protein	2.08

Table A.1 (cont.)

Locus tag	Gene description	log_2FC
Uncharacterized/functional unknown proteins		
EAMY_1737	hypothetical protein	2.03
EAMY_1067	hypothetical protein	2.01
EAMY_3111	hypothetical protein	1.99
EAMY_0945	hypothetical protein	1.98
EAMY_0140	hypothetical protein	1.95
EAMY_3061	hypothetical protein	1.93
EAMY_2121	hypothetical protein	1.92
EAMY_3523	hypothetical protein	1.91
EAMY_2819	*ygcL*, Cse1-family CRISPR-associated protein	1.90
EAMY_3112	hypothetical protein	1.88
EAMY_0291	hypothetical protein	1.88
EAMY_3060	hypothetical protein	1.88
EAMY_0449	polyketide synthase	1.84
EAMY_3522	hypothetical protein	1.83
EAMY_1634	*cho*, excinuclease	1.83
EAMY_0828	hypothetical protein	1.76
EAMY_3163	hypothetical protein	1.75
EAMY_2554	hypothetical protein	1.74
EAMY_1106	hypothetical protein	1.72
EAMY_3165	hypothetical protein	1.71
EAMY_3576	hypothetical protein	1.69
EAMY_1044	colicin A	1.68
EAMY_1104	hypothetical protein	1.67
EAMY_3164	hypothetical protein	1.64
EAMY_2122	hypothetical protein	1.62
EAMY_2419	hypothetical protein	1.62
EAMY_2818	*ygcK*, Cse2-family CRISPR-associated protein	1.61
EAMY_1886	hypothetical protein	1.61
EAMY_3529	hypothetical protein	1.59
EAMY_1105	hypothetical protein	1.59
EAMY_1299	hypothetical protein	1.59
EAMY_3622	hypothetical protein	1.58
EAMY_1983	hypothetical protein	1.57
EAMY_0705	*ppdA*, prepilin peptidase-dependent protein A	1.56
EAMY_1661	hypothetical protein	1.55
EAMY_0988	*ybaV*, AraC-family transcriptional regulator	1.52
EAMY_2589	ferredoxin	1.52
EAMY_3538	hypothetical protein	1.52
EAMY_2420	hypothetical protein	1.50
EAMY_2496	hypothetical protein	1.45
EAMY_2475	hypothetical protein	1.44

Table A.1 (cont.)

Locus tag	Gene description	log_2FC
Uncharacterized/functional unknown proteins		
EAMY_1991	hypothetical protein	1.43
EAMY_1103	hypothetical protein	1.42
EAMY_3403	hypothetical protein	1.41
EAMY_0677	hypothetical protein	1.40
EAMY_0501	hypothetical protein	1.39
EAMY_2817	*ygcJ*, Cse4-family CRISPR-associated protein	1.39
EAMY_2386	hypothetical protein	1.39
EAMY_2048	hypothetical protein	1.38
EAMY_3063	hypothetical protein	1.37
EAMY_3064	hypothetical protein	1.36
EAMY_3062	hypothetical protein	1.35
EAMY_3621	hypothetical protein	1.34
EAMY_2813	*ygbF*, CRISPR-associated protein Cas2	1.32
EAMY_2601	hypothetical protein	1.30
EAMY_1548	*mltE*, membrane-bound lytic murein transglycosylase E	1.30
EAMY_3553	hypothetical protein	1.29
EAMY_0039	*rbn*, tRNA processing exoribonuclease BN	1.29
EAMY_1187	*rhsA*, type IV secretion protein	1.28
EAMY_0452	hypothetical protein	1.28
EAMY_0824	hypothetical protein	1.27
EAMY_2047	hypothetical protein	1.24
EAMY_2649	hypothetical protein	1.22
EAMY_2816	*ygcI*, CRISPR-associated protein Cas5	1.21
EAMY_1888	hypothetical protein	1.21
EAMY_0293	*aaeB*, *p*-hydroxybenzoic acid efflux pump subunit	1.19
EAMY_0205	hypothetical protein	1.18
EAMY_1549	hypothetical protein	1.18
EAMY_0823	hypothetical protein	1.16
EAMY_2123	iodotyrosine dehalogenase I	1.15
EAMY_3290	transposase	1.15
EAMY_0897	hypothetical protein	1.15
EAMY_2506	*narQ*, two-component system histidine kinase	1.15
EAMY_2963	hypothetical protein	1.13
EAMY_2815	*ygcH*, Cse3-family CRISPR-associated protein	1.12
EAMY_1734	hypothetical protein	1.11
EAMY_3654	hypothetical protein	1.10
EAMY_1550	hypothetical protein	1.10
EAMY_3287	*soxS*, transcriptional regulator	1.09
EAMY_1969	hypothetical protein	1.09
EAMY_1641	hypothetical protein	1.08
EAMY_0666	hypothetical protein	1.07

Table A.1 (cont.)

Locus tag	Gene description	log_2FC
Uncharacterized/functional unknown proteins		
EAMY_3101	*yqjA*, YdjX-Z family transporter	1.06
EAMY_2118	hypothetical protein	1.06
EAMY_0576	hypothetical protein	1.05
EAMY_0363	*nahA*, *N*-acetyl-beta-hexosaminidase	1.05
EAMY_3446	hypothetical protein	1.04
EAMY_0946	hypothetical protein	1.03
EAMY_3524	hypothetical protein	1.02
EAMY_3321	hypothetical protein	1.01
EAMY_2637	hypothetical protein	1.00

Table A.2 Down-regulated genes in the *csrA* mutant (adjusted *P*-value < 0.05)

Locus tag	Gene description	log_2FC
Amino acid transport and metabolism		
EAMY_2839	*aroP*, aromatic amino acid transport protein	-2.32
EAMY_1712	*ydgR*, tripeptide transporter permease	-2.05
EAMY_1628	*astC*, succinylornithine transaminase	-1.95
EAMY_2504	*ansP*, L-asparagine permease	-1.93
EAMY_1755	*gdhA*, glutamate dehydrogenase	-1.78
EAMY_1631	*astB*, succinylarginine dihydrolase	-1.56
EAMY_1629	*astA*, arginine N-succinyltransferase	-1.51
EAMY_2275	*aroQ*, chorismate mutase	-1.42
EAMY_1271	*glnQ*, glutamine ABC transporter ATP-binding protein	-1.39
EAMY_3190	*asnB*, asparagine synthetase	-1.31
EAMY_0641	*gcvH*, glycine cleavage system H protein	-1.28
EAMY_1321	*poxB*, pyruvate oxidase	-1.27
EAMY_2932	*carA*, carbamoyl-phosphate synthase small subunit	-1.27
EAMY_3416	*pabA*, glutamine amidotransferase	-1.20
EAMY_2604	*glyA*, glycine/serine hydroxymethyltransferase	-1.16
EAMY_2218	*yeeF*, putrescine transporter	-1.16
EAMY_1272	*glnP*, glutamine ABC transporter	-1.15
EAMY_0640	*gcvT*, aminomethyltransferase	-1.11
EAMY_0493	*ggt*, gamma-glutamyltransferase	-1.08
EAMY_1320	*ltaA*, threonine aldolase	-1.07
EAMY_0278	*aroQ*, 3-dehydroquinate dehydratase II	-1.06
EAMY_0664	*lysA*, diaminopimelate decarboxylase	-1.04
Carbohydrate transport and metabolism		
EAMY_3043	*ydfJ*, major facilitator superfamily permease	-2.03
EAMY_0495	*bglH*, beta-glucosidase	-2.00
EAMY_0497	*celB*, PTS system transporter subunit EIIC	-1.88
EAMY_0496	*celC*, PTS system transporter subunit EIIA	-1.88
EAMY_0494	*bglA*, 6-phospho-beta-glucosidase	-1.84
EAMY_3254	*treF*, cytoplasmic trehalase	-1.80
EAMY_1644	*yniA*, fructosamine kinase	-1.73
EAMY_3189	major facilitator superfamily permease	-1.72
EAMY_2458	*yvrE*, gluconolactonase	-1.66
EAMY_1482	*ptsG*, PTS system glucose-specific transporter subunit II BC	-1.64
EAMY_0498	*celA*, PTS system transporter subunit EIIB	-1.58
EAMY_3473	*gntK*, gluconate kinase	-1.50
EAMY_3665	*kdgK*, 2-dehydro-3-deoxygluconokinase	-1.42
EAMY_2146	*amyA*, alpha-amylase	-1.37
EAMY_3635	*yahK*, alcohol dehydrogenase	-1.34
EAMY_1682	*pykF*, pyruvate kinase	-1.16
EAMY_2305	*fruB*, PTS system fructose-specific EIIA component	-1.14
EAMY_3419	*yhfC*, major facilitator superfamily transporter	-1.10

Table A.2 (cont.)

Locus tag	Gene description	log_2FC
Carbohydrate transport and metabolism		
EAMY_1552	*treA*, periplasmic trehalase	-1.04
Coenzyme transport and metabolism		
EAMY_1206	*bioB*, biotin synthetase	-2.97
EAMY_1208	*bioC*, biotin synthesis protein	-2.77
EAMY_1209	*bioD*, dethiobiotin synthetase	-2.64
EAMY_1207	*bioF*, 8-amino-7-oxononanoate synthase	-2.48
EAMY_1182	*pnuC*, nicotinamide mononucleotide transporter	-2.17
EAMY_3546	*cpoF*, alpha/beta hydrolase	-1.88
EAMY_3194	*panE*, ketopantoate reductase	-1.38
EAMY_0277	*accB*, biotin carboxyl carrier protein	-1.36
EAMY_1321	*poxB*, pyruvate oxidase	-1.27
EAMY_3302	*yjbQ*, mechanosensitive ion channel family transporter	-1.21
EAMY_3416	*pabA*, glutamine amidotransferase	-1.20
EAMY_0033	*hemN*, oxygen-independent coproporphyrinogen III oxidase	-1.16
EAMY_1786	*yhjG*, FAD monooxygenase	-1.14
EAMY_3191	*panC*, panthothenate synthetase	-1.12
Cell motility		
EAMY_1453	*flgB*, flagellar basal body protein	-6.34
EAMY_1454	*flgC*, flagellar basal body rod protein	-5.18
EAMY_1510	*fliG*, flagellar motor switch protein	-4.93
EAMY_0532	*hrcN*, type III secretion system ATPase	-4.90
EAMY_1509	*fliH*, flagellar assembly protein	-4.59
EAMY_1455	*flgD*, flagellar hook capping protein	-4.57
EAMY_1505	*fliL*, flagellar basal body-associated protein	-4.33
EAMY_1457	*flgF*, flagellar basal body rod protein	-4.28
EAMY_1507	*fliJ*, flagellar biosynthesis chaperone	-4.27
EAMY_1511	*fliF*, flagellar M-ring protein	-4.16
EAMY_1456	*flgE*, flagellar hook protein	-4.14
EAMY_1508	*fliI*, flagellum-specific ATP synthase	-3.97
EAMY_2085	*flhB*, flagellar biosynthetic protein	-3.97
EAMY_1503	*fliN*, flagellar motor switch protein	-3.83
EAMY_1459	*flhH*, flagellar L-ring protein	-3.81
EAMY_1504	*fliM*, flagellar motor switch protein	-3.68
EAMY_1460	*flgI*, flagellar P-ring protein	-3.61
EAMY_1458	*flgG*, flagellar basal body rod protein	-3.49
EAMY_2141	*fliC*, filament structural protein	-3.22
EAMY_1502	*fliO*, flagellar biogenesis protein	-3.08
EAMY_1461	*flgJ*, flagellar rod assembly protein	-3.07
EAMY_1506	*fliK*, flagellar hook-length control protein	-3.02
EAMY_2097	*motA*, flagellar motor protein	-2.96
EAMY_1452	*flgA*, flagellar basal body P-ring biosynthesis protein	-2.82

Table A.2 (cont.)

Locus tag	Gene description	log_2FC
Cell motility		
EAMY_2143	*fliS*, flagellin-specific chaperone	-2.72
EAMY_2142	*fliD*, flagellar capping protein	-2.71
EAMY_1501	*fliP*, flagellar biosynthetic protein	-2.64
EAMY_1512	*fliE*, flagellar hook-basal body protein	-2.63
EAMY_1500	*fliQ*, flagellar biosynthetic protein	-2.44
EAMY_2096	*motB*, flagellar motor protein	-2.25
EAMY_2095	*cheA*, chemotactic sensory histidine kinase	-2.21
EAMY_1451	*flgM*, negative regulator of flagellin synthesis	-2.16
EAMY_2084	*flhA*, flagellar biosynthesis protein	-2.10
EAMY_2094	*cheW*, chemotaxis signal transduction protein	-2.07
EAMY_1463	*flgL*, flagellar hook-associated protein	-1.92
EAMY_1499	*fliR*, flagellar biosynthetic protein	-1.88
EAMY_1462	*flgK*, flagellar hook-associated protein	-1.83
EAMY_1450	*flgN*, flagella synthesis protein	-1.77
EAMY_3607	*wssA*, cellulose synthase operon protein	-1.73
EAMY_1585	*spaO*, surface presentation of antigens protein	-1.21
EAMY_2695	*fliE*, flagellar hook-basal body protein	-1.16
EAMY_2687	*fliM*, flagellar motor switch protein	-1.10
Cell wall/membrane/envelope biogenesis		
EAMY_1461	*flgJ*, flagellar rod assembly protein	-3.07
EAMY_0413	*ompU*, outer membrane protein, porin	-2.55
EAMY_2750	*hlpA*, outer membrane chaperone	-1.89
EAMY_1239	glycosyltransferase	-1.76
EAMY_0090	*wabM*, glycosyltransferase	-1.67
EAMY_0951	*gtrB*, bactoprenol glucosyl transferase	-1.63
EAMY_2438	*vacJ*, lipoprotein	-1.57
EAMY_1386	*ompA*, outer membrane protein	-1.53
EAMY_0933	*csgG*, Curli production assembly/transport component	-1.47
EAMY_3311	*gtrB*, bactoprenol glucosyl transferase	-1.34
EAMY_2705	*tsx*, nucleoside-binding outer membrane protein	-1.28
EAMY_3595	*yhjG*, AsmA family protein	-1.28
EAMY_3172	*blc*, lipoprotein	-1.19
EAMY_1268	*ybiO*, mechanosensitive ion channel family transporter	-1.19
EAMY_2945	acyltransferase	-1.16
EAMY_2498	*amiA*, *N*-acetylmuramoyl-*L*-alanine amidase	-1.15
EAMY_0900	membrane protein	-1.14
EAMY_2844	outer membrane protease	-1.13
EAMY_2309	*spr*, lipoprotein	-1.10
EAMY_0092	*wabK*, lipopolysaccharide core biosynthesisglycosyltransferase	-1.06
EAMY_1281	outer membrane efflux protein	-1.05
EAMY_1231	*pbpG*, *D*-alanyl-*D*-alanine carboxypeptidase	-1.04

Table A.2 (cont.)

Locus tag	Gene description	log_2FC
Defense mechanisms		
EAMY_1068	*osmC*, peroxiredoxin	-1.94
EAMY_1275	*dps*, DNA-binding ferritin-like protein	-1.39
EAMY_2212	*yeeO*, Na^+-driven multidrug efflux pump	-1.34
EAMY_1422	multidrug resistance efflux pump	-1.10
EAMY_0364	*yjgF*, translation initiation inhibitor	-1.01
Energy production and conversion		
EAMY_1093	*cydA*, cytochrome bd-type quinol oxidase subunit I	-2.73
EAMY_1489	hypothetical protein	-1.94
EAMY_1905	*acnA*, aconitate hydratase	-1.77
EAMY_1092	*cydB*, cytochrome bd-type quinol oxidase subunit II	-1.72
EAMY_2837	*aceE*, pyruvate dehydrogenase E1 component	-1.66
EAMY_1630	*astD*, NAD-dependent aldehyde dehydrogenase	-1.43
EAMY_3707	*atpE*, ATP synthase subunit C	-1.32
EAMY_2836	*aceF*, pyruvate dehydrogenase	-1.24
EAMY_3706	*atpF*, ATP synthase subunit B protein	-1.24
EAMY_0975	*cyoB*, cytochrome o ubiquinol oxidase subunit I	-1.22
EAMY_3705	*atpH*, F0F1-type ATPase delta subunit	-1.22
EAMY_1262	aspartate/glutamate/hydantoin racemase	-1.16
EAMY_2439	*ccmI*, cytochrome c biogenesis factor	-1.15
EAMY_1170	*sucC*, succinyl-CoA synthetase beta subunit	-1.15
EAMY_3702	*atpD*, F0F1-type ATP synthase beta subunit	-1.11
EAMY_1786	*yhjG*, FAD monooxygenase	-1.14
EAMY_3704	*atpA*, F0F1-type ATP synthase alpha subunit	-1.09
EAMY_3703	*atpG*, F0F1-type ATP synthase gamma subunit	-1.09
EAMY_0976	*cyoA*, cytochrome o ubiquinol oxidase subunit II	-1.08
EAMY_3708	*atpB*, F0F1-type ATP synthase subunit A	-1.06
General function prediction only		
EAMY_3000	type VI secretion system-associated protein	-2.01
EAMY_1204	*yncB*, NADP-dependent oxidoreductases	-1.96
EAMY_0472	*yghA*, oxidoreductase	-1.96
EAMY_3546	*cpoF*, alpha/beta hydrolase	-1.88
EAMY_3003	type VI secretion system-associated protein	-1.88
EAMY_3245	*gdh*, glucose 1-dehydrogenase	-1.61
EAMY_3009	type VI secretion system-associated protein	-1.42
EAMY_2999	*rhs*, Rhs family protein	-1.38
EAMY_3249	*yedU*, intracellular protease/amidase	-1.34
EAMY_3079	*pqqE*, coenzyme PQQ synthesis protein	-1.33
EAMY_1434	*yceA*, sulfurtransferase	-1.15
EAMY_1551	*yeaQ*, membrane protein	-1.07
EAMY_1435	hypothetical protein	-1.01

Table A.2 (cont.)

Locus tag	Gene description	log_2FC
Inorganic ion transport and metabolism		
EAMY_1069	hypothetical protein	-1.85
EAMY_2474	*yrhG*, formate/nitrite family transporter	-1.44
EAMY_2472	*mntH*, manganese transport protein	-1.31
EAMY_3693	*pstC*, phosphate ABC transporter	-1.25
EAMY_3694	*pstS*, phosphate ABC transporter substrate-binding protein	-1.24
EAMY_3690	*phoU*, phosphate uptake regulator	-1.18
EAMY_1183	*ybgR*, zinc transporter	-1.05
Intracellular trafficking, secretion and vesicular transport		
EAMY_1509	*fliH*, flagellar assembly protein	-4.59
EAMY_1511	*fliF*, flagellar M-ring protein	-4.16
EAMY_1508	*fliI*, flagellum-specific ATP synthase	-3.97
EAMY_1503	*fliN*, flagellar motor switch protein	-3.83
EAMY_3020	type VI secretion system-associated protein	-2.73
EAMY_3021	type VI secretion system-associated protein	-2.72
EAMY_2143	*fliS*, flagellin-specific chaperone	-2.72
EAMY_3019	type VI secretion system-associated protein	-2.49
EAMY_3022	type VI secretion system-associated protein	-2.27
EAMY_3025	type VI secretion system-associated protein	-2.08
EAMY_3027	type VI secretion system-associated protein	-2.06
EAMY_3000	type VI secretion system-associated protein	-2.01
EAMY_2969	heme/hemopexin utilization protein B	-1.94
EAMY_3003	type VI secretion system-associated protein	-1.88
EAMY_3026	type VI secretion system-associated protein	-1.86
EAMY_1450	*flgN*, flagella synthesis protein	-1.77
EAMY_1586	*spaP*, type III secretion apparatus protein	-1.60
EAMY_3024	type VI secretion system-associated protein	-1.57
EAMY_3008	type VI secretion system-associated protein	-1.46
EAMY_1275	*dps*, DNA-binding ferritin-like protein	-1.39
Intracellular trafficking, secretion and vesicular transport		
EAMY_1574	*prgK*, lipoprotein	-1.37
EAMY_3007	type VI secretion system-associated protein	-1.27
EAMY_1585	*spaO*, surface presentation of antigens protein	-1.21
Lipid transport and metabolism		
EAMY_0222	*fadA*, acetyl-CoA acetyltransferase	-2.29
EAMY_0223	*fadB*, fatty acid oxidation complex subunit alpha	-2.16
EAMY_0472	*yghA*, oxidoreductase	-1.96
EAMY_2828	*fadD*, acyl-CoA synthase	-1.83
EAMY_2827	*vraB*, 3-ketoacyl-CoA thiolase	-1.72
EAMY_0276	*accC*, biotin carboxylase	-1.67
EAMY_3245	*gdh*, glucose 1-dehydrogenase	-1.61
EAMY_2829	acyl-CoA thioester hydrolase	-1.46

Table A.2 (cont.)

Locus tag	Gene description	log_2FC
Lipid transport and metabolism		
EAMY_1427	*ymdC*, phospholipase D family protein	-1.44
EAMY_1686	*cfa*, cyclopropane-fatty-acyl-phospholipid synthase	-1.38
EAMY_3270	*sbmA*, ABC-type long-chain fatty acid transporter	-1.37
EAMY_0277	*accB*, biotin carboxyl carrier protein	-1.36
EAMY_2984	*yjjU*, patatin family protein	-1.11
Nucleotide transport and metabolism		
EAMY_2052	*purT*, phosphoribosylglycinamide formyltransferase II	-2.63
EAMY_0262	*purH*, bifunctional purine biosynthesis protein	-2.10
EAMY_2542	*purM*, phosphoribosylformylglycinamidine cyclo-ligase	-2.10
EAMY_0045	*yicE*, purine permease	-1.98
EAMY_2529	*purC*, SAICAR synthase	-1.96
EAMY_0366	*pyrB*, aspartate carbamoyltransferase	-1.96
EAMY_2543	*purN*, phosphoribosylglycinamide formyltransferase	-1.90
EAMY_2610	*purl*, FGAM synthase	-1.69
EAMY_1532	*purB*, adenylosuccinate lyase	-1.61
EAMY_2404	*purF*, amidophosphoribosyltransferase	-1.56
EAMY_0261	*purD*, phosphoribosylamine-glycine ligase	-1.41
EAMY_0365	*pyrI*, aspartate carbamoyltransferase	-1.32
EAMY_2932	*carA*, carbamoyl-phosphate synthase small subunit	-1.27
EAMY_2568	*guaB*, inosine-5'-monophosphate dehydrogenase	-1.23
EAMY_1050	*purE*, phosphoribosylaminoimidazole carboxylase	-1.09
EAMY_2540	*uraA*, uracil permease	-1.07
EAMY_3192	*purD*, phosphoribosylamine-glycine ligase	-1.04
Post-translational modification, protein turnover and chaperones		
EAMY_0595	peroxiredoxin	-3.08
EAMY_0594	*dsbD*, cytochrome c biogenesis protein	-3.01
EAMY_2750	*hlpA*, outer membrane chaperone	-1.89
EAMY_3005	*clpV*, type VI secretion system core protein ATPase	-1.48
EAMY_1445	*grxB*, glutaredoxin II	-1.43
Post-translational modification, protein turnover and chaperones		
EAMY_3417	*ppiA*, peptidyl-prolyl *cis-trans* isomerase	-1.36
EAMY_0491	*lidJ*, disulphide bond formation protein	-1.31
EAMY_2439	*ccmI*, cytochrome *c* biogenesis factor	-1.15
EAMY_0915	*aspH*, membrane-bound beta-hydroxylase	-1.00
Replication, recombination and repair		
EAMY_2326	helicase	-3.42
EAMY_3144	*priB*, primosomal replication protein N	-1.43
Secondary metabolites biosynthesis, transport and catabolism		
EAMY_2517	*entF*, non-ribosomal peptide synthetase	-3.52
EAMY_1204	*yncB*, NADP-dependent oxidoreductases	-1.96
EAMY_0472	*yghA*, oxidoreductase	-1.96

Table A.2 (cont.)

Locus tag	Gene description	log_2FC
Secondary metabolites biosynthesis, transport and catabolism		
EAMY_2828	*fadD*, acyl-CoA synthase	-1.83
EAMY_3245	*gdh*, glucose 1-dehydrogenase	-1.61
EAMY_0463	*yqhE*, 2,5-diketo-*D*-gluconate reductase	-1.39
EAMY_1693	*gloA*, lactoylglutathione lyase	-1.25
EAMY_1787	*pvcB*, pyoverdine biosynthesis protein	-1.09
EAMY_3239	*dfoA*, desferrioxamine biosynthesis protein	-1.02
Signal transduction mechanisms		
EAMY_0513	*cstA*, carbon starvation protein	-3.33
EAMY_0808	*csrA*, carbon storage regulator	-2.88
EAMY_2095	*cheA*, chemotactic sensory histidine kinase	-2.21
EAMY_2094	*cheW*, chemotaxis signal transduction protein	-2.07
EAMY_3011	type VI secretion system-associated protein	-1.80
EAMY_2126	*phoH*, phosphate starvation-inducible protein	-1.65
EAMY_1498	*rcsA*, colanic acid capsular biosynthesis activation protein	-1.42
EAMY_0511	*yehT*, DNA-binding response regulator	-1.23
EAMY_1565	*yjdH*, two-component system histidine kinase	-1.21
EAMY_3004	type VI secretion system-associated protein	-1.11
EAMY_2628	*rseC*, sigma-E factor regulatory protein	-1.08
EAMY_1564	*yjdG*, two-component system response regulator	-1.08
Transcription		
EAMY_0536	*hrpL*, RNA polymerase sigma factor	-5.58
EAMY_2139	*fliA*, RNA polymerase sigma factor	-5.35
EAMY_3636	*yiaG*, transcriptional regulator	-2.91
EAMY_0593	*sigD*, RNA polymerase sigma factor	-2.77
EAMY_1451	*flgM*, negative regulator of flagellin synthesis	-2.16
EAMY_0148	*oxyR*, hydrogen peroxide-inducible genes activator	-2.11
EAMY_2838	*pdhR*, transcriptional regulator	-1.75
EAMY_0012	*alsR*, transcriptional regulator	-1.73
EAMY_1420	*marR*, transcriptional regulator	-1.43
EAMY_1498	*rcsA*, colanic acid capsular biosynthesis activation protein	-1.42
EAMY_3358	*zntR*, transcriptional regulator	-1.38
EAMY_3301	hypothetical protein	-1.36
EAMY_3042	*rbsR*, transcriptional repressor	-1.28
EAMY_0511	*yehT*, DNA-binding response regulator	-1.23
EAMY_1564	*yjdG*, two-component system response regulator	-1.08
Translation, ribosomal structure and biogenesis		
EAMY_3387	*rpsJ*, ribosomal protein S10	-3.42
EAMY_3384	*rplW*, ribosomal protein L23	-3.39
EAMY_3386	*rplC*, ribosomal protein L3	-3.37
EAMY_0031	*yihI*, GTPase-activating protein	-3.35
EAMY_3385	*rplD*, ribosomal protein L4	-3.33

Table A.2 (cont.)

Locus tag	Gene description	log_2FC
Translation, ribosomal structure and biogenesis		
EAMY_3381	*rplV*, ribosomal protein L22	-2.91
EAMY_3380	*rpsC*, ribosomal protein S3	-2.87
EAMY_3383	*rplB*, ribosomal protein L2	-2.83
EAMY_3382	*rpsS*, ribosomal protein S19	-2.48
EAMY_3379	*rplP*, ribosomal protein L16	-2.33
EAMY_3378	*rpmC*, ribosomal protein L29	-2.00
EAMY_3377	*rpsQ*, ribosomal protein S17	-1.90
EAMY_1382	*rmf*, ribosome modulation factor	-1.64
EAMY_3391	*rpsL*, ribosomal protein S12	-1.52
EAMY_0236	*rplA*, ribosomal protein L1	-1.49
EAMY_3145	*rpsF*, ribosomal protein S6	-1.45
EAMY_3104	*yqjD*, membrane protein	-1.43
EAMY_3370	*rplR*, ribosomal protein L18	-1.40
EAMY_0235	*rplK*, ribosomal protein L11	-1.39
EAMY_3193	*hisS*, histidyl-tRNA synthetase	-1.36
EAMY_3372	*rpsH*, ribosomal protein S8	-1.35
EAMY_3143	*rpsR*, ribosomal protein S18	-1.35
EAMY_3390	*rpsG*, ribosomal protein S7	-1.33
EAMY_1347	*rpsA*, ribosomal protein S1	-1.29
EAMY_3369	*rpsE*, ribosomal protein S5	-1.29
EAMY_3195	*hisZ*, histidyl-tRNA synthetase	-1.27
EAMY_3375	*rplX*, ribosomal protein L24	-1.15
EAMY_3142	*rplI*, ribosomal protein L9	-1.14
EAMY_3371	*rplF*, ribosomal protein L9	-1.11
EAMY_3376	*rplN*, ribosomal protein L14	-1.09
EAMY_3373	*rpsN*, ribosomal protein S14	-1.04
EAMY_0819	*rplS*, ribosomal protein L19	-1.04
EAMY_3389	*fusA*, Translation elongation factor	-1.00
Type III secretion system		
EAMY_0542	*hrpA*, Hrp pili protein	-6.87
EAMY_0552	*hrpN*, harpin protein	-6.50
EAMY_0543	*hrpB*, type III secretion system protein	-6.20
EAMY_0556	*hrpW*, harpin protein	-5.82
EAMY_0533	*hrpQ*, type III secretion system protein	-5.79
EAMY_0544	*hrcJ*, type III secretion inner-membrane protein	-5.78
EAMY_0547	*hrpF*, type III secretion protein	-5.67
EAMY_0535	*hrpJ*, type III secretion system protein	-5.59
EAMY_0536	*hrpL*, RNA polymerase sigma factor	-5.58
EAMY_0548	*hrpG*, type III secretion protein	-5.57
EAMY_0534	*hrcV*, type III secretion inner-membrane protein	-5.45
EAMY_0545	*hrpD*, type III secretion protein	-5.43

Table A.2 (cont.)

Locus tag	Gene description	log_2FC
Type III secretion system		
EAMY_0531	*hrpO*, type III secretion protein	-5.30
EAMY_0555	*orfC*, HrpW-specific chaperone	-5.28
EAMY_0558	*dspF*, Hrp secreted pathogenicity-like protein	-5.20
EAMY_0557	*dspE*, Hrp secreted pathogenicity-like protein	-5.20
EAMY_0549	*hrcC*, type III secretion system outer membrane pore	-5.07
EAMY_0532	*hrcN*, type III secretion system ATPase	-4.90
EAMY_0553	*orfA*, Tir chaperone family protein	-4.81
EAMY_0551	*hrpV*, type III secretion protein	-4.75
EAMY_0550	*hrpT*, type III secretion lipoprotein	-4.71
EAMY_0530	*hrpP*, type III secretion protein	-4.35
EAMY_0527	*hrcS*, type III secretion protein	-4.29
EAMY_0546	*hrpE*, type III secretion apparatus protein	-3.94
EAMY_0554	*orfB*, avirulence protein	-3.78
EAMY_0528	*hrcR*, type III secretion apparatus protein	-3.76
EAMY_0653	*eop2*, type III effector	-3.62
EAMY_0525	*hrcU*, type III secretion protein	-3.17
EAMY_0529	*hrcQ*, type III secretion system apparatus protein	-3.12
EAMY_0526	*hrcT*, type III secretion apparatus protein	-2.66
EAMY_0520	*hsvA*, Hrp-associated systemic virulence protein	-2.52
EAMY_0519	*hrpK*, pathogenicity locus protein	-2.39
EAMY_0539	*hrpS*, sigma-54-dependent enhancer-binding protein	-1.78
EAMY_3175	*avrRpt2*, cysteine protease avirulence protein	-1.61
EAMY_0521	*hsvB*, Hrp-associated systemic virulence protein	-1.47
EAMY_0522	*hsvC*, Hrp-associated systemic virulence protein	-1.10
Uncharacterized/functional unknown proteins		
EAMY_3325	*yjbJ*, CsbD family protein	-4.52
EAMY_0524	biphenyl 2,3-dioxygenase	-4.40
EAMY_2100	*flhD*, flagellar transcriptional activator	-4.29
EAMY_0920	hypothetical protein	-4.23
EAMY_2099	*flhC*, flagellar transcriptional activator	-4.10
EAMY_2098	hypothetical protein	-3.99
EAMY_3016	hypothetical protein	-3.49
EAMY_2997	hypothetical protein	-3.36
EAMY_0512	hypothetical protein	-3.26
EAMY_3017	type VI secretion system-associated protein	-3.23
EAMY_2138	*fliZ*, flagellar regulatory protein	-3.18
EAMY_2327	endonuclease	-3.14
EAMY_3015	type VI secretion system-associated protein	-3.11
EAMY_2998	hypothetical protein	-3.06
EAMY_3018	type VI secretion system-associated protein	-2.92
EAMY_1155	hypothetical protein	-2.78

Table A.2 (cont.)

Locus tag	Gene description	log_2FC
Uncharacterized/functional unknown proteins		
EAMY_1426	hypothetical protein	-2.66
EAMY_1906	hypothetical protein	-2.63
EAMY_3014	type VI secretion system-associated protein	-2.62
EAMY_3013	type VI secretion system-associated protein	-2.62
EAMY_2034	methyl-accepting chemotaxis protein	-2.51
EAMY_1567	*ygdR*, lipoprotein	-2.50
EAMY_0032	hypothetical protein	-2.48
EAMY_2177	hypothetical protein	-2.48
EAMY_2137	*yedO*, tryptophan synthase subunit beta	-2.47
EAMY_1181	*nadA*, Quinolinate synthetase	-2.44
EAMY_1004	hypothetical protein	-2.43
EAMY_2136	hypothetical protein	-2.39
EAMY_3243	hypothetical protein	-2.34
EAMY_3581	*prtA*, zinc-binding metalloprotease	-2.33
EAMY_1184	*ybgS*, homeobox protein	-2.29
EAMY_1230	*yohC*, YIP1 family protein	-2.29
EAMY_1566	lipoprotein	-2.29
EAMY_0011	*ygiW*, TIGR00156 family protein	-2.28
EAMY_3012	type VI secretion system-associated protein	-2.27
EAMY_3664	hypothetical protein	-2.20
EAMY_0720	lipoprotein	-2.19
EAMY_3028	hypothetical protein	-2.19
EAMY_0523	hypothetical protein	-2.18
EAMY_1784	*srfB*, virulence factor	-2.17
EAMY_3696	bacteriophage protein	-2.16
EAMY_3697	hypothetical protein	-2.15
EAMY_1063	hypothetical protein	-2.11
EAMY_1898	hypothetical protein	-2.10
EAMY_1841	acid-shock protein	-2.09
EAMY_0918	hypothetical protein	-2.08
EAMY_3319	hypothetical protein	-2.05
EAMY_0886	*crl*, sigma factor-binding protein	-1.98
EAMY_1575	hypothetical protein	-1.96
EAMY_0950	membrane protein	-1.95
EAMY_3088	hypothetical protein	-1.94
EAMY_0957	*ygaU*, peptidoglycan-binding protein	-1.93
EAMY_3359	hypothetical protein	-1.93
EAMY_1855	hypothetical protein	-1.91
EAMY_2176	*sqdD*, glycosyltransferase	-1.90
EAMY_0956	lipoprotein	-1.89
EAMY_0010	hypothetical protein	-1.88

Table A.2 (cont.)

Locus tag	Gene description	log_2FC
Uncharacterized/functional unknown proteins		
EAMY_3244	hypothetical protein	-1.88
EAMY_1785	*srfC*, virulence factor	-1.86
EAMY_2144	*fliT*, flagellar export chaperone	-1.85
EAMY_1514	hypothetical protein	-1.84
EAMY_2134	*yedO*, 1-aminocyclopropane-1-carboxylate deaminase	-1.83
EAMY_3173	hypothetical protein	-1.80
EAMY_2101	hypothetical protein	-1.77
EAMY_2877	hypothetical protein	-1.76
EAMY_3029	hypothetical protein	-1.75
EAMY_2053	hypothetical protein	-1.74
EAMY_3010	type VI secretion system-associated protein	-1.72
EAMY_1647	hypothetical protein	-1.70
EAMY_1783	*srfA*, myosin light chain kinase	-1.68
EAMY_1895	lipoprotein	-1.68
EAMY_1091	hypothetical protein	-1.67
EAMY_0914	*psiF*, phosphate starvation-inducible protein	-1.66
EAMY_3197	*nikS*, carbamoyl-phosphate synthase large subunit	-1.64
EAMY_1539	hypothetical protein	-1.64
EAMY_2379	hypothetical protein	-1.64
EAMY_3668	hypothetical protein	-1.62
EAMY_3001	hypothetical protein	-1.59
EAMY_0574	hypothetical protein	-1.58
EAMY_0622	acyltransferase	-1.57
EAMY_3002	flagellar L-ring protein	-1.56
EAMY_0091	*waaL*, O-antigen ligase	-1.56
EAMY_0934	lipoprotein	-1.54
EAMY_2274	hypothetical protein	-1.54
EAMY_3312	hypothetical protein	-1.52
EAMY_2842	hypothetical protein	-1.52
EAMY_1540	hypothetical protein	-1.51
EAMY_2450	oxidoreductase	-1.50
EAMY_2985	hypothetical protein	-1.50
EAMY_2570	*prt*, metalloprotease	-1.48
EAMY_0275	*yhdT*, membrane protein	-1.46
EAMY_3638	hypothetical protein	-1.45
EAMY_0044	hypothetical protein	-1.45
EAMY_2135	*D*-cysteine desulfhydrase	-1.45
EAMY_3105	*yqjE*, membrane protein	-1.44
EAMY_3608	*bcsO*, cellulose biosynthesis protein	-1.42
EAMY_2992	hypothetical protein	-1.42
EAMY_0894	hypothetical protein	-1.42

Table A.2 (cont.)

Locus tag	Gene description	log_2FC
Uncharacterized/functional unknown proteins		
EAMY_1274	hypothetical protein	-1.41
EAMY_2847	hypothetical protein	-1.41
EAMY_3106	hypothetical protein	-1.41
EAMY_0899	hypothetical protein	-1.40
EAMY_3695	*lscC*, levansucrase	-1.39
EAMY_2846	hypothetical protein	-1.36
EAMY_2091	hypothetical protein	-1.36
EAMY_2566	*intS*, integrase	-1.36
EAMY_2523	hypothetical protein	-1.35
EAMY_2563	hypothetical protein	-1.35
EAMY_2145	hypothetical protein	-1.34
EAMY_3196	ribosomal protein L11 methylase	-1.33
EAMY_2686	*fliN*, flagellar motor switch protein	-1.33
EAMY_2449	GNAT family acetyltransferase	-1.33
EAMY_1645	*ydiZ*, hypothetical protein	-1.33
EAMY_3637	hypothetical protein	-1.32
EAMY_2986	*osmY*, lipoprotein	-1.32
EAMY_2405	*cvpA*, colicin V production protein	-1.32
EAMY_0999	*ybaY*, lipoprotein	-1.30
EAMY_1403	*agp*, glucose-1-phosphatase	-1.28
EAMY_3203	hypothetical protein	-1.28
EAMY_2603	hypothetical protein	-1.28
EAMY_1543	prophage membrane protein	-1.28
EAMY_2451	*rcsC*, two-component system histidine kinase	-1.28
EAMY_0058	hypothetical protein	-1.27
EAMY_3078	*pqqF*, coenzyme PQQ synthesis protein	-1.27
EAMY_2708	hypothetical protein	-1.27
EAMY_0389	SAM-dependent methyltransferase	-1.27
EAMY_3103	*yqjC*, hypothetical protein	-1.26
EAMY_0775	*prgH*, type III secretion system protein	-1.26
EAMY_1280	*emrB*, major facilitator superfamily transporter	-1.25
EAMY_3269	hypothetical protein	-1.25
EAMY_3604	*bcsC*, cellulose synthase operon protein	-1.24
EAMY_2602	*csiE*, transcriptional anti-terminator	-1.24
EAMY_3253	hypothetical protein	-1.23
EAMY_3603	*bcsD*, cellulose synthase subunit D	-1.23
EAMY_2457	hypothetical protein	-1.22
EAMY_1003	hypothetical protein	-1.22
EAMY_1842	hypothetical protein	-1.22
EAMY_2995	ferric aerobactin receptor	-1.22
EAMY_0390	chromosome segregation ATPases	-1.22

Table A.2 (cont.)

Locus tag	Gene description	log_2FC
Uncharacterized/functional unknown proteins		
EAMY_2654	*flhC*, flagellar transcriptional activator	-1.22
EAMY_2565	*intS*, phage-related integrase	-1.20
EAMY_3080	*pqqD*, coenzyme PQQ synthesis protein	-1.20
EAMY_3238	*dfoJ*, glutamate decarboxylase	-1.19
EAMY_3174	hypothetical protein	-1.18
EAMY_1432	*msyB*, acidic protein	-1.17
EAMY_3242	hypothetical protein	-1.15
EAMY_2571	hypothetical protein	-1.15
EAMY_2270	hypothetical protein	-1.14
EAMY_2768	hypothetical protein	-1.14
EAMY_0608	colicin V secretion/processing ATP-binding protein	-1.13
EAMY_3580	*inh*, proteinase inhibitor	-1.13
EAMY_2704	hypothetical protein	-1.13
EAMY_2104	DUF1275 family protein	-1.12
EAMY_0778	*prgK*, invasion protein	-1.11
EAMY_3023	type VI secretion system-associated protein	-1.11
EAMY_2843	hypothetical protein	-1.11
EAMY_3605	*bcsB*, cellulose synthase regulator	-1.10
EAMY_0492	phytochelatin synthase	-1.09
EAMY_0060	hypothetical protein	-1.08
EAMY_1768	hypothetical protein	-1.08
EAMY_1573	*orgA*, oxygen-regulated invasion protein	-1.07
EAMY_1494	hypothetical protein	-1.06
EAMY_1703	hypothetical protein	-1.06
EAMY_1896	hypothetical protein	-1.05
EAMY_2970	nuclear pore complex protein	-1.05
EAMY_1602	*hypothetical protein*	-1.05
EAMY_1576	*prgH*, type III secretion system protein	-1.04
EAMY_2032	hypothetical protein	-1.03
EAMY_2456	hypothetical protein	-1.03
EAMY_3631	membrane protein	-1.02
EAMY_0059	retron reverse transcriptase	-1.02
EAMY_3533	*uspB*, universal stress protein	-1.02
EAMY_1568	hypothetical protein	-1.02
EAMY_3594	hypothetical protein	-1.02
EAMY_3625	HNH endonuclease	-1.02
EAMY_3463	hypothetical protein	-1.01
EAMY_0587	*yggN*, hypothetical protein	-1.00
EAMY_1061	hypothetical protein	-1.00
EAMY_1079	hypothetical protein	-1.00

Table A.3 Up-regulated genes in the *csrB* mutant (adjusted *P*-value < 0.05)

Locus tag	Gene description	log_2FC
Amino acid transport and metabolism		
EAMY_0826	*aroF*, phospho-2-dehydro-3-deoxyheptonate aldolase	4.12
EAMY_0827	*tyrA*, prephenate dehydrogenase	2.79
EAMY_1749	*dcp*, dipeptidyl carboxypeptidase II	1.99
EAMY_3339	*lysC*, aspartate kinase	1.63
EAMY_2196	*adhB*, alcohol dehydrogenase	1.59
EAMY_1805	*dppA2*, ABC transporter substrate-binding protein	1.53
EAMY_3609	*dppF*, ABC transporter ATP-binding protein	1.50
EAMY_2275	*aroQ*, chorismate mutase	1.43
EAMY_0995	*glnK*, nitrogen regulatory protein PII	1.39
EAMY_3611	*dppC*, ABC transporter	1.27
EAMY_3610	*dppD*, ABC transporter ATP-binding protein	1.27
EAMY_3471	*asd*, aspartate-semialdehyde dehydrogenase	1.22
EAMY_3612	*dppB*, ABC transporter	1.21
EAMY_2218	*yeeF*, putrescine transporter	1.03
EAMY_0466	*ddc*, *L*-2,4-diaminobutyrate decarboxylase	1.00
Carbohydrate transport and metabolism		
EAMY_2249	*amsB*, glycosyltransferase	2.24
EAMY_1670	*ppsA*, phosphoenolpyruvate synthase	2.01
EAMY_3469	*glgB*, 1,4-alpha-glucan branching protein	1.55
EAMY_3468	*glgX*, glycogen debranching enzyme	1.49
EAMY_3566	*gnl*, gluconolactonase	1.47
EAMY_0912	beta-galactosidase	1.44
EAMY_2103	*otsB*, trehalose-6-phosphate phophatase	1.38
EAMY_3467	*glgC*, ADP-glucose pyrophosphorylase	1.37
EAMY_3466	*glgA*, glycogen synthase	1.16
EAMY_2102	*otsA*, trehalose-6-phosphate synthase	1.15
EAMY_2469	*pdc*, pyruvate decarboxylase	1.08
Coenzyme transport and metabolism		
EAMY_2469	*pdc*, pyruvate decarboxylase	1.08
EAMY_1371	*ssuD*, alkanesulfonate monooxygenase	1.03
Cell motility		
EAMY_2141	*fliC*, filament structural protein	3.42
EAMY_2090	methyl-accepting chemotaxis protein	3.15
EAMY_2089	*cheR*, methyl-accepting chemotaxis protein methyltransferase	3.08
EAMY_2088	*cheB*, chemotaxis regulator	2.87
EAMY_2086	*cheZ*, chemotaxis protein	2.64
EAMY_3273	*aer*, methyl-accepting chemotaxis protein	2.08
EAMY_0532	*hrcN*, type III secretion system ATPase	1.78
EAMY_1463	*flgL*, flagellar hook-associated protein	1.75
EAMY_1451	*flgM*, negative regulator of flagellin synthesis	1.70
EAMY_1810	methyl-accepting chemotaxis protein	1.70

Table A.3 (cont.)

Locus tag	Gene description	log_2FC
Cell motility		
EAMY_1462	*flgK*, flagellar hook-associated protein	1.65
EAMY_1450	*flgN*, flagella synthesis protein	1.64
EAMY_2142	*fliD*, flagellar capping protein	1.62
EAMY_2096	*motB*, flagellar motor protein	1.57
EAMY_1515	*cheV*, chemotaxis signal transduction protein	1.54
EAMY_2097	*motA*, flagellar motor protein	1.46
EAMY_2095	*cheA*, chemotactic sensory histidine kinase	1.44
EAMY_3131	methyl-accepting chemotaxis protein	1.37
EAMY_2094	*cheW*, chemotaxis signal transduction protein	1.33
EAMY_2143	*fliS*, flagellin-specific chaperone	1.26
EAMY_2093	methyl-accepting chemotaxis protein	1.15
Cell wall/membrane/envelope biogenesis		
EAMY_2247	*amsD*, glycosyltransferase	2.60
EAMY_2253	*amsG*, UDP-phosphate galactose phosphotransferase	2.36
EAMY_2244	*amsJ*, exopolysaccharide biosynthesis protein	2.23
EAMY_2250	*amsA*, tyrosine-protein kinase	2.01
EAMY_2243	*amsK*, glycosyltransferase	1.97
EAMY_0739	*O*-acetyltransferase	1.94
EAMY_2252	*amsH*, amylovoran export outer membrane protein	1.89
EAMY_2945	acyltransferase	1.79
EAMY_2242	*amsL*, exopolysaccharide biosynthesis protein	1.52
EAMY_3658	*yiaD*, outer membrane protein	1.52
EAMY_1364	*ompN*, outer membrane protein porin	1.40
EAMY_1987	*wbaP*, undecaprenyl-phosphate galactose phosphotransferase	1.26
Energy production and conversion		
EAMY_1489	hypothetical protein	3.26
EAMY_1373	*ssuE*, NAD(P)H-dependent FMN reductase	1.88
EAMY_3274	*gltP*, proton glutamate symport protein	1.01
General function prediction only		
EAMY_2470	glyceraldehyde 3-phosphate reductase	1.77
EAMY_2196	*adhB*, alcohol dehydrogenase	1.59
EAMY_2469	*pdc*, pyruvate decarboxylase	1.08
EAMY_1371	*ssuD*, alkanesulfonate monooxygenase	1.03
Inorganic ion transport and metabolism		
EAMY_3084	*sul*, sulfate permease	1.71
EAMY_3085	*yadF*, carbonate dehydratase	1.69
EAMY_1198	*modA*, molybdate ABC transporter substrate-binding protein	1.42
EAMY_3611	*dppC*, ABC transporter	1.27
EAMY_3610	*dppD*, ABC transporter ATP-binding protein	1.27
EAMY_3612	*dppB*, ABC transporter	1.21
EAMY_0996	*amtB*, ammonia transporter	1.11

Table A.3 (cont.)

Locus tag	Gene description	log_2FC
Inorganic ion transport and metabolism		
EAMY_3405	*tauC*, taurine ABC transporter permease	1.02
EAMY_2162	*sitC*, iron ABC transporter	1.02
Intracellular trafficking, secretion and vesicular transport		
EAMY_1450	*flgN*, flagella synthesis protein	1.64
EAMY_0786	*spaQ*, surface presentation of antigens protein	1.44
EAMY_2143	*fliS*, flagellin-specific chaperone	1.26
Lipid transport and metabolism		
EAMY_0110	*cdh*, CDP-diacylglycerol pyrophosphatase	1.10
Nucleotide transport and metabolism		
EAMY_2473	*nupC*, sodium/nucleoside cotransporter	1.18
Post-translational modification, protein turnover and chaperones		
EAMY_0491	*lidJ*, disulphide bond formation protein	2.84
EAMY_3180	*groE*, molecular chaperone	1.58
EAMY_3179	*groL*, molecular chaperone	1.57
EAMY_0131	*hslU*, ATP-dependent protease	1.26
EAMY_0132	*hslV*, ATP-dependent protease	1.17
EAMY_1019	*htpG*, molecular chaperone	1.17
Signal transduction mechanisms		
EAMY_2090	methyl-accepting chemotaxis protein	3.15
EAMY_2089	*cheR*, methyl-accepting chemotaxis protein methyltransferase	3.08
EAMY_2088	*cheB*, chemotaxis regulator	2.87
EAMY_1498	*rcsA*, colanic acid capsular biosynthesis activation protein	2.73
EAMY_2086	*cheZ*, chemotaxis protein	2.64
EAMY_3273	*aer*, methyl-accepting chemotaxis protein	2.08
EAMY_2251	*amsI*, protein-tyrosine-phosphatase	2.02
EAMY_1810	methyl-accepting chemotaxis protein	1.70
EAMY_1515	*cheV*, chemotaxis signal transduction protein	1.54
EAMY_2095	*cheA*, chemotactic sensory histidine kinase	1.44
EAMY_0995	*glnK*, nitrogen regulatory protein PII	1.39
EAMY_3131	methyl-accepting chemotaxis protein	1.37
EAMY_2094	*cheW*, chemotaxis signal transduction protein	1.33
EAMY_2093	methyl-accepting chemotaxis protein	1.15
Transcription		
EAMY_1498	*rcsA*, colanic acid capsular biosynthesis activation protein	2.73
EAMY_0330	*nlp*, sugar fermentation stimulation protein	2.25
EAMY_2717	*emrR*, transcriptional regulator	1.88
Transcription		
EAMY_1451	*flgM*, negative regulator of flagellin synthesis	1.70
EAMY_0536	*hrpL*, RNA polymerase sigma factor	1.68
EAMY_2139	*fliA*, RNA polymerase sigma factor	1.09

Table A.3 (cont.)

Locus tag	Gene description	log_2FC
Translation, ribosomal structure and biogenesis		
EAMY_0658	*prfB*, peptide chain release factor I	1.43
EAMY_0659	*lysS*, lysyl-tRNA synthetase	1.35
Type III secretion system		
EAMY_0520	*hsvA*, Hrp-associated systemic virulence protein	3.47
EAMY_0521	*hsvB*, Hrp-associated systemic virulence protein	3.40
EAMY_0522	*hsvC*, Hrp-associated systemic virulence protein	2.52
EAMY_0519	*hrpK*, pathogenicity locus protein	2.07
EAMY_0552	*hrpN*, harpin protein	1.98
EAMY_0528	*hrcR*, type III secretion apparatus protein	1.93
EAMY_0526	*hrcT*, type III secretion apparatus protein	1.90
EAMY_0556	*hrpW*, harpin protein	1.90
EAMY_0527	*hrcS*, type III secretion protein	1.89
EAMY_0653	*eop2*, type III effector	1.85
EAMY_0533	*hrpQ*, type III secretion system protein	1.83
EAMY_0531	*hrpO*, type III secretion protein	1.81
EAMY_0546	*hrpE*, type III secretion apparatus protein	1.81
EAMY_0555	*orfC*, HrpW-specific chaperone	1.80
EAMY_0529	*hrcQ*, type III secretion system apparatus protein	1.80
EAMY_0530	*hrpP*, type III secretion protein	1.80
EAMY_0550	*hrpT*, type III secretion lipoprotein	1.79
EAMY_0553	*orfA*, Tir chaperone family protein	1.79
EAMY_0534	*hrcV*, type III secretion inner-membrane protein	1.78
EAMY_0549	*hrcC*, type III secretion system outer membrane pore	1.78
EAMY_0532	*hrcN*, type III secretion system ATPase	1.78
EAMY_0551	*hrpV*, type III secretion protein	1.75
EAMY_0545	*hrpD*, type III secretion protein	1.73
EAMY_0547	*hrpF*, type III secretion protein	1.73
EAMY_0535	*hrpJ*, type III secretion system protein	1.73
EAMY_0548	*hrpG*, type III secretion protein	1.73
EAMY_0542	*hrpA*, Hrp pili protein	1.72
EAMY_0554	*orfB*, avirulence protein	1.71
EAMY_0525	*hrcU*, type III secretion protein	1.71
EAMY_0536	*hrpL*, RNA polymerase sigma factor	1.68
EAMY_0543	*hrpB*, type III secretion system protein	1.67
EAMY_0544	*hrcJ*, type III secretion inner-membrane protein	1.66
EAMY_0557	*dspE*, Hrp secreted pathogenicity-like protein	1.58
EAMY_0558	*dspF*, Hrp secreted pathogenicity-like protein	1.57
EAMY_3175	*avrRpt2*, cysteine protease avirulence protein	1.54
Uncharacterized/functional unknown proteins		
EAMY_0657	hypothetical protein	4.24
EAMY_0492	phytochelatin synthase	3.41

Table A.3 (cont.)

Locus tag	Gene description	log_2FC
Uncharacterized/functional unknown proteins		
EAMY_2140	HNH endonuclease	3.00
EAMY_2087	*cheY*, chemotaxis regulator	2.83
EAMY_3567	hypothetical protein	2.77
EAMY_2091	hypothetical protein	2.71
EAMY_3269	hypothetical protein	2.65
EAMY_3334	*ymcB*, lipoprotein	2.61
EAMY_2248	*amsC*, exopolysaccharide biosynthesis protein	2.43
EAMY_2246	*amsE*, glycosyltransferase	2.40
EAMY_2477	hypothetical protein	2.39
EAMY_3333	*ymcA*, lipoprotein	2.38
EAMY_3335	*ymcC*, lipoprotein	2.38
EAMY_2202	hypothetical protein	2.23
EAMY_2270	hypothetical protein	2.16
EAMY_2245	*amsF*, exopolysaccharide biosynthesis protein	2.12
EAMY_1490	hypothetical protein	2.09
EAMY_1492	hypothetical protein	1.89
EAMY_0745	hypothetical protein	1.88
EAMY_2269	hypothetical protein	1.88
EAMY_0828	hypothetical protein	1.85
EAMY_0523	hypothetical protein	1.80
EAMY_0524	biphenyl 2,3-dioxygenase	1.80
EAMY_0744	*hopPtoC*, cysteine protease avirulence protein	1.75
EAMY_2092	hypothetical protein	1.74
EAMY_0652	hypothetical protein	1.71
EAMY_1768	hypothetical protein	1.59
EAMY_2133	*ycfT*, acyltransferase	1.56
EAMY_0661	hypothetical protein	1.53
EAMY_1548	*mltE*, membrane-bound lytic murein transglycosylase E	1.50
EAMY_2134	*yedO*, 1-aminocyclopropane-1-carboxylate deaminase	1.48
EAMY_0660	hypothetical protein	1.46
EAMY_2135	*D*-cysteine desulfhydrase	1.41
EAMY_2144	*fliT*, flagellar export chaperone	1.23
EAMY_2136	hypothetical protein	1.22
EAMY_1549	hypothetical protein	1.17
EAMY_1806	hypothetical protein	1.15
EAMY_3268	heme-regulated cyclic AMP phosphodiesterase	1.13
EAMY_1004	hypothetical protein	1.09
EAMY_3439	*yrfF*, membrane protein	1.08
EAMY_1769	*yafP*, acetyltransferase	1.07
EAMY_1488	hypothetical protein	1.06

Table A.3 (cont.)

Locus tag	Gene description	log_2FC
Uncharacterized/functional unknown proteins		
EAMY_3470	hypothetical protein	1.04
EAMY_2338	hypothetical protein	1.01

Table A.4 Down-regulated genes in the *csrB* mutant (adjusted *P*-value < 0.05)

Locus tag	Gene description	log_2FC
Amino acid transport and metabolism		
EAMY_2799	*medA*, methionine gamma-lyase	-1.16
EAMY_1632	*astE*, succinylglutamate desuccinylase	-1.09
EAMY_1628	*astC*, succinylornithine transaminase	-1.07
EAMY_3478	*ggt*, gamma-glutamyltranspeptidase	-1.04
EAMY_1629	*astA*, arginine *N*-succinyltransferase	-1.00
Carbohydrate transport and metabolism		
EAMY_0451	*smvA*, major facilitator superfamily transporter	-1.59
EAMY_3665	*kdgK*, 2-dehydro-3-deoxygluconokinase	-1.58
EAMY_1644	*yniA*, fructosamine kinase	-1.43
EAMY_3666	*tub*, major facilitator superfamily transporter	-1.31
EAMY_2552	major facilitator superfamily transporter	-1.23
EAMY_1495	*yedP*, mannosyl-3-phosphoglycerate phosphatase	-1.20
EAMY_3254	*treF*, cytoplasmic trehalase	-1.15
EAMY_2501	*talA*, transaldolase A	-1.09
EAMY_1738	*ynfM*, major facilitator superfamily transporter	-1.04
EAMY_1227	glucoamylase	-1.01
Coenzyme transport and metabolism		
EAMY_0444	*mcyE*, Glutamate-1-semialdehyde aminotransferase	-2.94
EAMY_0441	creatininase	-2.67
EAMY_1182	*pnuC*, nicotinamide mononucleotide transporter	-2.12
EAMY_1786	*yhjG*, FAD monooxygenase	-1.87
Cell wall/membrane/envelope biogenesis		
EAMY_1814	acetyltransferase	-2.12
EAMY_1239	glycosyltransferase	-1.52
EAMY_3264	acyltransferase	-1.26
EAMY_0627	*yhjL*, oxoglutarateaminotransferase	-1.26
EAMY_2498	*amiA*, *N*-acetylmuramoyl-*L*-alanine amidase	-1.15
EAMY_0249	*ompT*, outer membrane protease	-1.02
Defense mechanisms		
EAMY_2814	*ygbT*, CRISPR-associated protein Cas1	-2.01
EAMY_1068	*osmC*, peroxiredoxin	-1.75
EAMY_2820	*ygcB*, CRISPR-associated helicase Cas3	-1.69
EAMY_1275	*dps*, DNA-binding ferritin-like protein	-1.65
EAMY_2212	*yeeO*, Na^+-driven multidrug efflux pump	-1.34
Energy production and conversion		
EAMY_1786	*yhjG*, FAD monooxygenase	-1.87
EAMY_1905	*acnA*, aconitate hydratase	-1.37
EAMY_3265	alcohol dehydrogenase	-1.19
EAMY_1404	*gabD*, NAD-dependent aldehyde dehydrogenase	-1.05
EAMY_1262	aspartate/glutamate/hydantoin racemase	-1.03

Table A.4 (cont.)

Locus tag	Gene description	log_2FC
General function prediction only		
EAMY_1847	short-chain dehydrogenase	-1.89
EAMY_1551	*yeaQ*, membrane protein	-1.49
EAMY_0472	*yghA*, oxidoreductase	-1.29
EAMY_3266	GMC family oxidoreductase	-1.19
EAMY_3249	*yedU*, intracellular protease/amidase	-1.18
EAMY_1204	*yncB*, NADP-dependent oxidoreductases	-1.12
EAMY_3245	*gdh*, glucose 1-dehydrogenase	-1.02
Inorganic ion transport and metabolism		
EAMY_1069	hypothetical protein	-1.68
EAMY_1275	*dps*, DNA-binding ferritin-like protein	-1.65
EAMY_1771	*katA*, catalase	-1.40
EAMY_1183	*ybgR*, zinc transporter	-1.28
EAMY_3324	*yjbK*, peroxide operon regulator	-1.21
EAMY_3694	*pstS*, phosphate ABC transporter substrate-binding protein	-1.14
EAMY_3693	*pstC*, phosphate ABC transporter	-1.01
Lipid transport and metabolism		
EAMY_0472	*yghA*, oxidoreductase	-1.29
EAMY_1427	*ymdC*, phospholipase D family protein	-1.27
EAMY_3266	GMC family oxidoreductase	-1.19
EAMY_2423	*fabB*, 3-oxoacyl-(acyl-carrier-protein) synthase	-1.15
EAMY_1686	*cfa*, cyclopropane-fatty-acyl-phospholipid synthase	-1.09
EAMY_3245	*gdh*, glucose 1-dehydrogenase	-1.02
Nucleotide transport and metabolism		
EAMY_0442	dihydroorotate dehydrogenase	-2.74
Post-translational modification, protein turnover and chaperones		
EAMY_3285	*gstA*, glutathione S-transferase	-1.23
EAMY_1445	*grxB*, glutaredoxin II	-1.11
EAMY_0984	*clpX2*, ATP-dependent Clp protease ATP-binding subunit	-1.01
Replication, recombination and repair		
EAMY_2326	helicase	-2.02
EAMY_1654	*ihfA*, integration host factor alpha subunit	-1.20
Secondary metabolites biosynthesis, transport and catabolism		
EAMY_1788	*pvcA*, pyoverdine biosynthesis protein	-4.80
EAMY_1787	*pvcB*, pyoverdine biosynthesis protein	-4.12
EAMY_0447	*sypC*, gramicidin S synthetase II	-2.96
EAMY_0448	*ppsD*, polyketide synthase	-2.82
EAMY_0441	creatininase	-2.67
EAMY_0472	*yghA*, oxidoreductase	-1.29
EAMY_0463	*yqhE*, 2,5-diketo-*D*-gluconate reductase	-1.27
EAMY_1047	*ybbA*, ABC transporter ATP-binding protein	-1.23
EAMY_2423	*fabB*, 3-oxoacyl-(acyl-carrier-protein) synthase	-1.15

Table A.4 (cont.)

Locus tag	Gene description	log_2FC
Secondary metabolites biosynthesis, transport and catabolism		
EAMY_1204	*yncB*, NADP-dependent oxidoreductases	-1.12
EAMY_3245	*gdh*, glucose 1-dehydrogenase	-1.02
Signal transduction mechanisms		
EAMY_0054	LuxR-family transcriptional regulator	-1.48
EAMY_2463	*uspA*, universal stress protein	-1.27
Transcription		
EAMY_0148	*oxyR*, hydrogen peroxide-inducible genes activator	-2.66
EAMY_0054	LuxR-family transcriptional regulator	-1.48
EAMY_0253	*yjaE*, regulator of sigma D	-1.16
EAMY_1420	*marR*, transcriptional regulator	-1.14
Translation, ribosomal structure and biogenesis		
EAMY_2355	hypothetical protein	-1.24
EAMY_3104	*yqjD*, membrane protein	-1.21
EAMY_0830	*yfiA*, ribosomal subunit interface protein	-1.04
Uncharacterized/functional unknown proteins		
EAMY_1078	*inlA*, leucine-rich repeat protein	-4.71
EAMY_3696	bacteriophage protein	-4.29
EAMY_3695	*lscC*, levansucrase	-4.06
EAMY_1888	hypothetical protein	-3.86
EAMY_1889	lipoprotein	-3.32
EAMY_3697	hypothetical protein	-3.24
EAMY_0443	hypothetical protein	-3.11
EAMY_1890	lipoprotein	-2.99
EAMY_3325	*yjbJ*, CsbD family protein	-2.90
EAMY_1514	hypothetical protein	-2.79
EAMY_0446	*irp*, polyketide synthase	-2.79
EAMY_1891	lipoprotein	-2.78
EAMY_1181	*nadA*, Quinolinate synthetase	-2.73
EAMY_1058	hypothetical protein	-2.48
EAMY_0445	*mcyE*, beta-ketoacyl synthase	-2.36
EAMY_3111	hypothetical protein	-2.29
EAMY_2818	*ygcK*, Cse2-family CRISPR-associated protein	-2.25
EAMY_2817	*ygcJ*, Cse4-family CRISPR-associated protein	-2.22
EAMY_2816	*ygcI*, CRISPR-associated protein Cas5	-2.21
EAMY_2819	*ygcL*, Cse1-family CRISPR-associated protein	-2.20
EAMY_1230	*yohC*, YIP1 family protein	-2.19
EAMY_0449	polyketide synthase	-2.14
EAMY_1426	hypothetical protein	-2.11
EAMY_2815	*ygcH*, Cse3-family CRISPR-associated protein	-2.10
EAMY_3664	hypothetical protein	-2.01
EAMY_2327	endonuclease	-2.01

Table A.4 (cont.)

Locus tag	Gene description	log_2FC
Uncharacterized/functional unknown proteins		
EAMY_3622	hypothetical protein	-2.00
EAMY_0825	hypothetical protein	-1.98
EAMY_1823	hypothetical protein	-1.93
EAMY_1186	hypothetical protein	-1.91
EAMY_1077	hypothetical protein	-1.86
EAMY_2475	hypothetical protein	-1.81
EAMY_0957	*ygaU*, peptidoglycan-binding protein	-1.80
EAMY_1274	hypothetical protein	-1.76
EAMY_0956	lipoprotein	-1.75
EAMY_1737	hypothetical protein	-1.74
EAMY_2176	*sqdD*, glycosyltransferase	-1.73
EAMY_2813	*ygbF*, CRISPR-associated protein Cas2	-1.71
EAMY_1895	lipoprotein	-1.70
EAMY_0914	*psiF*, phosphate starvation-inducible protein	-1.69
EAMY_2800	*rcsV*, LuxR-family transcriptional regulator	-1.68
EAMY_1090	hypothetical protein	-1.67
EAMY_0920	hypothetical protein	-1.67
EAMY_0450	gramicidin S synthetase	-1.66
EAMY_1789	hypothetical protein	-1.63
EAMY_1196	hypothetical protein	-1.62
EAMY_1855	hypothetical protein	-1.61
EAMY_2177	hypothetical protein	-1.60
EAMY_1061	hypothetical protein	-1.60
EAMY_0453	hypothetical protein	-1.60
EAMY_1060	hypothetical protein	-1.59
EAMY_0699	hypothetical protein	-1.59
EAMY_0799	hypothetical protein	-1.58
EAMY_1405	hypothetical protein	-1.57
EAMY_1567	*ygdR*, lipoprotein	-1.57
EAMY_3088	hypothetical protein	-1.56
EAMY_1813	hypothetical protein	-1.56
EAMY_0440	hypothetical protein	-1.55
EAMY_2570	*prt*, metalloprotease	-1.54
EAMY_0798	transcriptional regulator	-1.53
EAMY_1637	*osmE*, osmotically-inducible lipoprotein	-1.52
EAMY_2877	hypothetical protein	-1.50
EAMY_0918	hypothetical protein	-1.49
EAMY_3203	hypothetical protein	-1.48
EAMY_1759	hypothetical protein	-1.47
EAMY_3243	hypothetical protein	-1.47
EAMY_1841	acid-shock protein	-1.46

Table A.4 (cont.)

Locus tag	Gene description	log_2FC
Uncharacterized/functional unknown proteins		
EAMY_1566	lipoprotein	-1.45
EAMY_2506	*narQ*, two-component system histidine kinase	-1.45
EAMY_0698	hypothetical protein	-1.44
EAMY_1645	*ydiZ*, hypothetical protein	-1.41
EAMY_1896	hypothetical protein	-1.40
EAMY_3103	*yqjC*, hypothetical protein	-1.40
EAMY_1063	hypothetical protein	-1.39
EAMY_0574	hypothetical protein	-1.38
EAMY_3573	K^+-transporting ATPase subunit F	-1.37
EAMY_3516	hypothetical protein	-1.37
EAMY_0720	lipoprotein	-1.36
EAMY_2034	methyl-accepting chemotaxis protein	-1.35
EAMY_2500	hypothetical protein	-1.35
EAMY_3242	hypothetical protein	-1.35
EAMY_3244	hypothetical protein	-1.34
EAMY_0501	hypothetical protein	-1.33
EAMY_0622	acyltransferase	-1.33
EAMY_1922	BON domain-containing protein	-1.32
EAMY_2571	hypothetical protein	-1.29
EAMY_1062	hypothetical protein	-1.29
EAMY_0382	hypothetical protein	-1.29
EAMY_2274	hypothetical protein	-1.28
EAMY_3267	gluconate 2-dehydrogenase	-1.27
EAMY_0058	hypothetical protein	-1.27
EAMY_1403	*agp*, glucose-1-phosphatase	-1.25
EAMY_2100	*flhD*, flagellar transcriptional activator	-1.24
EAMY_2049	hypothetical protein	-1.23
EAMY_1003	hypothetical protein	-1.22
EAMY_1897	hypothetical protein	-1.21
EAMY_1842	hypothetical protein	-1.21
EAMY_1779	hypothetical protein	-1.20
EAMY_3173	hypothetical protein	-1.20
EAMY_2602	*csiE*, transcriptional anti-terminator	-1.20
EAMY_1316	*ybjP*, lipoprotein	-1.19
EAMY_0502	acetyltransferase	-1.19
EAMY_0999	*ybaY*, lipoprotein	-1.19
EAMY_3105	*yqjE*, membrane protein	-1.18
EAMY_1497	hypothetical protein	-1.17
EAMY_2721	*trxC*, thioredoxin-like protein	-1.17
EAMY_1494	hypothetical protein	-1.15
EAMY_3077	hypothetical protein	-1.15

Table A.4 (cont.)

Locus tag	Gene description	log_2FC
Uncharacterized/functional unknown proteins		
EAMY_2359	hypothetical protein	-1.15
EAMY_2173	hypothetical protein	-1.14
EAMY_1898	hypothetical protein	-1.13
EAMY_2462	hypothetical protein	-1.13
EAMY_3148	hypothetical protein	-1.13
EAMY_1228	hypothetical protein	-1.13
EAMY_1647	hypothetical protein	-1.13
EAMY_2099	*flhC*, flagellar transcriptional activator	-1.13
EAMY_3533	*uspB*, universal stress protein	-1.12
EAMY_2358	hypothetical protein	-1.12
EAMY_0894	hypothetical protein	-1.12
EAMY_2379	hypothetical protein	-1.12
EAMY_1184	*ybgS*, homeobox protein	-1.11
EAMY_3054	hypothetical protein	-1.10
EAMY_3106	hypothetical protein	-1.09
EAMY_3253	hypothetical protein	-1.08
EAMY_3621	hypothetical protein	-1.08
EAMY_1156	*ybgA*, membrane protein	-1.07
EAMY_0301	*yhcB*, cytochrome d uniquinol oxidase subunit	-1.07
EAMY_3423	hypothetical protein	-1.07
EAMY_1076	hypothetical protein	-1.05
EAMY_1079	hypothetical protein	-1.05
EAMY_1089	hypothetical protein	-1.05
EAMY_1638	hypothetical protein	-1.04
EAMY_1440	*yceP*, biofilm formation regulatory protein	-1.03
EAMY_2970	nuclear pore complex protein	-1.03
EAMY_0606	hypothetical protein	-1.02
EAMY_3582	hypothetical protein	-1.01
EAMY_3518	hypothetical protein	-1.01